REPROCESSABLE CROSS-LINKED POLYURETHANES

A Dissertation

Presented to the Faculty of the Graduate School

of Cornell University

In Partial Fulfillment of the Requirements for the Degree of

Doctor of Philosophy

by

David Joseph Fortman

May 2018

REPROCESSABLE CROSS-LINKED POLYURETHANES

David Joseph Fortman, Ph. D.

Cornell University 2018

Thermosets are a ubiquitous class of polymeric materials used due to their excellent mechanical properties and stability resulting from their covalently cross-linked architecture. Unfortunately, these covalent cross-links preclude the reshaping or reprocessing these materials, which limits both the technological applications and sustainable use of these materials. Recent efforts have focused on the incorporation of dynamic covalent bonds into cross-linked materials to enable their continuous reprocessing (Chapter 1). We have focused on applying these strategies to cross-linked polyurethane networks, since these are the most prevalent class of cross-linked polymers. We first demonstrated that the synthesis of cross-linked polyhydroxyurethanes (PHUs) generates cross-linked resins that are inherently reprocessable, likely through mechanically-activated transcarbamoylation reactions that occur at elevated temperature (Chapter 2). We further studied how the polymer structure affects the thermal stability and reprocessability of PHUs (Chapter 3). Due to the slow and incomplete reprocessing observed in these systems, we incorporated more dynamic disulfide bonds into PHU networks as one strategy to enable rapid, quantitative reprocessing of these materials (Chapter 4). Through our many studies on the reprocessing of these and related materials, we have discovered that cross-linked polyurethane resins are inherently dynamic under mild conditions in the presence of certain catalysts, and we demonstrate the potential to use this finding to reprocess PUs traditionally considered to be thermoset materials (Chapter 5).

BIOGRAPHICAL SKETCH

David Joseph Fortman was born in Buffalo, NY on December 26, 1991, and grew up in Tonawanda, NY. His interest in chemistry began during his high school years in the Honors and AP Chemistry classes of Mr. Matthew Hellerer at St. Joseph's Collegiate Institute in Kenmore, NY. Upon graduating high school in 2009, David attended Canisius College in Buffalo, NY as a chemistry major and physics minor. During his time there, he was introduced to research by Dr. Steven Szczepankiewicz, with whom he worked on developing inorganic photocatalysts, and by Dr. Timothy Gregg, who provided him with his introduction to organic synthesis. David decided to apply his organic synthesis skills toward the development of new organic materials, and joined the group of Prof. William Dichtel at Cornell University in 2013. In 2016, he moved with the rest of the Dichtel Group to Northwestern University, where he completed his thesis work developing reprocessable, cross-linked polymers. Upon graduation, David will begin a position as a Research Chemist at PPG Industries in Pittsburgh, PA. In his free time, David enjoys socializing with friends, playing basketball and volleyball, and rooting for the Buffalo Bills and Sabres.

This dissertation is dedicated to my family, friends, and colleagues, for their constant support, especially my parents, Dave and Marsha Fortman.

ACKNOWLEDGMENTS

All of the work reported herein and all of my accomplishments during graduate school would not have been possible without the contributions of countless others. I would like to begin by thanking Prof. William Dichtel for his guidance and mentorship throughout my graduate career; his constant professionalism and unmatched work ethic have set a terrific example for how to be a successful scientist. I would further like to thank Prof. Geoffrey Coates and Prof. Brett Fors for their helpful input as members of my committee, as well as all other faculty at both Cornell and Northwestern University who I've had the opportunity to interact with.

Any successful scientific outcomes would not be possible without the direct contributions of the scientific collaborators I've worked closely with throughout my time in the Dichtel Group. I owe a huge amount of gratitude to Dr. Jacob Brutman and Prof. Marc Hillmyer for their initial and continued help with polymer rheology and mechanical testing, as well as countless discussions on various vitrimer systems we've explored. I'd also like to thank the younger members of "Team Vitrimer", Rachel Snyder, Guilhem De Hoe, Hannah Bates, and, most recently, Daylan Sheppard for their past and continued help in characterizing and understanding these cross-linked polymers. I'd also like to thank Prof. Chris Cramer, Dr. Goliath Beniah and Prof. John Torkelson, and Dr. Catherine Mulzer, Dr. Ryan Bisbey, Dr. Kenneth Hernandez-Burgos, and Prof. Hector Abruña for their valuable scientific collaborations during my time as a graduate student.

Furthermore, this research would not have been possible without the financial support provided by many funding agencies. This research was supported by the National Science Foundation (NSF) through the Center for Sustainable Polymers (CHE-1413862). This research made use of the Cornell Center for Materials Research User Facilities, which are supported by the NSF (DMR-1120296), the Materials Characterization and Imagining Facility, which receives support from the MRSEC Program (NSF DMR-1121262) of the Materials Research Center at Northwestern University, and the Integrated Molecular Structure Education and

Research Center at Northwestern University, which has received support from the Soft and Hybrid Nanotechnology Experimental Resource (NSF NNCI-1542205), the State of Illinois, and the International Institute for Nanotechnology.

I'd like to thank all members, past and present, of the Dichtel Research Group for making it a special place to work. As much as research can be difficult at times, the passionate and intelligent folks in the DRG have made for a fun and stimulating environment in which to do science. I'd particularly like to thank Dr. Catherine Mulzer and Dr. Ryan Bisbey for their guidance as I began my graduate career. I also would like to specially thank Rachel Snyder, Anton Chavez, and Dr. Edon Vitaku for going beyond the contributions of normal labmates, although everyone in the Dichtel Group deserves thanks for some positive contribution to my time in graduate school.

Finally, I'd like to give the most important thanks to all my family & friends. Their constant support has made graduate school a fun and rewarding experience, and I am extremely grateful to have a large support group whose constant encouragement has made graduate school an enjoyable time in my life.

TABLE OF CONTENTS

LIST OF FIGURES

LIST OF TABLES

LIST OF SCHEMES

LIST OF ABBRIVATIONS AND SYMBOLS

5CC	Five-membered cyclic carbonate
6CC	Six-membered cyclic carbonate
DA	Diels-Alder
DBTDL	Dibutyltin dilaurate
DFT	Density functional theory
DMTA	Dynamic mechanical thermal analysis
DSC	Differential scanning calorimetry
E	Young's modulus
ε_b	Strain at break
E′	Storage modulus
E″	Loss modulus
E_a	Arrhenius energy of activation
FT-IR	Fourier transform infrared spectroscopy
FurMal	Furan-maleimide
GC-MS	Gas chromatography-mass spectrometry
HMDA	Hexamethylenediamine
MDI	4,4′-methylenebis(phenyl isocyanate)
NMR	Nuclear magnetic resonance
PDMS	Polydimethylsiloxane
PEG	Poly(ethylene glycol)

PHU	Polyhydroxyurethane
PLA	Polylactide
PU	Polyurethane
RDA	Retro-Diels-Alder
σ_b	Tensile strength
SRA	Stress relaxation analysis
τ^*	Characteristic relaxation time
T_c	Ceiling temperature
T_d	Thermal decomposition temperature
T_g	Glass transition temperature
TGA	Thermogravimetric analysis
TREN	Tris(2-aminoethyl)amine
TS	Transition state
T_v	Topology freezing temperature

CHAPTER ONE

APPROACHES TO SUSTAINABLE AND CONTINUALLY RECYCLABLE CROSS-LINKED POLYMERS

1.1 Abstract

Cross-linked polymers are ubiquitous in daily life, finding applications as tires, insulation, adhesives, automotive parts, and countless other products. The covalent cross-links in these materials render them more mechanically robust, chemically resistant, and thermally stable than their thermoplastic counterparts. Unfortunately, these covalent linkages also prevent recycling these materials into similar value goods. Furthermore, cross-linked polymers are typically produced from petroleum-based feedstocks and their hydrocarbon backbones render them non-degradable, making them unsustainable in the long-term. In recent years, much effort has focused on the development of recycling strategies for cross-linked polymeric materials. In the following Chapter, we discuss many of these approaches, and highlight efforts to produce recyclable cross-linked polymers sustainably. We present future challenges that must be overcome to enable widespread, viable, and more sustainable implementation of these materials, including sustainable sourcing of feedstocks, long-term environmental stability of inherently dynamic polymers, and moving toward industrially viable synthesis and reprocessing methods.

This chapter was written in collaboration with Rachel Snyder, and Dr. Jacob Brutman, Guilhem X. De Hoe, and Prof. Marc Hillmyer in the Department of Chemistry at the University of Minnesota.

1.2 Introduction

Over the last century, plastics have become pervasive in most aspects of our lives, with applications ranging from consumer products to medical devices and industrial goods. The emergence of plastics is attributed to their high strength, low density, and remarkable affordability. However, most plastics used today, including polyethylene, polypropylene, poly(vinyl chloride), and polystyrene, are derived from non-renewable petroleum sources and persist in the environment for decades or centuries, long after their functional lifetimes. Though some plastics are recyclable, only 2% of plastic packaging products are recycled into similar value products in the US (Figure 1.1).[1] More alarmingly, approximately 40% of plastic packaging is landfilled and about 32% ends up dispersed in the environment, and some current estimates predict that the weight of plastic in the ocean will surpass that of marine life by 2050.[1] One relatively immediate way to reduce the environmental impact of plastic waste accumulation is to increase the types and amounts of plastics recycled into similar value products. However, this feat is not straightforward as traditional primary recycling techniques involve high-temperature melt-processing which often leads to deleterious chain-scission processes.[2] Furthermore, the performance of recycled products is compromised if contaminants such as incompatible polymers, dyes, and plasticizers are present during reprocessing.[3,4]

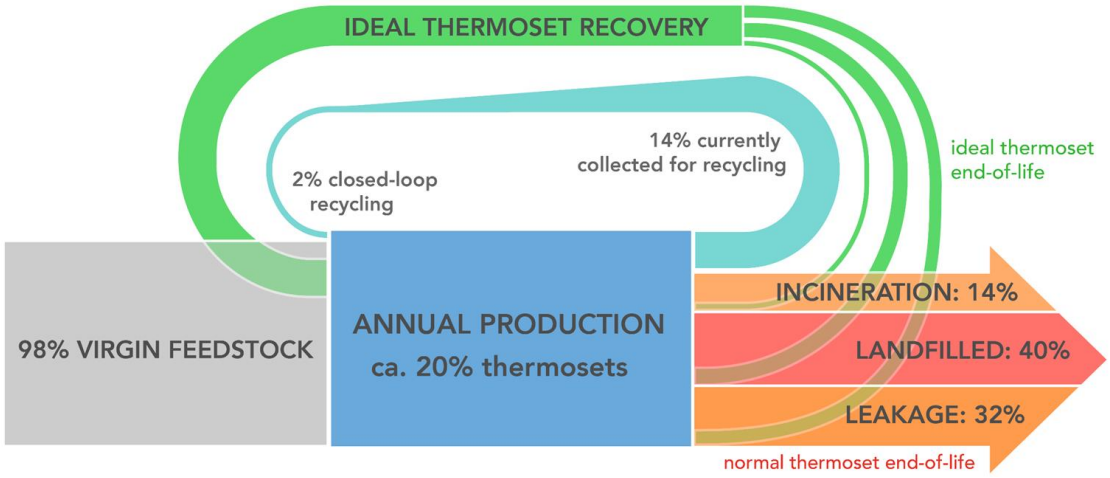

Figure 1.1. Schematic of the outcomes for plastic packaging in 2013, according to a study by the World Economic Forum, the Ellen MacArthur Foundation, and McKinsey & Company.[1] Closed-loop recycling is the recycling of plastics into similar value products. This analysis likely understates the problem for polymeric materials used in other sectors because nearly all thermosets are not capable of closed-loop recycling. This Chapter will discuss reprocessing processes and design criteria that will allow more closed-loop recycling and environmental degradation of thermosets**.**

Even if a high rate of recycling can be achieved, current fossil fuel resources are unlikely to represent a truly sustainable source for our growing plastic use. Although only about 8% of crude oil is required for annual plastics production,[4] fossil fuel generation occurs over thousands to millions of years.[5] Combined with the aforementioned environmental impacts of plastic waste generation, we believe there is a significant social and economic impetus to shift polymer production towards renewable feedstocks. However, only ~1% of plastics are currently produced from renewable resources. Polylactide (PLA) is the most common commercially available, bio-based plastic, with an estimated global demand of 360,000 tons in 2013.[6] PLA offers improved sustainability because it is both industrially compostable and biocompatible; however, the need for industrial composting conditions (60 °C, high humidity) introduces a requirement for specialized facilities. Various other plastics have been

developed that can be environmentally degraded into benign products after disposal, and offer an alternative solution to modulating plastic waste.[7-12] We believe that improving the sustainability of plastics will depend on both improving the efficiency of recycling processes and synthesizing novel plastics that degrade in the environment on reasonable timescales, while keeping in mind the ultimate benefits of using bio-sourced starting materials.

Covalently cross-linked polymers, often referred to as thermosets, are another ubiquitous class of materials comprising *ca*. 15-20% of polymers produced.[13] Traditional recycling of cross-linked polymers via mechanical reprocessing is impractical because their structure precludes flow, even at elevated temperatures. Thermosets are insoluble, such that solution reprocessing is also not viable. Although some of these materials are down-cycled into lower value products, nearly all thermosets are incinerated, landfilled, or otherwise unaccounted for (leakage, Figure 1.1). Still, the high strength and chemical stability of thermosets renders them essential in tires, engineering composites, foams, adhesives, and many other applications. Developing strategies to recycle these materials without compromising their performance represents a formidable challenge.

Recently, significant research effort has been focused on the development of continually reprocessable/recyclable cross-linked polymers by incorporating dynamic covalent bonds into these polymer networks.[3,14-18] Despite rapidly growing interest in reprocessable cross-linked polymers, other aspects of sustainability (*i.e.* renewability and degradability) are rarely integrated into their development. In this Chapter, we will highlight promising approaches for continual recycling of cross-linked polymer

materials via depolymerization strategies or dynamic exchange reactions. We hope to provide insight into the outstanding challenges these materials face towards replacing traditional non-recyclable thermosets and limiting the adverse environmental impacts of this important class of materials.

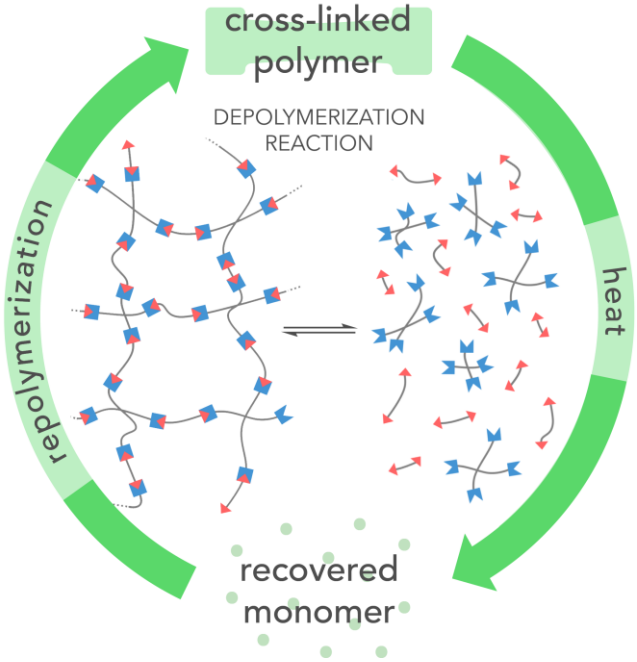

Figure 1.2. Depolymerization strategies such as pyrolysis, solvolysis, hydrolysis, or the design of polymers that depolymerize or dissociate under mild conditions enable reprocessing through conversion of polymers to monomers, then synthesizing new polymers of similar performance**.**

1.3. Depolymerization Strategies

1.3.1 Thermal Depolymerization

Pyrolysis breaks large molecules into smaller ones through high temperature treatment (typically >600 °C), such as petroleum cracking in the petrochemical industry. Both thermoplastic and cross-linked polymers are capable of complete breakdown via pyrolysis,[19-21] and various commodity plastics, including polyethylene,[22] polypropylene,[23] poly(methyl methacrylate),[24] and polystyrene,[25] undergo pyrolysis to

yield a complex mixture of potentially valuable chemicals. The mixtures obtained from petroleum cracking are separated into desirable compounds, and a similar process could be envisioned for recovery of high-value chemical feedstocks from complex mixtures of waste plastics. This method is of particular interest for cross-linked polymers, which typically have limited options for reprocessing. Unlike many of the chemistries discussed below, pyrolysis is theoretically applicable to all polymers. While industrial-scale pyrolysis has been demonstrated as a reliable method to produce fuel mixtures,[26,27] to our knowledge, the production of useful polymer feedstocks via pyrolysis is not practiced due to the complex, energy-intensive separations that would be required. Plastics that selectively depolymerize to recover pure, reusable monomer feedstocks would prevent the need for complex purifications and likely require less energy.

Selective depolymerization at lower temperatures than those required for pyrolysis (<250 °C) has been demonstrated for several polymers.[28-31] The most common examples are lactone-based polyesters, but poly(phthalaldehyde),[32] poly(tetramethylene oxide),[33] poly(methyl methacrylate),[25] certain polycarbonates,[34] and poly(trimethylene urethane)[35] also depolymerize to regenerate their monomers. Depolymerization is induced by heating above the ceiling temperature (T_c), at which the rate of polymerization and depolymerization are equal. Typical recovery processes yield high-purity monomer, reducing the need for further purification. This strategy has been used to recycle cross-linked polymers; for example, cross-linked poly(β-methyl-δ-valerolactone) (PMVL) was depolymerized to recover over 90% of the original monomer (Scheme 1.1) from cross-linked polyurethane foams or robust polyester elastomers.[27,36] This strategy is applicable to any polymer with an appropriate T_c and

could become even more prevalent with the development of new monomer feedstocks capable of controlled thermal depolymerization to their monomers. Further research on monomer feedstocks with optimized polymerization/depolymerization thermodynamics could provide powerful chemical recycling processes. We also stress that the scope of polymers with ceiling temperatures accessible for selective depolymerization extends beyond lactones and developing strategies to incorporate other depolymerizable backbones into cross-linked resins might also benefit thermoset recycling. Ideal polymers for this strategy would also be derived from renewable feedstocks via efficient chemistry.

Scheme 1.1 Poly(β-methyl-δ-valerolactone) backbone "unzipping" to monomer, and its incorporation into chemically recyclable cross-linked polymers**.**

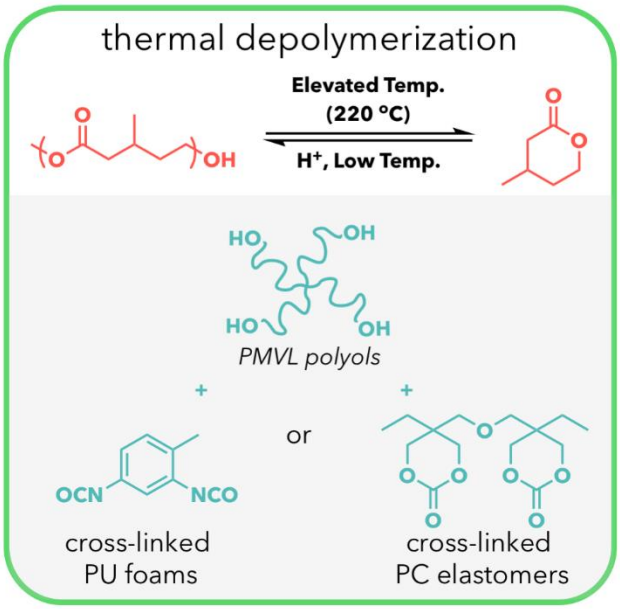

1.3.2 Solvent-assisted Depolymerization

Almost all polymers can be pyrolyzed, but the recovered compounds cannot necessarily be used to manufacture similar value products. For instance, polyurethanes[37,38] and polyesters[39-42] can be difficult to pyrolyze into useful small-

molecules. The urethane and ester functional groups of these polymers are susceptible to reactions with nucleophiles such as water or alcohols, allowing them to be depolymerized to compounds suitable for repolymerization. This strategy is amenable to any material in which a hydrolysable functional group is part of the polymer backbone. The most successful application of solvent-assisted depolymerization is the hydrolysis or alcoholysis of poly(ethylene terephthalate), a common commodity thermoplastic.[38] Although polyurethane foams are traditionally considered non-recyclable, they also can be subjected to alcoholysis to obtain various urethane-alcohols that can be used to produce materials of similar value.[36] The development of efficient catalysts[43] and optimization of engineering processes could make this strategy highly practical and for the recycling of cross-linked polyesters, polyurethanes, polyamides, and polyacetals.

1.3.3 Hemiaminals/Hexahydrotriazines

Developing thermoset materials that undergo solvolysis under milder conditions represents a promising route to improving the energy costs associated with solvent-assisted depolymerization. Hemiaminals and hexahydrotriazines can hydrolyze at ambient temperatures, yet still may be incorporated into materials with mechanical properties comparable to high-performance nitrogen-containing thermosets (Scheme 1.2). The condensation of three equivalents of a primary amine with two equivalents of paraformaldehyde under mild conditions yields hemiaminal linkages, which dissociate at similar rates as acetal/hemiacetal linkages.[44] Upon further heating, hemiaminals condense to form hexahydrotriazines,[45-50] which have been employed as cross-links in non-dynamic polymer systems.[51,52] Hedrick and coworkers demonstrated that these two

sequential trifunctional moieties enable the synthesis of easily recyclable, high performance cross-linked polymers.[44] The mechanical properties of these materials exceeded most thermosets, but the hemiaminal and hexahydrotriazine linkages were hydrolyzed in acidic conditions at room temperature to recover the amine monomer. Li *et al.* synthesized a nanocomposite hemiaminal dynamic covalent network film with bacterial cellulose and reported materials that demonstrated improved mechanical strength without compromising their recyclability.[53] Hemiaminal dynamic covalent organogels from amine-terminated, oligomeric poly(ethylene glycol) (PEG) were also synthesized by Fox *et al*. These materials heal in seconds at room temperature and are capable of complete reversion to monomer in water at room temperature.[54] Hexahydrotriazine-based epoxy resins were reported using efficient epoxide-amine reactions to give fast curing, high-performance networks that degrade under mild conditions, illustrating that solvent-depolymerizable hexahydrotriazine networks can be applied to commercially-relevant materials.[55]

Hemiaminal and hexahydrotriazine-linked networks couple facile synthesis, excellent mechanical properties, and mild and selective depolymerization. This facile degradation represents a sustainable approach to the synthesis of high-performance polymer composites, as it allows for easy recycling of these typically intractable materials. However, their rapid degradation under acidic conditions must be considered in application designs. Solvent-free production would also improve their viability.[55] Additionally, these materials could prove more useful if direct mechanical reprocessing is demonstrated via this chemistry. This could potentially be achieved via incorporation of an acid catalyst to enable mechanical recycling via cross-link exchange.

Scheme 1.2 Synthesis and hydrolysis of hexahydrotriazines, and their incorporation into hydrolyzable cross-linked polymers**.**

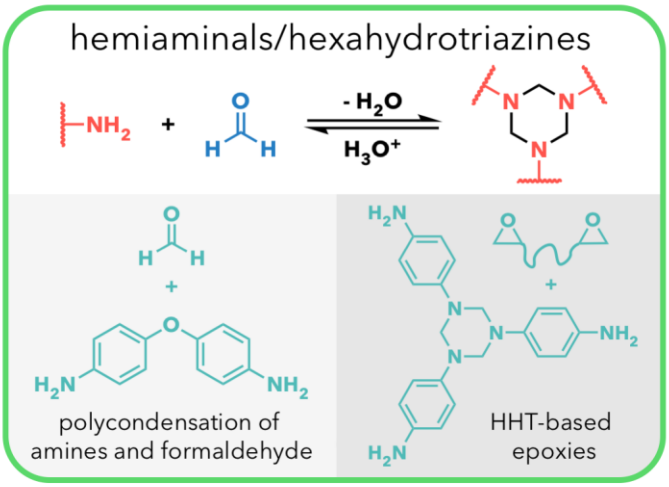

1.3.4 Dissociative Depolymerization/Diels-Alder Cycloadducts

Another effective approach towards continually reprocessable cross-linked polymers is to control the reversible transformation between a cross-linked and uncross-linked state (Figure 1.2), allowing the polymers to flow. Diels-Alder (DA) reactions are the most prominently explored and promising design examples. Cross-linked polymer networks based on thermoreversible DA cycloadducts between furans and maleimides (FurMal) were first described in a 1969 U.S. patent,[56] and many other reprocessable polymer networks based on this linkage have been reported subsequently (Scheme 1.3).[57-59] A comprehensive review published in 2013 on the use of FurMal linkages in reprocessable polymers indicates that this interest has persisted.[60] Though not as widely studied as the FurMal system, the reversible dimerization of cyclopentadiene was introduced into reprocessable polymers in a 1974 US patent.[61]

Scheme 1.3 Diels-Alder equilibrium of FurMal cycloadducts, and Modulating their Recyclability with Light

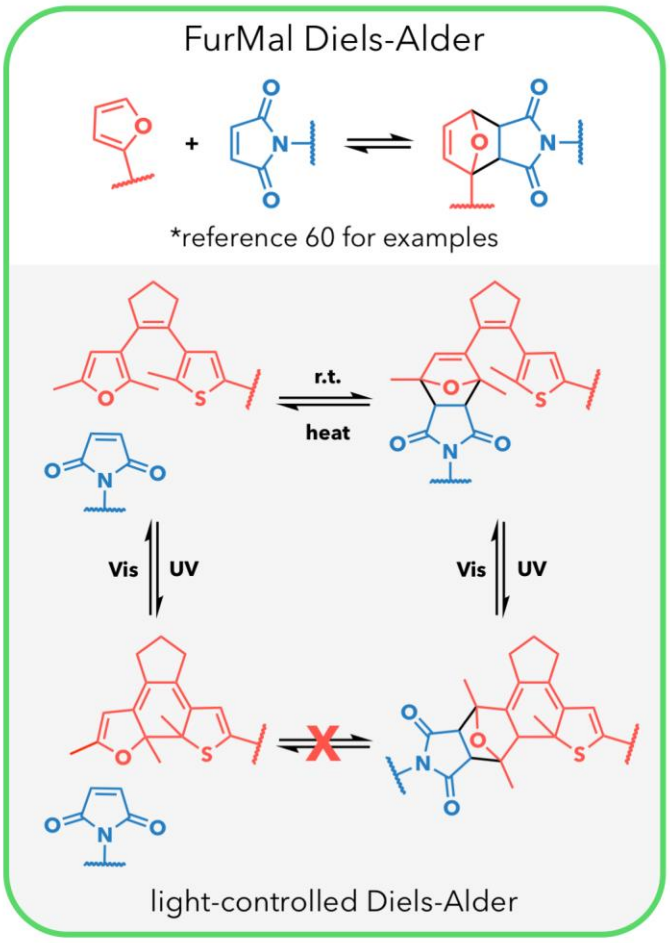

The tunability and selectivity of reversible DA cycloadduct formation imparts many benefits for its use in reprocessing cross-linked polymers. The kinetics and thermodynamics of the DA reaction can be tuned by the selected diene and dieneophile, as well as the steric bulk and regiochemistry of their substituents. The FurMal linkages are commonly studied because of their fast rates of cycloadduct formation, and because their dissociation occurs within temperature ranges that are compatible with many polymer backbones.[62] Still, the breadth of available diene/dienophiles and substitution patterns enables tuning of the solubility of monomers, oxidative and hydrolytic stability

of resins, and temperatures required for cross-linking/de-cross-linking, which is valuable for developing polymers for specific applications.

Both the DA and retro-Diels-Alder (RDA) reactions are highly functional-group-tolerant, allowing DA adducts to serve as reversible cross-links for commodity polymers. FurMal linkages have been applied to reprocessable networks based on polyolefins, polyesters, polyethers, polyurethanes, polyamides, polyoxazilines, polyketones, and polysiloxanes.[59] DA linkages have also been incorporated into sustainable polymers, including poly(ε-caprolactone),[63] poly(lactide),[64] and hyaluronic acid,[65] or into networks synthesized from biorenewable feedstocks including abietic acid,[66] epoxidized soybean oil,[67] and trehalose.[68] Furan-based DA systems are partially renewable, as furan derivatives can be obtained from hemicellulose, an abundant agricultural waste product.[59,69] Maleimides can be produced renewably from succinic anhydride, although this is not the current industrial method for their production.

DA moieties can be incorporated into a variety of industrially relevant resins due to their functional group tolerance.[57,70,71] While most reported DA-functionalized plastics and rubbers require specialized polymer synthesis and/or solvent casting methods to generate bulk materials, recent work from Magana *et al.* demonstrated that DA linkages can be incorporated into a commercially available polyethylene terpolymer via reactive extrusion with a FurMal cycloadduct-based monomer.[72] More recent reports regarding poly(ε-caprolactone) networks show that extrusion and bulk mixing are feasible methods to obtain reprocessable DA networks.[73,74] These are crucial developments to eventually replace conventional cross-linked materials with recyclable alternatives.

In some cases, the low temperatures at which RDA becomes relevant can compromise the cross-linked material at high temperatures and render them soluble as monomer dissolution shifts the equilibrium towards depolymerization.[75] One promising proof-of-concept to overcome these thermal limitations was demonstrated by Fuhrmann, *et al.*, who used a tetrafuryl-substituted diarylethene as the diene that allows for modulating the recyclability of the material via light-induced isomerization of the diarylethene moiety (Scheme 1.3).[76] Additionally, many applications require cross-linked materials without requiring extreme temperature and solvent resistance (e.g., some adhesives and coatings). The depolymerization of DA under relatively mild conditions without catalyst or solvent, in combination with the amenability to renewable substrates and polymers, indicate great potential for dynamic networks capable of reversible DA cycloadduct formation.

1.4 Vitrimers and Related Materials

While thermal, solvent-assisted, and dissociative depolymerization strategies are amenable to the recycling of cross-linked networks, direct mechanical reprocessing may be a more ideal processing strategy in many cases. An approach allowing for direct recyclability was developed, whereby dynamic bonds that undergo associative exchange-reactions are incorporated into polymer networks (Figure 1.3). These networks, termed vitrimers by Leibler and coworkers,[77] show strong-glass forming behavior: when force is applied at reprocessing temperatures, vitrimers relax stress more like silica-based glasses than typical thermoplastics, which have an abrupt drop in the viscosity just above their T_g. While some reactions discussed in this section may proceed through a dissociative intermediate, their high association constants are likely the cause

of their vitrimer-like behavior (e.g. they remain insoluble at high temperature). Vitrimer chemistry has been reviewed extensively elsewhere.[78-80] Here, we outline promising chemistries developed for vitrimers and related materials, and comment on their prospects for widespread, sustainable implementation.

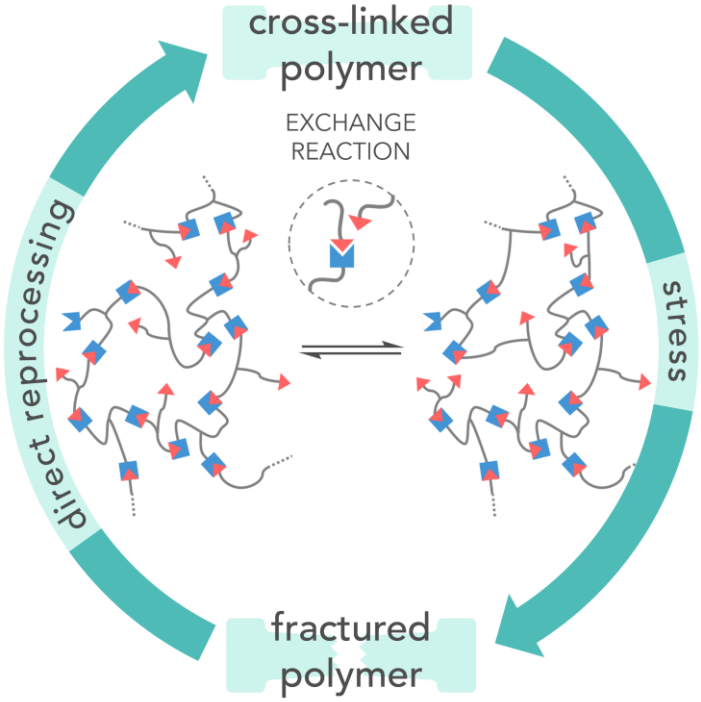

Figure 1.3. Illustration of vitrimers, whereby a cross-linked polymer is broken and can be directly reprocessed into a similar value material, due to dynamic covalent exchange reactions within the network**.**

1.4.1 Transesterification

The transesterification of esters with free alcohols, usually in the presence of a Lewis acid or organic catalyst, is a prototypical vitrimer exchange reaction (Scheme 1.4).[81] In 2011, Montarnal *et al*. synthesized polyester-based epoxy networks containing a Zn(II) transesterification catalyst.[78] These networks possess mechanical properties competitive with traditional epoxy resins, but can be injection-molded after curing and reprocessed to give materials with similar properties to the as-synthesized resins. The

networks display gradual changes in viscosity related to the thermally-activated, associative exchange reactions. This unique capability allows for welding and processing of these polymers by methods similar to silica glass, which is unlikely for dissociating networks.[82] Capelot, *et al.* further showed that changing the catalyst structure and loading enables control of the viscosity changes and reprocessing rates in these networks.[83]

Scheme 1.4 Transesterification & strategies for implementation in cross-linked polymers.

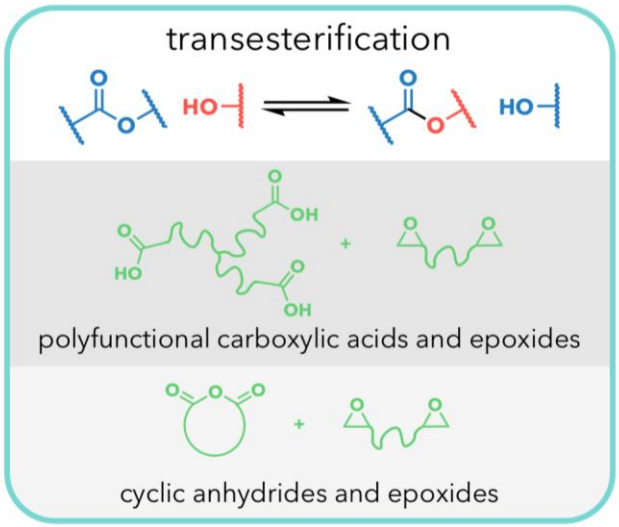

Due to the robustness of the transesterification reaction and the ease with which ester-based networks can be synthesized using common feedstocks, vitrimers based upon transesterification have been widely studied. Commercially available epoxy/anhydride resins have enabled fundamental studies on the rheology of vitrimers with varying cross-link densities and glass transition temperatures,[84-86] and this knowledge has been used to tune properties from rigid thermoset-like materials to cross-linked polyester elastomers.[87] Further emerging applications that incorporate this chemistry include photocurable resins and coatings,[88] carbon fiber-[89] and silica-epoxy[90]

composites with enhanced mechanical properties, and shape memory materials[91-93] that respond to various external stimuli.

Transesterification also represents an ideal chemistry for the large-scale implementation of sustainable materials with high-performance and recyclability. In fact, the first polyester vitrimers were partially bio-based, comprising vegetable oil-derived, oligomeric fatty acids as a primary component.[78] Later, Altuna *et al*. reported fully bio-based polyester vitrimers via the reaction of epoxidized soybean oil and citric acid.[94] These networks showed sufficient reprocessability using excess carboxylic acid groups to catalyze transesterification instead of transition metals. These examples point the way toward fully sustainable polyester vitrimer systems. Many bio-derived/sustainable polymers are polyesters derived from sugar feedstocks,[95] which provide a plethora of diverse monomers through which the properties of bio-based networks can be tuned for appropriate applications. Furthermore, significant research has focused on the development of fully sustainable epoxy networks,[96] many of which could be made reprocessable by the incorporation of transesterification catalysts into the network.

In addition to improving the renewability of these networks, further investigation into the robustness of this exchange chemistry and its application to scalable manufacturing techniques will enable widespread use of these networks. This includes exploring the ability to reprocess these materials multiple times with clear demonstrations of the reproducibility of reshaping and stress relaxation processes. There are also open questions about the long-term environmental stability of resins containing Lewis acid or organocatalysts to catalyst leaching, hydrolysis, etc. Further opportunities

exist for the development of more active catalysts, as many of these materials do not display rapid enough dynamics to enable reprocessing by direct extrusion or injection-molding; however, we note that recent applications of solid-state polymerization[97] and reactive extrusion[98] to produce these materials highlight the potential scalability of this approach.

1.4.2 Sulfur Chemistries

Dynamic sulfur-based chemistries are commonly used in vitrimer-like reprocessable cross-linked networks and have the potential to significantly impact the recycling of many consumer products. The most common method of producing cross-linked elastomers is vulcanization of polyisoprene and polybutadiene—both of which can be renewably derived—with elemental sulfur, predominately used in the production of tires. While vulcanization is known to occur through a radical process, the average number of sulfur atoms in each link is difficult to elucidate. In 1946, Stern and Tobolsky showed that various vulcanized unsaturated polyolefin rubbers exhibit stress relaxation and creep at slightly elevated temperatures (≥60 °C), representing the first example of potential reprocessability in sulfur-containing networks.[99] While it was suggested that a metathesis-type mechanism was responsible for relaxation, Tobolsky *et al*. later demonstrated that these vulcanized rubbers relaxed through homolytic S-S radical scission followed by rapid recombination (Scheme 1.5).[100] This work was eventually confirmed by Nevajans *et al*. through model compound studies, which also showed that the presence of a base enhances the rate of exchange and can enable exchange through a thiolate anion mediated mechanism.[101]

Scheme 1.5: Radical disulfide exchange, and its implementation in cross-linked polymer networks.

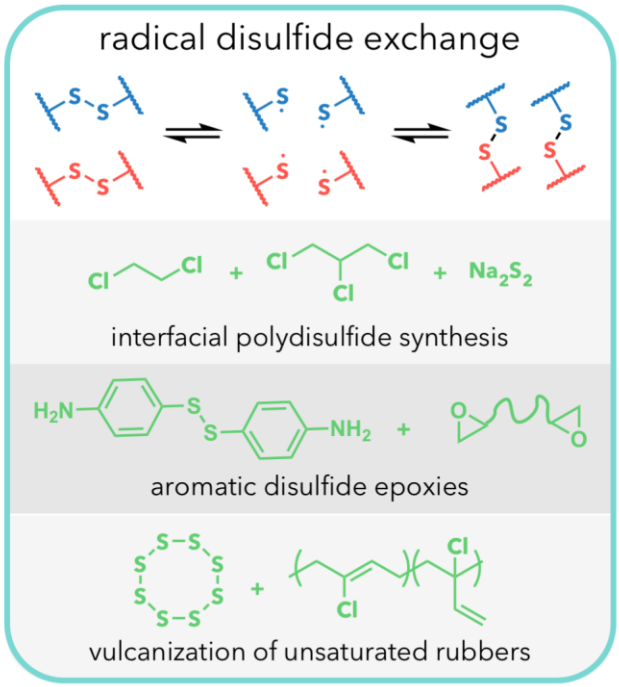

Disulfide linkages were first used to recycle cross-linked polymers in 1990[102,103] when Tesoro *et al*. recycled disulfide-containing epoxy resins by reducing the disulfide linkages into thiols and subsequently re-oxidizing the thiols to disulfides. Since this study, recycling of vulcanized rubbers has been investigated,[104-106] with recent studies focusing on developing single step, catalyst-free disulfide exchange systems.[107] In particular, the use of aryl disulfides instead of alkyl disulfides significantly increases the rate of exchange, allowing for elastomers that heal at room temperature and high T_g polymers that show excellent reprocessability.[108,109] The library of sulfur-based monomers is quite large, enabling a high degree of tunability in the recycling conditions and mechanical properties of the materials. A recent study incorporated disulfide linkages into renewable epoxy resins, indicating that reprocessability of sulfur-based

materials can be extended to bio-derived materials.[110] Although most dynamic sulfur methodologies feature some dissociative cross-links, one study demonstrated reprocessability through the reaction of thiols with disulfides.[111] Unlike the aforementioned examples, these materials solely reprocess via associative cross-link exchange, which has potential benefits over dissociative processes; however, thiols are prone to oxidation in air, which may limit their applicability. Regardless, the environment would benefit greatly from recycling facilities for sulfur-based materials due to the sheer volume of commercial sulfur cross-linked materials. We note that while industrial-scale bio-derived sulfur sources are rare, elemental sulfur is currently produced as an industrial-scale waste product in petroleum refining and is therefore currently a desirable feedstock from a sustainability perspective.[112]

1.4.3 Olefin Metathesis

In addition to sulfur-based vulcanization, unsaturated polyolefin rubbers can also be cross-linked through radical alkene polymerization.[113,114] As these materials lack S-S bonds which allow for reprocessing of vulcanized rubbers, they are incapable of being reprocessed via the methods discussed above. However, these networks often contain residual alkene moieties that enable reprocessing via metal-catalyzed alkene metathesis.

In 2012, Lu *et al.* published two studies regarding alkene metathesis within radically cross-linked poly(butadiene) using the second-generation Grubbs ruthenium alkylidene catalyst (Scheme 1.6).[115,116] These materials rapidly relax stress and reprocess at room temperature. Furthermore, full recovery of tensile properties was observed after reprocessing materials that contained as little as 0.005 mol% catalyst.

Neal *et al.* improved the mechanical performance of these materials by incorporating amide groups into the network,[117] which increase their toughness through hydrogen bonding. These promising systems would further benefit from more efficient catalyst incorporation protocols, such as including the catalyst before cross-linking or by mechanical methods just before reprocessing, followed by subsequent recovery of the catalyst. Further developments could include increasing the functional lifetime of the catalyst by preventing degradation;[118] using a latent metathesis catalyst[119-121] such that the reaction can be (de)activated by external stimuli, resulting in a more robust material; development of this technology for biorenewable feedstocks such as polyisoprene (which is capable of cross-metathesis);[122] and exploration of the potential for metal-free metathesis[123] to address cost concerns associated with the precious metal catalysts used.

Scheme 1.6 Alkene metathesis, and its implementation in cross-linked polymers.

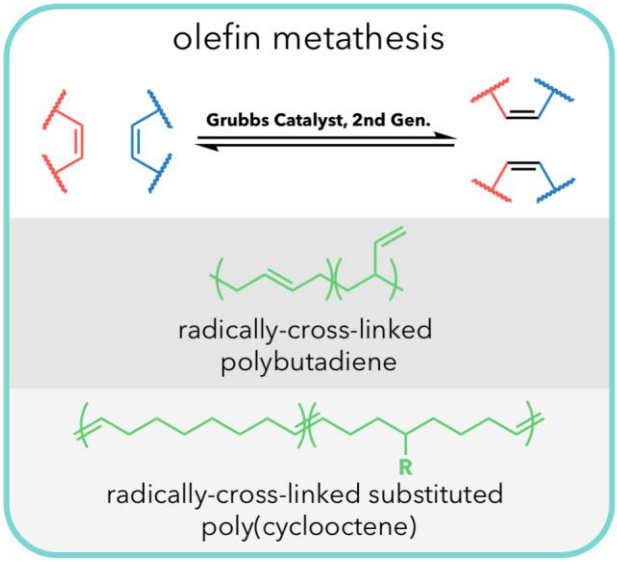

1.4.4 Alkoxyamines

Alkoxyamines undergo reversible homolytic bond cleavage at mild temperatures (*ca.* 100 °C) to yield stable, nitroxyl/aminoxyl and carbon-centered

radicals (Scheme 1.7). This reversible bonding has been used to develop nitroxide-mediated radical polymerizations,[124] whereby the growth of radically-propagating polymers is modulated through an equilibrium activation-deactivation. Several cross-linked systems use these stable nitroxyl radicals to achieve reprocessability. In the earliest applications to repairable cross-linked polymers, 2,2,6,6-tetramethyl-1-piperidinyloxy (TEMPO) moieties were incorporated via multiple synthetic steps as cross-linkers for polystyrene,[125,126] poly(methyl methacrylate),[127] or polyurethane resins.[128] In all cases, these polymers display dynamic behavior at elevated temperatures and can be reprocessed to recover ca. 75% of tensile properties. Jin *et al.* used commercially available TEMPO-substituted methacrylate to cross-link styrene-butadiene rubber in a one-step controlled curing process;[129] these rubbers show near-quantitative reprocessing efficiencies over multiple compression molding cycles.

Scheme 1.7. Alkoxyamine equilibrium, and its implementation in cross-linked polymers.

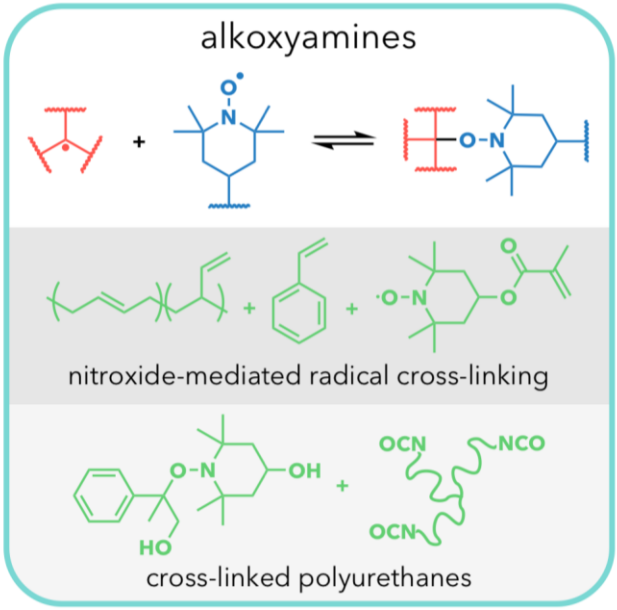

From our perspective, this approach has significant potential because it can be applied directly to any network based on controlled radical polymerization, and can be amended to traditional polymers based on acrylic, styrenic, and other olefinic monomers. This strategy should also be compatible with renewable feedstocks, especially as the syntheses of traditional petrochemical feedstocks from renewable resources are made more efficient. While networks reported to-date do not have mechanical properties comparable to traditional materials (perhaps due to cross-linking by the relatively weak alkoxyamine bond) and tend to show limitations in reprocessing efficiency (low recovery in mechanical properties after reprocessing) at higher cross-link densities, the toughening of these materials through additives and further developments in the chemistry of controlled radicals might overcome these present challenges.

1.4.5 Imine and Vinylogous Urethane Exchange

Imines, or Schiff bases (Scheme 1.8A), are commonly used to develop dynamic covalent molecular systems.[130] The exchange of imine bonds occurs under relatively mild conditions, and the ability to control dynamics by stimuli such as heat, water content, and pH changes offer numerous possibilities for designing vitrimer-like systems. Taynton *et al.* demonstrated the synthesis of polyimine networks via the direct condensation of polyfunctional amines and aldehydes.[131] These networks demonstrate very fast stress relaxation compared to most vitrimers (characteristic relaxation times less than 1 minute at 130 °C, which can be accelerated by the presence of water) and maintain high reprocessing efficiencies. Additional studies demonstrated the reprocessing of polyimine-carbon fiber composites,[132] the mechanical tuning of

polyimine networks via aldehyde and amine selection,[133] and their ultimate degradation under appropriate conditions.[134] Given the fast dynamics compared to most other vitrimers, further investigation should focus on understanding the long-term hydrolytic stability of these networks in environmental conditions.

Scheme 1.8. A. Imine exchange and B. vinylogous urethane exchange, and their implementation in cross-linked polymers.

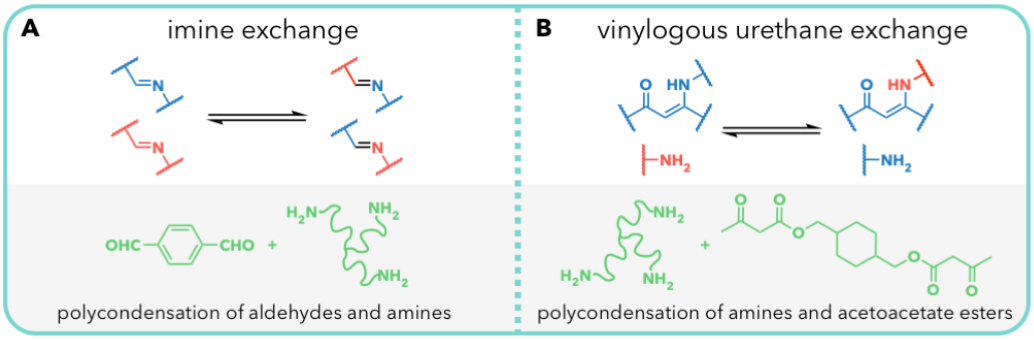

Another promising chemistry exploiting the nucleophilicity of amines is the reversible conjugate addition of amines to vinylogous urethanes. Denissen *et al.* synthesized vinylogous urethane vitrimers via the condensation of polyfunctional amines (an excess of amine functionality is required) and acetoacetate esters (Scheme 1.8B).[135] These vitrimers demonstrate fast relaxation rates (characteristic relaxation times of ca. 100 s at 170 °C) without external catalyst and near-quantitative reprocessing over five reprocessing cycles. Acidic or basic additives capable of catalyzing or inhibiting this exchange reaction tune the exchange reaction rate by greater than an order of magnitude at a given temperature.[136] Changing the structure from vinylogous urethanes to vinylogous ureas further enhances the relaxation rates in the presence of acid catalyst, and enables reprocessing of fiber-reinforced composites.[137] The practicality of water removal, as well as the long-term stability of the free-amines in

these systems to oxidation, carbon dioxide exposure, and other environmental degradation-inducing conditions, are opportunities for further study in these efficient systems. Imine or vinylogous urethane materials could be quite promising as sustainable cross-linked materials, especially if the indefinite recyclability is practical under typical service conditions.

1.4.6 Urea/Urethane Exchange

Polyurethanes (PUs) are commodity polymers derived from the polyaddition of isocyanates and alcohols to produce foams, elastomers, sealants, coatings, and adhesives.[138,139] Ranked sixth in terms of global production,[140] PUs are among the most common polymers used in cross-linked polymer architectures and therefore are a prime target for cross-linked polymer recycling. While solvent-assisted depolymerization approaches have been developed for the chemical recycling of oligomers and small molecules, these approaches have many limitations (see above).[36,37] Much work has focused on incorporating other dynamic bonds into PU networks; however, we will focus on directly exploiting the dynamics of the urethane or urea bonds to enable reprocessing.

One promising approach takes advantage of the fact that the reaction of an alcohol and isocyanate is an equilibrium process, such that urethane linkages will dissociate at elevated temperatures into their constituent alcohol and isocyanate (Scheme 1.9A). This equilibrium has long been known as a source of stress relaxation in cross-linked PU materials,[141,142] but this property has been leveraged only recently for the reprocessing and reshaping of cross-linked PUs. Zheng *et al.* reported that PU elastomers containing catalytic dibutyltin dilaurate show rapid, Arrhenius-type stress

relaxation behavior and plasticity at elevated temperatures.[143] This behavior occurs even in the absence of free alcohol, suggesting the tin-catalyzed dissociation of urethanes as the dominant relaxation mechanism. Further investigation on the dynamics and reprocessing of urethane cross-linked PLA and PEG has shown that, in the presence of tin(II), polyurethane exchange occurs more appreciably than transesterification.[144-146] Although this methodology likely proceeds through a dissociative mechanism, these PUs likely show vitrimer-like behavior because only a small number of carbamates are dissociated under typical reprocessing conditions. These findings demonstrate that any traditional cross-linked PU should show vitrimer-like behavior in the presence of an appropriate catalyst. Therefore, PUs synthesized from sustainable polycarbonate-[147] and polyester-[28,148,149] based polyols and bio-derived isocyanates can be explored for their direct recyclability. Further investigation should also focus on the development of non-toxic metal or organocatalysts for reprocessing.[150] While many of these systems have been shown to relax stress and demonstrate plasticity, reprocessability has been demonstrated but not been thoroughly investigated in most of these systems,[142] and remains an area requiring further investigation.

Scheme 1.9. A. Urethane-urethane exchange B. exchange of sterically-hindered ureas and C. hydroxyl-mediated transcarbamoylation, and their implementation in cross-linked polymers.

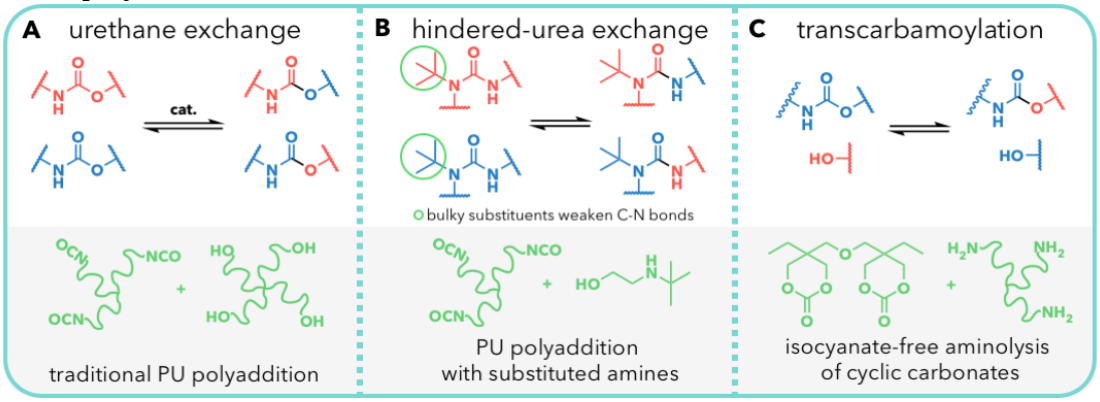

Another approach to enable dynamics at milder temperatures in urethane resins is the incorporation of more readily dissociative urethane analogues into PU networks, reminiscent of the blocked isocyanates commonly used for one-component curing of urethane adhesives and coatings.[151] Amino-alcohols containing sterically-hindered amines were reacted with isocyanates to generate hindered urea bonds (Scheme 1.9B).[152-154] Bulkier amine substitution yielded faster dynamics,[155] such that when a *t*-butyl-substituted amine is used, these hindered urea bonds undergo exchange at room temperature. Hindered ureas have since been incorporated into self-healing elastomers[149] and rigid thermosets[150] that are reprocessable at temperatures above their T_g. These networks are synthesized by incorporating substituted amino-alcohols into traditional PU formulations, which can be directly coupled with renewably-sourced polyols and isocyanates to develop more sustainable variants. Expansion of the scope of this approach from hindered amine to oxime blocking agents indicates the generality and tunability of this approach.[156] Currently, none of the aforementioned methodologies have been applied to the recycling of PU foams, which make up a large percentage of cross-linked PUs; we believe that demonstrating facile foam recyclability would be the next stage towards commercialization of this PU recycling process.

Due the toxicity of isocyanates, regulatory bodies in both the United States and Europe are moving to reduce or remove their use in PU synthesis.[157] Developing alternate chemistries to synthesize cross-linked PU resins is imperative. We have studied the reprocessability of cross-linked PUs synthesized from bis(cyclic carbonates) and amines to produce polyhydroxyurethanes (PHUs).[158] These networks display Arrhenius-type stress relaxation via associative transcarbamoylation (Scheme 1.9C),

likely owing to the thermally stable *N*-alkyl-*O*-alkyl urethanes and stoichiometric equivalence of hydroxyl moieties. Excellent mechanical properties coupled with promising reprocessability make these materials an exciting strategy for producing isocyanate-free, reprocessable PUs. Although promising, PHUs have significantly slower curing times than isocyanate-based PUs and are not currently suitable for producing foams. Quantitative reprocessing has been achieved in 5-membered cyclic carbonate-based PHUs in the presence of catalysts,[159] but reprocessing has been limited to elastomeric materials due to the limited thermal stability of β-hydroxyurethanes.[160] Thus, the efficient synthesis of six-membered cyclic carbonates remains an important target. Developments in six-membered cyclic carbonate synthesis from feedstocks such as CO_2[161] and urea,[162] as well as the development of renewable amines[163] will profoundly impact the sustainability of these materials. Furthermore, improved catalysis of both the cross-linking and transcarbamoylation reactions will enable faster and more efficient (re)processing of these materials.

1.4.7 Siloxane Exchange

Cross-linked siloxane polymers, most notably polydimethylsiloxane (PDMS), are commonly used as elastomers where very low glass transition temperatures are required,[164] though composites with silica fillers have more robust mechanical properties.[165] The Si-O bond is stable to water, air, and radical coupling conditions, but can undergo exchange with nucleophiles, such as silonates (Scheme 1.10). As a result, siloxane exchange reactions are prominent in applications that require fast and efficient reactions, such as microencapsulated healing agents.[166-168] Both acid and base-catalyzed siloxane exchange was rigorously studied in the mid-1900s, [159,169-171] and the reaction is

thought to occur through an associative S_N2-like transition state. These studies demonstrated stress relaxation of cross-linked PDMS elastomers, suggesting their potential to serve as vitrimer-like materials.

Scheme 1.10 Siloxane-silonate exchange, and its implementation in cross-linked polymers.

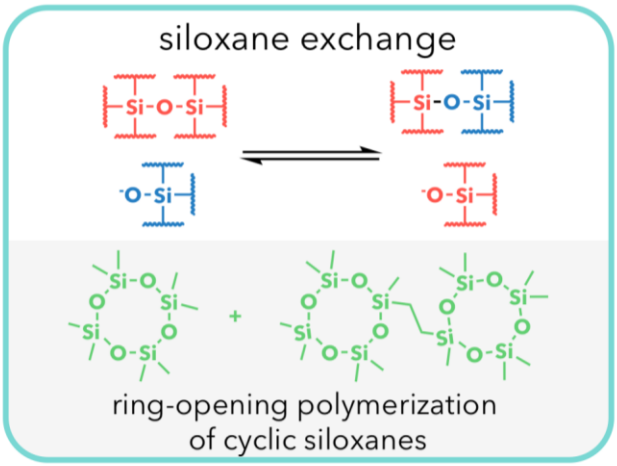

In 2012, Zheng *et al.* described reprocessable, cross-linked PDMS elastomers.[172] Cross-linked networks synthesized via the catalytic ring-opening polymerization of octamethylcyclotetrasiloxane give clear, colorless elastomers that heal completely at 90 °C in 24 h via the exchange of tetramethylammonium silonates with Si-O bonds. The authors showcased several reshaping experiments of the networks, and found this chemistry afforded quantitative recycling. Schmolke *et al.*[173] expanded upon these initial studies by probing the effects of both catalyst concentration and cross-linking density on the dynamics of the network. By increasing catalyst loading, networks are capable of rapid stress relaxation at temperatures as low as 5 °C. However, increased catalyst loading also decreased the mechanical integrity of the polymers, which was attributed to a reduction in viscosity due to increased reaction rates.

These dynamic siloxane systems are promising because they demonstrate some of the fastest stress relaxation of any dynamic covalently cross-linked networks, while maintaining quantitative reprocessing efficiencies. Furthermore, polysiloxanes are well known to be non-toxic, having the same environmental impact as sand and glass. To expand the applications of these materials, the fast and selective silonate exchange must be coupled with more robust polymer backbones to prevent flow and depolymerization at service temperatures. Recent work by Nishimura, *et al.* demonstrates that the incorporation of silyl ether bonds into hydroxyl-containing networks will combine the benefits of robust exchange with enhanced mechanical properties, enabling wider application of this exchange chemistry.[174]

1.4.8 Boronic Ester Exchange

Boronic acid derivatives such as cyclic boronic and boronate esters have been implemented as dynamic covalent linkages in polymer networks. These two functional groups evolve from the reaction between a boronic acid and a 1,2- or 1,3-diol to form a cyclic boronic ester in anhydrous conditions or a cyclic boronate ester in basic aqueous media. To date, most reports incorporating dynamic bonds with anionic boronates focus on water-mediated self-healing of low-toxicity hydrogels for biomedical applications,[175-179] but several vitrimer-like cross-linked systems with boronic esters have been reported.

In 2015, Cash *et al.* described networks synthesized via thiol-ene reactions between a tetrafunctional thiol and a difunctional vinyl monomer containing a boronic ester.[180] These networks heal in the presence of water at room temperature over three days. The use of water for successful healing implies that the primary mechanism for

reprocessing is dissociative (i.e., hydrolysis and re-esterification) rather than associative. Although water aids the healing of these materials, it does not readily degrade them, likely due to the hydrophobic character of the network. A similar boronic-ester-based polysiloxane was later reported by Zuo *et al.*, demonstrating compatibility with other polymer backbones.[181]

Later, Cromwell *et al.* described the synthesis of reprocessable polyolefin networks containing 1,2-diol moieties and difunctional boronic ester cross-linkers.[182] In tertiary amine-containing networks, healing occurs in the absence of water or alcohol; however, poor healing was observed in the absence of tertiary amines, suggesting an amine-catalyzed boronic ester metathesis mechanism. Recently, Rottger *et al.* demonstrated that boronic ester cross-links could be installed in commodity plastics such as polystyrene, high-density polyethylene (HDPE), and poly(methyl methacrylate) via functionalized monomers or post-polymerization modification.[183] Model boronic esters were shown to undergo thermally-activated metathesis, allowing for the synthesis of materials with greater thermal and oxidative stability (Scheme 1.11). These vitrimers relax stress, can be reprocessed by heating (≥130 °C), and do not require water or catalyst to induce healing. The authors used industrially relevant techniques such as extrusion and injection molding to (re)process these materials. This promising application of boronic ester metathesis to conventional polymers demonstrates huge potential for modification of industrially ubiquitous thermoplastics into reprocessable, high-performance vitrimers.

Scheme 11: Boronic ester metathesis, and its implementation in cross-linked polymers.

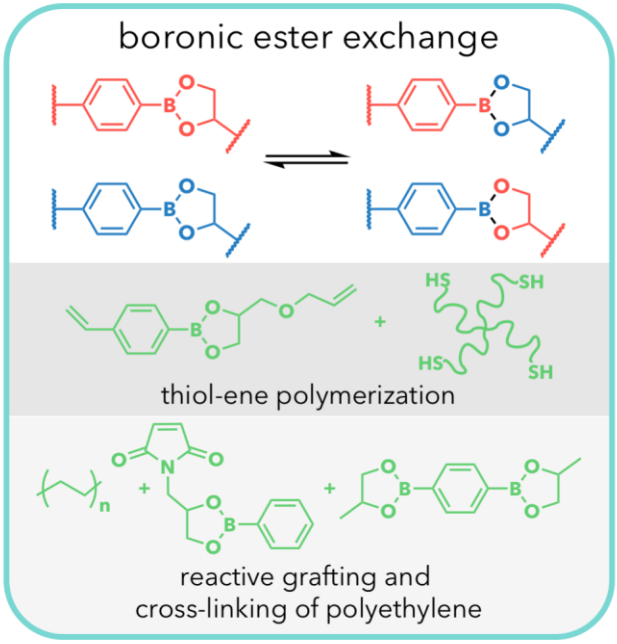

While boron-based polymers are not generally considered renewable,[184] their hydrolysis product is non-toxic boric acid, which is beneficial from a sustainability standpoint.[179,185] We believe future studies on boron-based networks should involve the optimization of their susceptibility to hydrolysis, allowing for tunable degradation of these materials in the environment after their functional lifetimes.

1.5 Conclusion

We have highlighted many promising approaches towards addressing the lack of reprocessability and recyclability in traditional thermoset polymers. The methodologies vary from pyrolysis to the introduction of dynamic functional groups for traditional melt-processing. We stress that the chemistries highlighted above are an incomplete list of strategies applied to this problem. All of the highlighted approaches have advantages and disadvantages in terms of reprocessing efficiencies, methods, cost,

thermal stability, etc.; consequently, a combination of many of these chemistries will be developed to optimize materials for specific applications.

With that in mind, we believe that a continued understanding of the fundamental chemistry and physics governing these materials will be required to enable their commercial implementation. For example, a fundamental understanding of equilibrium thermodynamics will allow precise temperature control of depolymerization to monomers. Developments in dynamic covalent chemistry will enable a material's design to be tailored towards exemplary reprocessability. Beyond this, further study of the behavior of these materials outside controlled laboratory conditions remains a hurdle towards the implementation of these systems. Since these polymers are inherently reactive/dynamic, factors such as long-term exposure to moisture, oxygen, and sunlight will ultimately determine their large-scale use.

More developments are required to improve the sustainability of reprocessable polymers reported to date. A common goal in the field of sustainable polymers is to create materials that are useful for precise amounts of time, before degrading rapidly to benign compounds. Therefore, developing materials that display both enhanced functional lifetimes and controlled degradation could have significant added value over current systems. Furthermore, developing extremely robust materials with recycling efficiencies comparable to or better than thermoplastics could have large impacts in decreasing the amount of plastic waste generated, another crucial aspect to mitigating the present socioeconomic issues related to polymer recycling.

Finally, we stress that many of these chemistries can and should be applied to sustainable polymer feedstocks, such as polylactide, saccharides, and cellulose

derivatives, allowing plastics to begin decoupling from petroleum feedstocks. These same sustainable polymers are often capable of biodegradation to non-toxic small-molecules, which will further prevent significant environmental damage from the disposal of plastics. Although current recycling of polymers is inefficient at best, we believe that the strong research push to develop these continuously recyclable, high-performance polymers can only benefit our environment as we move forward, especially if researchers aim to make these materials truly sustainable in all facets of their life cycle.

References

(1) *The New Plastics Economy - Rethinking the future of plastics*; World Economic Forum, Ellen MacArthur Foundation, and McKinsey & Company: 2016.

(2) Rahimi, A.; García, J. M. *Nat. Rev. Chem.* **2017**, *1*, 1-11.

(3) Helms, B. A.; Russell, T. P. *Chem.* **2016,** *1*, 816-818.

(4) Hopewell, J.; Dvorak, R.; Kosior, E. *Philos. Trans. R. Soc., B* **2009**, *364*, 2115-2126.

(5) Conaway, C. F. 2. Petroleum Origins and Accumulation. In *Petroleum Industry - A Nontechnical Guide*, PennWell: 1999.

(6) Grand View Research. Lactic Acid Market Analysis by Application (Industrial, F&B, Pharmaceuticals, Personal Care) & Polylactic Acid (PLA) Market Analysis by Application (Packaging, Agriculture, Transport, Electronics, Textiles), And Segment Forecasts, 2014-2025. May, 2017.

(7) Williams, C. K.; Hillmyer, M. A. *Polym. Rev.* **2008,** *48*, 1-10.

(8) Miller, S. *ACS Macro Lett.* **2013**, *2*, 550-554.

(9) Hillmyer, M. A.; Tolman, W. B. *Acc. Chem. Res.* **2014,** *47*, 2390-2396.

(10) Ma, S.; Li, T.; Liu, X.; Zhu, J. *Polym. Int.* **2016**, *65*, 164-173.

(11) Zhu, Y.; Romain, C.; Williams, C. *Nature* **2016**, *540*, 354-362.

(12) Schneiderman, D. K.; Hillmyer, M. A. *Macromolecules* **2017,** *50*, 3733-3749.

(13) American Chemistry Council, U.S. Resin Production and Sales, March 2017. https://plastics.americanchemistry.com/Sales-Data-by-Resin.pdf

(14) Wu, D. Y.; Meure, S.; Solomon, D. *Prog. Polym. Sci.* **2008,** *33*, 479-522

(15) Wool, R. P. *Soft Matter* **2008,** *4*, 400-418.

(16) Tyagi, P.; Deratani, A.; Quemener, D. *Isr. J. Chem.* **2013,** *53*, 53-60.

(17) Kloxin, C.; Bowman, C. *Chem. Soc. Rev*. **2013**, *42*, 7161-7173.

(18) Wojtecki, R. J.; Meador, M. A.; Rowan, S. J. *Nat. Mater*. **2011**, *10*, 14–27.

(19) Buekens, A. Introduction to Feedstock Recycling of Plastics. In *Feedstock Recycling and Pyrolysis of Waste Plastics*, John Wiley & Sons, Ltd: 2006; pp 1-41.

(20) Butler, E.; Devlin, G.; McDonnell, K. *Waste and Biomass Valoriz.* **2011,** *2*, 227-255.

(21) Kaitz, J. A.; Lee, O. P.; Moore, J. S. *MRS Comm.* **2015,** *5*, 191-204.

(22) Bagri, R.; Williams, P. T. *J. Anal. Appl. Pyrol.* **2002,** *63*, 29-41.

(23) Kiran Ciliz, N.; Ekinci, E.; Snape, C. E. *Waste Manag.* **2004,** *24*, 173-181.

(24) Kaminsky, W.; Franck, J. *J. Anal. Appl. Pyrol.* **1991,** *19*, 311-318.

(25) Achilias, D. S.; Kanellopoulou, I.; Megalokonomos, P.; Antonakou, E.; Lappas, A. A. *Macromol. Mater. Eng.* **2007,** *292*, 923-934.

(26) American Chemistry Council, Economic Impact of Plastics-to-Oil Facilities in the U.S. October, 2014.

(27) Sharuddin, S. D. A.; Abnisa, F.; Daud, W. M. A. W.; Aroua, M. K. *Energy Convers. Manag*. **2016**, *115*, 308-326.

(28) Schneiderman, D. K.; Vanderlaan, M. E.; Mannion, A. M.; Panthani, T. R.; Batiste, D. C.; Wang, J. Z.; Bates, F. S.; Macosko, C. W.; Hillmyer, M. A. *ACS Macro Lett.* **2016**, 515-518.

(29) Hong, M.; Chen, E. Y. X. *Nat. Chem.* **2016,** *8*, 42-49.

(30) MacDonald, J. P.; Shaver, M. P. *Polym. Chem.* **2016,** *7*, 553-559.

(31) Hong, M., Chen, E. Y. X. *Green Chem.* **2017**, 19, 3692-3706.

(32) Ito, H.; Willson, C. G. *Polym. Eng. Sci.* **1983,** *23*, 1012-1018.

(33) Enthaler, S.; Trautner, A. *ChemSusChem* **2013,** *6*, 1334-1336.

(34) Olsen, P.; Undin, J.; Odelius, K.; Keul, H.; Albertsson, A-C. *Biomacromolecules* **2016**, *17*, 3995-4002.

(35) Neffgen, S.; Keul, H.; Hocker, H. *Macromol. Rapid Commun.* **1996**, *17*, 373-382.

(36) Brutman, J. P.; De Hoe, G. X.; Schneiderman, D. K.; Le, T. N.; Hillmyer, M. A. *Ind. Eng. Chem. Res.* **2016,** *55*, 11097-11106.

(37) Zia, K. M.; Bhatti, H. N.; Ahmad Bhatti, I. *React. Funct. Polym.* **2007,** *67*, 675-692.

(38) Yang, W.; Dong, Q.; Liu, S.; Xie, H.; Liu, L.; Li, J. *Procedia Environ. Sci.* **2012,** *16*, 167-175.

(39) Paszun, D.; Spychaj, T. *Ind. Eng. Chem. Res.* **1997,** *36*, 1373-1383.

(40) Bassampour, Z. S.; Budy, S. M.; Son, D. Y. *J. Appl. Polym. Sci.* **2017,** *134*, 44620.

(41) Fukushima, K.; Lecuyer, J. M.; Wei, D. S.; Horn, H. W.; Jones, G. O.; Al-Megren, H. A.; Alabdulrahman, A. M.; Alsewailem, F. D.; McNeil, M. A.; Rice, J. E.; Hedrick, J. L. *Polym. Chem.* **2013,** *4*, 1610-1616.

(42) Shi, Q.; Yu, K.; Dunn, M. L.; Wang, T.; Qi, H. J. *Macromolecules* **2016**, *49*, 5527-5537.

(43) Zhang, X.; Fevre, M; Jones, G. O.; Waymouth, R. M. *Chem. Rev.* **2018**, *118*, 839-885.

(44) Garcia, J. M.; Jones, G. O.; Virwani, K.; McCloskey, B. D.; Boday, D. J.; ter Huurne, G. M.; Horn, H. W.; Coady, D. J.; Bintaleb, A. M.; Alabdulrahman, A. M. S.; Alsewailem, F.; Almegren, H. A. A.; Hedrick, J. L. *Science* **2014**, *344*, 732-735.

(45) Bouchemma, A.; Mccabe, P. H.; Sim, G. A. *J. Chem. Soc. Perkin Trans. 2* **1989**, *6*, 583-587.

(46) Nielsen, A. T.; Atkins, R. L.; Moore, D. W.; Scott, R.; Mallory, D.; LaBerge, J. M. *J. Org. Chem.* **1973**, *38*, 3288-3295.

(47) Nielsen, A. T.; Moore, D. W.; Ogan, M. D.; Atkins, R. L. *J. Org. Chem.* **1979**, *44*, 1678-1684.

(48) Singh, A. K. S., S.K.; Quraishi, M.A. *J. Mater. Environ. Sci.* **2011**, *2*, 403-306.

(49) Ghandi, M.; Salimi, F.; Olyaei, A. *Molecules* **2006**, *11*, 556.

(50) Dandia, A.; Arya, K.; Sati, M.; Sarawgi, P. *J. Fluorine Chem.* **2004**, *125*, 1273-1277.

(51) Kong, L.-Z.; Pan, C.-Y. *Polymer* **2008**, *49*, 3450-3456.

(52) Dienys, G.; Sereikaitė, J.; Gavėnas, G.; Kvederas, R.; Bumelis, V.-A. *Bioconjugate Chem.* **1998**, *9*, 744-748.

(53) Li, Z.; Qiu, J.; Pei, C. *Cellulose* **2016**, *23*, 2449-2455.

(54) Fox, C. H.; ter Hurrne, G. M.; Wojtecki, R. J.; Jones, G. O.; Horn, H. W.; Meijer, E. W.; Frank, C. W.; Hedrick, J. L.; Garcia, J. M. *Nat. Commun.* **2015**, *6*, 8417.

(55) You, S.; Ma, S.; Dai, J.; Jia, Z.; Liu, X.; Zhu, J. *ACS Sus. Chem. Eng.* **2017**, *5*, 4683-4689.

(56) Craven, J. M. US Patent 3,435,003, March 25, 1969.

(57) Chujo, Y.; Sada, K.; Saegusa, T. *Macromolecules* **1990**, *23*, 2636–2641.

(58) Canary, S. A.; Stevens, M. P. *J. Polym. Sci. A Polym. Chem.* **1992**, *30*, 1755–1760.

(59) Chen, X.; Dam, M. A.; Ono, K.; Mal, A.; Shen, H.; Nutt, S.; Sheran, K.; Wudl, F. *Science* **2002**, *295*, 1698–1702.

(60) Gandini, A. *Prog. Polym. Sci.* **2013**, *38*, 1–29.

(61) Takeshita, Y.; Uoi, M.; Hirai, Y.; Uchiyama, M. US Patent 3,826,760, July 30, 1974.

(62) Boutelle, R. C.; Northrop, B. H. *J. Org. Chem.* **2011**, *76*, 7994-8002.

(63) Ikeda, T.; Oikawa, D.; Shimasaki, T.; Teramoto, N.; Shibata, M. *Polymer* **2013**, *54*, 3206–3216.

(64) Iji, M.; Inoue, K.; Yamashiro, M. *Polym. J.* **2008**, *40*, 657–662.

(65) Nimmo, C. M.; Owen, S. C.; Shoichet, M. S. *Biomacromolecules* **2011**, *12*, 824–830.

(66) Mustață, F.; Bicu, I. *Angew. Makromol. Chem.* **1999**, *264*, 21–29.

(67) Amato, D. N.; Strange, G. A.; Swanson, J. P.; Chavez, A. D.; Roy, S. E.; Varney, K. L.; Machado, C. A.; Amato, D. V.; Costanzo, P. J. *Polym. Chem.* **2013**, *5*, 69–76.

(68) Teramoto, N.; Arai, Y.; Shibata, M. *Carbohydr. Polym.* **2006**, *64*, 78–84.

(69) Binder, J. B.; Blank, J. J.; Cefali, A. V.; Raines, R. T. *ChemSusChem* **2010**, *3*, 1268–1272.

(70) Bai, N.; Saito, K.; Simon, G. P. *Polym. Chem.* **2013**, *4*, 724–730.

(71) Bai, J.; Li, Z.; Shi, Z.; Yin, J. *Macromolecules* **2015**, *48*, 3539–3546.

(72) Magana, S.; Zerroukhi, A.; Jegat, C.; Mignard, N. *React. Funct. Polym.* **2010**, *70*, 442–448.

(73) Raquez, J.-M.; Vanderstappen, S.; Meyer, F.; Verge, P.; Alexandre, M.; Thomassin, J.-M.; Jérôme, C.; Dubois, P. *Chem. Eur. J.* **2011**, *17*, 10135–10143.

(74) Mallek, H.; Jegat, C.; Mignard, N.; Abid, M.; Abid, S.; Teha, M. *J. Appl. Polym. Sci.* **2012**, *129*, 954–964.

(75) Zhang, Y.; Broekhuis, A. A.; Picchioni, F. *Macromolecules* **2009,** *42*, 1906-1912.

(76) Fuhrmann, A.; Göstl, R.; Wendt, R.; Kötteritzsch, J.; Hager, M. D.; Schubert, U. S.; Brademann-Jock, K.; Thünemann, A. F.; Nöchel, U.; Behl, M.; Hecht, S. *Nat. Commun.* **2016,** *7*, 13623.

(77) Montarnal, D.; Capelot, M.; Tournilhac, F.; Leibler, L. *Science* **2011,** *334*, 965-968.

(78) Denissen, W.; Winne, J.; Du Prez, F. *Chem. Sci*. **2016**. *7*, 30-38.

(79) Imbernon, L.; Norvez, S. *Eur. Polym. J.* **2016,** *82*, 347-376.

(80) Zou, W. K.; Dong, J. T.; Luo, Y. W.; Zhao, Q.; Xie, T. *Adv. Mater*. **2017**, *29*, 1606100.

(81) Otera, J. *Chem. Rev.* **1993**, *93*, 1449-1470.

(82) Capelot, M.; Montarnal, D.; Tournilhac, F.; Leibler, L. *J. Am. Chem. Soc.* **2012,** *134*, 7664-7667.

(83) Capelot, M.; Unterlass, M. M.; Tournilhac, F.; Leibler, L. *ACS Macro Lett.* **2012,** *1*, 789-792.

(84) Yu, K.; Taynton, P.; Zhang, W.; Dunn, M. L; Qi, H. J. *RSC Adv.* **2014**, *4*, 48682-48690.

(85) Snijkers, F.; Rossana, P.; Maffezzoli, A. *Soft Matter* **2017**, *13*, 258-268.

(86) Snyder, R.; Fortman, D.; De Hoe, G.; Hillmyer, M.; Dichtel, W. *Macromolecules* **2018**, *51*, 389-397.

(87) Imbernon, L.; Norvez, S.; Leibler, L. *Macromolecules* **2016**, *49*, 2172-2178.

(88) Lyon, G. B.; Cox, L. M.; Goodrich, J. T.; Baranek, A. D.; Ding, Y.; Bowman, C. N. *Macromolecules* **2016**, *49*, 8905-8913.

(89) Chabert, E.; Vial, J.; Cauchois, J-P.; Mihaluta, M.; Tournilhac, F. *Soft Matter* **2016**, *12*, 4838-4845.

(90) Aurelie, L.; Soulie-Ziakovic, C. *Macromolecules* **2016**, *49*, 5893-5902.

(91) Pei, Z.; Yang, Y.; Chen, Q.; Terentjev, E. M.; Wei, Y.; Ji, Y. *Nat. Mater.* **2014,** *13*, 36-41.

(92) Yang, Y.; Pei, Z.; Li, Z.; Wei, Y.; Ji, Y. *J. Am. Chem. Soc*. **2016**, *138*, 2118-2121.

(93) Yang, Z.; Wang, Q.; Wang, T. *ACS Appl. Mater. Interfaces* **2016**, *8*, 21691-21699.

(94) Altuna, F. I.; Pettarin, V.; Williams, R. J. J. *Green Chem.* **2013**, *15*, 3360-3366.

(95) Vilela, C.; Sousa, A.; Fonseca, A.; Serra, A.; Coelho, J.; Freire, C.; Silvestre, A. *Polym. Chem.* **2014**, *5*, 3119-3141.

(96) Auvergne, R.; Caillol, S.; David, G.; Boutevin, B.; Pascault, J-P. *Chem. Rev.* **2014**, *114*, 1082-1115.

(97) Zhou, Y.; Goossens, J. G. P..; Sijbesma, R. P.; Heuts, J. P. A. *Macromolecules* **2017**, *50*, 6742-6751.

(98) Demongeot, A.; Groote, R.; Goossens, H.; Hoeks, T.; Tournilhac, F.; Leibler, L. *Macromolecules* **2017**, *50*, 6117-6127.

(99) Stern, M. D.; Tobolsky, A. V. *J. Chem. Phys.* **1946,** *14*, 93-100.

(100) Tobolsky, A. V.; MacKnight, W. J.; Takahashi, M. *J. Phys. Chem.* **1964,** *68*, 787-790.

(101) Nevejans, S.; Ballard, N.; Miranda, J. I.; Reck, B.; Asua, J. M. *Phys. Chem. Chem. Phys.* **2016,** *18*, 27577-27583.

(102) Tesoro, G. C.; Sastri, V. *J. Appl. Polym. Sci.* **1990,** *39*, 1425-1437.

(103) Sastri, V. R.; Tesoro, G. C. *J. Appl. Polym. Sci.* **1990,** *39*, 1439-1457.

(104) Adhikari, B.; De, D.; Maiti, S. *Prog. Polym. Sci.* **2000,** *25*, 909-948.

(105) Rajan, V. V.; Dierkes, W. K.; Joseph, R.; Noordermeer, J. W. M. *Prog. Polym. Sci.* **2006,** *31*, 811-834.

(106) Xiang, H. P.; Rong, M. Z.; Zhang, M. Q. *ACS Sustain. Chem. Eng.* **2016,** *4*, 2715-2724.

(107) Canadell, J.; Goossens, H.; Klumperman, B. *Macromolecules* **2011,** *44*, 2536-2541.

(108) Rekondo, A.; Martin, R.; Ruiz de Luzuriaga, A.; Cabanero, G.; Grande, H. J.; Odriozola, I. *Mater. Horiz.* **2014,** *1*, 237-240.

(109) Ruiz de Luzuriaga, A.; Martin, R.; Markaide, N.; Rekondo, A.; Cabanero, G.; Rodriguez, J.; Odriozola, I. *Mater. Horiz.* **2016**. *3*, 241-247.

(110) Ma, Z.; Wang, Y.; Zhu, J.; Yu, J.; Hu, Z. *J. Polym. Sci. Part A Polym. Chem.* **2017**. *55*, 1790-1799.

(111) Pepels, M.; Filot, I.; Klumperman, B.; Goossens, H. *Polym. Chem.* **2013,** *4*, 4955-4965.

(112) Chung, W. J.; Griebel, J. J.; Kim, E. T.; Yoon, H.; Simmonds, A. G.; Ji, H. J.; Dirlam, P. T.; Glass, R. S.; Wie, J. J.; Nguyen, N. A.; Guralnick, B. W.; Park, J.; Somogyi, A.; Theato, P.; Mackay, M. E.; Sung, Y-E.; Char, K.; Pyun, J. *Nat. Chem*. **2013**, *5*, 518-524.

(113) Loan, L. *Pure Appl. Chem.* **1972,** *30*, 173-180.

(114) Coran, A. Y. 7 - Vulcanization - Mark, James E. In *Science and Technology of Rubber (Third Edition)*, Erman, B.; Eirich, F. R., Eds. Academic Press: Burlington, 2005; pp 321-366.

(115) Lu, Y.-X.; Tournilhac, F.; Leibler, L.; Guan, Z. *J. Am. Chem. Soc.* **2012,** *134*, 8424-8427.

(116) Lu, Y.-X.; Guan, Z. *J. Am. Chem. Soc.* **2012,** *134*, 14226-14231.

(117) Neal, J. A.; Mozhdehi, D.; Guan, Z. *J. Am. Chem. Soc.* **2015,** *137*, 4846-4850.

(118) Nickel, A. Storage of Grubbs Catalysts. http://allthingsmetathesis.com/storage-of-grubbs-catalysts/ (accessed May 16, 2017).

(119) Ben-Asuly, A.; Tzur, E.; Diesendruck, C. E.; Sigalov, M.; Goldberg, I.; Lemcoff, N. G. *Organometallics* **2008,** *27*, 811-813.

(120) Ben-Asuly, A.; Aharoni, A.; Diesendruck, C. E.; Vidavsky, Y.; Goldberg, I.; Straub, B. F.; Lemcoff, N. G. *Organometallics* **2009,** *28*, 4652-4655.

(121) Ginzburg, Y.; Anaby, A.; Vidavsky, Y.; Diesendruck, C. E.; Ben-Asuly, A.; Goldberg, I.; Lemcoff, N. G. *Organometallics* **2011,** *30*, 3430-3437.

(122) Solanky, S. S.; Campistron, I.; Laguerre, A.; Pilard, J.-F. *Macromol. Chem. Phys.* **2005,** *206*, 1057-1063.

(123) Ogawa, K. A.; Goetz, A. E.; Boydston, A. J. *J. Am. Chem. Soc.* **2015**, *137*, 1400-1403.

(124) Nicolas, J.; Guillaneuf, Y.; Lefay, C.; Bertin, D.; Gigmes, D.; Charleux, B. *Prog. Polym. Sci*. **2013**, *38*, 63-235.

(125) Yuan, C.; Rong, M. Z.; Zhang, M. Q.; Zhang, Z. P.; Yuan, Y. C. *Chem. Mater*. **2011**, *23*, 5076-5081.

(126) Wang, F.; Rong, M. Z.; Zhang, M. Q. *J. Mater. Chem.* **2012**, *22*, 13076-13084.

(127) Higaki, Y.; Otsuka, H.; Takahara, A. *Macromolecules* **2006**, *39*, 2121-2125.

(128) Yuan, C.; Rong, M. Z.; Zhang, M. Q. *Polymer* **2014**, *55*, 1782-1791.

(129) Jin, K.; Li, L.; Torkelson, J. M. *Adv. Mater*. **2016**, *28*, 6746-6750.

(130) Belowich, M. E.; Stoddart, J. F. *Chem. Soc. Rev*. **2012**, *41*, 2003-2024.

(131) Taynton, P.; Yu, K.; Shoemaker, R. K.; Jin, Y.; Qi, H. J.; Zhang, W. *Adv. Mater*. **2014**, *26*, 3938-3942.

(132) Taynton, P.; Ni, H.; Zhu, C.; Yu, K.; Loob, S.; Jin, Y.; Qi, H.J.; Zhang, W. *Adv. Mater*. **2016**, *28*, 2904-2909.

(133) Taynton, P.; Zhu, C.; Loob, S.; Shoemaker, R.; Pritchard, J.; Jin, Y.; Zhang, W. *Polym. Chem.* **2016**, *7*, 7052-7056.

(134) Li, H.; Bai, J.; Shi, Z.; Yin, J. *Polymer* **2016,** *85*, 106-113.

(135) Denissen, W.; Rivero, G.; Nicolaÿ, R.; Leibler, L.; Winne, J. M.; Du Prez, F. E. *Adv. Funct. Mater.* **2015**, *25*, 2451–2457.

(136) Denissen, W.; Droesbeke, M.; Nicolaÿ, R.; Leibler, L.; Winne, J. M.; Du Prez, F. E. *Nat. Commun.* **2017,** *8*, 14857.

(137) Denissen, W.; De Baere, I.; Van Paepegem, W.; Leibler, L.; Winne, J. Du Prez, F. E. *Macromolecules* **2018**, *51*, 2054-2064.

(138) Oertel, G. *Polyurethane Handbook*. 2nd ed.; 1994.

(139) Engels, H.-W.; Pirkl, H.-G.; Albers, R.; Albach, R. W.; Krause, J.; Hoffmann, A.; Casselmann, H.; Dormish, J. *Angew. Chem. Int. Ed*. **2013**, *52*, 9422-9441.

(140) Cerasana, Market Study: Polyurethanes (PUR) and Isocyanates (MDI & TDI) [Second Edition] January, 2016.

(141) Offenbach, J. A.; Tobolsky, A. V. *J. Colloid Sci.* **1956**, *11*, 39-47.

(142) Colodny, P.C.; Tobolsky, A. V. *J. Am. Chem. Soc*. **1957**, *79*, 4320-4323.

(143) Zheng, N.; Fang, Z.; Zou, W.; Zhao, Q.; Xie, T. *Angew. Chem. Int. Ed.* **2016**, *55*, 11421–11425.

(144) Brutman, J. P.; Delgado, P. A.; Hillmyer, M. A. *ACS Macro Lett.* **2014**, *3*, 607-610.

(145) Brutman, J. P.; Fortman, D. J.; De Hoe, G. X.; Dichtel, W. R.; Hillmyer, M. A. *Submitted*.

(146) Yan, P.; Zhao, W.; Fu, X.; Liu, Z.; Kong, W.; Zhou, C.; Lei, J. *RSC Adv.* **2017**, *7*, 26858-26866.

(147) Allen, S. D.; Byrne, C. M.; Coates, G. W. *ACS Symp. Ser.* **2006**, *921*, 116-129.

(148) Xiong, M.; Schneiderman, D. K.; Bates, F. S.; Hillmyer, M. A.; Zhang, K. *Proc. Natl. Acad. Sci. U.S.A.* **2014**, *111*, 8357-8362.

(149) Schneiderman, D. K.; Hillmyer, M. A. *Macromolecules* **2016**, *49*, 2419-2428.

(150) Sardon, H.; Pascual, A.; Mecerreyes, D.; Taton, D.; Cramail, H.; Hedrick, J. L. *Macromolecules* **2015**, *48*, 3153-3165.

(151) Delebecq, E.; Pascault, J.-P.; Boutevin, B.; Ganachaud, F. *Chem. Rev*. **2013**, *113*, 80-118.

(152) Ying, H.; Cheng, J. *J. Am. Chem. Soc.* **2014**, *136*, 16974-16977.

(153) Ying, H.; Zhang, Y.; Cheng, J. *Nat. Commun.* **2014**, *5*, 3218-3227.

(154) Zhang, Y.; Ying, H.; Hart, K. R.; Wu, Y.; Hsu, A. J.; Coppola, A. M.; Kim, T. A.; Yang, K.; Sottos, N. R.; White, S. R.; Cheng, J. *Adv. Mater*. **2016**, *28*, 7646–7651.

(155) Zhang, L.; Rowan, S. *Macromolecules* **2017**, *50*, 5051-5060.

(156) Liu, W.; Zhang, C.; Zhang, H.; Zhao, N.; Yu, Z.; Xu, J. *J. Am. Chem. Soc*. **2017**, *139*, 8678-8684.

(157) Verheugen, G. Commission Regulation (EC) No 552/2009 amending Regulation (EC) No 1907/2006 of the European Parliament and of the Council on the Registration, Evaluation, Authorisation and Restriction of Chemicals (REACH) as regards Annex XVII. *J. Eur. Union* **2009**, L164/7.

(158) Fortman, D. J.; Brutman, J. P.; Cramer, C. J.; Hillmyer, M. A.; Dichtel, W. R. *J. Am. Chem. Soc.* **2015**, *137*, 14019-14022.

(159) Chen, X.; Li, L.; Jin, K.; Torkelson, J. *Polym. Chem.* **2017**, *8*, 6349-6355.

(160) Fortman, D. J.; Brutman, J. P.; Hillmyer, M. A.; Dichtel, W. R. *J. Appl. Polym. Sci*. **2017**, 44984.

(161) Gabriele, B.; Mancuso, R.; Salerno, G.; Ruffolo, G.; Costa, M; Dibenedetto, A. *Tet. Lett*. **2009**, *50*, 7330-7332.

(162) Li, Q.; Zhang, W.; Zhao, N.; Wei, W.; Sun, Y. *Catal. Today*. **2006**, *115*, 111-116.

(163) Froidevaux, V.; Negrell, C.; Caillo, S.; Pascault, J.; Boutevin, B. *Chem. Rev*. **2016**, *116*, 14181-14224.

(164) Burkhard, C. A.; Rochow, E. G.; Booth, H. S.; Hartt, J. *Chem. Rev.* **1947**, *41*, 97-149.

(165) Zheng, P.; McCarthy, T. J. *Langmuir* **2010**, *26*, 18585-18590.

(166) Cho, S. H.; White, S. R.; Braun, P. V. *Adv. Mater.* **2009**, *21*, 645-649.

(167) Keller, M. W.; White, S. R.; Sottos, N. R. *Adv. Funct. Mater.* **2007**, *17*, 2399-2404.

(168) Keller, M. W.; White, S. R.; Sottos, N. R. *Polymer* **2008**, *49*, 3136-3145.

(169) Hurd, D. T.; Osthoff, R. C.; Corrin, M. L. *J. Am. Chem. Soc.* **1954**, *76*, 249-252.

(170) Osthoff, R. C.; Bueche, A. M.; Grubb, W. T. *J. Am. Chem. Soc.* **1954**, *76*, 4659-4663.

(171) Kantor, S. W.; Grubb, W. T.; Osthoff, R. C. *J. Am. Chem. Soc.* **1954,** *76*, 5190-5197.

(172) Zheng, P. W.; McCarthy, T. J. *J. Am. Chem. Soc.* **2012**, *134*, 2024-2027.

(173) Schmolke, W.; Perner, N.; Seiffert, S. *Macromolecules* **2015**, *48*, 8781-8788.

(174) Nishimura, Y.; Chung, J.; Muradyan, H.; Guan, Z. *J. Am. Chem. Soc.* **2017**, *139*, 14881-14884.

(175) Cambre, J. N.; Sumerlin, B. S. *Polymer* **2011**, *52*, 4631–4643.

(176) Deng, C. C.; Brooks, W. L. A.; Abboud, K. A.; Sumerlin, B. S. *ACS Macro Lett.* **2015**, *4*, 220–224.

(177) He, L.; Fullenkamp, D. E.; Rivera, J. G.; Messersmith, P. B. *Chem. Commun.* **2011**, *47*, 7497–7499.

(178) Wang, Y.; Li, L.; Kotsuchibashi, Y.; Vshyvenko, S.; Liu, Y.; Hall, D.; Zeng, H.; Narain, R. *ACS Biomater. Sci. Eng.* **2016**, *2*, 2315–2323.

(179) Guan, Y.; Zhang, Y. *Chem. Soc. Rev.* **2013**, *42*, 8106–8121.

(180) Cash, J. J.; Kubo, T.; Bapat, A. P.; Sumerlin, B. S. *Macromolecules*, **2015**, *48*, 2098–2106.

(181) Zuo, Y.; Gou, Z.; Zhang, C.; Feng, S. *Macromol. Rapid Commun.* **2016**, *37*, 1052–1059.

(182) Cromwell, O. R.; Chung, J.; Guan, Z. *J. Am. Chem. Soc.* **2015**, *137*, 6492–6495.

(183) Röttger, M.; Domenech, T.; van der Weegen, R.; Breuillac, A.; Nicolaÿ, R.; Leibler, L. *Science*, **2017**, *356*, 62–65.

(184) Hall, D. G. Boronic Acids: Structure, Properties, and Preparation of Boronic Acid Derivatives. In *Boronic Acids: Preparation and Applications in Organic Synthesis, Medicine and Materials*; Hall, D. G., Ed; Wiley-VCH Verlag GmbH & Co. KGaA: Weinheim, Germany, 2011, pp. 1–133.

(185) Benderdour, M.; Bui-Van, T.; Dicko, A.; Belleville, F. *J. Trace Elem. Med. Biol.* **1998,** *12*, 2-7.

CHAPTER TWO

MECHANICALLY-ACTIVATED, CATALYST-FREE POLYHYDROXYURETHANE VITRIMERS

2.1 Abstract

Vitrimers are polymer networks whose cross-links undergo associative exchange processes at elevated temperature, usually in the presence of an embedded catalyst. This design feature enables the reshaping of materials with mechanical properties similar to thermoset resins. Here we report a new class of vitrimers consisting of polyhydroxyurethanes (PHUs) derived from six-membered cyclic carbonates and amines. PHU networks relax stress and may be molded into arbitrary shapes at elevated temperature and pressure in the absence of an external catalyst. The as-synthesized networks exhibit tensile properties comparable to leading thermosets and recover ca. 75% of their as-synthesized values following reprocessing. Stress relaxation occurs through an associative process involving the nucleophilic addition of free hydroxyl groups to the carbamate linkages, and is characterized by an Arrhenius activation energy (111 ± 10 kJ/mol) lower than that observed for molecular model compounds (148 ± 7 kJ/mol). These findings suggest that transcarbamoylation is activated by mechanical stress, which we attribute, based on density functional theory (DFT) calculations, to the twisting of N lone pairs out of conjugation with the carbonyl π-orbitals. PHU vitrimers are a promising new class of repairable networks because of their outstanding mechanical properties, avoidance of toxic isocyanate monomers, and catalyst-free repair processes.

This work was performed in collaboration with Dr. Jacob Brutman, Prof. Marc Hillmyer, and Prof. Chris Cramer in the Department of Chemistry at the University of Minnesota. This work was first published in the *Journal of the American Chemical Society*: Fortman, D. J.; Brutman, J. P.; Cramer, C. J.; Hillmyer, M. A.; Dichtel, W. R. *J. Am. Chem. Soc.* **2015**, *137*, 14019-14022 and is reproduced with permission.

2.2 Introduction

Thermosets are cross-linked polymer networks with outstanding mechanical strength and solvent resistance used in durable goods, adhesives, and composites. Their static cross-links cause thermosets to be irreparable and difficult to recycle. Cross-links capable of dynamic exchange[1–10] impart repair and reshaping capabilities but reduce toughness and shape persistence unless controlled precisely. A subset of dynamic cross-linked polymers, classified as vitrimers,[1,2] combine excellent mechanical properties at service temperatures and malleability at elevated temperatures by employing cross-links that undergo associative, rather than dissociative, exchange reactions. This design results in gradual viscosity changes with respect to temperature, in contrast to the abrupt viscosity change observed just above the glass transition temperatures of thermoplastics, enabling vitrimers to be easily reprocessed.

Broadening the chemical scope of vitrimers beyond polyester resins (based on transesterification)[11–16] and polybutadiene rubbers (based on alkene metathesis)[17,18] provides a means to improve and expand both the performance and sustainability of cross-linked polymers. Polyurethanes (PU) comprise a large class of industrially produced thermosets and are used extensively for cushioning and thermal insulation,

yet the efficient reprocessing of PU thermosets is poorly established. Associative transcarbamoylation processes are sluggish for carbamates because of their reduced electrophilicity relative to esters, and the dissociative reversion of carbamates to isocyanates and alcohols that typically occurs at high temperatures (>200 °C) can be associated with deleterious side-reactions. As such, existing healable cross-linked PUs either incorporate additional dynamic functional groups and/or are limited to elastomeric materials.[19–26] Inspired by historic reports of enhanced stress relaxation in cross-linked polyurethanes containing free hydroxyl groups,[27,28] we evaluated the vitrimeric properties of polyhydroxyurethane (PHU) networks, whose synthesis from polyfunctional cyclic carbonates and amines provides one hydroxyl group per carbamate linkage, avoids the use of toxic isocyanates, and is amenable to monomers derived from renewable sources.[29,30]

Here we report PHU networks derived from six-membered cyclic carbonates and polyfunctional amines as a new class of vitrimers that does not require the incorporation of an external catalyst. Stress relaxation in these polymers is consistent with an associative transcarbamoylation process, yet exhibits a lower Arrhenius activation energy in the polymer than that observed in molecular model compounds. We attribute this phenomenon to mechanical activation of the transcarbamoylation reaction, associated with twisting the carbamate nitrogen lone pair out of conjugation from the carbonyl group, and present supporting density functional theory (DFT) calculations. The combined thermal and mechanical activation of vitrimers represents a new and desirable reprocessing mechanism that will increase the utility of repairable polymer networks and the scope of chemical transformations available to these materials.

2.3 Results and Discussion

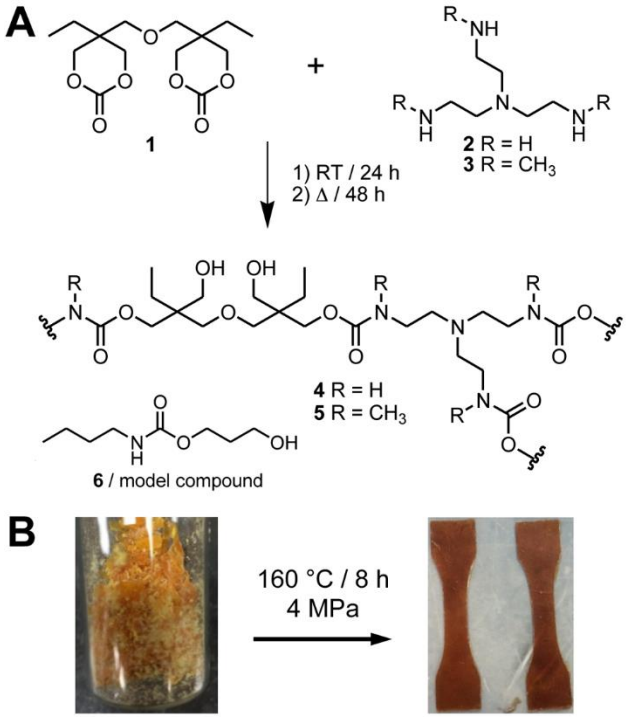

Figure 2.1. A. The reaction of bis(cyclic carbonate) **1** and triamines **2** and **3** provides PHUs **4** and **5**, respectively. **6** is a hydroxyurethane model compound used for transcarbamoylation studies. B. Photograph of a ground sample of **4** (left), which was reprocessed into tensile bars (right) by heating to 160 °C at 4 MPa pressure for 8 h.

A cross-linked PHU (**4**) was prepared through the reaction of bis(cyclic carbonate) **1** and tris(2-aminoethyl)amine **2** (Figure 2.1A) in CH_2Cl_2 at room temperature, after which the solvent was removed by heating to 90 °C under reduced pressure for 48 h. Polymer **4** was isolated as an orange solid that conformed to the shape of its mold. The FT-IR spectrum of **4** (Figure S2.1) exhibits a single peak in the carbonyl region at 1690 cm^{-1}, corresponding to a hydrogen-bonded carbamate C=O stretch. The spectrum also contains a new broad stretch at 3300 cm^{-1}, corresponding to the O-H stretch of hydroxyl groups, and no C=O stretch signals associated with residual cyclic

carbonates. Swelling tests of the polymer in THF (25 °C, 24 h) indicate gel fractions in excess of 0.98, consistent with a densely cross-linked network. As-synthesized samples of **4** had average Young's moduli (E) of 2.2 ± 0.4 GPa, strain-at-break (ε_b) of 6.9 ± 3.8%, and 72 ± 11 MPa tensile strength (σ_b), all competitive materials properties for typical thermosets.[1,5,6,15] Also, **4** shows little weight loss up to 250 °C, as determined by thermogravimetric analysis (TGA, Figure S2.4), and exhibits a glass transition temperature (T_g) of 54 °C, as determined by differential scanning calorimetry (DSC, Figure S2.3). Dynamic mechanical thermal analysis (DMTA) revealed that the modulus of solid **4** decreased by two orders of magnitude near 61 °C, similar to the T_g determined by DSC. Above this temperature, the material has a constant plateau modulus of 7.5 MPa, corresponding to an estimated molar mass between cross-links of 1.2 kg/mol (Figure S2.6). These combined observations indicate that **1** and **2** readily condense to provide a densely cross-linked, rigid PHU network.

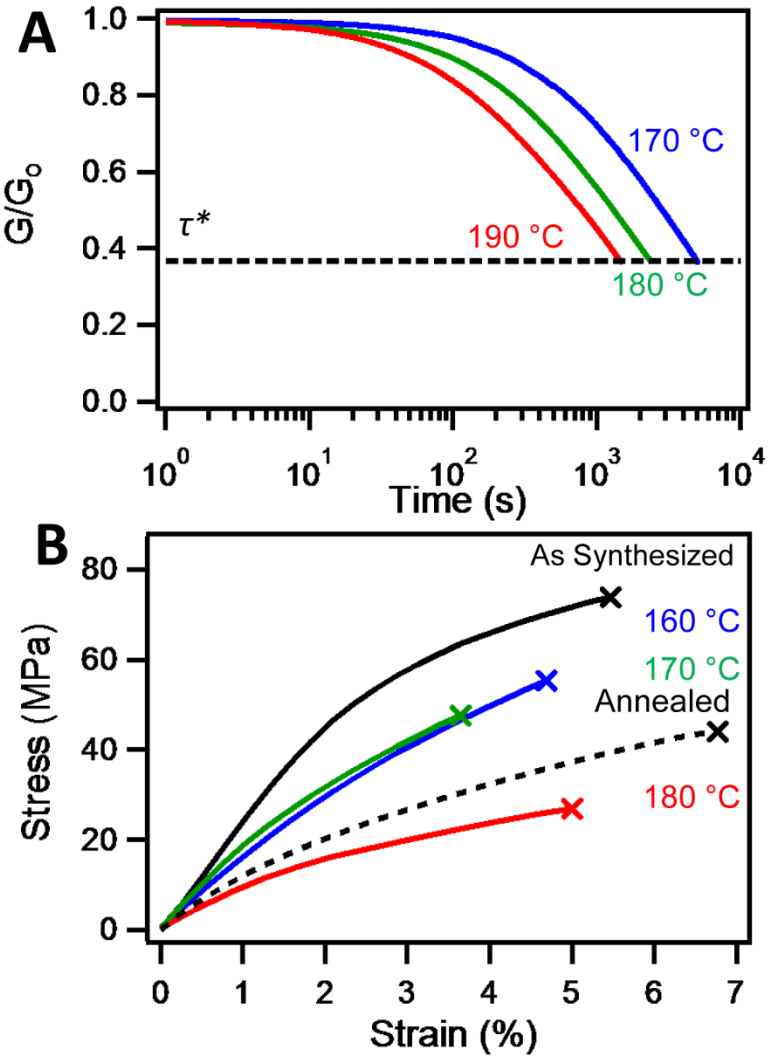

Figure 2.2. A. Normalized stress relaxation analysis performed on **4** at elevated temperature. The dashed-black line represents where $G/G_0 = e^{-1}$, defined as the characteristic relaxation time, τ^*. B. Representative tensile tests of the as-synthesized (black) **4**, samples reprocessed (See Figure 2.1B) for $3\tau^*$ at 160 °C (blue), 170 °C (green), and 180 °C (red) and 4 MPa pressure, and an as-synthesized sample annealed for $3\tau^*$ at 160 °C (dashed black).

The dynamic properties of **4** were characterized using tensile stress relaxation analysis (SRA) at elevated temperatures in the linear viscoelastic regime (Figure 2.2A). Samples were thermally equilibrated, subjected to a controlled strain of 5%, and the characteristic relaxation lifetime ($\tau^* = G/G_0 = e^{-1}$) was measured. SRA was performed

at 170, 180 and 190 °C and was reproducible. The topology freezing transition temperature (T_v), at which viscosity (η) crosses the traditionally defined solid-to-liquid transition of 10^{12} Pa·s,[31] was 111 °C (see Appendix); below T_v **4** behaves as a traditional thermoset. FT-IR spectra recorded after SRA performed at each temperature were unchanged relative to those of the as-synthesized networks, suggesting no significant change in the network functionality (Figures S2.8) and indicated the stability of **4** to the reprocessing conditions and stress relaxation through degenerate carbamate exchange reactions.

Uniaxial tensile testing was performed on both pristine and recycled dogbone samples to characterize the mechanical properties and reprocessibility of polymer **4**. The process of repairing and reshaping broken samples by compression molding was optimized with respect to reprocessing temperature and time. Reprocessing performed at 160 °C for 3τ* (*ca*. 8 h; Figure 2.1B) provided the maximum recovery of tensile properties relative to a tensile bar prepared directly from the polymerization (Figure 2B), with E = 1.6 ± 0.2 GPa (76% recovery), ε_b = 4.8 ± 0.8% (69% recovery), and σ_b = 53 ± 8 MPa (74% recovery). We attribute the incomplete recovery of the tensile properties to minor decomposition in the network that occurs slowly at elevated temperature over long times, as evidenced by the discoloration of the materials and TGA isotherms showing modest mass loss (ca. 7% over 5 h at 190 °C, Figure S2.5). Furthermore, tensile bars prepared directly from the polymerization that were heated to 160 °C for 3τ* prior to the analysis exhibited similarly reduced tensile properties as the recycled samples (Figure 2.2B, Table S2.2), suggesting that the bond-formation process is efficient but that the polymers also undergo slight decomposition. Consistent with the

FT-IR analysis after the SRA experiments (Figure S2.8), FT-IR spectra of reprocessed samples are identical to those of as-synthesized samples, corroborating isodesmic carbamate exchange reactions being responsible for stress relaxation. A similar T_g and an 80% recovery of the plateau modulus were observed by DMTA after reprocessing (Figure S2.6), further indicating that the dynamic bonds preserve the cross-linking density and mechanical properties of **4**.

The temperature dependence of the SRA experiments (Figure 2.2A) indicates that the PHU network **4** undergoes more rapid transcarbamoylation than model compounds under similar conditions. The temperature dependence of τ^* for **4** was fit to an Arrhenius relationship to determine the apparent activation energy (E_a, Figure 2.3A) of 111 ± 10 kJ/mol, which is significantly lower than that of uncatalyzed transcarbamoylation observed in model compound **6** (148 ± 7 kJ/mol, Figures S2.10, S2.11) and similar to the lowest reported values of catalyzed transcarbamoylation in traditional urethanes [$Bi(OTf)_3$, E_a = 112 ± 9 kJ/mol].[32] We hypothesize that this phenomenon arises from the mechanical activation of the transcarbamoylation reaction, as model hydroxyurethane **6** shows relatively little transcarbamoylation and no significant side reactions, in the presence of excess alcohol at similar temperatures and timescales (Figure S2.10). Previous vitrimers have shown consistent E_a values between their stress relaxation behavior and their catalyzed exchange reactions,[1,6] with the notable exception of another urethane-containing material.[15] Therefore, we probed the mechanism of stress relaxation in PHUs further, both to confirm an associative process and to understand why it occurs more readily within the polymer networks.

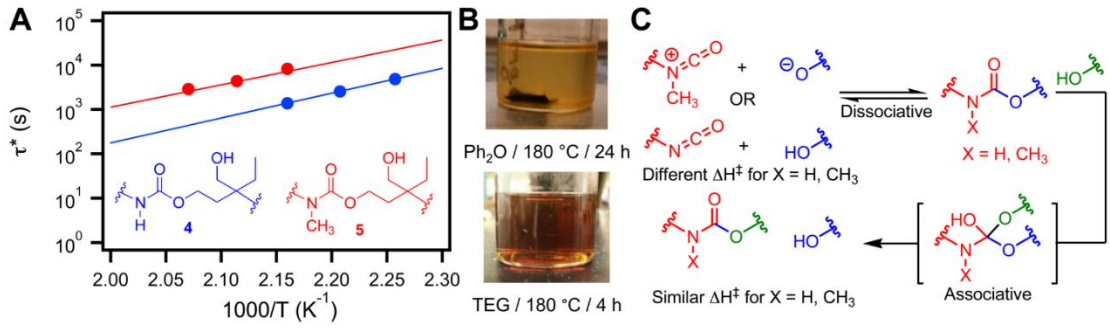

Figure 2.3. A. An Arrhenius plot for the thermal activation of stress relaxation in **4** (blue) and **5** (red) is consistent with vitrimeric behavior. B. Swelling in Ph_2O (180 °C, 24 h, top) does not dissolve **4**, but **4** fully dissolves in tetraethylene glycol after 4 h (bottom). C. The similar activation energies for the stress relaxation **4** and **5** are suggestive of an associative transcarbamoylation mechanism.

The decomposition of carbamates to isocyanates and alcohols, the most likely dissociative stress relaxation mechanism, generally occurs at much higher temperatures than those at which **4** exhibits rapid stress relaxation, particularly for urethanes derived from aliphatic isocyanates (>250 °C).[33] Swell tests of **4** in Ph_2O (180 °C, 24 h, Figure 2.3B) showed no evidence of dissolution, consistent with associative exchange in the presence of an unreactive solvent.[34] On the other hand, the network dissolved completely in the reactive tetraethylene glycol (TEG) within 4 h under identical conditions, consistent with transcarbamoylation being the dominant exchange mechanism. Stress relaxation experiments performed on **5**, which is linked by *N*-methyl urethanes incapable of forming neutral isocyanates (Figure 2.3C), exhibited similar E_a (101 ± 7 kJ/mol) for stress relaxation as **4**. These experiments cast doubt that the reversion of carbamates to isocyanates is significant under the stress relaxation conditions and demonstrate that alcohols significantly contribute to the stress relaxation. Stress relaxation rates of **5** were significantly slower than **4**, indicating a difference in

pre-exponential factor which may be associated with steric effects related to nucleophilic addition to the methyl-substituted carbamate. The absence of isocyanate or isocyanurate peaks in the FT-IR spectra of both **4** and **5** (Figures S2.8, S2.9) after SRA is consistent with negligible isocyanate formation. To further support an associatve mechanism of reprocessing, the reprocessibility of the polymer was characterized after the hydroxyl groups of ground polymer **4** were acetylated (Scheme S2.6, Figure S2.12). The acetylated polymers showed only a ca. 10 % recovery of mechanical properties, indicating the necessity of free hydroxyl groups for efficient reprocessing (Figure S2.13); we attribute the partial recovery observed to incomplete acetylation of the free hydroxyl groups. These combined observations suggest that PHU stress relaxation and reprocessing occurs primarily through associative transcarbamoylation reactions, which is a key feature for accessing the desirable toughness, malleability, and creep resistance associated with vitrimers.

The discrepancy in activation energy between PHU stress relaxation and model compound transcarbamoylation, along with dissociative exchange processes appearing to be inoperative, suggests that transcarbamoylation reactions are mechanically activated. Thermoplastic PUs previously exhibited decreased molar mass and increased dispersity when subjected to mechanical strain at high temperatures.[35] These changes were attributed to the breaking of urethane bonds, whose rate increases with increased polymer size, a common trait of mechanically activated reactions in polymeric systems.[36] We propose that transcarbamoylation is accelerated when mechanical strain causes the lone pair of the nitrogen atom to twist out of conjugation from the carbonyl π-electron system, thereby rendering the carbamate more susceptible to nucleophilic

attack by hydroxyl groups in the network. The resulting orthocarbamate intermediate is most likely to reform the carbamate by expelling the alkoxy group so as to relieve the most stress.

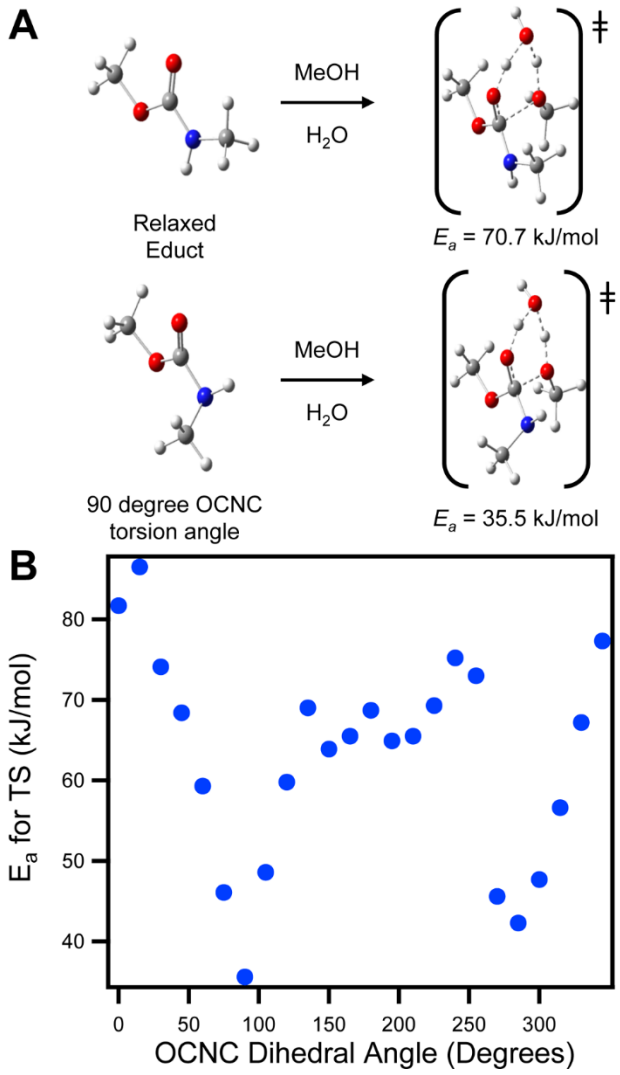

Figure 2.4. A. DFT calculated structures for *N*,*O*-dimethylcarbamate with their corresponding transition state (TS) structures for water-catalyzed transcarbamoylation with methanol (above); H, C, N, and O atoms are shown as white, gray, blue, and red, respectively. B. The vertical E_a to reach a constrained TS from a constrained educt as a function of the O=C(OCH$_3$)N(H)CH$_3$ dihedral angle.

To assess this hypothesis, DFT calculations were undertaken at the M06-2X/6-311+G(d,p) level of theory (see Appendix) to predict E_a values for the water catalyzed reaction of MeOH with *N*,*O*-dimethyl carbamate to generate the product orthocarbamate. To address the potential influence of torsional strain, the energies of possible reactant and transition-state (TS) structures were computed for fixed OCNC dihedral angles of O=C(OCH_3)N(H)CH_3. Interestingly, the E_a values associated with many torsionally strained educt and TS structures, where the torsion was assumed to be attained through mechanical activation, were predicted to be much lower than for the analogous fully relaxed reaction (Figure 2.4). In particular, compared to the adiabatic E_a of 70.7 kJ/mol that is predicted for fully relaxed structures in this model reaction, at an OCNC torsion angle of 90 degrees, the E_a is predicted to drop to 35.5 kJ/mol (Figure 2.4; see Figure S2.20 for the full torsional coordinate). This reduction is quite similar to the difference in E_a observed for the stress relaxation of **4** and transcarbamoylation processes of the model system. Importantly, computed TS-structure energies for water-catalyzed reversion of *N*,*O*-dimethyl carbamate were found to increase greatly due to torsional strain when compared with the educt, further consistent with the conclusion that isocyanate formation is not responsible for strain relief in the present system.

2.4 Conclusion

In conclusion, we have demonstrated that cross-linked PHUs derived from six-membered cyclic carbonates and amines display vitrimeric behavior in the absence of an embedded catalyst typically incorporated into such networks. Furthermore, we have posited that transcarbamoylation is the principal relaxation mechanism in PHU

networks. These materials display mechanical properties competitive with traditional PU thermosets, yet enable reshaping and repair that will enhance their long-term utility. Moreover, these networks are prepared from readily accessible and general monomer classes, which will facilitate the full exploration and tuning of their properties. We will continue to develop both sustainably derived, reconfigurable thermosets with outstanding properties, and an improved understanding of their stress relaxation processes.

References

(1) Montarnal, D.; Capelot, M.; Tournilhac, F.; Leibler, L. *Science* **2011**, *334*, 965.

(2) Denissen, W.; Winne, J. M.; Du Prez, F. E. *Chem. Sci.* **2016**, *7*, 30.

(3) Chen, X.; Dam, M.; Kanji, O.; Mal, A.; Shen, H.; Nutt, S.; Sheran, K.; Wudl, F. *Science* **2002**, *295*, 1698.

(4) Pepels, M.; Filot, I.; Klumperman, B.; Goossens, H. *Polym. Chem.* **2013**, *4*, 4955.

(5) Obadia, M. M.; Mudraboyina, B. P.; Serghei, A.; Montarnal, D.; Drockenmuller, E. *J. Am. Chem. Soc.* **2015**, *137*, 6078.

(6) Denissen, W.; Rivero, G.; Nicolaÿ, R.; Leibler, L.; Winne, J. M.; Du Prez, F. E. *Adv. Funct. Mater.* **2015**, *25*, 2451.

(7) Ying, H.; Zhang, Y.; Cheng, J. *Nat. Commun.* **2014**, *5*, 3218.

(8) Zheng, P.; McCarthy, T. J. *J. Am. Chem. Soc.* **2012**, *134*, 2024.

(9) Cromwell, O. R.; Chung, J.; Guan, Z. *J. Am. Chem. Soc.* **2015**, *137*, 6492.

(10) Taynton, P.; Yu, K.; Shoemaker, R. K.; Jin, Y.; Qi, H. J.; Zhang, W. *Adv. Mater.* **2014**, *26*, 3938.

(11) Capelot, M.; Montarnal, D.; Tournilhac, F.; Leibler, L. *J. Am. Chem. Soc.* **2012**, *134*, 7664.

(12) Capelot, M.; Unterlass, M. M.; Tournilhac, F.; Leibler, L. *ACS Macro Lett.* **2012**, *1*, 789.

(13) Yang, Y.; Pei, Z.; Zhang, X.; Tao, L.; Wei, Y.; Ji, Y. *Chem. Sci.* **2014**, *5*, 3486.

(14) Pei, Z.; Yang, Y.; Chen, Q.; Terentjev, E. M.; Wei, Y.; Ji, Y. *Nat. Mater.* **2013**, *13*, 36.

(15) Brutman, J. P.; Delgado, P. A.; Hillmyer, M. A. *ACS Macro Lett.* **2014**, *3*, 607.

(16) Altuna, F. I.; Pettarin, V.; Williams, R. J. J. *Green Chem.* **2013**, *15*, 3360.

(17) Lu, Y.-X.; Tournilhac, F.; Leibler, L.; Guan, Z. *J. Am. Chem. Soc.* **2012**, *134*, 8424.

(18) Lu, Y.-X.; Guan, Z. *J. Am. Chem. Soc.* **2012**, *134*, 14226.

(19) Lin, Y.; Li, G. *J. Mater. Chem. B* **2014**, *2*, 6878.

(20) Chen, S.; Mo, F.; Yang, Y.; Stadler, F. J.; Chen, S.; Yang, H.; Ge, Z. *J. Mater. Chem. A* **2015**, *3*, 2924.

(21) Du, P.; Wu, M.; Liu, X.; Zheng, Z.; Wang, X.; Joncheray, T.; Zhang, Y. *J. Appl. Polym. Sci.* **2014**, *131*, 40234.

(22) Huang, L.; Yi, N.; Wu, Y.; Zhang, Y.; Zhang, Q.; Huang, Y.; Ma, Y.; Chen, Y. *Adv. Mater.* **2013**, *25*, 2224.

(23) Ling, J.; Rong, M. Z.; Zhang, M. Q. *Polymer* **2012**, *53*, 2691.

(24) Zhong, Y.; Wang, X.; Zheng, Z.; Du, P. *J. Appl. Polym. Sci.* **2015**, *132*, 41944.

(25) Heo, Y.; Sodano, H. A. *Adv. Funct. Mater.* **2014**, *24*, 5261.

(26) Yang, Y.; Urban, M. W. *Angew. Chem. Int. Ed.* **2014**, *53*, 12142.

(27) Offenbach, J.; Tobolsky, A. *J. Colloid Sci.* **1956**, *11*, 39.

(28) Colodny, P.; Tobolsky, A. *J. Am. Chem. Soc.* **1957**, *79*, 4320.

(29) Nohra, B.; Candy, L.; Blanco, J.-F.; Guerin, C.; Raoul, Y.; Mouloungui, Z. *Macromolecules* **2013**, *46*, 3771.

(30) Blattmann, H.; Fleischer, M.; Bähr, M.; Mülhaupt, R. *Macromol. Rapid Commun.* **2014**, *35*, 1238.

(31) Dyre, J. C. *Rev. Mod. Phys.* **2006**, *78*, 953.

(32) Jousseaume, B.; Laporte, C.; Toupance, T.; Bernard, J.-M. *Tetrahedron Lett.* **2002**, *43*, 6305.

(33) Yang, W; Macosko, C. W.; Wellinghoff, S. *Polymer* **1986**, *27*, 1235.

(34) Zhang, Y.; Broekhuis, A. A.; Picchioni, F. *Macromolecules* **2009**, *42*, 1906.

(35) Endres, W.; Lechner, M.; Steinberger, R. *Macromol. Mater. Eng.* **2003**, *288*, 525.

(36) Caruso, M. M.; Davis, D. A.; Shen, Q.; Odom, S. A.; Sottos, N. R.; White, S. R.; Moore, J. S. *Chem. Rev.* **2009**, *109*, 5755.

CHAPTER TWO APPENDIX

Table of Contents

A. Materials. All reagents were purchased from Sigma-Aldrich. Tris(2-aminoethyl)amine (**2**) and tris[2-(methylamino)ethyl]amine (**3**) were stirred over CaH_2 and distilled prior to use; all other reagents were used without further purification. Dichloromethane (DCM), triethylamine (Et_3N), and tetrahydrofuran (THF) were purchased from commercial sources and purified using a custom-built alumina-column based solvent purification system. Other solvents were purchased from commercial sources and used without further purification.

Instrumentation. Infrared spectra were recorded on a Thermo Nicolet iS10 or a Bruker Alpha Platinum; both were equipped with a diamond ATR attachment and spectra were uncorrected.

Gas chromatography was performed on an Agilent 6890N Network GC System with a flame ionization detector. Concentrations were determined from a linear calibration of peak area to concentration relative to di-*tert*-butylbiphenyl as an internal standard.

NMR spectra were recorded on a Varian 400 MHz, a Varian 500 MHz or a Bruker ARX 300 MHz spectrometer using a standard $^1H/X$ Z-PFG probe at ambient temperature with a 20 Hz sample spin rate.

Thermogravimetric analysis (TGA) was performed on a TA Instruments Q500 Thermogravimetric Analyzer. Samples were heated under a nitrogen atmosphere at a rate of 10 °C/min from 25 ºC to 600 ºC. Isotherms were taken by heating samples under nitrogen to the desired temperature at a rate of 20 ºC/min, then maintaining constant temperature for five hours.

Differential scanning calorimetry (DSC) was performed on a TA instruments Q1000 Differential Scanning Calorimeter. Samples were heated at a rate of 10 °C/min to 175

°C to erase thermal history, cooled to -190 °C at 10 °C/min, and then heated to 175 °C at 10 °C/min. All data shown are taken from the second heating ramp.

Dynamic mechanical thermal analysis (DMTA) was performed on a TA Instruments RSA-G2 analyzer (New Castle, DE) utilizing dog bone shaped tensile bars (*ca.* 0.5 mm (T) × 3 mm (W) × 25 mm (L) and a gauge length of 16 mm). The axial force was adjusted to 0 N and a strain adjust of 30% was set with a minimum strain of 0.05%, a maximum strain of 5%, and a maximum force of 1 N in order to prevent the sample from buckling or going out of the specified strain. Furthermore, a force tracking mode was set such that the axial force was twice the magnitude of the oscillation force. A temperature ramp was then performed from 30 °C to 200 °C at a rate of 5 °C/min, with an oscillating strain of 0.05% and an angular frequency of 6.28 rad s^{-1} (1 Hz). The T_g was calculated from the maximum value of the loss modulus (G"). Estimated cross-linking density was determined as in the literature.[1]

Uniaxial tensile testing was conducted using dog bone shaped tensile bars (*ca.* 0.5 mm (T) × 3 mm (W) × 25 mm (L) and a gauge length of 16 mm). The samples were aged for at least 48 h at 25 °C in a desiccator prior to testing. Tensile measurements were performed on a Shimadzu Autograph AGS-X Series tensile tester (Columbia, MD) at 22 °C with a uniaxial extension rate of 5 mm/min. Young's modulus (*E*) values were calculated using the Trapezium software by taking the slope of the stress-strain curve from 0 to 1 N of force applied. Reported values are the average and standard deviations of at least five samples.

Stress relaxation analysis (SRA) was performed on a TA Instruments RSA-G2 analyzer (New Castle, DE) utilizing rectangular films (*ca.* 0.5 mm (T) × 5 mm (W) ×

10 mm (L)) or dog bone shaped tensile bars (*ca.* 0.5 mm (T) × 3 mm (W) × 25 mm (L) and a gauge length of 16 mm). The SRA experiments were performed in a strain control at specified temperature (150-210 °C). The samples were allowed to equilibrate at this temperature for approximately 10 minutes, after which the axial force was then adjusted to 0 N with a sensitivity of 0.05 N. Subsequently, each sample was subjected to an instantaneous 5% strain. The stress decay was monitored, while maintaining a constant strain (5%), until the stress relaxation modulus had relaxed to at least 37% (1/e) of its initial value. This was performed three times for each sample. The activation energy (E_a) and freezing transition temperature (T_v) were determined utilizing the methodology in literature.[1,2]

In order to reprocess the materials, the polymer was ground in an electric coffee grinder and then placed into a dog bone shaped mold (*ca.* 0.5 mm (T) × 3 mm (W) × 25 mm (L) and a gauge length of 16 mm) between two thin Teflon® sheets. This assembly was placed in a Wabash-MPI compression mold (Wabash, IN), which was preheated to the desired temperature. The material was allowed to thermally equilibrate for two minutes, following a two minute period of rapidly increasing the pressure to 4 MPa then reducing back to 0 MPa in order to remove air bubbles. The pressure was then increased to 4 MPa and allowed to heat for varying periods of time and then rapidly cooled to room temperature over the course of 5 minutes using the water cooling function of the compression mold. The resulting tensile bars were then allowed to age for 48 h in a desiccator and subjected to uniaxial tensile testing in order to determine their recovery in mechanical properties. Reported values are the average and standard deviations of at least five samples.

B. Synthetic Procedures

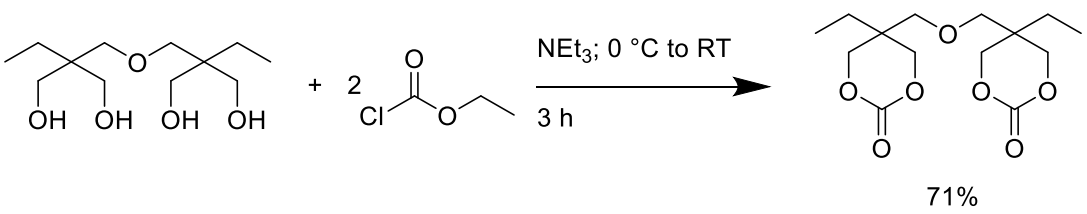

Synthesis of 1: To a flame-dried round-bottom flask under nitrogen atmosphere was added di(trimethylol)propane (10.0 g, 40 mmol) and 250 mL anhydrous THF. To the suspension was added ethyl chloroformate (25.2 g, 232 mmol) under stirring. The mixture was cooled to 0°C, triethylamine (24.6 g, 242 mmol) was added dropwise, and a white precipitate began to form. The mixture was warmed to room temperature and allowed to stir for 3 hours. The solid was removed via filtration, and solvent was removed at reduced pressure to yield a white solid. The solid was recrystallized from THF to obtain compound **1** as a white solid (8.6 g, 71%). ^{1}H NMR (400 MHz, $CDCl_3$) δ 4.29 (d, *J* = 10.1 Hz, 4H, -C*H*$_2$OCOOC*H*$_2$-), 4.17 (d, *J* = 10.5 Hz, 4H, -C*H*$_2$OCOOC*H*$_2$-), 3.50 (s, 4H, -C*H*$_2$OC*H*$_2$-), 1.50 (q, *J* = 7.5 Hz, 4H, -CH_3C*H*$_2$C-), 0.91 (t, *J* = 7.6 Hz, 6H, C*H*$_3$$CH_2$C-).^{13}C NMR (75 MHz, $CDCl_3$) δ 148.32 (-O*C*OO-), 72.76 (-O*C*H_2O*C*H_2O-), 70.71 (-*C*H_2O*C*H_2-), 35.36 (-[CH_2]$_2$*C*[CH_2]-), 23.55 (CH_3*C*H_2-), 7.34 (*C*$H_3$$CH_2$). IR (solid, ATR) 2972, 2918, 2881, 1732 (C=O stretch), 1463, 1412, 1165, 1106, 762 cm^{-1}. The ^{1}H and ^{13}C NMR spectra match those previously reported in the literature.[3]

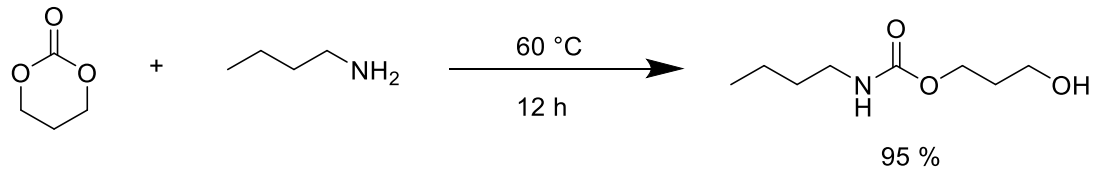

Synthesis of 6: To a vial was added solid trimethylene carbonate (1.286 g, 12.6 mmol); the vial was heated to 60 °C, resulting in a clear melt. Butylamine (920 mg, 12.6 mmol) was added via syringe, and the mixture was heated at 60 °C for 12 hours. The resulting oil was chromatographed on silica gel in ethyl acetate to yield compound **6** as a colorless oil (2.09 g, 95%). ^{1}H NMR (400 MHz, $CDCl_3$) δ 4.71 (br s, 1H, -N*H*-), 4.24 (t, *J* = 5.8 Hz, 2H, -C*H*$_2$O), 3.70-3.63 (m, 2H, -C*H*$_2$OH), 3.21-3.12 (m, 2H, -CH_2C*H*$_2$NH), 2.86 (br s, 1H, -O*H*), 1.85 (quintet, *J* = 6.1 Hz, 2H, -CH_2C*H*$_2$$CH_2$OH), 1.52-1.42 (m, 2H, -$CH_2$C*H*$_2$$CH_2$NH-), 1.41-1.25 (m, 2H, -CH_2C*H*$_2$$CH_3$), 0.93 (t, *J* = 7.3 Hz, 3H, -CH_2C*H*$_3$). ^{13}C NMR (100 MHz, $CDCl_3$) δ 157.2, 61.5, 58.7, 40.7, 32.2, 31.9, 19.8, 13.6. IR (liquid, ATR) 3324, 2958, 2932, 2874, 1690 (C=O stretch), 1538 (N-H deformation), 1248, 1053 HRMS (ESI) calcd. for $[C_8H_{17}NO_3+Na]^+$ 198.11006, found 198.10956.

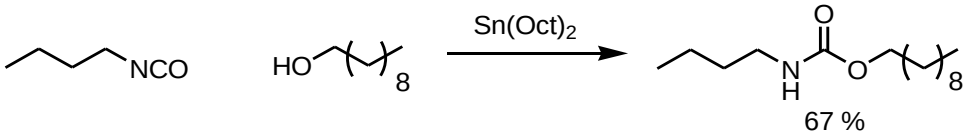

Synthesis of 7: In a flame-dried round-bottom flask under nitrogen atmosphere, *n*-butylisocyanate (436 mg, 4.4 mmol) was dissolved in 5.0 ml anhydrous THF. Decanol (633 mg, 4.0 mmol) was added via syringe, followed by a solution of tin (II) octoate (32 mg, 2 mol %) in 0.2 ml anhydrous THF. The solution was allowed to stir at room temperature for 48 hours and solvent was removed at reduced pressure. The residue was chromatographed on silica gel in 20% EtOAc/Hexanes to yield **7** as a white solid (690 mg, 67%). ^{1}H-NMR (300 MHz, $CDCl_3$) δ 4.59 (br s, 1H, -N*H*-), 4.03 (t, *J* = 6.7 Hz, 2H,

-OCH_2-), 3.21-3.11 (m, 2H, -NHCH_2-), 1.66-1.22 (m, 20H), 0.96-0.84 (m, 6H) ^{13}C-NMR (75 MHz, $CDCl_3$) δ 156.8, 64.8, 40.6, 32.0, 31.8, 29.5 (2C), 29.2 (2C), 29.0, 25.7, 22.6, 19.8, 14.0, 13.6 IR (solid, ATR) 3318 (N-H stretch), 2957, 2917, 2849, 1688 (C=O stretch), 1538 (N-H deformation), 1468, 1250, 1147, 1029, 1013 HRMS (DART) calcd. for $[C_{15}H_{31}NO_2+H]^+$ 258.24276, found 258.24355

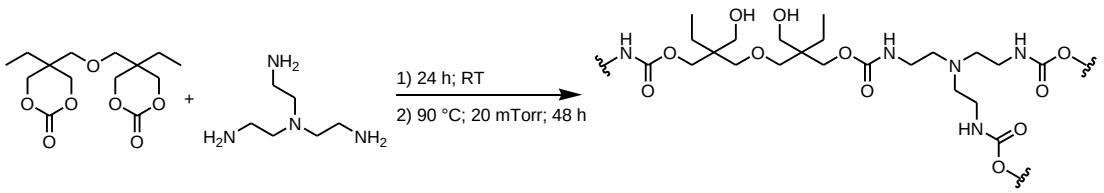

Synthesis of 4: 1 (798.0 mg, 2.639 mmol, 1 eq. cyclic carbonate) was dissolved in a minimal amount of anhydrous DCM (*ca.* 2.5 mL) along with tris(2-aminoethyl)amine **2** (257.3 mg, 1.760 mmol, 1 eq. amine to cyclic carbonate). Solutions were sonicated for one minute to ensure homogeneity, then poured into an aluminum mould (60 mm D x 10 mm H), and allowed to stand at room temperature for *ca*. 24 hours. Samples were cut from the resulting films, and placed under reduced pressure at 90 °C and 20 mTorr for *ca*. 48 hours to ensure complete cross-linking and removal of solvent. Swell tests were performed on the resulting materials in THF and a gel fraction of greater than 0.98 was found in all cases. IR (solid, ATR) 3297, 2962, 2880, 1689 (C=O stretch), 1527 (N-H deformation), 1460, 1257, 1105, 1020 cm^{-1}. See Table S1 and S2 for mechanical and tensile properties.

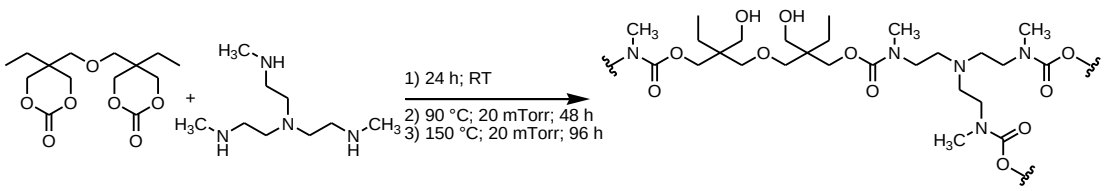

Synthesis of 5: 1 (733 mg, 1 eq. cyclic carbonate) was dissolved in a minimal amount of anhydrous DCM (*ca*. 2.5 mL) along with tris[2-(methylamino)ethyl]amine **3** (304.5 mg, 1 eq. amine to cyclic carbonate). Solutions were sonicated for one minute to ensure homogeneity. The solutions were poured into an aluminum mould (60 mm D x 10 mm H), and allowed to stand at room temperature for *ca*. 48 hours. Samples were cut from the resulting films, and placed under reduced pressure at 90 °C and 20 mtorr for *ca*. 48 hours; due to the lower reactivity of the secondary amines, the materials were post-cured for 96 hours at 150 °C and 20 mTorr to drive the reaction to higher conversion. IR (solid, ATR) 3427, 2931, 2879, 1677 (C=O stretch), 1459, 1402, 1186, 1111, 1039 cm^{-1}.

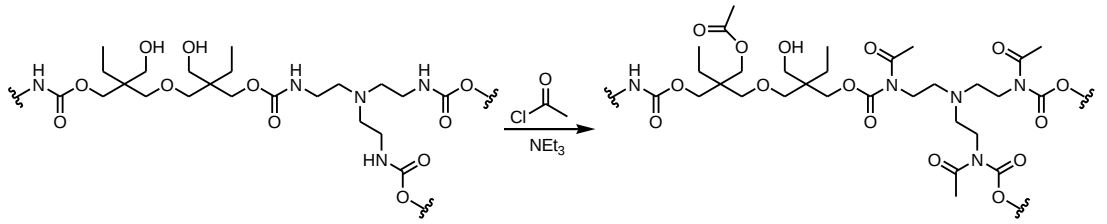

Synthesis of 8: **4** was repeatedly ground in a burr coffee grinder and sifted until a fine powder was obtained. The fine powder of **4** (1.0 g, 5.0 mmol hydroxyl, 1 eq. hydroxyl) was then placed in a 250 mL round-bottom flask along with acetyl chloride (7.13 mL, 20 eq. to hydroxyl) and 100 mL of anhydrous THF. The heterogenous mixture was cooled to 0 °C and triethylamine (13.9 mL, 20 eq. to hydroxyl) was added dropwise over 20 min while stirring and a white precipitate began to form. The mixture rapidly heated to 35 °C and then cooled to room temperature. It was allowed to stir for 24 h

after which the solid was collected by filtration and rinsed with distilled water until the salts were removed. The remaining solid was further rinsed with an excess of acetone, then toluene and dried for 48 h under high vacuum (*ca.* 50 mTorr) yielding a yellow-orange solid (1.2 g). IR spectroscopy indicated full surface acetylation of –OH groups, as well as acetylation of urethane –NH groups; the obtained yield is indicative that functionalization is not quantitative due to limited swelling of the densely-cross-linked network. The product structure in Scheme S7, therefore, is a representative structure of the obtained polymer. IR (solid, ATR) 2962, 2886, 1732 (acetyl C=O stretch), 1698 (urethane C=O stretch), 1682 (N-acetylated urethane C=O stretch), 1525 (N-H deformation, weak), 1462, 1366, 1227, 1158, 1111, 1034, 975, 771 cm^{-1}.

C. Characterization Tables and Figures

Table S2.1: Material properties of polyhydroxyurethane **4**.

Polymer	Gel %	T_d (°C; 5%)	T_g (°C; DSC)	T_g (°C; DMTA)	E' at 100 °C (MPa)	E_a (kJ/mol)	T_v (°C)
4	99	263	54	61	7.5	110 ± 10	111

Table S2.2: Tensile properties of polyhydroxyurethane **4** before and after reprocessing at various temperatures, and attempted reprocessing of acetylated polyhydroxyurethane **8**.

		As Synthesized		
		σ_b (MPa)	ε_b (%)	E (GPa)
		72.1 ± 11.1	6.93 ± 3.78	2.17 ± 0.37
		After Reprocessing, Polymer 4		
Reprocessing Temp. (°C)	Reprocessing Time (min)	σ_b (MPa)	ε_b (%)	E (GPa)
160	**480**	53.1 ± 8.1	4.79 ± 0.79	1.64 ± 0.19
170	**320**	43.1 ± 3.3	7.29 ± 1.04	1.38 ± 0.17
170	**240**	46.1 ± 5.6	4.10 ± 1.41	1.93 ± 0.14
170	**160**	35.0 ± 9.9	4.74 ± 2.74	1.48 ± 0.98
180	**120**	26.6 ± 3.7	4.79 ± 1.72	1.10 ± 0.24
		After Reprocessing, Acetylated Polymer 8		
160	**480**	3.2 ± 0.9	6.90 ± 2.21	0.17 ± 0.12

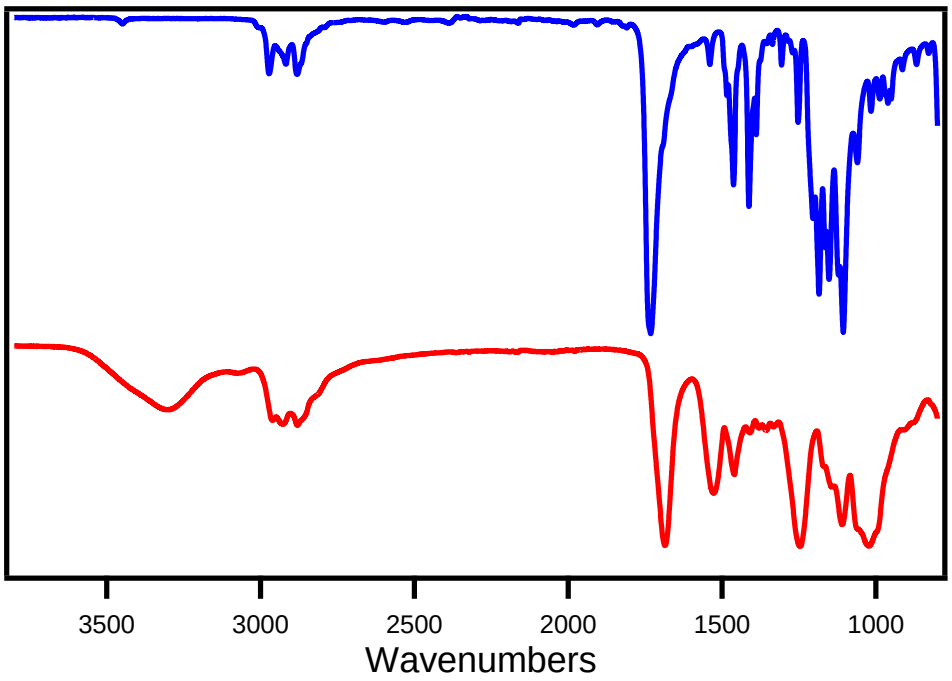

Figure S2.1. FT-IR spectra of monomer **1** (blue) and polymer **4** (red).

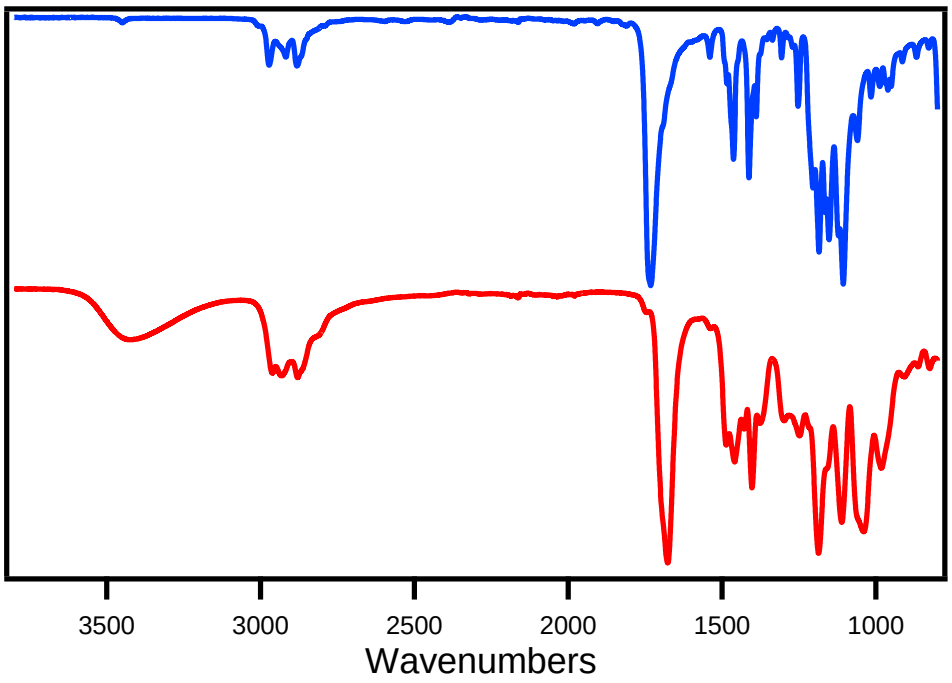

Figure S2.2. FT-IR spectra of monomer **1** (blue) and polymer **5** (red).

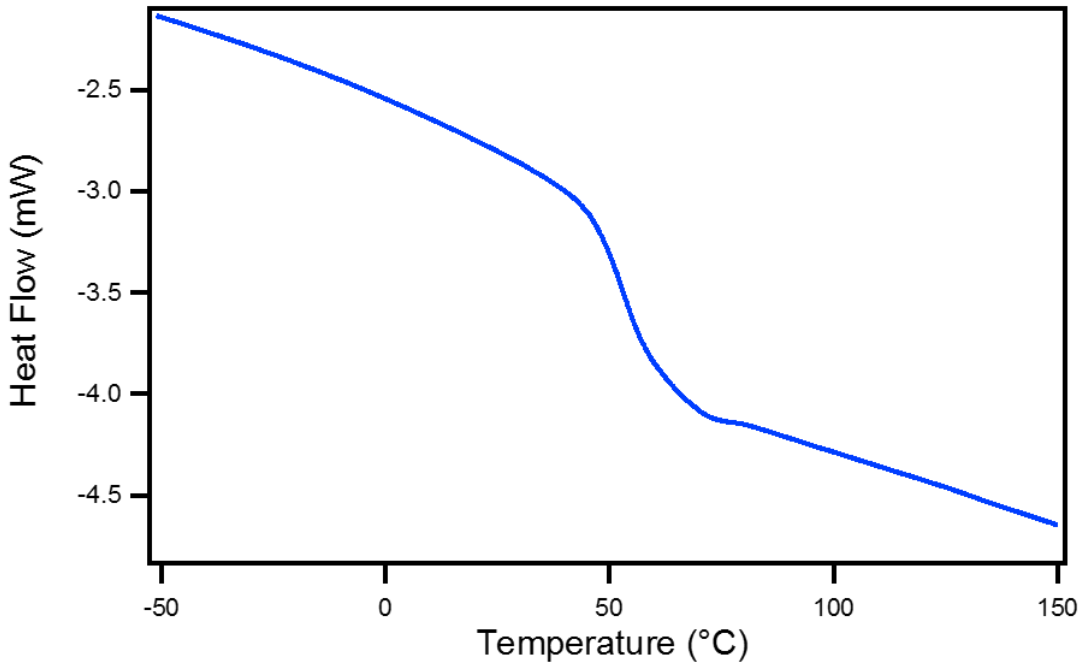

Figure S2.3. Differential scanning calorimetry of polymer **4** performed at a heating rate of 10 °C/min.

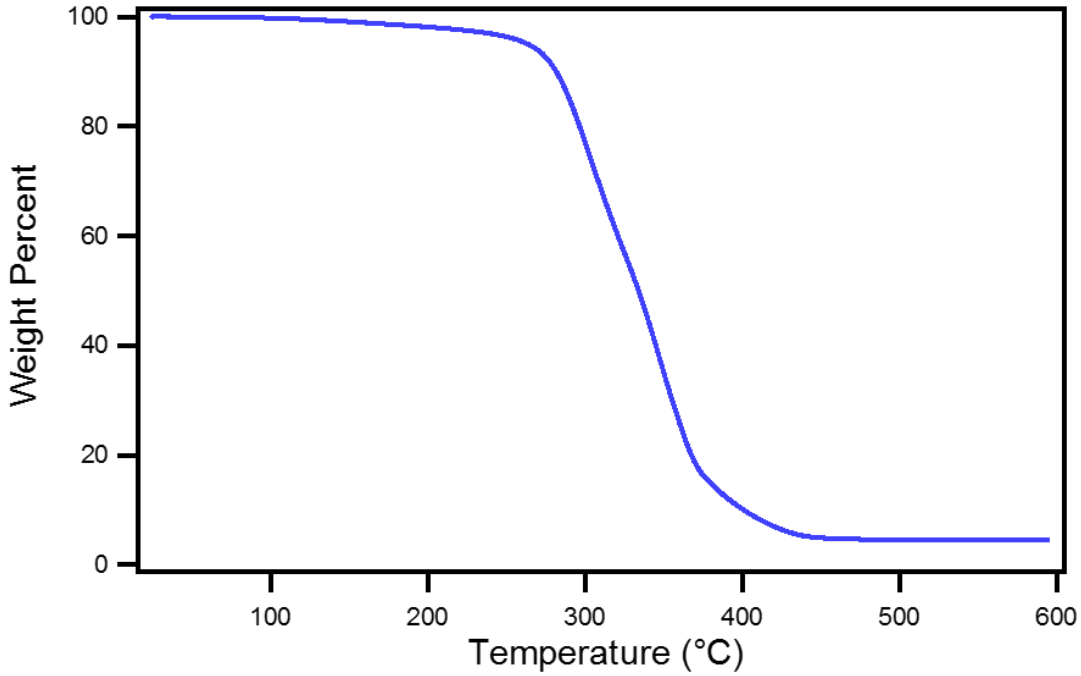

Figure S2.4. Thermogravimetric analysis of polymer **4** performed at a heating rate of 10 °C/min under nitrogen atmosphere.

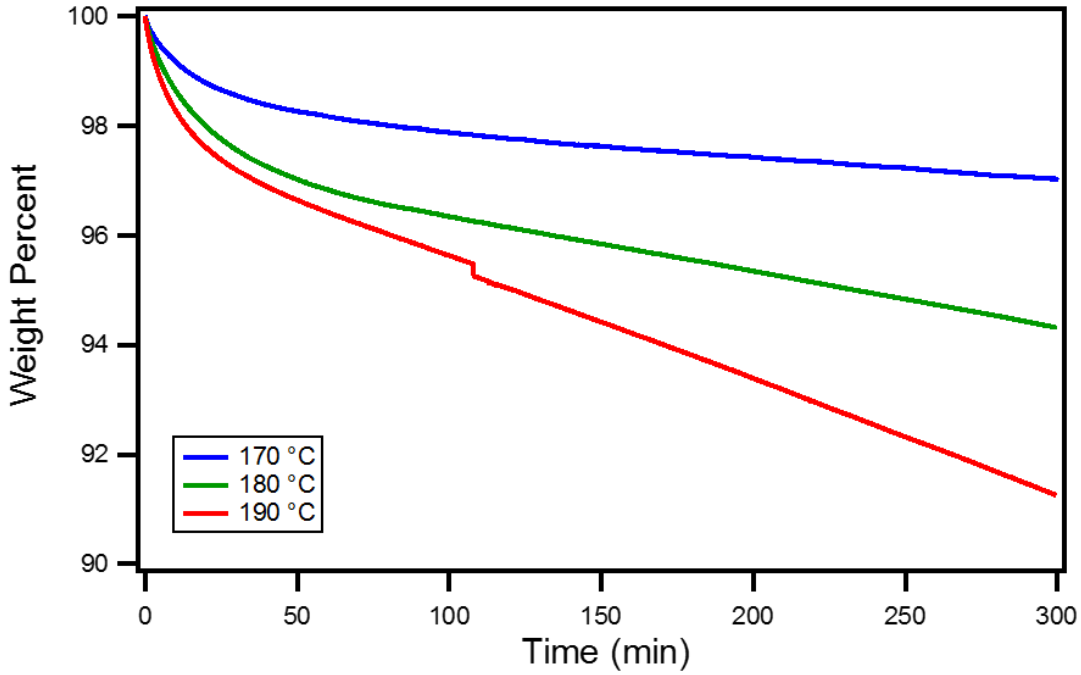

Figure S2.5. Thermogravimetric analysis isotherms of polymer **4** under nitrogen atmosphere.

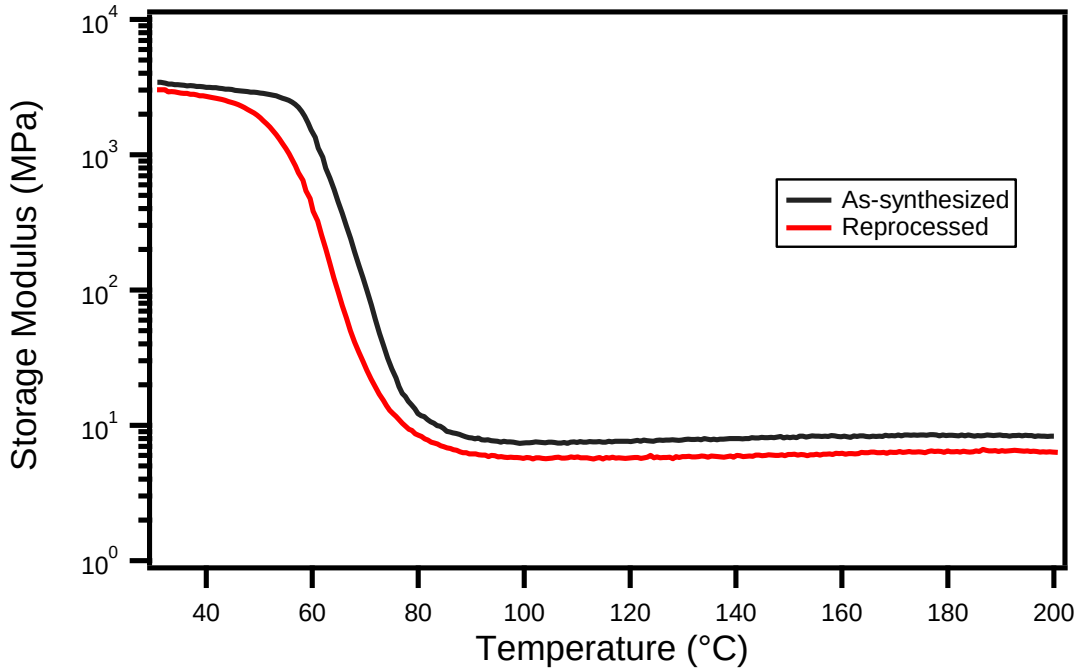

Figure S2.6. Dynamic mechanical analysis of polymer **4** before and after reprocessing (160 ºC, 480 min) from 30 to 200 °C at 1 Hz, 0.05% oscillating strain, at a heating rate of 5 °C/min.

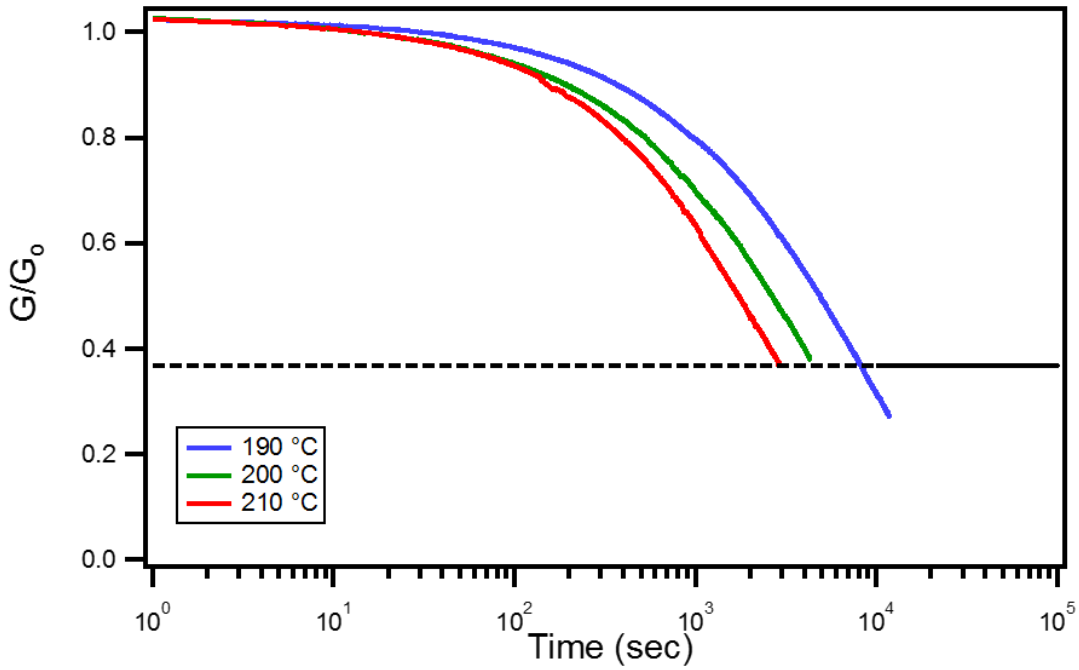

Figure S2.7. Stress relaxation analysis of polymer **5**.

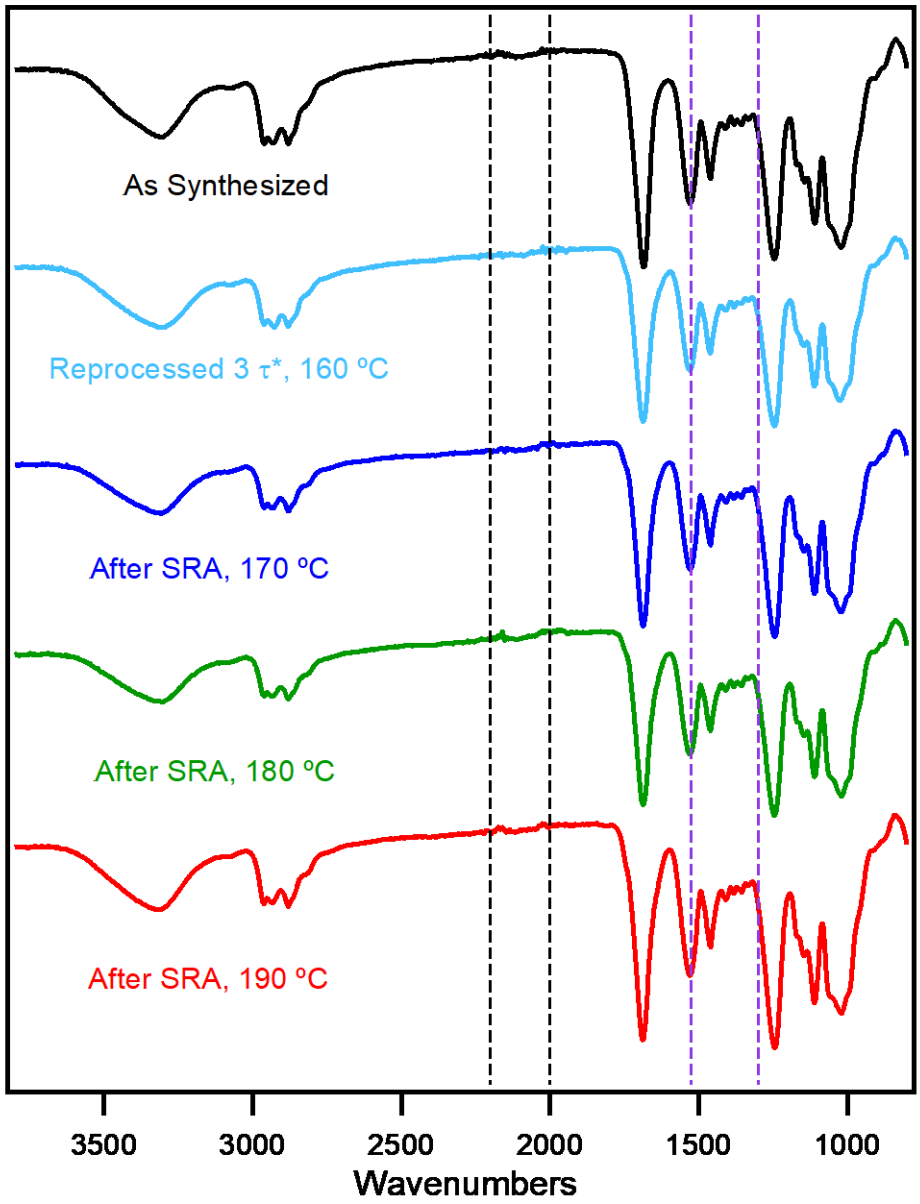

Figure S2.8. FT-IR spectra of **4** before & after stress relaxation analysis, and after reprocessing. The regions where isocyanate and isocyanurate signals would be expected are highlighted in black and purple, respectively.

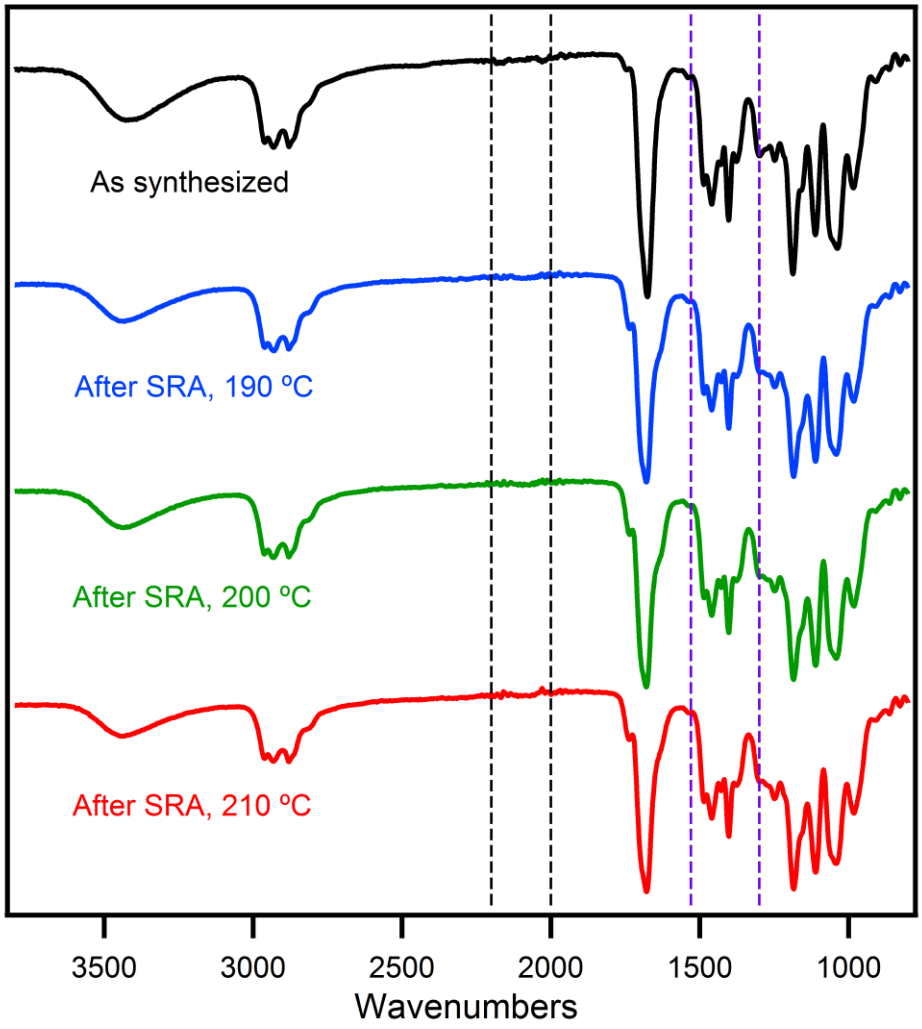

Figure S2.9. FT-IR spectra of **5** before & after stress relaxation analysis. The regions where isocyanate and isocyanurate signals would be expected are highlighted in black and purple, respectively.

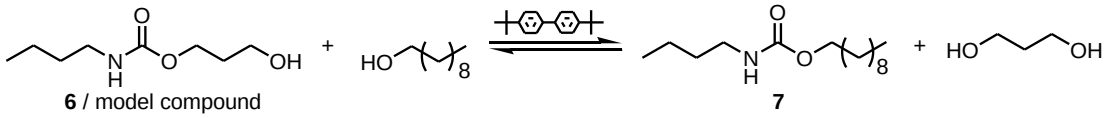

Kinetics of Transcarbamoylation of 6: To a vial was added hydroxyurethane model compound **6** (70 mg, 0.40 mmol), 1-decanol (632 mg, 4.0 mmol), and di-*tert*-butylbiphenyl (10 mg, 0.038 mmol) as an internal standard. The resulting mixture was heated in an oil bath preheated to the desired temperature (170-210 ºC), aliquots were taken via syringe at various time points, and analyzed via GC analysis with FID detection (Figure S2.10). Concentrations of the transcarbamoylation product **7** were determined from a calibration curve of independently synthesized **7**.

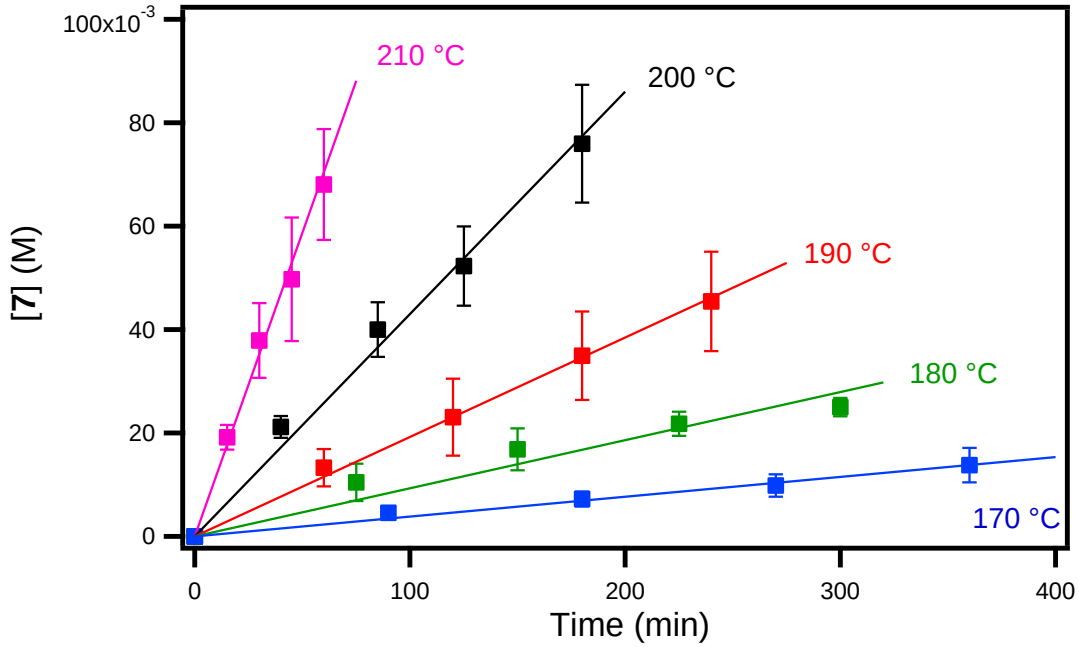

Figure S2.10. Plots of transcarbomylation product **7** concentration versus time for transcarbamoylation of model compound **6** with 1-decanol as a function of temperature. Concentrations shown are the average of four independent trials at a given temperature; error bars indicate one standard deviation. Linear fits are shown for initial rates under pseudo-first order kinetic conditions.

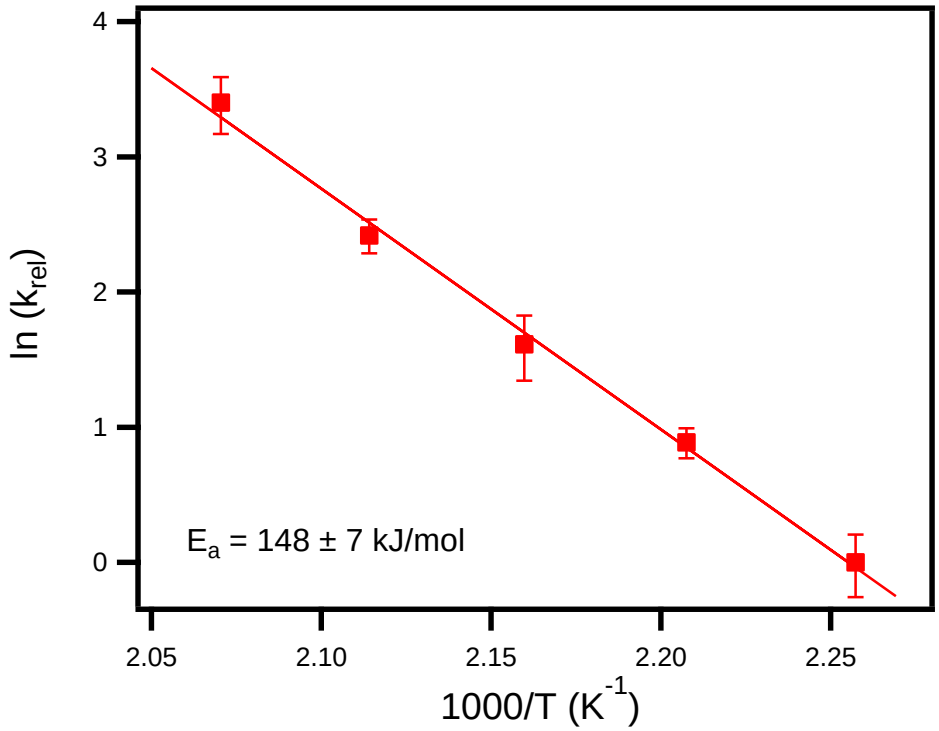

Figure S2.11. Arrhenius plot for determination of activation energy of transcarbamoylation in model compound **6**. Relative rates shown are the average of four independent trials; error bars indicate one standard deviation.

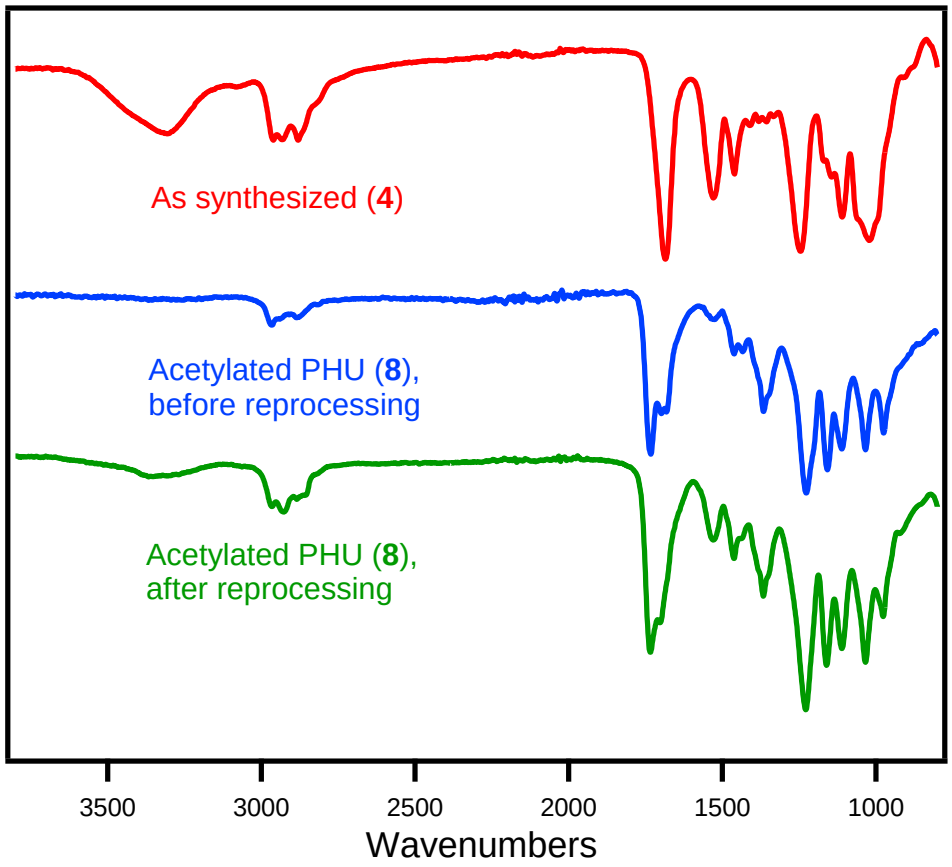

Figure S2.12. FT-IR spectra of as-synthesized polymer **4** (red), ground and acetylated polymer **8** before attempted reprocessing (blue), and acetylated polymer **8** after attempted reprocessing (green).

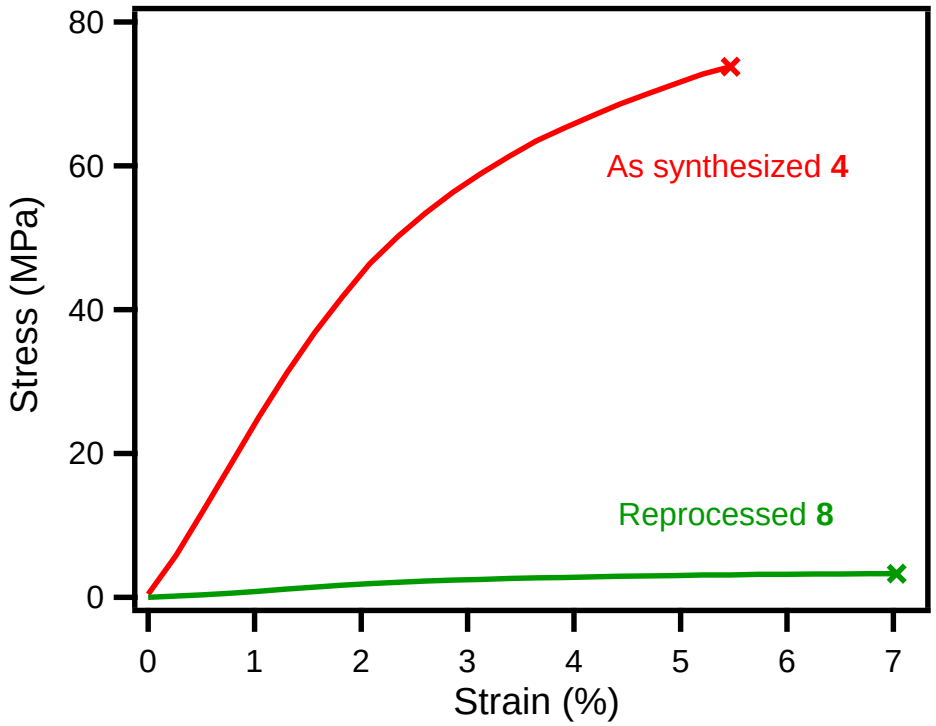

Figure S2.13. Representative tensile tests of as-synthesized polymer **4** (red) and reprocessed acetylated polymer **8** (green), showing limited reprocessability in the absence of a large concentration of free hydroxyl groups.

D. NMR Spectra

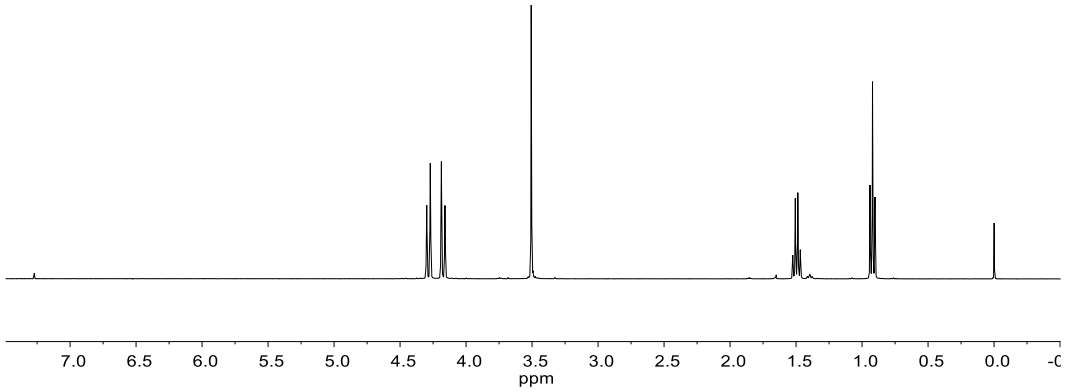

Figure S2.14. ^{1}H NMR ($CDCl_3$, 400 MHz, 298 K) of monomer **1**.

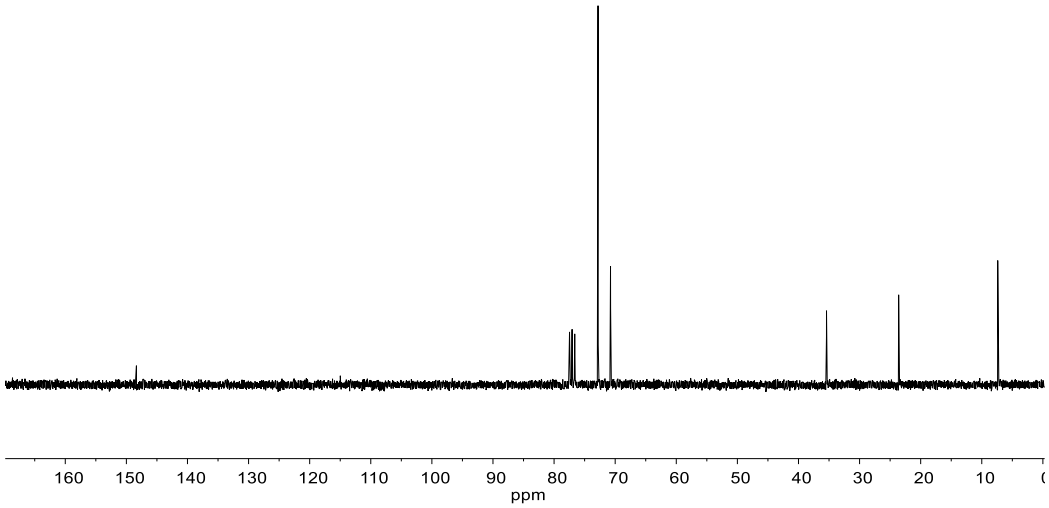

Figure S2.15. ^{13}C NMR ($CDCl_3$, 100 MHz, 298 K) of monomer **1**.

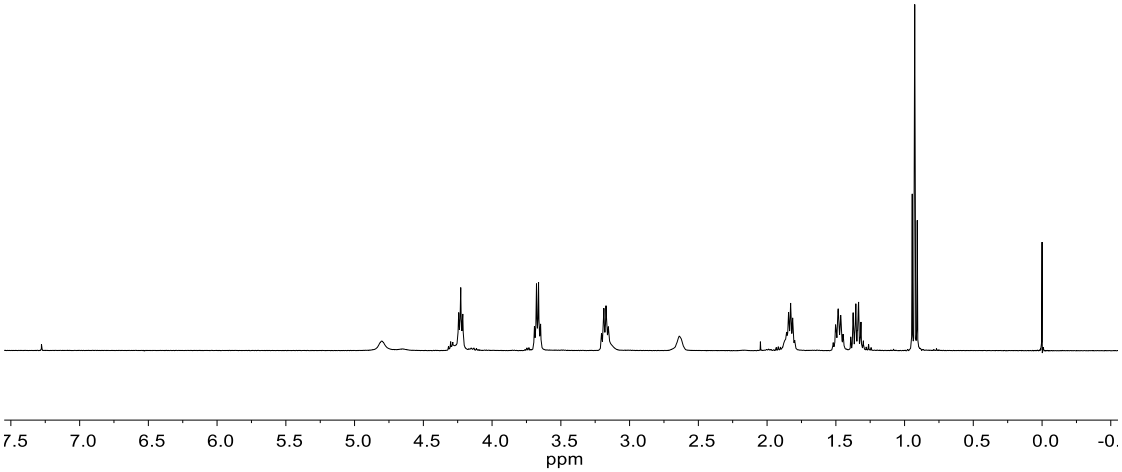

Figure S2.16. ^{1}H-NMR ($CDCl_3$, 400 MHz, 298 K) of hydroxyurethane model compound **6**.

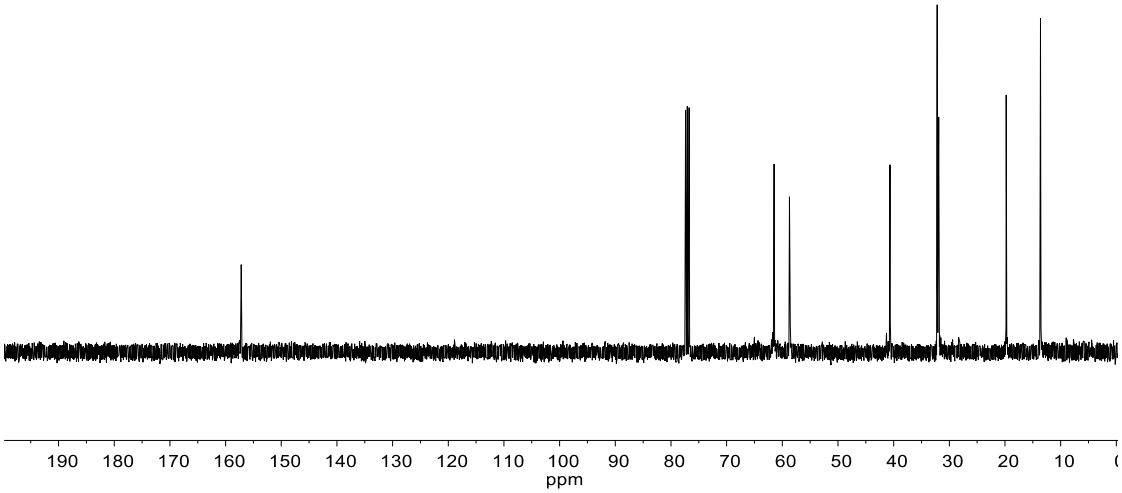

Figure S2.17. ^{13}C NMR ($CDCl_3$, 100 MHz, 298 K) of hydroxyurethane model compound **6**.

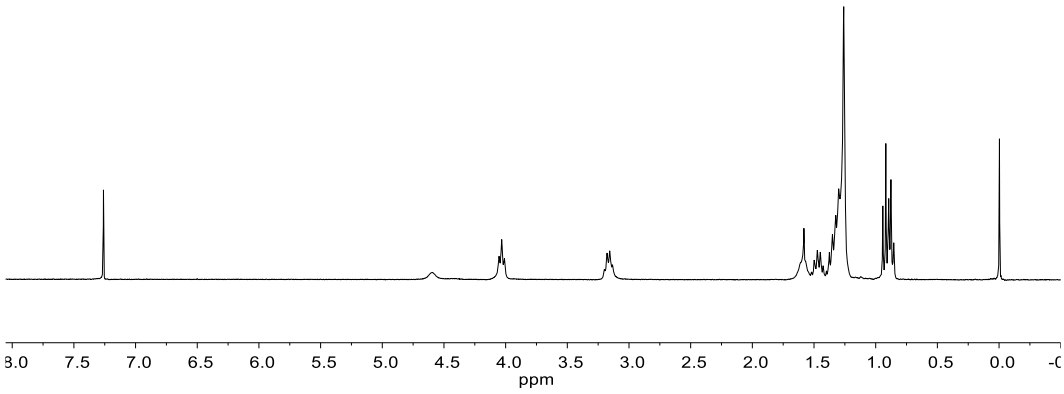

Figure S2.18. ^{1}H NMR ($CDCl_3$, 300 MHz, 298 K) of urethane **7**.

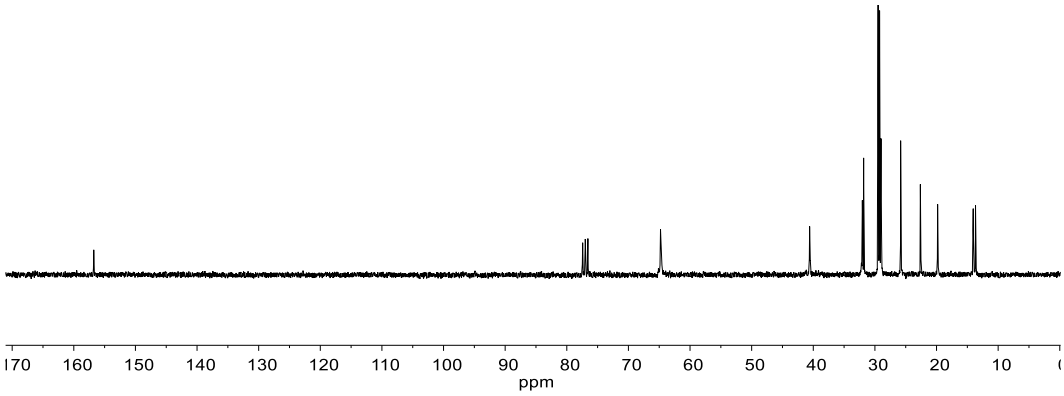

Figure S2.19. ^{13}C NMR ($CDCl_3$, 75 MHz, 298 K) of urethane **7**.

E. Computational Studies

All molecular structures were optimized, either fully or subject to a torsional constraint, at the M06-2X level[4] of density functional theory employing the 6-311+G(d,p) basis set.[5] Along the torsional coordinate, the N atom of *N*,*O*-dimethylcarbamate can pyramidalize, leading to different energies for *R* and *S* chiralities when the remainder of the system is asymmetric relative to the pyramidalization. In addition, the ester of the carbamate may be adopt either *s*-cis or *s*-trans orientations. For the transition-state (TS) structures, both possible ester orientations and nitrogen pyramidalizations were considered in order to identify the lowest-energy TS structure for a given torsion angle. Figure S2.20 provides the relative enthalpies of all structures relevant to the transcarbamoylation reaction as a function of torsion angle. Water-catalyzed reversion TS structures were also computed. They are not shown in Figure S2.20, but their enthalpies rise as a function of torsion angle more rapidly than do those of the reactant until the point is reached at which the TS structure can no longer be located because the geometry necessary for proton transfer can no longer be achieved.

Thermal contributions to molecular enthalpies were computed from analytical frequency calculations for all structures employing the conventional particle-in-a-box, rigid rotator, quantum mechanical harmonic oscillator approximations; molecular enthalpies of activation were converted to Arrhenius activation energies by addition of RT taking T = 180 °C.[6] The effects of increasing the basis set size to 6-311+G(2df,2p) and of including solvation effects for ethyl acetate to mimic the vitrimer condensed phase, were examined through single point calculations on relevant structures.[7] Computed relative energies for relevant structures remained unchanged to within 2

kJ/mol. All calculations were accomplished using the Gaussian09 suite of electronic structure programs.[8]

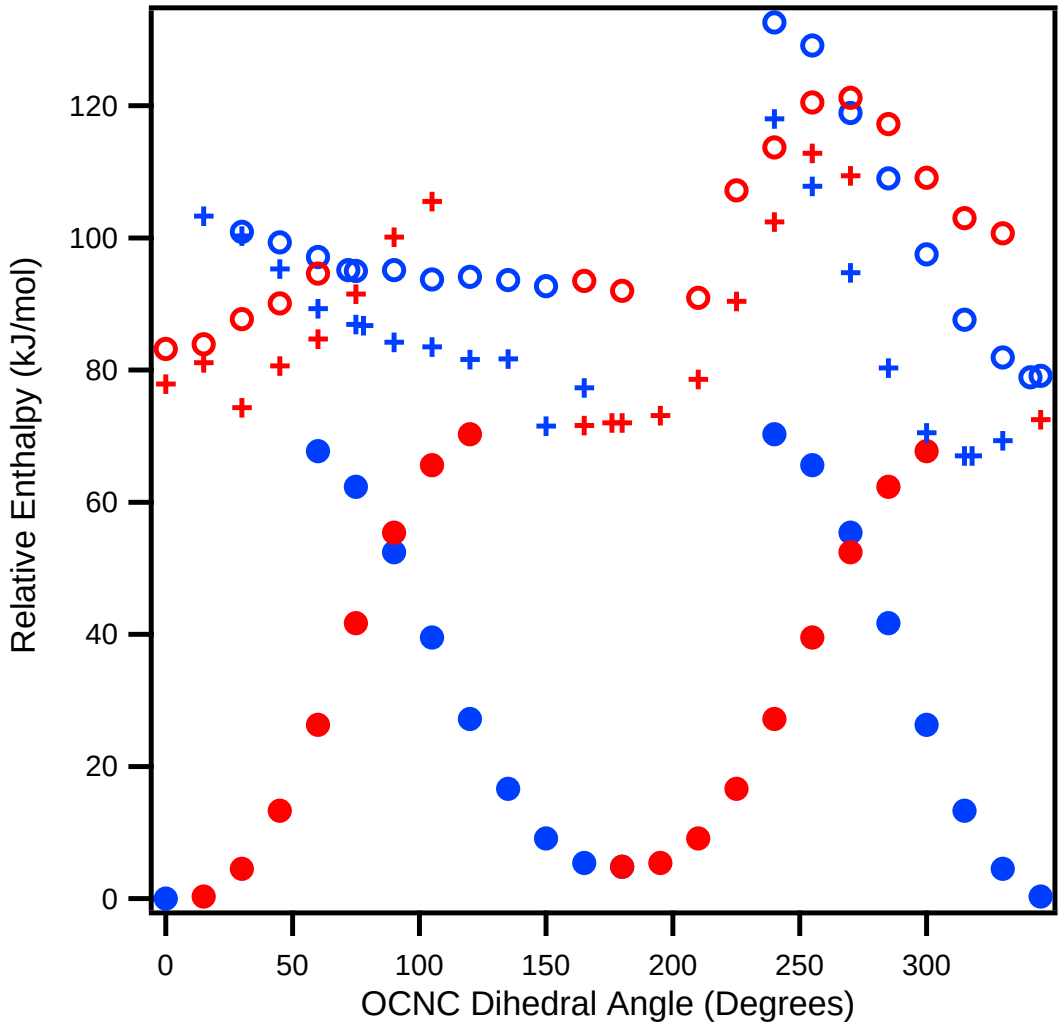

Figure S2.20. Enthalpies relative to global minimum separated reactant structures at the M06-2X/6-311+G(d,p) level of theory as a function of OCNC torsion angle in the *N*,*O*-dimethylcarbamate fragment. The educt enthalpies are represented by filled circles and TS-structure enthalpies are represented with crosses and open circles. Blue and red symbols refer to *R* and *S* local chirality at the nitrogen atom (the dots at torsion angles of 0 and 180 deg are arbitrarily colored as these structures have a planar N atom). Crosses and open circles refer to TS structures having ester groups with *s*-cis and *s*-trans stereochemistries, respectively.

To assess whether direct elongation, as opposed to torsional variations, might play a role in lowering the activation free energies for transcarbamoylation, we consider the

relative free energies of otherwise optimized reactant and TS structures in which the C-C distance between the two methyl groups on N,O-dimethylcarbamate were forced to separations 5% greater than those found for fully relaxed structures (i.e., corresponding to the strain employed in the experimental studies). We found that relative to the fully relaxed structures, the free energies of the stretched reactant and TS structures both went up by about 16 kJ/mol, i.e., no rate acceleration would be expected in transcarbamoylation exclusively from this elongation strain (which is manifest as a combination of angle-bending strain and bond-stretching strain). It is of some interest to note that the same distortion energy — about 16 kJ/mol — is required to reach the most torsionally strained reactant structures. Thus, to the extent that strain will be distributed into different modes throughout the polymer depending on the details of local condensed-phase structure, one would expect more reactive torsionally strained structures to indeed be accessible.

F. References:

(1) Brutman, J. P.; Delgado, P. A.; Hillmyer, M. A. *ACS Macro Lett.* **2014**, *3*, 607.

(2) Capelot, M.; Unterlass, M. M.; Tournilhac, F.; Leibler, L. *ACS Macro Lett.* **2012**, *1*, 789.

(3) Yang, L; He, B.; Meng, S.; Zhang, J.; Li, M.; Guo, J.; Guan, Y.; Li, J.; Gu, Z. *Polymer* **2013**, *54*, 2668.

(4) Zhao, Y.; Truhlar, D. G.*Theor. Chem. Acc.* **2008**, *120*, 215.

(5) Hehre, W. J.; Radom, L.; Schleyer, P. v. R.; Pople, J. A. *Ab Initio Molecular Orbital Theory*; Wiley: New York, 1986.

(6) Cramer, C. J. *Essentials of Computational Chemistry: Theories and Models*; 2nd ed.; John Wiley & Sons: Chichester, 2004.

(7) Marenich, A. V.; Cramer, C. J.; Truhlar, D. G. *J. Phys. Chem. B* **2009**, *113*, 6378.

(8) Frisch, M. J.; Trucks, G. W.; Schlegel, H. B.; Scuseria, G. E.; Robb, M. A.; Cheeseman, J. R.; Scalmani, G.; Barone, V.; Mennucci, B.; Petersson, G. A.; Nakatsuji, H.; Caricato, M.; Li, X.; Hratchian, H. P.; Izmaylov, A. F.; Bloino, J.; Zheng, G.; Sonnenberg, J. L.; Hada, M.; Ehara, M.; Toyota, K.; Fukuda, R.; Hasegawa, J.; Ishida, M.; Nakajima, T.; Honda, Y.; Kitao, O.; Nakai, H.; Vreven, T.; Montgomery, J. A.; Peralta, J. E.; Ogliaro, F.; Bearpark, M.; Heyd, J. J.; Brothers, E.; Kudin, K. N.; Staroverov, V. N.; Kobayashi, R.; Normand, J.; Raghavachari, K.; Rendell, A.; Burant, J. C.; Iyengar, S. S.; Tomasi, J.; Cossi, M.; Rega, N.; Millam, J. M.; Klene, M.; Knox, J. E.; Cross, J. B.; Bakken, V.; Adamo, C.; Jaramillo, J.; Gomperts, R.; Stratmann, R. E.; Yazyev, O.; Austin, A. J.; Cammi, R.; Pomelli, C.; Ochterski, J. W.; Martin, R. L.; Morokuma, K.; Zakrzewski, V. G.; Voth, G. A.; Salvador, P.; Dannenberg, J. J.; Dapprich, S.; Daniels, A. D.; Farkas, Ö.; Foresman, J. B.; Ortiz, J. V.; Cioslowski, J.; Fox, D. J. *Gaussian 09, Revision C.01*; Gaussian, Inc.: Wallingford, CT, 2010.

CHAPTER THREE

STRUCTURAL EFFECTS ON THE REPROCESSABILITY AND STRESS RELAXATION OF CROSS-LINKED POLYHYDROXYURETHANES

3.1 Abstract

Cross-linked polyhydroxyurethane (PHU) networks synthesized from difunctional six-membered cyclic carbonates and triamines are reprocessable at elevated temperatures through transcarbamoylation reactions. Here we study the structural effects on reprocessability and stress relaxation in cross-linked PHUs. Cross-linked PHUs derived from bis(five-membered cyclic carbonates) are shown to decompose at temperatures needed for reprocessing, likely via initial reversion of the PHU linkage and subsequent side reactions of the liberated amine and cyclic carbonate. Therefore, several six-membered cyclic carbonate-based PHUs with varying polymer backbones and cross-link densities were synthesized. These networks show large differences in the Arrhenius activation energy of stress relaxation (from 99 to 136 kJ/mol) that depend on the network structure, suggesting that transcarbamoylation reactions may be highly affected by both chemical and mechanical effects. Furthermore, all cross-linked PHUs derived from six-membered cyclic carbonates show mechanical properties typical of thermoset polymers, but recovered as much as 80% of their as-synthesized tensile properties after elevated temperature compression molding. These studies provide significant insight into factors affecting the reprocessability of PHUs and inform design criteria for the future synthesis of sustainable and repairable cross-linked PHUs.

This work was performed in collaboration with Dr. Jacob Brutman and Prof. Marc Hillmyer from the Department of Chemistry at the University of Minnesota. This chapter was first published in the *Journal of Applied Polymer Science*: Fortman, D. J.; Brutman, J. P.; Hillmyer, M. A.; Dichtel, W. R. *J. Appl. Polym. Sci*. **2017**, *134*, 44984, and is reproduced with permission.

3.2 Introduction

Thermosets are cross-linked polymer networks whose mechanically robust and solvent-resistant properties facilitate their use in demanding applications that require high dimensional stability. However, these desirable properties are no longer advantageous once thermosets are damaged or discarded, since their inability to dissolve or melt precludes reshaping or repair. The incorporation of covalent bonds capable of dynamic exchange into cross-linked polymers imparts self-healing to elastomeric materials and reprocessability to thermoset-like materials, yet compromises their toughness if not carefully controlled.[1–10] Polymer networks termed vitrimers are a subset of repairable cross-linked polymers with outstanding mechanical properties that rely on associative, rather than dissociative, exchange reactions to relax stress and undergo repair.[11,12] In their initial report,[13] Leibler and coworkers synthesized polyester-based epoxy resins containing free hydroxyl groups, which undergo catalyzed transesterification reactions at elevated temperatures that enable stress relaxation and reshaping. Nevertheless, these polymers have mechanical properties competitive with traditional epoxy resins at service temperatures. Another benefit of this design is that the viscosity of the polymer decreases gradually with temperature, because their flow

relies on activated cross-link exchange, rather than the abrupt Williams-Landel-Ferry-type changes in viscosity observed in thermoplastic materials above the glass transition temperature (T_g). This strong glass-forming behavior typically enables vitrimers to be reshaped, even without precise temperature control.

Early examples of vitrimers focused on polyester resins[14–18] and polybutadiene rubbers.[19-21] Other dynamic polymer networks have since emerged that incorporate dynamic functional groups including disulfides,[22–25] hindered ureas,[26,27] vinylogous urethanes,[28] alkylated triazoles,[29] siloxanes,[30,31] imines,[32] and boronate esters,[33] representing a significant expansion of dynamic chemistries that are compatible with the vitrimer concept. Yet developing vitrimeric materials with tunable mechanical properties that are economical and capable of efficient reprocessing remains an ongoing challenge. Polyhydroxyurethane (PHU) networks in particular show great potential as inexpensive, tunable, and sustainable vitrimers because their synthesis avoids toxic isocyanates and inherently provides a stoichiometric number of hydroxyl groups for cross-link exchange.[34] Polyurethanes (PUs) are used as coatings, adhesives, foams, and thermosets,[35] but are not typically reprocessed. Chemical recycling of cross-linked PUs has been explored as an effective approach to convert PUs into monomers or oligomeric molecules,[36–38] but this approach is limited by the high energy requirements and multistep processing. Effective approaches for directly reprocessing cross-linked PUs have been developed, but most require specialized monomers containing other dynamic functional groups or have less desirable mechanical properties.[22,39–41] Therefore, interest has arisen in controlling the dynamics of carbamate linkages themselves to enable reprocessing,[42] inspired by seminal work on cross-linked PU stress relaxation by

Tobolsky, *et. al*.[43,44] We recently reported that PHU networks synthesized from polyfunctional six-membered cyclic carbonates (6CCs) and amines demonstrate vitrimeric behavior in the absence of external catalysts, and attributed this behavior to associative transcarbamoylation reactions that might be facilitated by mechanical effects.[34] Here we analyze the effects of PHU structure on the thermal stability, stress relaxation behavior, and reprocessability of cross-linked networks. We establish that PHU networks based on five-membered cyclic carbonates (5CCs) undergo thermal reversion and subsequent side reactions at elevated temperature, making them poor candidates for PHU vitrimers. Vitrimeric behavior is observed in networks derived from several bis(6CCs), which inform design criteria for the development of thermally reprocessable PHUs.

3.3 Results & Discussion

We previously described the stress relaxation and reprocessing of two similar PHU networks derived from 6CCs at elevated temperatures.[34] Polyfunctional 5CCs are also attractive monomers because they are derived from inserting carbon dioxide into epoxides,[48] typically through solvent-free protocols. Polyfunctional epoxides are easily derived from many renewable feedstocks, thus, the corresponding PHUs are promising sustainable alternatives to PUs synthesized from isocyanate precursors.[49–51] However, 5CC-derived PHUs contain predominantly secondary hydroxyl groups,[52,53] as compared to the primary hydroxyl groups found in 6CC-derived networks. Given the lower nucleophilicity of secondary alcohols (which may or may not undergo transcarbamoylation reactions under similar conditions) and the much smaller concentration of primary hydroxyl groups in these PHUs, these materials might require

higher temperatures for stress relaxation. Therefore, we explored whether networks derived from 5CCs exhibit vitrimeric behavior.

Scheme 3.1. A. Reaction of bis(5-membered cyclic carbonate) **1** or bis(6-membered cyclic carbonate) **2** with **TREN** to give cross-linked polyhydroxyurethane **3** and **4**, respectively, highlighting the presence of secondary hydroxyl groups present in polymer **3**. B. Transcarbamoylation is the proposed mechanism of stress relaxation and reprocessing in cross-linked PHUs.

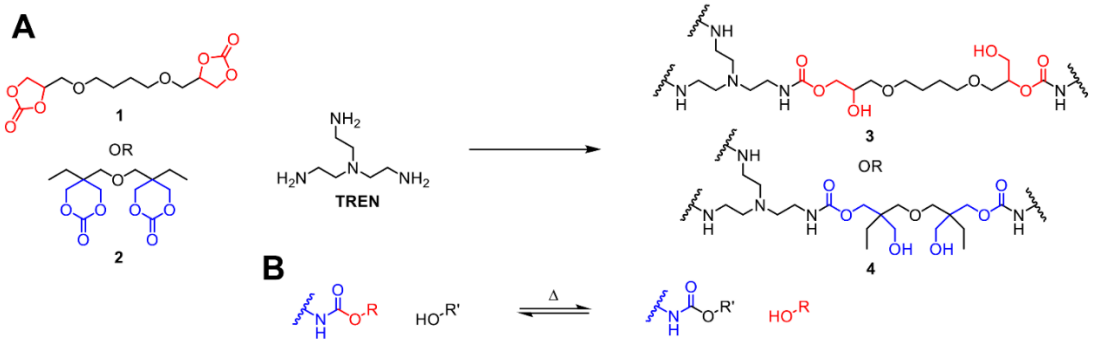

We synthesized bis(5CC) **1** via the insertion of carbon dioxide into 1,4-butanediol diglycidyl ether.[47] Monomer **1** was reacted with **TREN** using a 1:1 molar ratio of amine:5CC to give cross-linked PHU networks via reaction in CH_2Cl_2 at room temperature, followed by heating under vacuum to remove solvent and yield PHU **3** as an orange solid (Scheme 3.1; see Experimental Section). FT-IR spectroscopy showed complete disappearance of the initial cyclic carbonate C=O stretch (1790 cm^{-1}, Figure 1A), as well as the appearance of multiple absorbances associated with PHU structure: O-H stretch (3300 cm^{-1}), urethane C=O stretch (1690 cm^{-1}), and urethane N-H deformation (1530 cm^{-1}). Swelling tests of the polymers in CH_2Cl_2 show gel fractions in excess of 0.97, further supporting that these monomers react to high conversion under the synthesis conditions to give densely cross-linked PHU networks. To determine whether these networks would behave as vitrimers at elevated temperatures, we analyzed their stability to sustained heating to temperatures greater than 170 °C, where

stress relaxation occurred within a reasonable timeframe in 6CC-based PHUs.[34] New peaks appear in the FT-IR spectra of polymer **3** after heating for either 15 min or 5 h, indicating side reactions occurring at elevated temperatures (Figure 3.1A). Within 15 min, a new peak appeared at 1790 cm^{-1}, corresponding to partial reversion of the hydroxyurethane linkages to corresponding cyclic carbonate and amine. After extended heating, further decomposition was observed with the emergence of a new carbonyl peak associated with urea linkages (1640 cm^{-1}) and a shift in carbonyl absorbance from 1690 cm^{-1} to 1720 cm^{-1}. Identical experiments were performed with a PHU network synthesized from bis(6CC) **2** and **TREN** (Scheme 3.1);[34] this network (**4**) shows no detectable change in the IR spectra under identical conditions (Figure 3.1B), indicating that the 6CC-derived PHU linkages are more thermally stable than those derived from 5CCs.

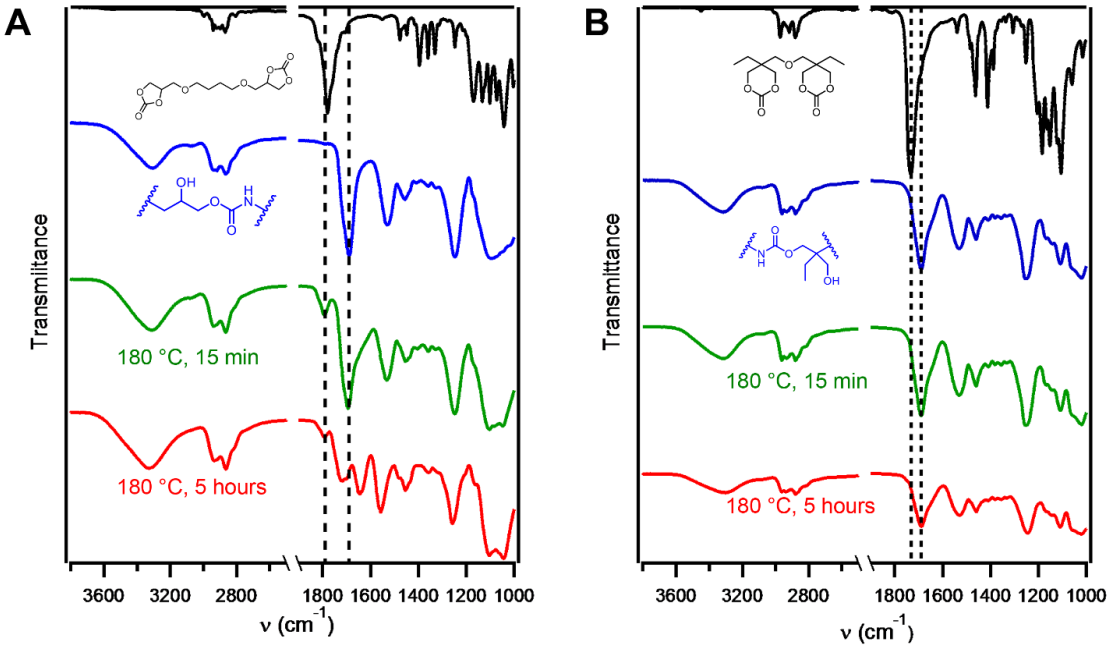

Figure 3.1. A. FT-IR spectra of monomer **1** (black), polymer **3** (blue), and polymer **3** after heating at 180 °C for 15 minutes (green) and 5 hours (red). B. FT-IR spectra of

monomer **2** (black), polymer **4** (blue), and polymer **4** after heating at 180 °C for 15 minutes (green) and 5 hours (red).

The difference in thermal stability between hydroxyurethanes derived from 6CCs and 5CCs was further explored using model compounds **5** and **6** (Figure 3.2). The 5CC model compound **5** was used as a mixture of secondary (**5a**) and primary (**5b**) hydroxyl-containing carbamates to most accurately model the likely structure of the PHU network. **5** and **6** were heated to 180 °C for up to 5 hours and analyzed by GC-MS at intermediate time points. After 60 min at 180 °C, **5** partially decomposes back to the 5CC from which it derives. This decomposition product is observed more prominently after 5 hours, along with additional secondary decomposition products. These include di-*n*-butylurea, which is presumably formed from the nucleophilic attack of liberated *n*-butylamine on the carbamate linkage of the model compound. The presence of the cyclic carbonate upon sustained heating was confirmed by ^{1}H NMR spectroscopy (Figure S3.1), providing further support of this decomposition mechanism. In contrast, no reversion is observed in the 6CC model carbamate **6** (Figure 3.2B, Figure S3.2) under the same conditions; the only other detectable species is a small amount of a compound containing two carbamates, originating from the reaction of the free hydroxyl group with another molecule of **6**. These observations are consistent with those of the polymer networks **3** and **4**, and likely reflect the greater thermodynamic stability of 5CCs compared to 6CCs. 6CCs are estimated to have ring strain of ca. 3 kcal/mol greater than 5CCs.[54]

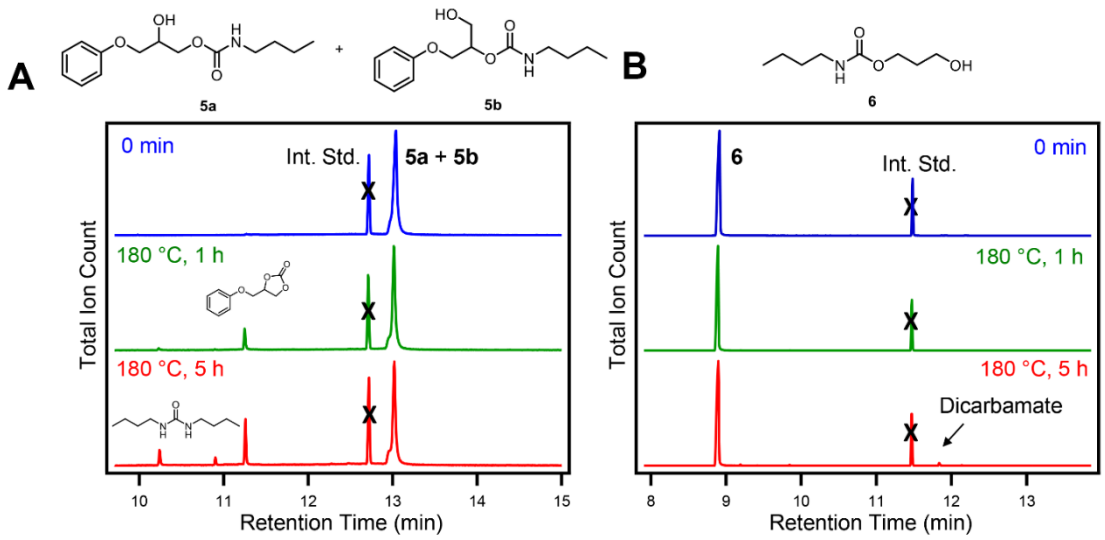

Figure 3.2. GC-MS chromatograms of A. model compound **5** and B. model compound **6** as-synthesized (blue) and after heating to 180 °C for 1 hour (green) and 5 hours (red).

Based on these observations, the likely decomposition pathway for 5CC-derived PHUs first involves the reversion of the hydroxyurethane linkage to the 5CC and free amine (Scheme 3.2a). Free amines may undergo several side reactions at elevated temperature. They can react with cyclic carbonates at higher temperatures via an undesired decarboxylative mechanism that gives linkages unable to undergo further exchange (Scheme 3.2b). Amines also add to carbamates to form ureas (Scheme 3.2c), thus impacting the network composition. Free hydroxyl groups in the network might also react with the cyclic carbonate moiety to give ether (Scheme 3.2d) or carbonate (Scheme 3.2e) linkages. Additional side reactions such as oxazolidone formation are also possible according to literature reports.[55] We have no direct evidence for the formation of these species but cannot rule out their presence at low concentrations in the decomposed networks. Given the propensity of 5CCs to undergo this deleterious decomposition process at temperatures needed for stress relaxation, strained cyclic

carbonates such as 6CCs, are more effective precursors for PHU networks that display vitrimer-like behavior.

Scheme 3.2. Proposed breakdown of hydroxyurethanes derived from 5CCs, labeled with the FT-IR frequency of the carbonyl species. At elevated temperatures, the hydroxyurethane reverts to cyclic carbonate and amine (a); subsequently, amine may react with cyclic carbonate in a decarboxylative manner (b), amine may react with urethane linkages to form ureas (c), or free hydroxyls may react with cyclic carbonate to form ether (d) or carbonate (e) linkages.

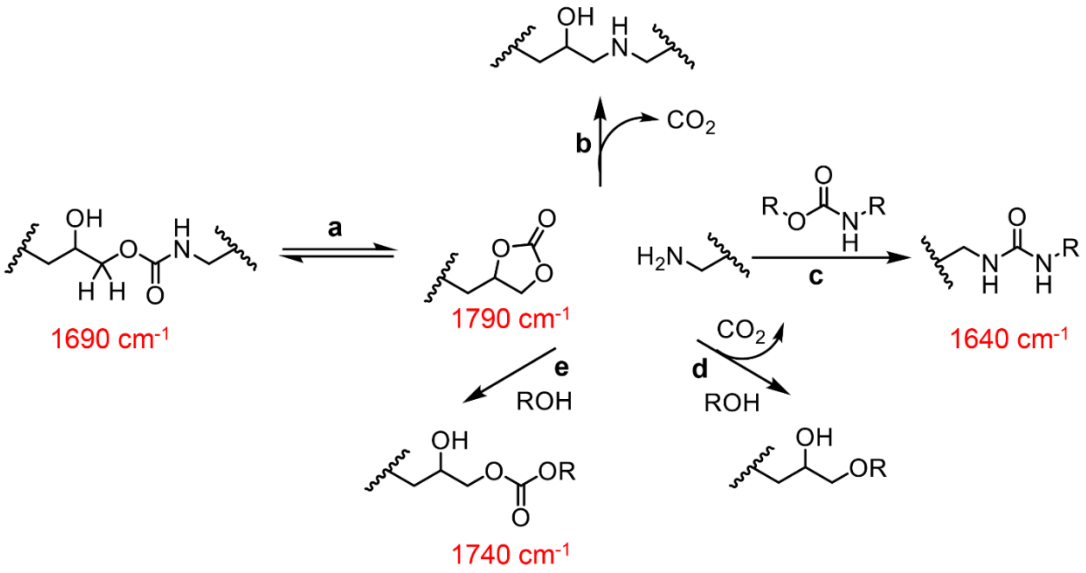

Scheme 3.3. Synthesis of PHUs based on bis(hydroxymethyl)propionic acid. Diols were esterified with carboxylic acid-containing 6CC **7** in the presence of DCC and DMAP. The resulting bis(6CC)s are reacted with **TREN** via gelation in CH_2Cl_2 and heating under vacuum to yield cross-linked polyhydroxyurethanes **8-11**.

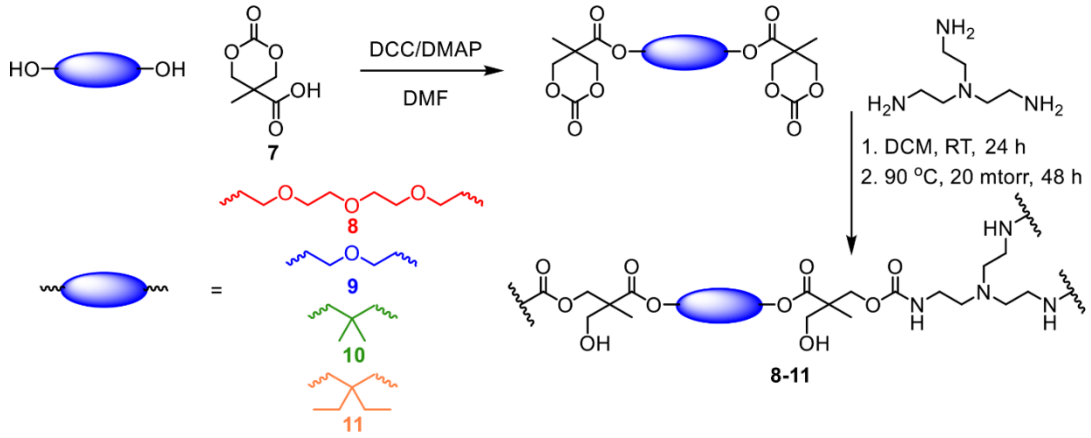

Table 3.1: Material Properties of Cross-linked Polyhydroxyurethanes

Polymer	Gel %	T_d (°C; 5%)	T_g (°C; DSC)	T_g (°C; DMTA)	E' at 100 °C (MPa)	E_a (kJ/mol)	T_v (°C)
4[Ref. 34]	99	263	54	61	7.5	110 ± 3	111
8	96	265	7	0	3.6	99 ± 6	93
9	99	270	35	25	4.5	108 ± 11	98
10	98	280	48	41	3.3	136 ± 8	115
11	94	276	54	51	2.0	134 ± 4	108
12	98	278	45	41	2.4	132 ± 9	111
13	98	292	45	47	1.6	128 ± 13	105
14	98	299	42	44	1.2	117 ± 11	95

Having established the superior thermal stability of 6CC-based PHUs, we designed a modular approach to evaluate structure-property relationships related to their stress relaxation (Scheme 3.3). Most reported 6CCs have been evaluated for controlled ring-opening polymerizations,[56–58] and only a few examples have been incorporated into PHUs.[59,60] Hedrick and coworkers studied the ring-opening polymerization of 6CC

monomers based on esterifying the pendant carboxylic acid of the 6CC **7**, which is derived from bis(hydroxymethyl)propionic acid.[46] Suitable monomers for PHU networks can be prepared by esterifying diols with **7** using the same approach. Diols based on oligoether chains of differing length provide materials with lower T_g's, and branched aliphatic diols provide higher T_g materials. In all cases, carbodiimide-mediated esterifications between the diols and **7** provided monomers of high purity, which were readily reacted with **TREN** to give densely cross-linked networks. FT-IR analysis of all polymers was consistent with the expected PHU structure (Figure S3.2). Amidation at the sterically hindered ester was not observed in model compounds under similar reaction conditions, as only products corresponding to carbamate formation were observed. No amide resonances were observed in the FT-IR spectra of the PHUs, and gel fractions and DMTA indicated the formation of highly cross-linked networks (Table 3.1, Figure 3.3A). Stress relaxation experiments at elevated temperatures in the linear viscoelastic regime (Figure 3.3B) showed markedly differing behavior between the samples. All of the 6CC-based PHUs exhibited reproducible stress relaxation with no change in their FT-IR spectra after extended heating (Figure S3.3 and S3.5). The low T_g PHUs **8** and **9** exhibit faster stress relaxation than the higher T_g materials **10** and **11**. The Arrhenius activation energies for the oligoether-based materials were markedly lower (99 ± 6 kJ/mol for **8**, and 108 ± 11 kJ/mol for **9**) than those of the aliphatic systems (136 ± 8 kJ/mol for **10**, and 134 ± 4 kJ/mol for **11**); this difference was unexpected, given that transcarbamoylation is expected to be responsible for stress relaxation in all cases. Although speculative, we hypothesize that these differences arise from the increased flexibility of the polymer chains in the oligoether-containing networks or

differences in dielectric constants of the ether-containing networks lowering the reaction barrier for transcarbamoylation.

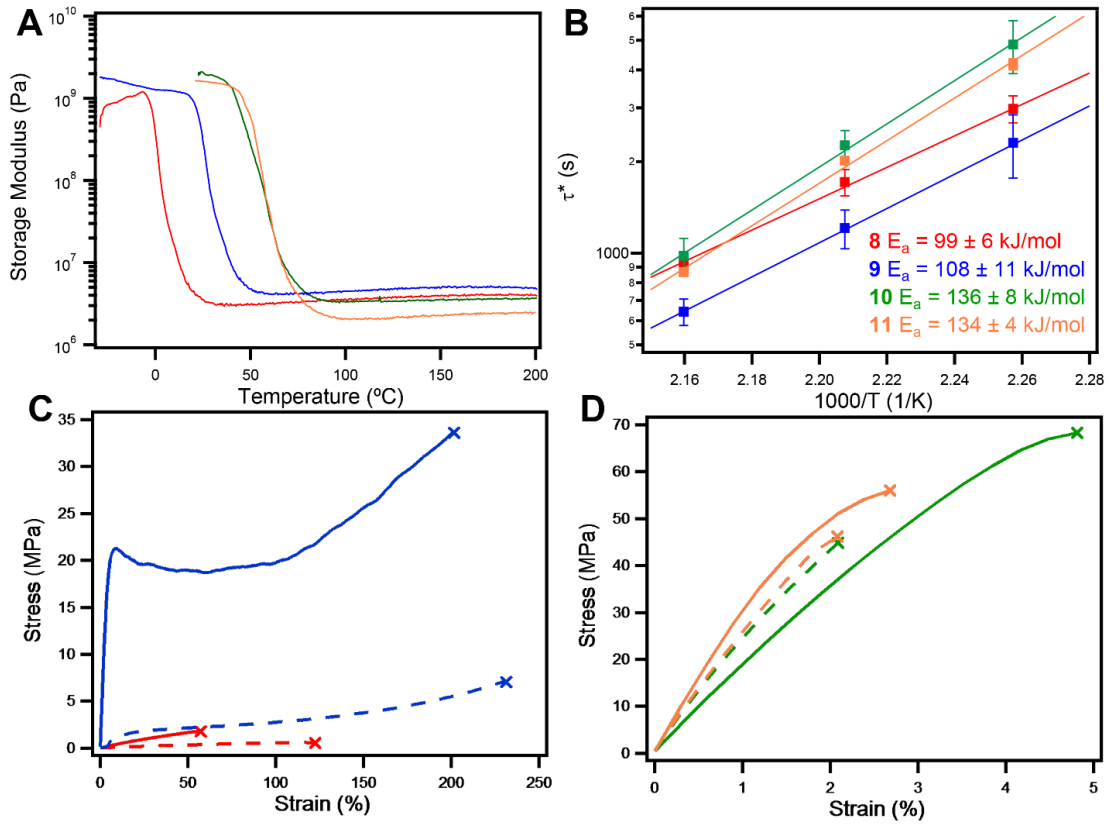

Figure 3.3. A. Dynamic mechanical thermal analysis, B. Arrhenius plots of characteristic stress relaxation times, and C. and D. tensile testing data of as-synthesized (solid) and reprocessed (dashed) polyhydroxyurethane **8** (red), **9** (blue), **10** (green), and **11** (orange).

Table 3.2: Tensile Properties of Polyhydroxyurethanes

As Synthesized				After Healing			
Polymer	σ_b (MPa)	ε_b (%)	E (GPa)	Temp (°C); Time (min) healed	σ_b (MPa)	ε_b (%)	E (GPa)
4[Ref. 34]	72 ± 11	6.9 ± 3.8	2.2 ± 0.4	160; 480	53 ± 8	4.8 ± 0.8	1.6 ± 0.2
8	1.9 ± 0.4	56 ± 8	(4.8 ± 0.5) x 10^{-3}	160; 280	0.57 ± 0.04	114 ± 9	(7.7 ± 0.6) x 10^{-4}
9	30 ± 6	198 ± 15	0.6 ± 0.5	160; 225	6.7 ± 2.4	216 ± 23	0.05 ± 0.04
10	66 ± 4	4.0 ± 0.5	1.9 ± 0.2	160; 570	34 ± 14	1.5 ± 0.5	2.5 ± 0.3
11	61 ± 6	2.2 ± 0.4	3.0 ± 0.4	160; 495	47 ± 4	2.1 ± 0.2	2.63 ± 0.05
12	82 ± 7	4.5 ± 0.4	2.3 ± 0.3	160; 580	37 ± 17	1.9 ± 0.8	2.4 ± 0.2
13	82 ± 10	4.3 ± 0.6	2.5 ± 0.2	160; 545	32 ± 7	1.5 ± 0.4	2.42 ± 0.08
14	69 ± 7	3.5 ± 0.3	2.4 ± 0.3	160; 400	49 ± 6	2.2 ± 0.3	2.5 ± 0.1

To further verify that this stress relaxation is the result of productive transcarbamoylation processes, rather than a result of degradation of the networks, we reprocessed damaged PHUs at elevated temperatures. In all cases, compression molding of crushed/broken samples provided fused, albeit discolored, cross-linked polymers. Compression molding of each material for three times its characteristic stress relaxation time (τ^*, defined as the time required for an applied stress to relax to $1/e$ of its original value) at 160 °C led to materials with similar macroscopic behavior, but reduced

mechanical properties as determined by tensile testing (Figure 3.3C and 3.3D, Table 3.2). The reprocessed oligoether-based polymers **8** and **9** recover only ca. 20-30% of their original tensile strength, but both show increased strain at break. The stiffer, aliphatic diol-based polymers **10** and **11** recover 50-75% of their original tensile strength and show Young's moduli comparable to as-synthesized samples, similar to results obtained in our initial reports on polymer **4**,[34] indicating that the presence of ethers versus esters in the backbone does not have a dramatic effect on reprocessability. A second reprocessing cycle was performed on polymer **11**, and a similar additional decrease in mechanical properties was observed (Figure S3.8, Table S3.1), indicating that the materials as currently formulated are not indefinitely recyclable. The more elastomeric behavior of the lower glass transition polymers **8** and **9**, as well as the decreased tensile properties of the higher glass transition polymers **10** and **11** are consistent with the reprocessed materials having lower cross-linking densities than the as-synthesized samples, similar to our initial study.[34] Despite these diminished properties, we note that FT-IR spectroscopy does not show any evidence of the structural changes in these networks.

To determine if the reduced mechanical properties are predominantly due to minor degradation processes or inefficient bond formation, we annealed as-synthesized tensile bars under N_2 for identical amounts of time. Annealed samples provided somewhat reduced tensile properties compared to as-synthesized samples (Figure S3.8, Table S3.1), but they do perform better than the reprocessed samples. This observation suggests that moderate decomposition may be occurring under the reprocessing conditions, but that bond formation has not reached the same extent as in as-synthesized

samples. Therefore, further work is required to determine optimal reprocessing conditions for each PHU, which either balance the competing bond formation and degradation processes or accelerate transcarbamoylation to allow reprocessing at lower temperatures.

To gain more insight into the factors that govern stress-relaxation phenomena in PHUs, we varied the cross-link density of the networks without significantly varying their chemical composition. Monomer **2** was reacted with varying ratios of **HMDA** and **TREN** (Figure 3.4A). FT-IR analysis of all polymers (Figure S3.4) indicated complete disappearance of the initial cyclic carbonate C=O stretch (1740 cm^{-1}), and the appearance of an O-H stretch (3300 cm^{-1}) and urethane C=O stretch (1690 cm^{-1}), indicating high conversion of the polymerization. The T_g of the networks, as determined by DSC, increased slightly with increasing cross-link density (from *ca*. 45-54 °C), consistent with limited change in the chemical structure of the network. DMTA indicated an expected increased rubbery plateau modulus/decreased molar mass between cross-links of these materials with increased cross-linker content (Figure 3.4B). Stress relaxation analysis performed from 170-190 °C in the linear viscoelastic regime shows a general trend of faster stress relaxation with lower cross-link density (Figure 3.4C, Figure S3.6), as has been reported in other vitrimer systems.[61] In all cases, FT-IR analysis after multiple stress relaxation experiments shows no detectable change in chemical functionality (Figure S3.4), indicating that the relaxation process is likely caused predominantly by transcarbamoylation reactions. The Arrhenius activation energy of stress relaxation is highest in samples with intermediate cross-link densities (132 ± 9 kJ/mol for **12** and 128 ± 13 kJ/mol for **13**), while lower activation energies

were measured at the lowest cross-link density (117 ± 11 kJ/mol for **14**) and highest cross-link density (110 ± 10 kJ/mol for **4**).[34] While some of these activation energy values are essentially within error of the measurement, differences in relaxation behavior between the polymers of varying cross-link density are evident (Figure S3.7). While we are unsure of the exact cause of this change, we note that similar trends in activation energy have been observed when changing network structure in polyester vitrimers when stress relaxation was performed at temperatures close to the T_g.[61] Given that the networks are of similar chemical composition, it is likely that chemical effects on transcarbamoylation dynamics are negligible, so we attribute this change in activation energy to differences in the stiffness of the materials. Although no clear trend is observed between the storage modulus and either the activation energy or pre-exponential factor of the Arrhenius model (Figure S3.7), it is possible that the urethane linkages may experience different levels of stress depending on the cross-link density. It is likely possible that the different stiffnesses of the PHUs might affect the ability of reactive groups to adopt appropriate trajectories for transcarbamoylation. Further investigation is required to fully understand the degree to which these mechanical factors impact PHU stress relaxation.

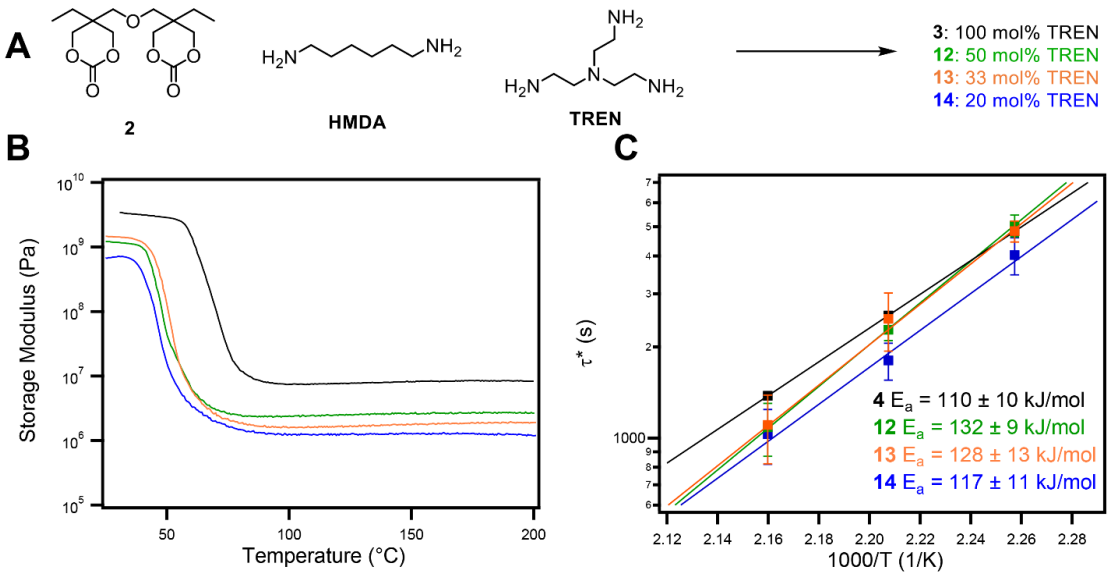

Figure 3.4. A. Synthesis of cross-linked polyhydroxyurethanes of varied cross-linked density via reaction of monomer **2** with mixtures of hexamethylenediamine (**HMDA**) and **TREN**. B. Dynamic mechanical thermal analysis and C. Arrhenius plots of characteristic stress relaxation times of cross-linked polyhydroxyurethane **4** (black, ref. 34), **12** (green), **13** (orange), and **14** (blue).

Reprocessing experiments were performed to determine how cross-link density affects reprocessability of the PHUs and further demonstrate that stress relaxation is caused by productive transcarbamoylation reactions. Reprocessing of all samples at 160 °C for 3τ* yields macroscopically repaired samples. Interestingly, while all samples discolor upon reprocessing, the samples with lowest TREN loadings discolor the least (Figure 3.5A), consistent with an increase in decomposition temperature of ca. 35 ºC observed with decreasing cross-linker content (Table 3.1). These observations suggest that tertiary amines are a source of decomposition in these materials. Tensile testing of the as-synthesized and reprocessed samples shows moderate reprocessing efficiencies (Figure 3.5B, Table 3.2), which are in agreement with expected trends in tertiary amine content. A second reprocessing cycle on polymer **14** yields similar reprocessing efficiency, resulting in further diminished mechanical properties (Figure S3.9). We note

that these reprocessing conditions are not fully optimized for any particular sample; therefore, better reprocessing efficiency is likely possible given the very similar Young's moduli of the as-synthesized, annealed (Figure S3.9, Table S3.1), and reprocessed samples (Table 3.1). This behavior suggests that design of future PHU vitrimers could benefit from the design of higher functional cyclic carbonate cross-linkers or of aliphatic polyamines that lack tertiary amines within the network.

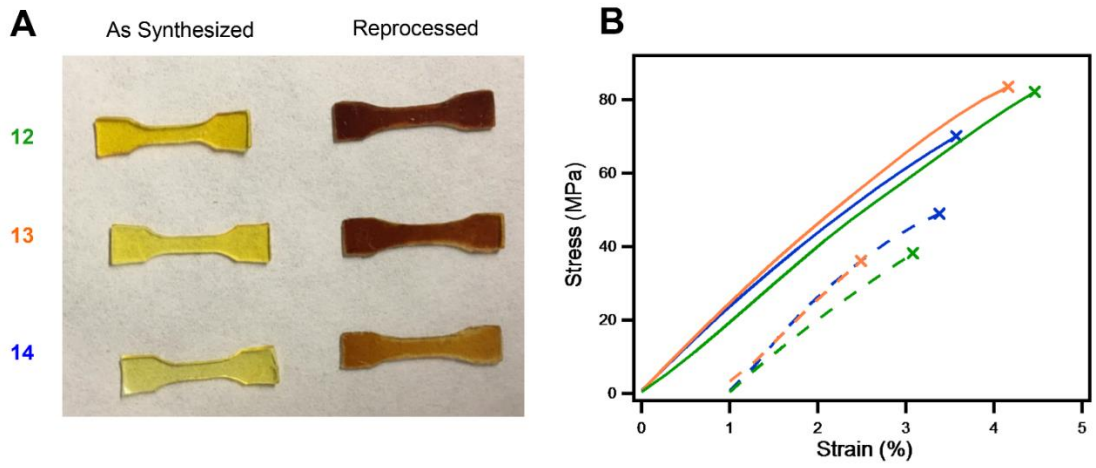

Figure 3.5. A. Photos of as-synthesized (left column) and reprocessed (right column) PHUs **12-14**. Annealed samples have the same level of discoloration as the reprocessed samples. B. Tensile testing data of as-synthesized (solid) and reprocessed (dashed) polyhydroxyurethane **12** (green), **13** (orange), and **14** (blue). Reprocessed samples are shifted right by 1% strain for easier visualization.

3.4 Conclusion

We have evaluated PHU networks derived from 5CCs and 6CCs as reprocessable cross-linked networks. The higher thermodynamic stability of 5CCs leads to reversion and subsequent decomposition in 5CC-derived PHUs at temperatures required for reprocessing in densely cross-linked thermosets, while this decomposition is not observed in networks derived from 6CCs. We have further determined that the Arrhenius activation energy of stress relaxation in a variety of PHUs is highly dependent

on the exact network structure, indicating that multiple processes may be possible for these relaxations or that transcarbamoylation is impacted by the exact nature of the polymer network, either by chemical or mechanical factors. Furthermore, we demonstrate that these cross-linked materials can be reprocessed, although with somewhat diminished mechanical properties; despite the loss of performance, most reprocessed materials would be appropriate for similar structural applications as the pristine materials. We observed that the loss of mechanical properties is more pronounced with increased concentration of tertiary amines within the polymer networks. Therefore, we suggest that development of polyfunctional six-membered cyclic carbonates or polyfunctional aliphatic amines containing no tertiary amines may allow for the synthesis of PHU networks with improved reprocessing capabilities. Taken together, this work demonstrates the promise and design criteria for employing PHUs as sustainable and reprocessable thermoset-like materials.

References

(1) Kloxin, C. J.; Bowman, C. N. *Chem. Soc. Rev.* **2013**, *42*, 7161–7173.

(2) Wojtecki, R. J.; Meador, M. A.; Rowan, S. J. *Nat. Mater.* **2011**, *10*, 14–27.

(3) Roy, N.; Bruchmann, B.; Lehn, J.-M. *Chem. Soc. Rev.* **2015**, *44*, 3786–3807.

(4) Chen, X.; Dam, M. A.; Ono, K.; Mal, A.; Shen, H.; Nutt, S. R.; Sheran, K.; Wudl, F. *Science* **2002**, *295*, 1698–1702.

(5) Scott, T. F.; Schneider, A. D.; Cook, W. D.; Bowman, C. N. *Science* **2005**, *308*, 1615–1617.

(6) Garcia, J. M.; Jones, G. O.; Virwani, K.; McCloskey, B. D.; Boday, D. J.; ter Huurne, G.; Horn, H. W.; Coady, D. J.; Bintaleb, A. M.; Alabdulrahman, A. M. S.; Alsaiwalem, F.; Almegren, H. A. A.; Hedrick, J. L. *Science* **2014**, *344*, 732–735.

(7) Baruah, R.; Kumar, A.; Ujjwal, R. R.; Kedia, S.; Ranjan, A.; Ojha, U. *Macromolecules* **2016**, *49*, 7814–7824.

(8) Imato, K.; Takahara, A.; Otsuka, H. *Macromolecules* **2015**, *48*, 5632–5639.

(9) Ghosh, B.; Urban, M. W. *Science* **2009**, *323*, 1458–1460.

(10) Jin, K.; Li, L.; Torkelson, J. M. *Adv. Mater.* **2016**, *28*, 6746–6750.

(11) Denissen, W.; Winne, J. M.; Du Prez, F. E. *Chem. Sci.* **2016**, *7*, 30–38.

(12) Imbernon, L.; Norvez, S. *Eur. Polym. J.* **2016**, *82*, 347–376.

(13) Montarnal, D.; Capelot, M.; Tournilhac, F.; Leibler, L. *Science* **2011**, *334*, 965–968.

(14) Capelot, M.; Montarnal, D.; Tournilhac, F.; Leibler, L. *J. Am. Chem. Soc.* **2012**, *134*, 7664–7667.

(15) Capelot, M.; Unterlass, M. M.; Tournilhac, F.; Leibler, L. *ACS Macro Lett.* **2012**, *1*, 789–792.

(16) Brutman, J. P.; Delgado, P. A.; Hillmyer, M. A. *ACS Macro Lett.* **2014**, *3*, 607–610.

(17) Pei, Z.; Yang, Y.; Chen, Q.; Terentjev, E. M.; Wei, Y.; Ji, Y. *Nat. Mater.* **2013**, *13*, 36–41.

(18) Altuna, F. I.; Pettarin, V.; Williams, R. J. J. *Green Chem.* **2013**, *15*, 3360-3366.

(19) Lu, Y.-X.; Guan, Z. *J. Am. Chem. Soc.* **2012**, *134*, 14226–14231.

(20) Lu, Y.-X.; Tournilhac, F.; Leibler, L.; Guan, Z. *J. Am. Chem. Soc.* **2012**, *134*, 8424–8427.

(21) Neal, J. A.; Mozhdehi, D.; Guan, Z. *J. Am. Chem. Soc.* **2015**, *137*, 4846–4850.

(22) Martin, R.; Rekondo, A.; Ruiz de Luzuriaga, A.; Cabañero, G.; Grande, H. J.; Odriozola, I. *J. Mater. Chem. A* **2014**, *2*, 5710-5715.

(23) Rekondo, A.; Martin, R.; Ruiz de Luzuriaga, A.; Cabañero, G.; Grande, H. J.; Odriozola, I. *Mater. Horiz.* **2014**, *1*, 237–240.

(24) Pepels, M.; Filot, I.; Klumperman, B.; Goossens, H. *Polym. Chem.* **2013**, *4*, 4955-4965.

(25) Imbernon, L.; Oikonomou, E. K.; Norvez, S.; Leibler, L. *Polym. Chem.* **2015**, *6*, 4271–4278.

(26) Ying, H.; Zhang, Y.; Cheng, J. *Nat. Commun.* **2014**, *5*, 3218-3227.

(27) Zhang, Y.; Ying, H.; Hart, K. R.; Wu, Y.; Hsu, A. J.; Coppola, A. M.; Kim, T. A.; Yang, K.; Sottos, N. R.; White, S. R.; Cheng, J. *Adv. Mater.* **2016**, *28*, 7646–7651.

(28) Denissen, W.; Rivero, G.; Nicolaÿ, R.; Leibler, L.; Winne, J. M.; Du Prez, F. E. *Adv. Funct. Mater.* **2015**, *25*, 2451–2457.

(29) Obadia, M. M.; Mudraboyina, B. P.; Serghei, A.; Montarnal, D.; Drockenmuller, E. *J. Am. Chem. Soc.* **2015**, *137*, 6078–6083.

(30) Zheng, P.; McCarthy, T. J. *J. Am. Chem. Soc.* **2012**, *134*, 2024–2027.

(31) Schmolke, W.; Perner, N.; Seiffert, S. *Macromolecules* **2015**, *48*, 8781–8788.

(32) Taynton, P.; Yu, K.; Shoemaker, R. K.; Jin, Y.; Qi, H. J.; Zhang, W. *Adv. Mater.* **2014**, *26*, 3938–3942.

(33) Cromwell, O. R.; Chung, J.; Guan, Z. *J. Am. Chem. Soc.* **2015**, *137*, 6492–6495.

(34) Fortman, D. J.; Brutman, J. P.; Cramer, C. J.; Hillmyer, M. A.; Dichtel, W. R. *J. Am. Chem. Soc.* **2015**, *137*, 14019–14022.

(35) Krol, P. *Prog. Mater. Sci.* **2007**, *52*, 915–1015.

(36) Zia, K. M.; Bhatti, H. N.; Ahmad Bhatti, I. *React. Funct. Polym.* **2007**, *67*, 675–692.

(37) Yang, W.; Dong, Q.; Liu, S.; Xie, H.; Liu, L.; Li, J. *Procedia Environ. Sci.* **2012**, *16*, 167–175.

(38) Schneiderman, D. K.; Vanderlaan, M. E.; Mannion, A. M.; Panthani, T. R.; Batiste, D. C.; Wang, J. Z.; Bates, F. S.; Macosko, C. W.; Hillmyer, M. A. *ACS Macro Lett.* **2016**, *5*, 515–518.

(39) Wang, Z.; Yang, Y.; Burtovyy, R.; Luzinov, I.; Urban, M. W. *J. Mater. Chem. A* **2014**, *2*, 15527-15534.

(40) Yang, Y.; Urban, M. W. *Angew. Chem. Int. Ed.* **2014**, *53*, 12142–12147.

(41) Zhong, Y.; Wang, X.; Zheng, Z.; Du, P. *J. Appl. Polym. Sci.* **2015**, *132*, 41944-41953.

(42) Zheng, N.; Fang, Z.; Zou, W.; Zhao, Q.; Xie, T. *Angew. Chem. Int. Ed.* **2016**, *55*, 11421–11425.

(43) Offenbach, J. A.; Tobolsky, A., V. *J. Colloid Sci.* **1956**, *11*, 39–47.

(44) Colodny, P. C.; Tobolsky, W. T. *J. Am. Chem. Soc.* **1957**, *79*, 4320–4323.

(45) Yang, L.-Q.; He, B.; Meng, S.; Zhang, J.-Z.; Li, M.; Guo, J.; Guan, Y.-M.; Li, J.-X.; Gu, Z.-W. *Polymer* **2013**, *54*, 2668–2675.

(46) Pratt, R. C.; Nederberg, F.; Waymouth, R. M.; Hedrick, J. L. *Chem. Commun.* **2008**, *1*, 114–116.

(47) Camara, F.; Benyahya, S.; Besse, V.; Boutevin, G.; Auvergne, R.; Boutevin, B.; Caillol, S. *Eur. Polym. J.* **2014**, *55*, 17–26.

(48) North, M.; Pasquale, R.; Young, C. *Green Chem.* **2010**, *12*, 1514-1539.

(49) Nohra, B.; Candy, L.; Blanco, J.-F.; Guerin, C.; Raoul, Y.; Mouloungui, Z. *Macromolecules* **2013**, *46*, 3771–3792.

(50) Blattmann, H.; Fleischer, M.; Bähr, M.; Mülhaupt, R. *Macromol. Rapid Commun.* **2014**, *35*, 1238–1254.

(51) Rokicki, G.; Parzuchowski, P. G.; Mazurek, M. *Polym. Adv. Technol.* **2015**, *26*, 707–761.

(52) Tomita, H.; Sanda, F.; Endo, T. *J. Polym. Sci. Part A: Polym. Chem.* **2001**, *39*, 3678–3685.

(53) Tomita, H.; Sanda, F.; Endo, T. *J. Polym. Sci. Part A: Polym. Chem.* **2001**, *39*, 851–859.

(54) Tomita, H.; Sanda, F.; Endo, T. *J. Polym. Sci. Part A: Polym. Chem.* **2001**, *39*, 162–168.

(55) Clements, J. H. *Ind. Eng. Chem. Res.* **2003**, *42*, 663–674.

(56) Mespouille, L.; Coulembier, O.; Kawalec, M.; Dove, A. P.; Dubois, P. *Prog. Polym. Sci.* **2014**, *39*, 1144–1164.

(57) Suriano, F.; Coulembier, O.; Hedrick, J. L.; Dubois, P. *Polym. Chem.* **2011**, *2*, 528–533.

(58) Brutman, J. P.; De Hoe, G. X.; Schneiderman, D. K.; Le, T. N.; Hillmyer, M. A. *Ind. Eng. Chem. Res.* **2016**, *55*, 11097–11106.

(59) Tomita, H.; Sanda, F.; Endo, T. *J. Polym. Sci. Part A: Polym. Chem.* **2001**, *39*, 860–867.

(60) Maisonneuve, L.; Wirotius, A.-L.; Alfos, C.; Grau, E.; Cramail, H. *Polym. Chem.* **2014**, *5*, 6142–6147.

(61) Yu, K.; Taynton, P.; Zhang, W.; Dunn, M. L.; Qi, H. J. *RSC Adv.* **2014**, *4*, 48682–48690.

CHAPTER THREE APPENDIX

Table of Contents

A. **Materials.** All reagents were purchased from Sigma-Aldrich or Fisher Scientific. Tris(2-aminoethyl)amine (**TREN**) was stirred over calcium hydride and distilled prior to use; all other reagents were used without further purification. Dichloromethane (CH_2Cl_2), tetrahydrofuran (THF), and dimethylformamide (DMF) were purchased from Fisher Scientific and purified using a custom-built alumina-column based solvent purification system. Other solvents were used without further purification. Di(trimethylolpropane)-based bis(cylic carbonate) **2**,[1] 6CC-based hydroxyurethane model compound **6**,[2] and carboxylic acid functionalized 6CC (**7**)[3] were synthesized according to the literature procedures.

General Characterization[2]

Infrared spectra were recorded on a Thermo Nicolet iS10 or a Bruker Alpha Platinum; both were equipped with a diamond ATR attachment and spectra were uncorrected.

Gas chromatography/electron impact mass spectrometry was performed on an Agilent 6890N Network GC System with a JEOL JMS-GCmate II Mass Spectrometer (magnetic sector). Di-tert-butylbiphenyl or triphenylmethane were utilized as internal standards.

NMR spectra were recorded on a Varian 400 MHz or an Agilent DD MR-400 400 MHz spectrometer using a standard ^{1}H/X Z-PFG probe at ambient temperature.

Thermogravimetric analysis (TGA) was performed on a Mettler Toledo SDTA851 Thermogravimetric Analysis System. Samples were heated under a nitrogen atmosphere at a rate of 10 °C/min from 30 ºC to 600 ºC.

Differential scanning calorimetry (DSC) was performed on a TA instruments Q1000 Differential Scanning Calorimeter or a Mettler Toledo DSC822 Differential Scanning Calorimeter. Samples were heated at a rate of 10 °C/min to at least 130 °C to erase thermal history, cooled to at least -30 °C at 10 °C/min, and then heated to at least 130 °C. All data shown are taken from the second heating ramp. The glass transition temperature (T_g) was calculated from the maximum value of the derivative of heat flow with respect to temperature.

Dynamic mechanical thermal analysis (DMTA) was performed on a TA Instruments RSA-G2 analyzer (New Castle, DE) utilizing rectangular films (*ca.* 0.5 mm (T) × 5 mm (W) × 10 mm (L)). The axial force was adjusted to 0 N and a strain adjust of 30% was set with a minimum strain of 0.05%, a maximum strain of 5%, and a maximum force of 1 N in order to prevent the sample from buckling or going out of the specified strain. Furthermore, a force tracking mode was set such that the axial force was twice the magnitude of the oscillation force. A temperature ramp was then performed from 20 °C to 200 °C (-40°C to 200 °C for low glass transition materials) at a rate of 5 °C/min, with an oscillating strain of 0.05% and an angular frequency of 6.28 rad s^{-1} (1 Hz). The glass transition temperature (T_g) was calculated from the maximum value of the loss modulus (G").

Uniaxial tensile testing was conducted using dog bone shaped tensile bars (*ca.* 0.5 mm (T) × 3 mm (W) × 25 mm (L) and a gauge length of 14 mm). The samples were aged for at least 48 h at 22 °C in a desiccator prior to testing. Tensile measurements were performed on a Shimadzu Autograph AGS-X Series tensile tester (Columbia, MD) at 22 °C with a uniaxial extension rate of 5 mm/min. Young's modulus (E) values were

calculated using the Trapezium software by taking the slope of the stress-strain curve from 0 to 1 N of force applied. Reported values are the average and standard deviations of at least five samples.

Stress relaxation analysis (SRA) was performed on a TA Instruments RSA-G2 analyzer (New Castle, DE) utilizing rectangular films (*ca.* 0.5 mm (T) × 5 mm (W) × 10 mm (L)). The SRA experiments were performed in a strain control at specified temperature (170-190 °C). The samples were allowed to equilibrate at this temperature for approximately 10 minutes, after which the axial force was then adjusted to 0 N with a sensitivity of 0.05 N. Subsequently, each sample was subjected to an instantaneous 5% strain. The stress decay was monitored, while maintaining a constant strain (5%), until the stress relaxation modulus had relaxed to at least 37% (1/*e*) of its initial value. This was performed three times for each sample. The activation energy (E_a) and freezing transition temperature (T_v) were determined utilizing the methodology in literature.[15,16]

To reprocess the materials, the polymer was broken into small pieces and then placed into a PTFE coated (Sprayon MR311) aluminum dog bone shaped mold (*ca.* 0.5 mm (T) × 3 mm (W) × 25 mm (L) and a gauge length of 14 mm) between two thin Teflon® sheets. This assembly was placed in a Wabash-MPI compression mold (Wabash, IN), which was preheated to the desired temperature. The material was allowed to thermally equilibrate for two minutes, following a two- minute period of rapidly increasing the pressure to 4 MPa then reducing back to 0 MPa in order to remove air bubbles. The pressure was then increased to 4 MPa and allowed to heat for varying periods of time and then rapidly cooled to room temperature over the course of 5 minutes using the water cooling function of the compression mold. A similar procedure

was performed for rubbery samples, which were compression molded in a square mold (5 cm x 5 cm), and tensile specimens were punched from the sheets after cooling. The resulting tensile bars were then allowed to age for 48 h in a desiccator and subjected to uniaxial tensile testing in order to determine their recovery in mechanical properties. Reported values are the average and standard deviations of at least five samples.

Annealed samples were prepared by heating as-synthesized tensile bars of the cross-linked polymers in an oven under a nitrogen atmosphere. The resulting tensile bars were aged for 48 h in a desiccator and subjected to uniaxial tensile testing to compare their mechanical properties to as-synthesized or reprocessed samples. Reported values are the average and standard deviations of at least five samples.

B. Synthetic Procedures

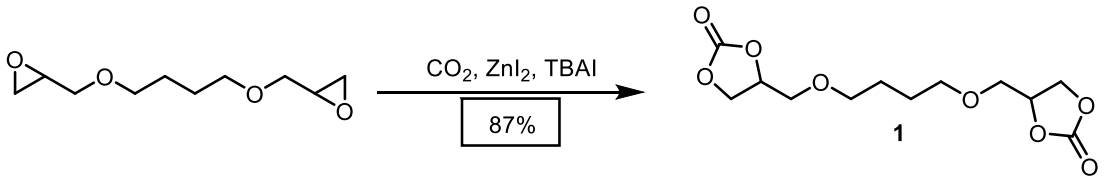

Synthesis of 1: To a stainless steel pressure reactor was added 1,4-butanediol diglycidyl ether (11.95 g, 59.2 mmol), zinc iodide (180 mg, 0.5 mmol), and tetrabutylammonium iodide (180 mg, 0.5 mmol). The reactor was sealed and pressurized with 100 psi carbon dioxide, then heated to 100 °C for 36 hours, while stirring the mixture. The reactor was allowed to cool and the residue was diluted with CH_2Cl_2 (300 mL), washed with H_2O (2 x 200 mL), dried over $MgSO_4$, filtered, and the solvent was removed at reduced pressure to yield an off-white solid. The solid was recrystallized from EtOH to yield **1** as a white solid (14.9 g, 87%). ^{1}H NMR (400 MHz, $CDCl_3$) δ 4.85-4.77 (m, 2H), 4.60 (t, *J* = 8.4 Hz, 2H), 4.44-4.37 (m, 2H), 3.74-3.47 (m, 8H), 1.68-1.61 (m, 4H). ^{13}C NMR (100 MHz, $CDCl_3$) δ 155.0, 75.1, 71.3, 69.4, 66.0, 25.8. IR (solid, ATR) 2869, 1779 (C=O), 1396, 1101, 1073, 1043, 767, 713 cm^{-1}. The ^{1}H and ^{13}C NMR data match those previously reported.[4]

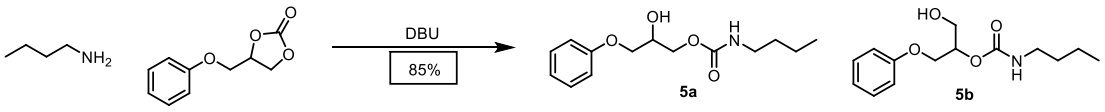

Synthesis of 5CC Hydroxyurethane Model Compound (5): In a round-bottom flask, 3-phenoxypropylenecarbonate (1.0 g, 5.13 mmol) and *n*-butylamine (413 mg, 5.64 mmol) were dissolved in anhydrous DMF (5.0 mL). The mixture was heated to 70 °C, and 1,8-diazabicyclo[5.4.0]undec-7-ene (DBU, 78 mg, 76 µL, 0.5 mmol) was added via syringe. The mixture was stirred at 70 ºC for 12 hours, then cooled to room temperature.

The solution was partitioned between H_2O (50 mL) and EtOAc (50 mL), and the aqueous layer was washed with EtOAc (2 x 50 mL). The combined organic layers were dried over $MgSO_4$, filtered, and solvent was removed at reduced pressure to yield a yellowish oil. The resulting oil was chromatographed in EtOAc to yield the mixture of products as a colorless oil, which slowly solidified to a white, waxy solid (1.16 g, 85 %). ^{1}H NMR (400 MHz, $CDCl_3$) δ 7.31-7.25 (m), 6.99-6.94 (m), 6.94-6.90 (m), 5.11-5.00 (m), 4.33-4.12 (m), 4.01 (d, *J* = 5.6 Hz, major), 3.89 (t, *J* = 5.2 Hz, minor), 3.50 (d, *J* = 4.0 Hz, minor), 3.17 (q, *J* = 6.5 Hz), 2.99 (t, *J* = 6.2 Hz, minor), 2.13 (s, major), 2.05 (s, major), 1.53-1.41 (m), 1.40-1.24 (m), 0.92 (t, *J* = 7.5 Hz). ^{13}C NMR (100 MHz, $CDCl_3$) δ 158.3, 156.8 (major C=O), 156.2 (minor C=O), 129.4, 121.1, 114.5, 73.4 (minor), 68.9 (major), 68.4 (major), 66.5 (minor), 65.9 (major), 62.2 (minor), 40.8, 31.8, 19.8, 13.6. IR (solid, ATR) 3337, 2957, 2871, 1689 (C=O stretch), 1540 (N-H deformation), 1232, 1059, 752 cm^{-1}. HRMS (ESI) calcd. for $[C_{14}H_{21}NO_4+Na]^+$ 290.1363 found 290.1369.

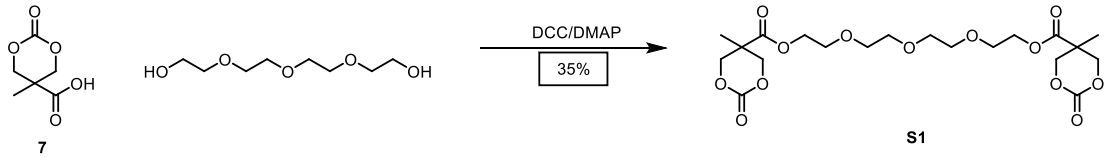

7 S1

Synthesis of S1. To a flame-dried round-bottom flask under nitrogen atmosphere was added **7** (4.00 g, 25 mmol), tetraethylene glycol (2.33 g, 12 mmol), and 25 mL anhydrous DMF. To the homogeneous solution was added 4-dimethylaminopyridine (300 mg, 2.5 mmol), and the solution was allowed to stir until the DMAP had fully dissolved. The solution was cooled to 0°C, solid N,N'-dicylcohexylcarbodiimide (5.30 g, 25.7 mmol) was added, and a white precipitate formed. The resulting mixture was

allowed to stir and warm to room temperature for 18 hours. The mixture was filtered, and solid was washed with 200 mL EtOAc. The EtOAc was removed at reduced pressure, and 250 mL Et_2O was added; this mixture was allowed to stand until an oil separated from the Et_2O layer. The resulting oil was chromatographed on silica gel in 20% acetone/EtOAc to yield **S1** as a colorless oil (2.0 g, 35%). ^{1}H NMR (300 MHz, $CDCl_3$) δ 4.71 (d, *J* = 10.9 Hz, 4H), 4.36 (m, 4H), 4.21 (d, *J* = 10.9 Hz, 4H), 3.70 (m, 4H), 3.63 (m, 8H), 1.32 (s, 6H). ^{13}C NMR (75 MHz, $CDCl_3$) δ 170.6, 146.9, 72.3, 69.7, 67.9, 64.1, 39.5, 16.4. IR (neat, ATR) 2924, 1755, 1732, 1464, 1403, 1237, 1172, 1132, 1097, 1029 cm^{-1}. HRMS (ESI) calcd. for $[C_{20}H_{30}O_{13}+H]^+$ 479.1759 found 479.1769.

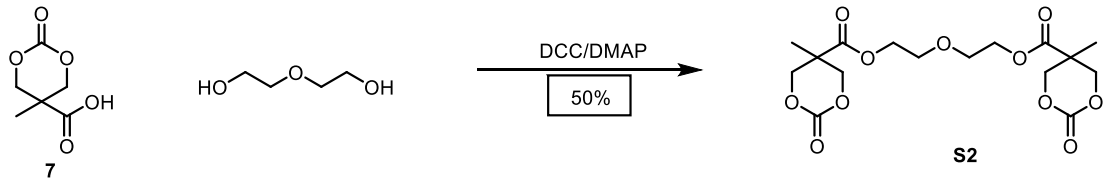

Synthesis of S2. To a flame-dried round-bottom flask under nitrogen atmosphere was added **7** (4.00 g, 25 mmol), diethylene glycol (1.28 g, 12 mmol), and 25 mL anhydrous DMF. To the homogeneous solution was added 4-dimethylaminopyridine (300 mg, 2.5 mmol), and the solution was allowed to stir until the DMAP had fully dissolved. The solution was cooled to 0°C, solid N,N'-dicylcohexylcarbodiimide (5.30 g, 25.7 mmol) was added, and a white precipitate formed. The resulting mixture was allowed to stir and warm to room temperature for 18 hours. The mixture was filtered, and solid was washed with 200 mL EtOAc. The EtOAc was removed at reduced pressure, 250 mL Et_2O was added, and the mixture was cooled, resulting in separation of a yellowish oil. The resulting oil was chromatographed on silica gel in 10% acetone/EtOAc to yield compound **S2** as a yellowish oil (2.37 g, 50%). ^{1}H NMR (400 MHz, $CDCl_3$) δ 4.71 (d,

J = 10.8 Hz, 4H), 4.35 (m, 4H), 4.28 (d, *J* = 10.8 Hz, 4H), 3.69 (m, 4H), 1.33 (s, 6H). ^{13}C NMR (100 MHz, $CDCl_3$) δ 171.0, 147.4, 72.8, 68.5, 64.7, 40.1, 17.2. IR (neat, ATR) 2962, 1747, 1728, 1463, 1403, 1236, 1170, 1131, 1096, 1031 cm^{-1}. HRMS (ESI) calcd. for $[C_{16}H_{22}O_{11}+H]^+$ 391.1235 found 391.1245.

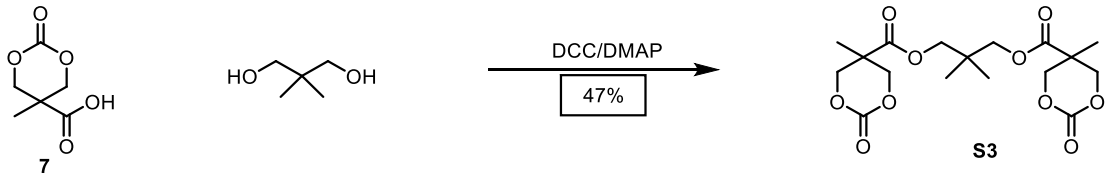

Synthesis of S3. To a flame-dried round-bottom flask under nitrogen atmosphere was added **7** (4.00 g, 25 mmol), neopentyl glycol (1.25 g, 12 mmol), and 25 mL anhydrous DMF. To the homogeneous solution was added 4-dimethylaminopyridine (300 mg, 2.5 mmol), and the solution was allowed to stir until the DMAP had fully dissolved. The solution was cooled to 0°C, solid N,N'-dicylcohexylcarbodiimide (5.30 g, 25.7 mmol) was added, and a white precipitate formed. The resulting mixture was allowed to stir and warm to room temperature for 18 hours. The mixture was filtered, and solid was washed with 200 mL EtOAc. The EtOAc was removed at reduced pressure, and 250 mL Et_2O was added, resulting in the formation of a white solid. The solid was recrystallized from 250 ml toluene to yield **S3** as white, needle-like crystals (2.2 g, 47%). ^{1}H NMR (300 MHz, DMSO) δ 4.56 (d, *J* = 10.4 Hz, 4H), 4.37 (d, *J* = 10.4 Hz, 4H), 3.97 (s, 4H), 1.18 (s, 6H), 0.94 (s, 6H). ^{13}C NMR (75 MHz, DMSO) δ 171.5, 147.2, 72.5, 69.4, 39.9, 34.7, 21.1, 16.3. IR (solid, ATR) 2965, 1741, 1725, 1469, 1397, 1237, 1172, 1133, 1095 cm^{-1}. HRMS (ESI) calcd. for $[C_{17}H_{24}O_{10}+H]^+$ 389.1442 found 389.1451.

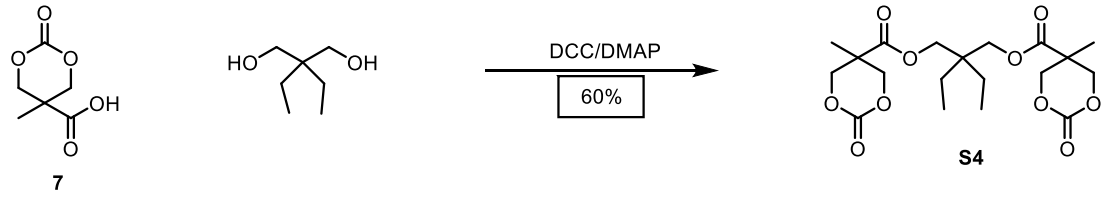

Synthesis of S4. To a flame-dried round-bottom flask under nitrogen atmosphere was added **7** (4.00 g, 25 mmol), 2,2-diethylpropane-1,3-diol (1.59 g, 12 mmol), and 25 mL anhydrous DMF. To the homogeneous solution was added 4-dimethylaminopyridine (300 mg, 2.5 mmol), and the solution was allowed to stir until the DMAP had fully dissolved. The solution was cooled to 0°C, solid N,N'-dicylcohexylcarbodiimide (5.30 g, 25.7 mmol) was added, and a white precipitate formed. The resulting mixture was allowed to stir and warm to room temperature for 18 hours. The mixture was filtered, and solid was washed with 200 mL EtOAc. The EtOAc was removed at reduced pressure, and 250 mL Et_2O was added, resulting in the formation of a white solid. The solid was recrystallized from 250 ml toluene to yield **S4** as white crystals (2.98 g, 60%). ^{1}H NMR (400 MHz, $CDCl_3$) δ 4.67 (d, *J* = 10.8 Hz, 4H), 4.22 (d, *J* = 10.8 Hz, 4H), 4.06 (s, 6H), 1.37 (q, *J* = 7.9 Hz, 4H), 1.32 (s, 6H), 0.96 (t, *J* = 7.9 Hz, 6H). ^{13}C NMR (100 MHz, $CDCl_3$) δ 170.9, 147.3, 72.9, 66.4, 40.4, 40.0, 22.8, 17.2, 6.8. IR (solid, ATR) 2976, 1754, 1724, 1469, 1396, 1233, 1173, 1134, 1096 cm^{-1}. HRMS (ESI) calcd. for $[C_{19}H_{28}O_{10}+H]^+$ 417.1755 found 417.1767.

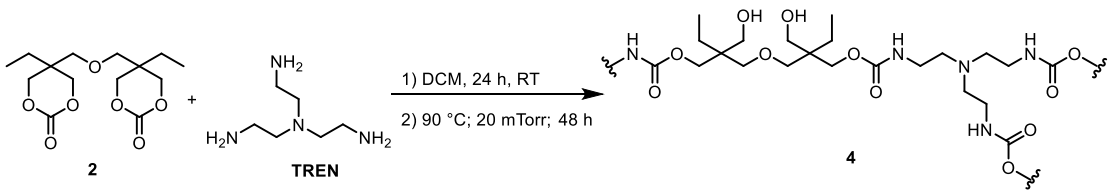

Synthesis of 4: 2 (798.0mg, 2.639 mmol, 1 eq. cyclic carbonate) was dissolved in a minimal amount of anhydrous DCM (*ca.* 3.0 mL) along with tris(2-aminoethyl)amine

(**TREN**) (257.3mg, 1.760mmol, 1 eq. amine to cyclic carbonate). Solutions were sonicated for one minute to ensure homogeneity, then poured into an aluminum mould (60 mm D x 10 mm H), and allowed to stand at room temperature for *ca*. 24 hours. Samples were cut from the resulting films, and placed under reduced pressure at 90 °C and 20 mTorr for *ca*. 48 hours to ensure complete cross-linking and removal of solvent, yielding polymer **4** as a hard, orange solid. IR (solid, ATR) 3297, 2962, 2880, 1689 (C=O stretch), 1527 (N-H deformation), 1460, 1257, 1105, 1020 cm^{-1}. The characterization data match those previously reported in the literature.[2]

Identical procedures were performed with appropriate cyclic carbonate and amine(s) to obtain the following polymers as orange solids; polymers **12**-**14** were first heated to 60 ºC at 20 mTorr vacuum to avoid bubbling:

3: IR (solid, ATR) 3316 (O-H stretch), 2940, 2866, 1688 (C=O stretch), 1530 (N-H deformation), 1456, 1247, 1104, 775 cm^{-1}.

8: IR (solid, ATR) 3360 (O-H stretch), 2880, 1716 (shoulder), 1695 (C=O stretch), 1530 (N-H deformation), 1456, 1242, 1121, 1047 cm^{-1}.

9: IR (solid, ATR) 3342 (O-H stretch), 2944, 1716 (shoulder), 1691 (C=O stretch), 1528 (N-H deformation), 1458, 1242, 1120, 1044 cm^{-1}.

10: IR (solid, ATR) 3366 (O-H stretch), 2962, 1720 (shoulder), 1694 (C=O stretch), 1529 (N-H deformation), 1463, 1241, 1126, 1045, 1019 cm^{-1}.

11: IR (solid, ATR) 3365 (O-H stretch), 2966, 1726 (shoulder), 1696 (C=O stretch), 1529 (N-H deformation), 1461, 1238, 1128, 1046 cm^{-1}.

12: IR (solid, ATR) 3317 (O-H stretch), 2930, 2880, 1687 (C=O stretch), 1531 (N-H deformation), 1461, 1250, 1110, 1031 cm^{-1}.

13: IR (solid, ATR) 3308 (O-H stretch), 2931, 2879, 1687 (C=O stretch), 1531 (N-H deformation), 1249, 1107, 1033 cm^{-1}.

14: IR (solid, ATR) 3298 (O-H stretch), 2929, 1688 (C=O stretch), 1532 (N-H deformation), 1462, 1250, 1107, 1033 cm^{-1}.

C. Characterization Tables and Figures

Table S3.1. Tensile Testing Data of Annealed Samples and Multiply Reprocessed Samples

	Annealed			
Polymer	σ_b (MPa)	ε_b (%)	E (GPa)	Temp (°C); Time (min) annealed
4 (Ref. 2)	72 ± 11	6.9 ± 3.8	2.2 ± 0.4	160; 480
8	1.37 ± 0.04	165 ± 12	(1.3 ± 0.1) x 10^{-3}	160; 280
9	16 ± 3	194 ± 7	0.5 ± 0.2	160; 225
10	70 ± 12	2.7 ± 0.4	3.0 ± 0.4	160; 570
11	63 ± 6	3.0 ± 0.4	2.5 ± 0.3	160; 495
12	78 ± 7	3.7 ± 0.3	2.5 ± 0.5	160; 580
13	76 ± 4	4.3 ± 0.4	2.4 ± 0.1	160; 545
14	69 ± 10	3.6 ± 0.7	2.5 ± 0.1	160; 400
Second Reprocessing Cycle				
11	35 ± 8	1.5 ± 0.4	2.4 ± 0.1	160; 495
14	32 ± 10	1.7 ± 0.8	2.1 ± 0.2	160; 400

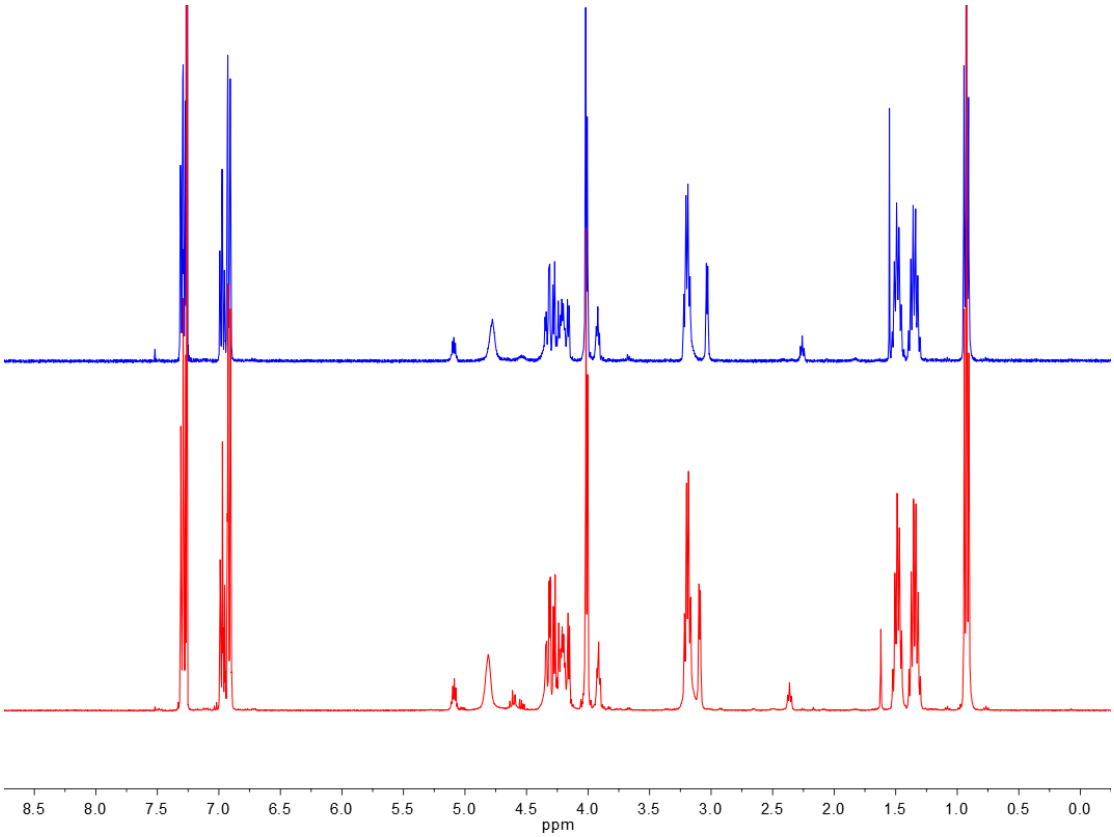

Figure S3.1. ^{1}H NMR Spectra (400 MHz, $CDCl_3$) of model compound mixture **5** before (blue) and after heating at 170 °C for 5 hours (red). The sharp peaks from *ca*. 4.50-4.65 are characteristic of the parent cyclic carbonate.

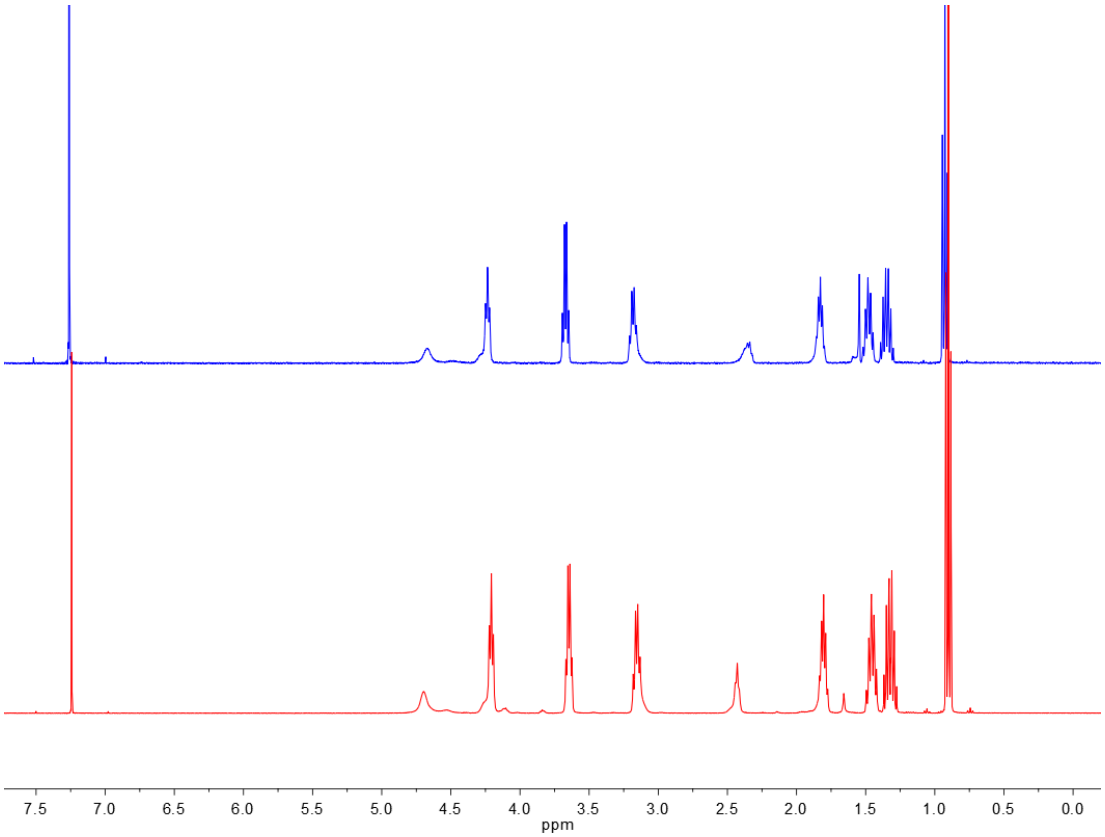

Figure S3.2. ^{1}H NMR Spectra (400 MHz, $CDCl_3$) of model compound **6** before (blue) and after heating at 170 °C for 5 hours (red). No cyclic carbonate is observed.

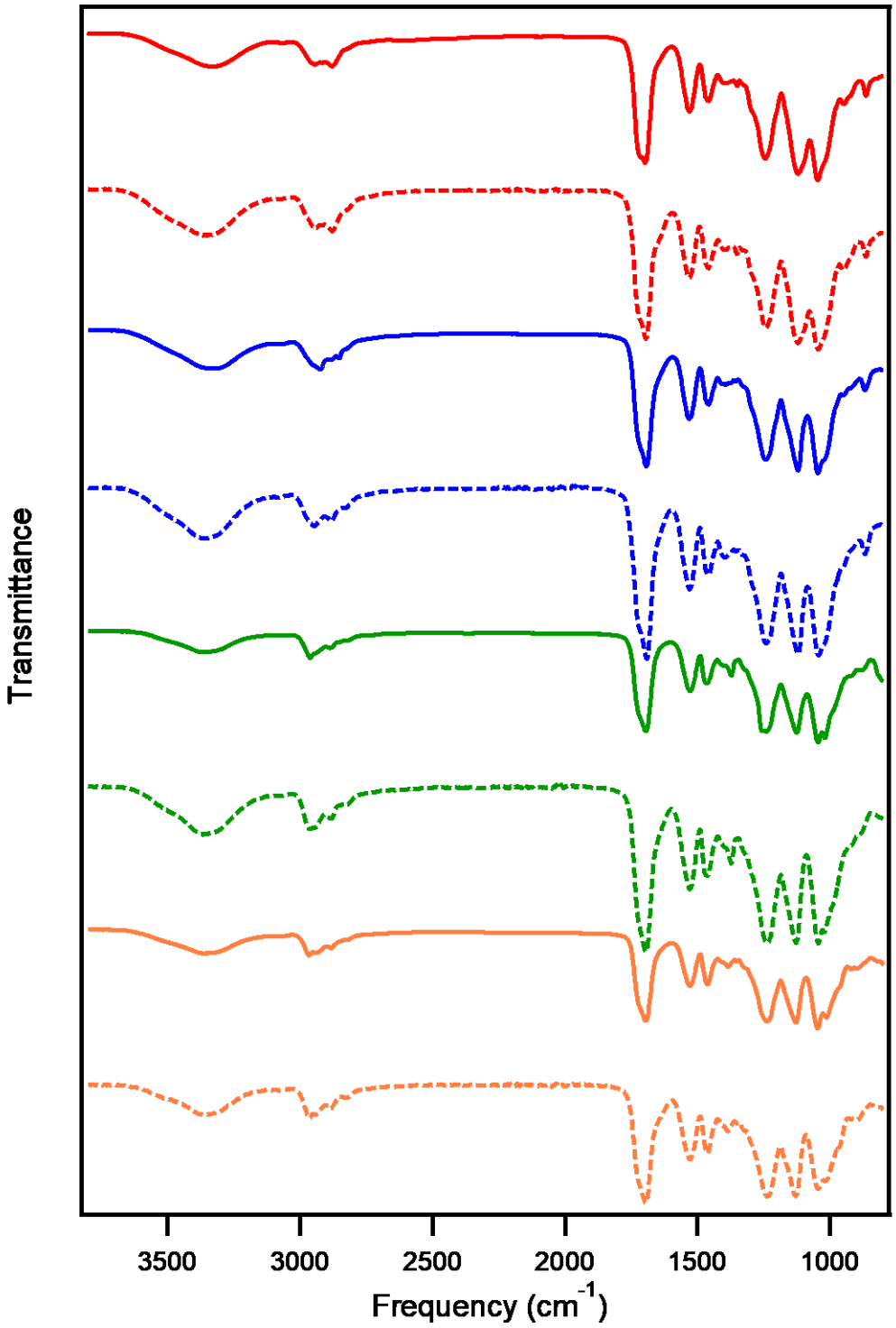

Figure S3.3. FT-IR spectra of **8** (red), **9** (blue), **10** (green), and **11** (orange) before (solid) and after (dashed) stress relaxation analysis at 190 ºC.

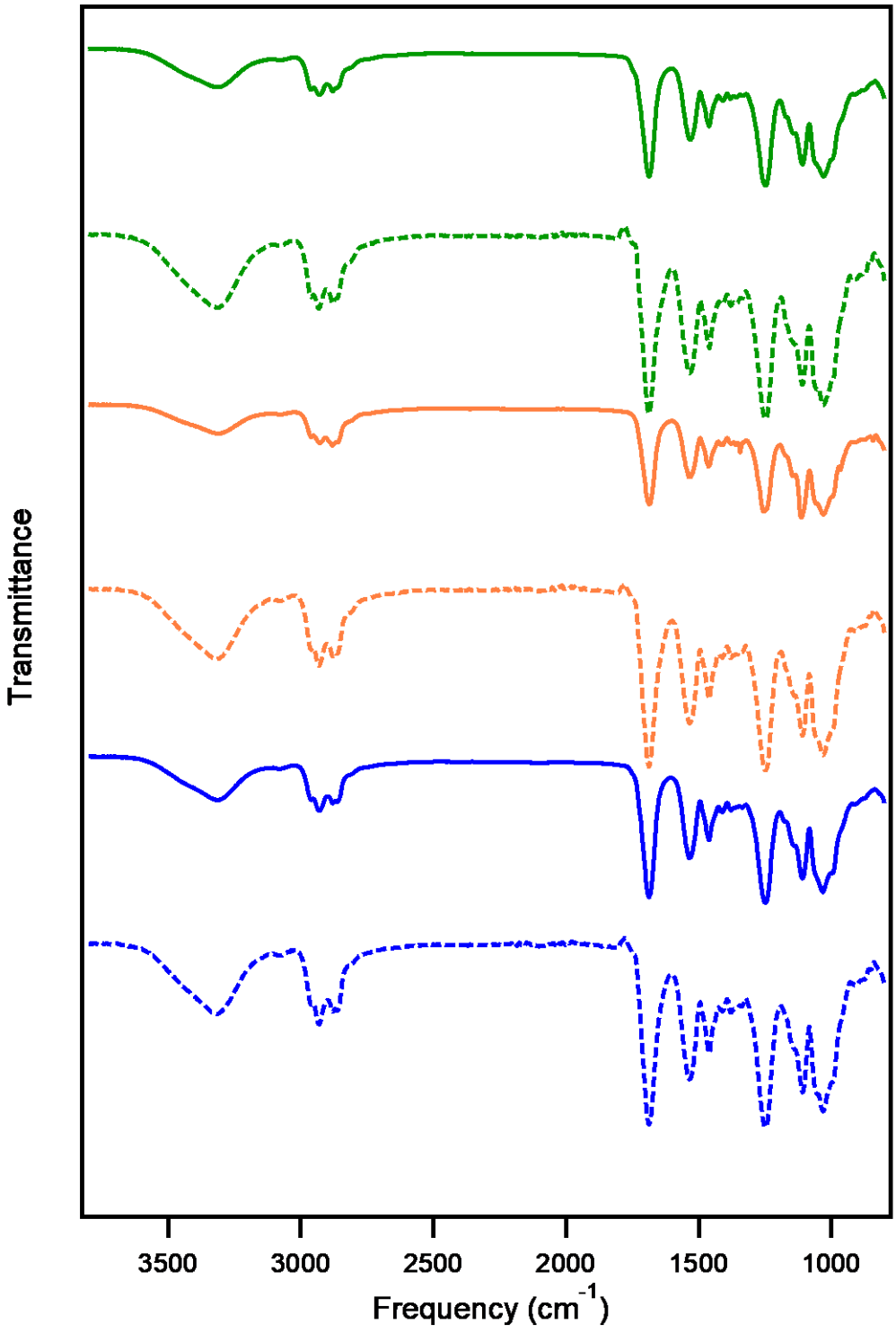

Figure S3.4. FT-IR spectra of **12** (green), **13** (orange), and **14** (blue), before (solid) and after (dashed) stress relaxation analysis at 190 ºC.

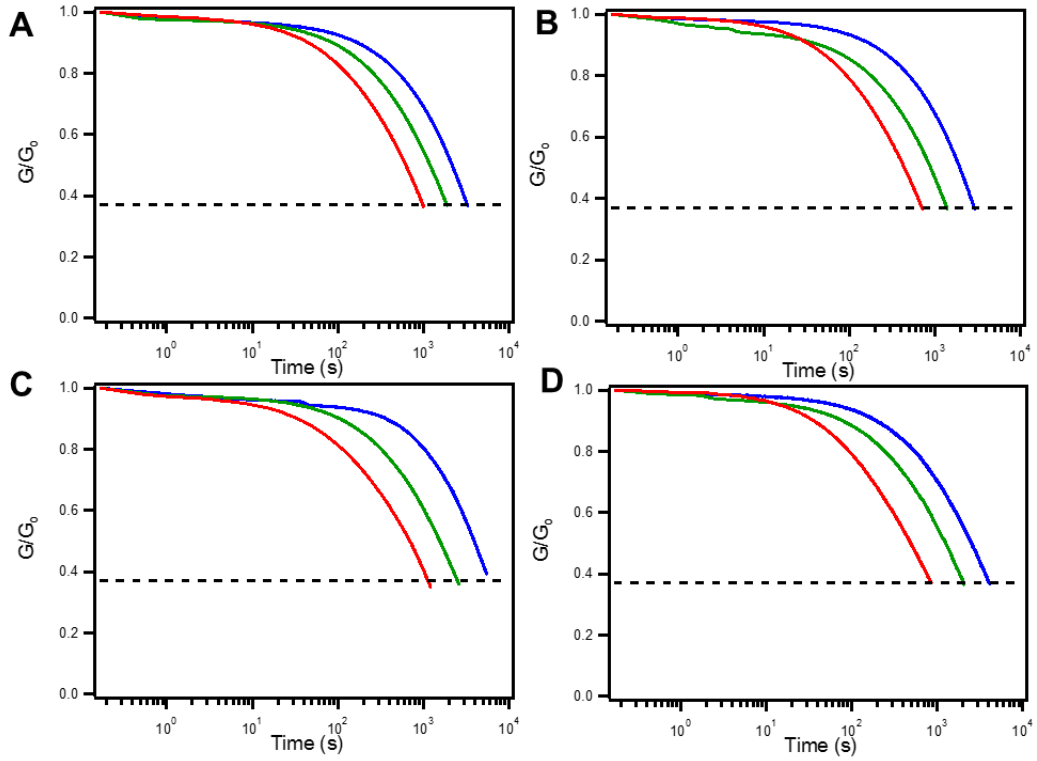

Figure S3.5. Representative normalized stress relaxation analysis curves for A. polymer **8**, B. polymer **9**, C. polymer **10**, and D. polymer **11** at 190 °C (red), 180 °C (green), and 170 °C (blue). The dashed line represents the characteristic relaxation time, τ*.

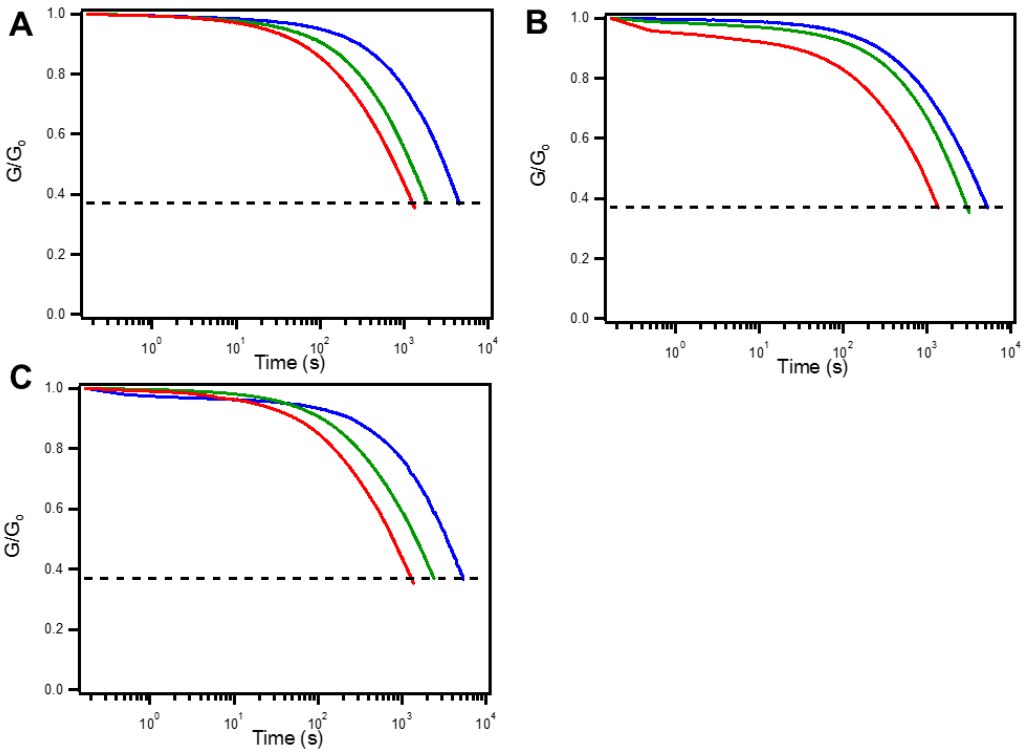

Figure S3.6. Representative normalized stress relaxation analysis curves for A. polymer **12**, B. polymer **13**, and C. polymer **14** at 190 °C (red), 180 °C (green), and 170 °C (blue). The dashed line represents the characteristic relaxation time, τ*.

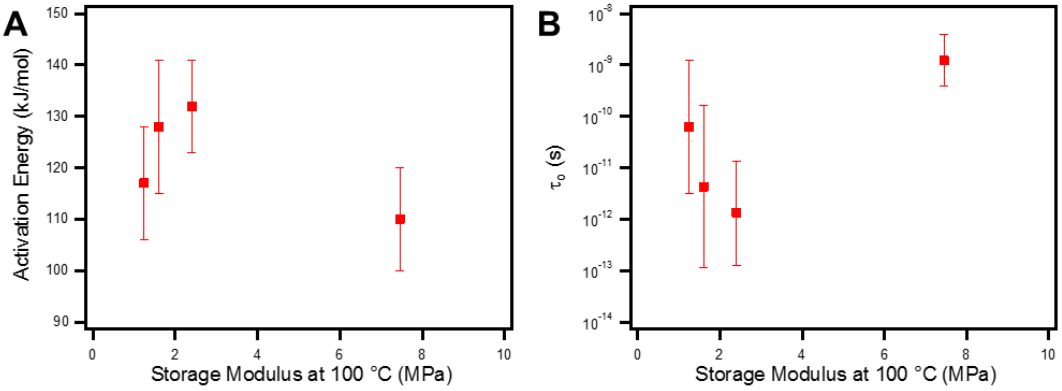

Figure S3.7. A. Arrhenius activation energy of stress relaxation and B. τ_o, the pre-exponential factor of the Arrhenius relationship between τ* and temperature as a function of rubbery storage modulus for polymers **4** and **12-14**.

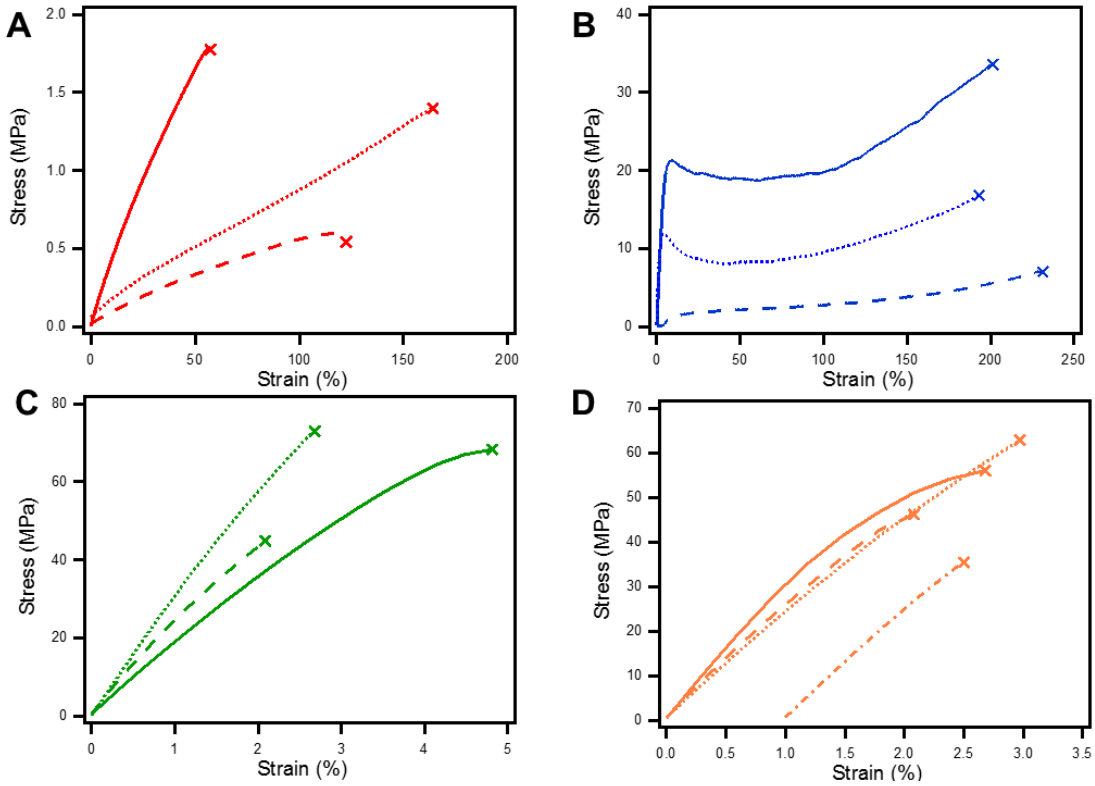

Figure S3.8. Representative stress-strain curves of as-synthesized (solid), annealed under nitrogen for 3τ* (dotted), and reprocessed via compression molding for 3τ* (dashed) A. polymer **8**, B. polymer **9**, C. polymer **10**, and D. polymer **11**. The results of a second reprocessing cycle on polymer **11** are shown in D, as a dashed-dotted line, which is offset by 1% strain for easier visualization.

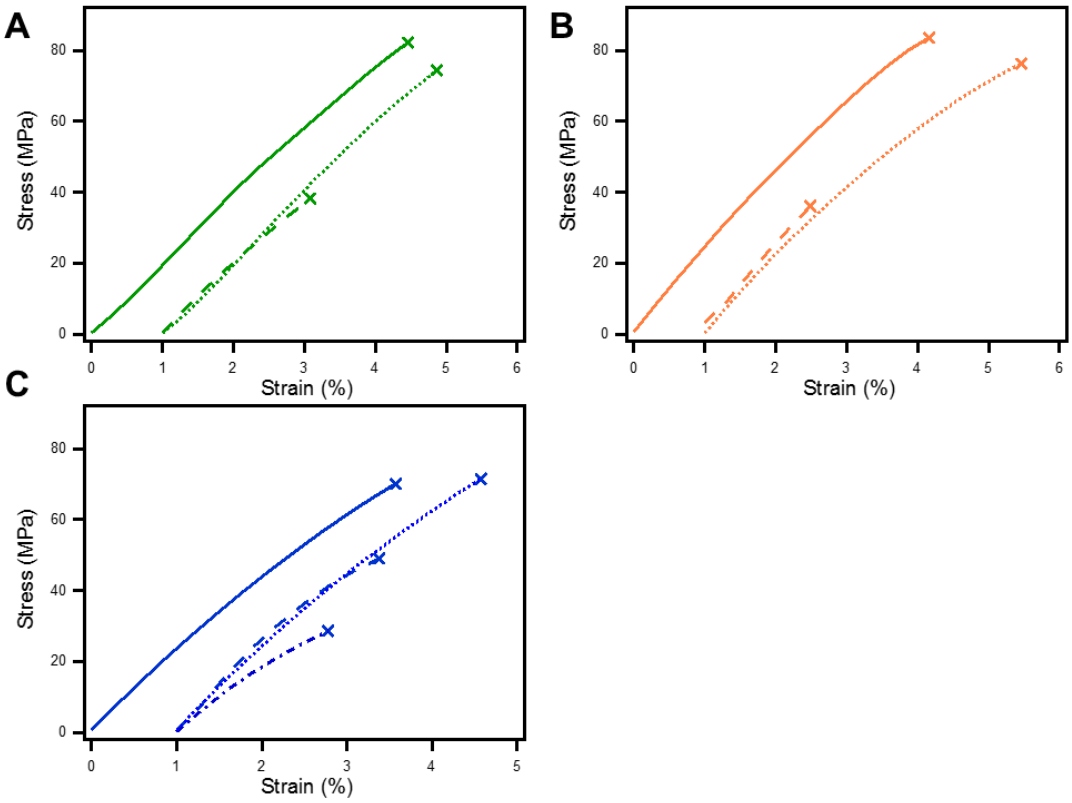

Figure S3.9. Representative stress-strain curves of as-synthesized (solid), annealed under nitrogen for 3τ* (dotted), and reprocessed via compression molding for 3τ* (dashed) A. polymer **12**, B. polymer **13**, and C. polymer **14**. The annealed and reprocessed traces are shifted to the right by 1% strain for easier visualization. The results of a second reprocessing cycle on polymer **14** are shown in C, as a dashed-dotted line, which is also offset by 1% strain for easier visualization.

D. NMR Spectra

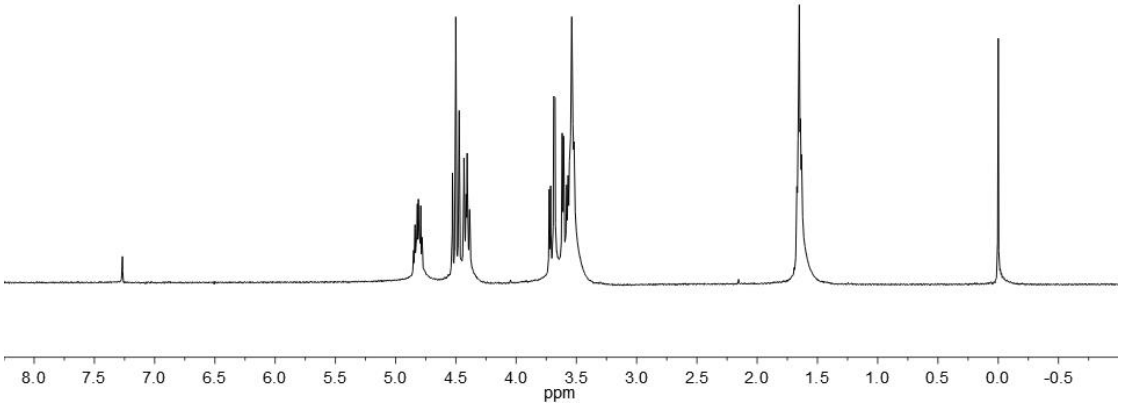

Figure S3.10. ^{1}H NMR ($CDCl_3$, 300 MHz, 298K) of bis(cyclic carbonate) **1**.

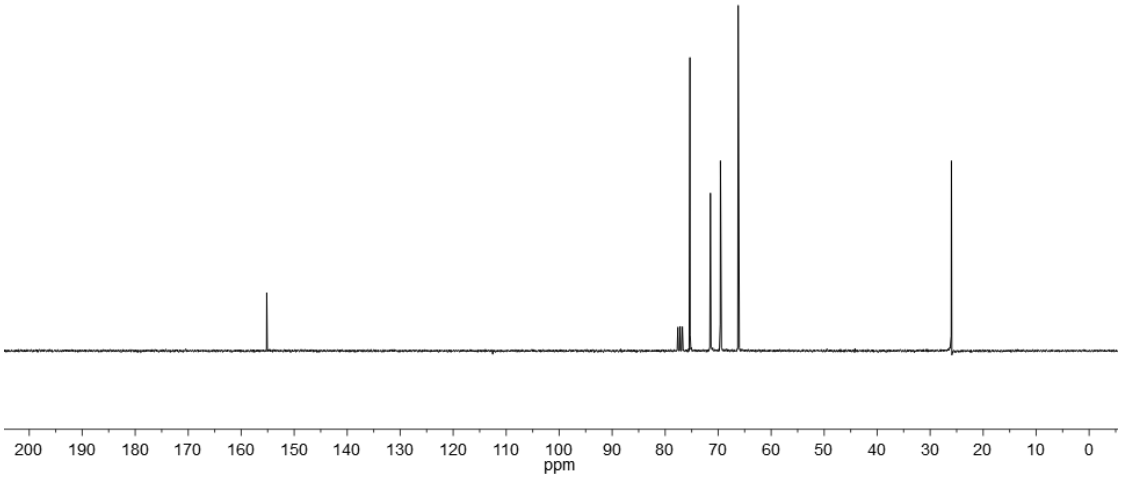

Figure S3.11. ^{13}C NMR ($CDCl_3$, 75 MHz, 298K) of bis(cyclic carbonate) **1**.

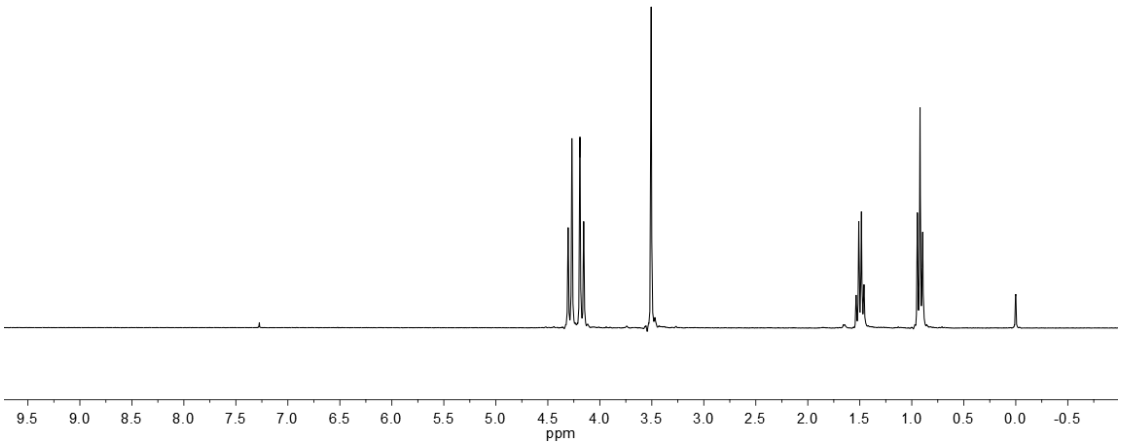

Figure S3.12. ^{1}H NMR ($CDCl_3$, 300 MHz, 298 K) of bis(cyclic carbonate) **2.**

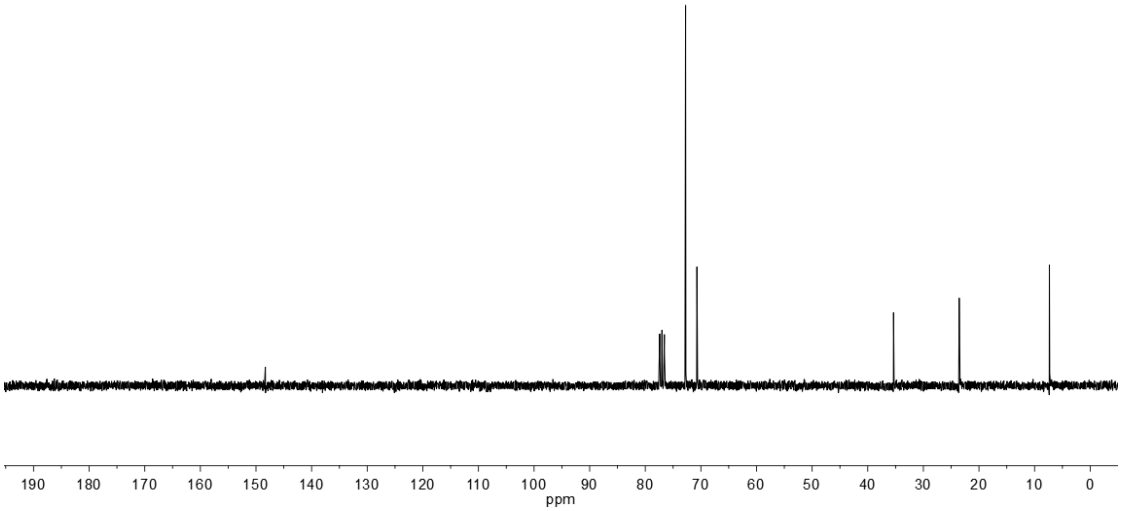

Figure S3.13. ^{13}C NMR ($CDCl_3$, 75 MHz, 298 K) of bis(cyclic carbonate) **2**.

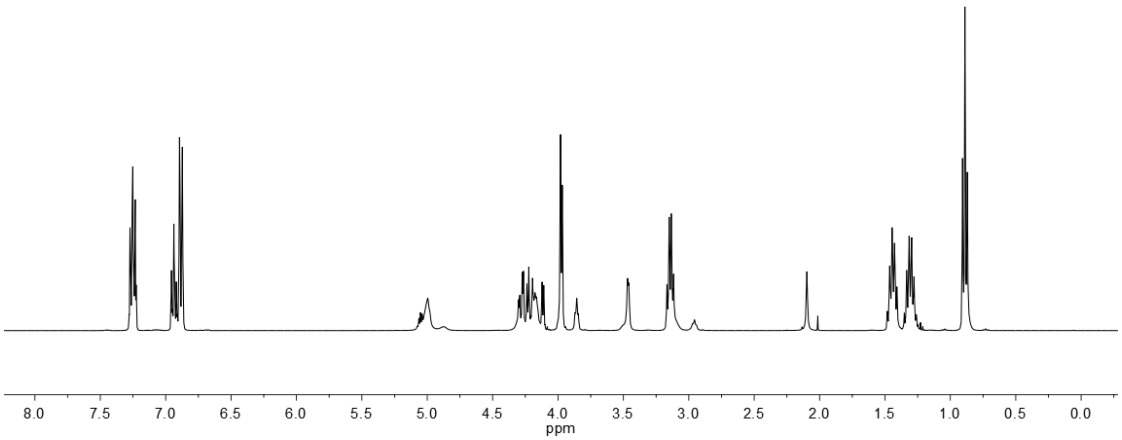

Figure S3.14. ^{1}H NMR (400 MHz, $CDCl_3$, 298K) of hydroxyurethane mixture **5**.

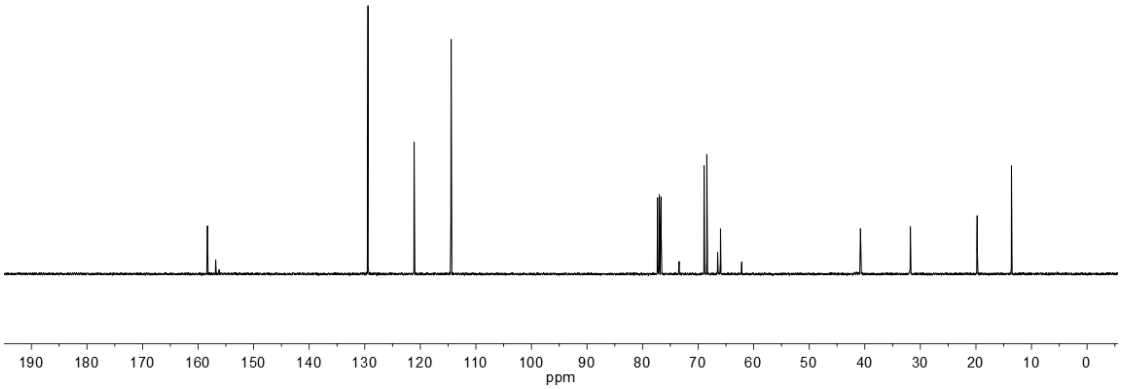

Figure S3.15. ^{13}C NMR (100 MHz, $CDCl_3$, 298K) of hydroxyurethane mixture **5**.

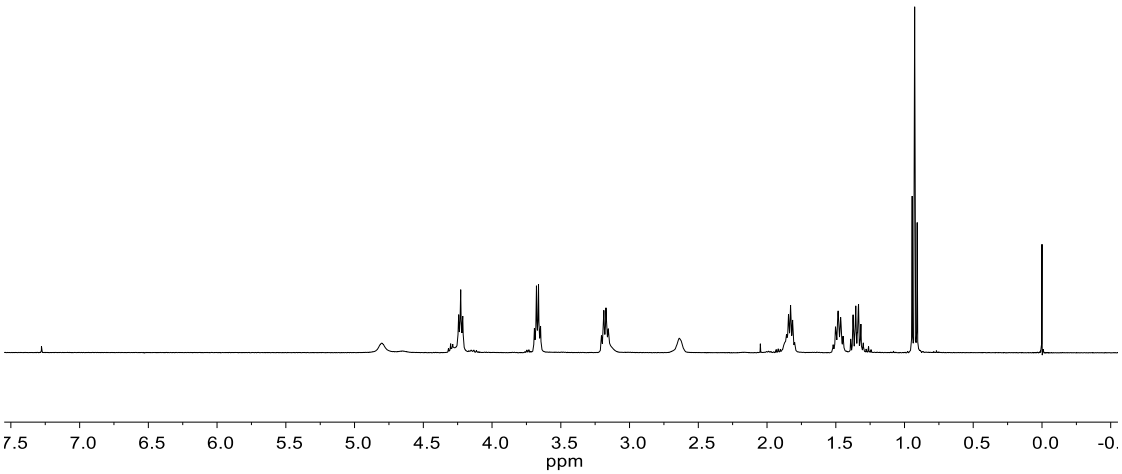

Figure S3.16. ^{1}H-NMR ($CDCl_3$, 300 MHz, 298 K) of hydroxyurethane model compound **6**.

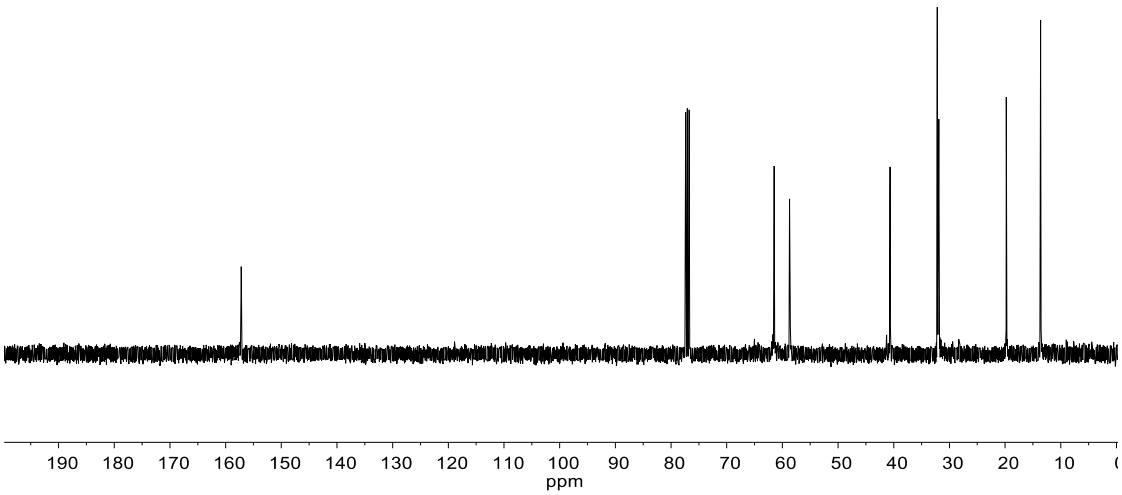

Figure S3.17. ^{13}C NMR ($CDCl_3$, 75 MHz, 298 K) of hydroxyurethane model compound **6**.

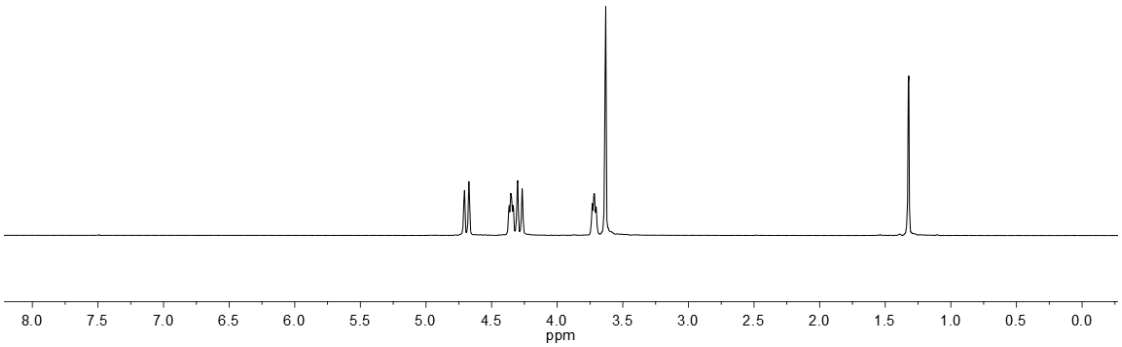

Figure S3.18. ^{1}H NMR ($CDCl_3$, 300 MHz, 298 K) of bis(cyclic carbonate) **S1**.

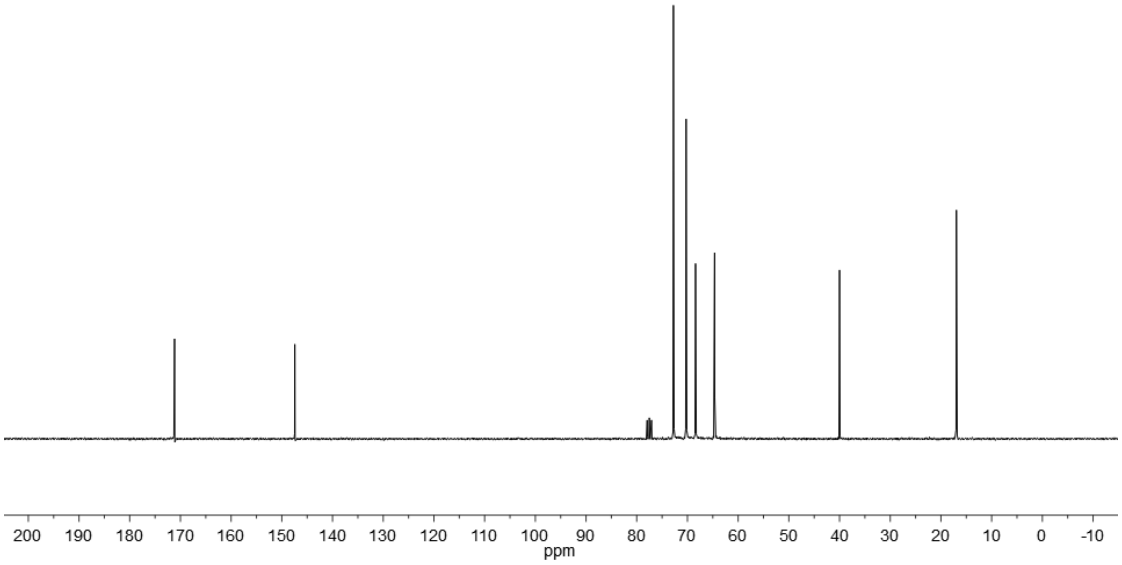

Figure S3.19. ^{13}C NMR ($CDCl_3$, 75 MHz, 298 K) of bis(cyclic carbonate) **S1**.

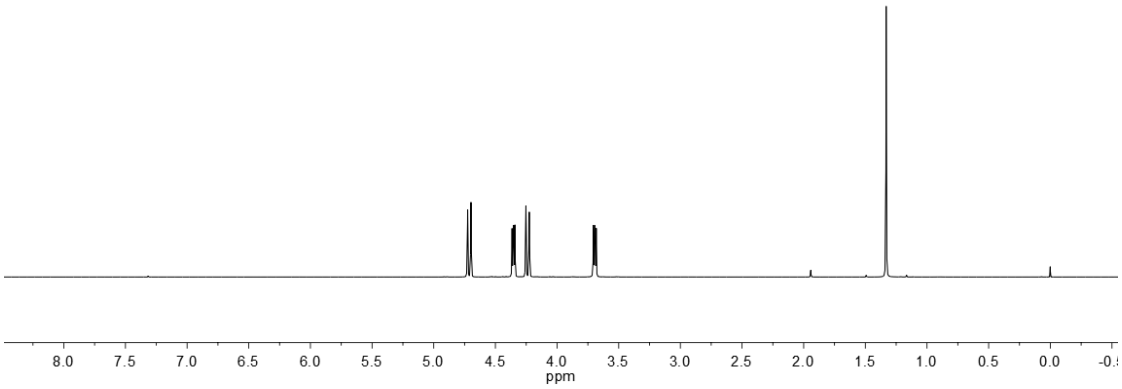

Figure S3.20. ^{1}H NMR ($CDCl_3$, 400 MHz, 298 K) of bis(cyclic carbonate) **S2**.

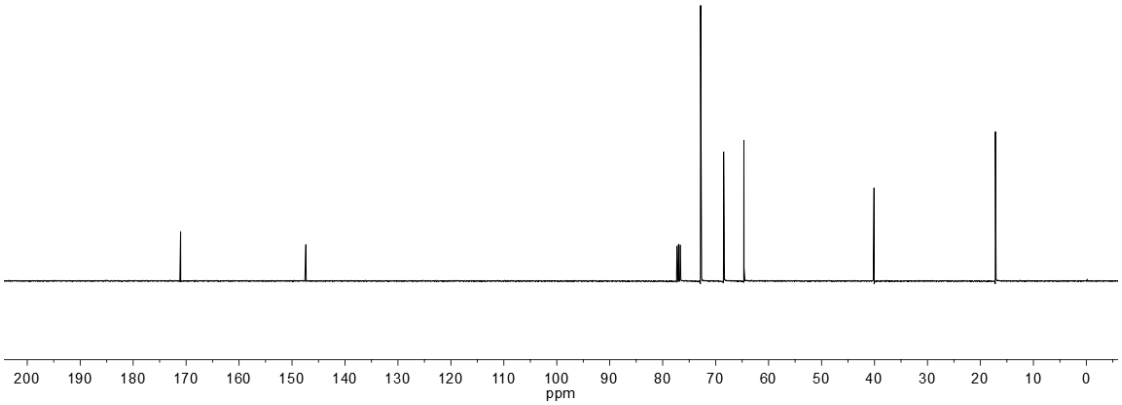

Figure S3.21. ^{13}C NMR ($CDCl_3$, 100 MHz, 298 K) of bis(cyclic carbonate) **S2**.

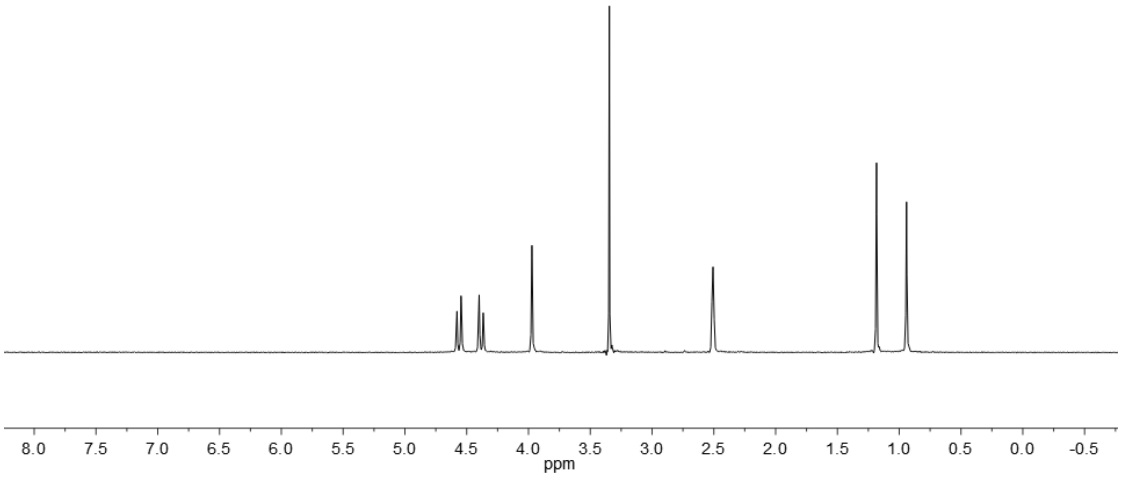

Figure S3.22. ^{1}H NMR (DMSO, 300 MHz, 298 K) of bis(cyclic carbonate) **S3**.

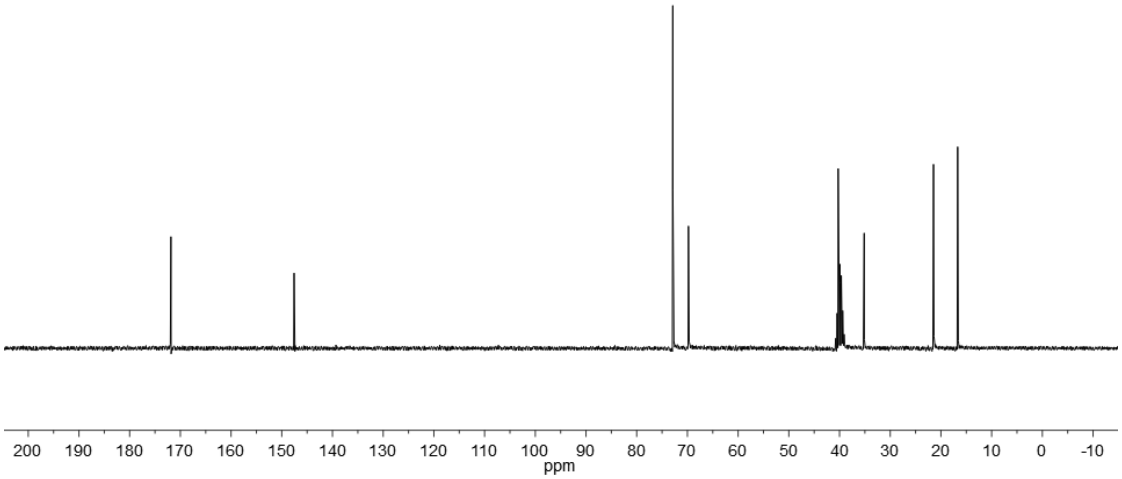

Figure S3.23. ^{13}C NMR (DMSO, 75 MHz, 298 K) of bis(cyclic carbonate) **S3**.

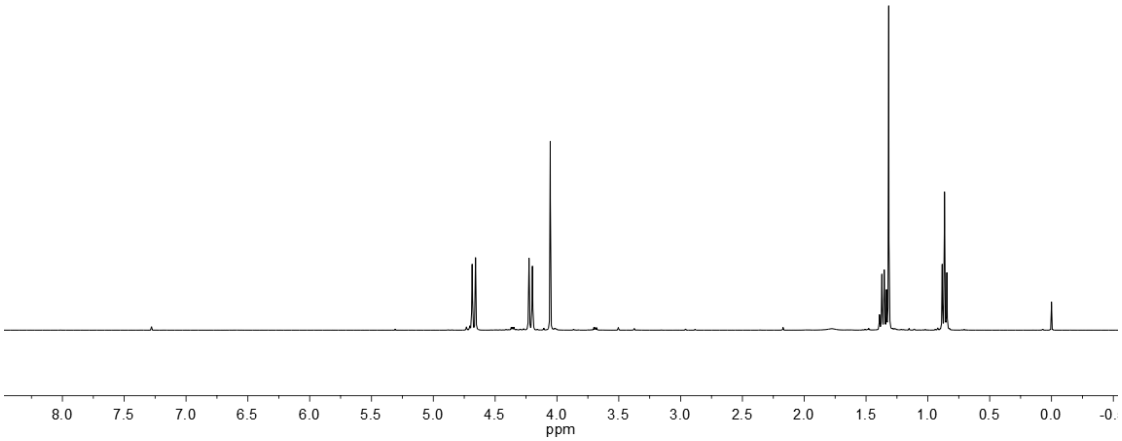

Figure S3.24. ^{1}H NMR ($CDCl_3$, 400 MHz, 298 K) of bis(cyclic carbonate) **S4**.

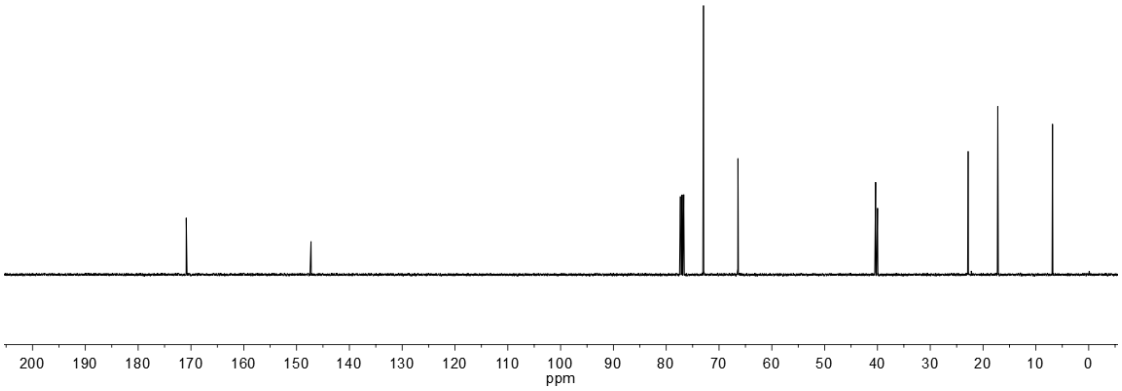

Figure S3.25. ^{13}C NMR ($CDCl_3$, 100 MHz, 298 K) of bis(cyclic carbonate) **S4**.

E. References:

(1) Yang, L.-Q.; He, B.; Meng, S.; Zhang, J.-Z.; Li, M.; Guo, J.; Guan, Y.-M.; Li, J.-X.; Gu, Z.-W. *Polymer* **2013**, *54*, 2668–2675.

(2) Fortman, D. J.; Brutman, J. P.; Cramer, C. J.; Hillmyer, M. A.; Dichtel, W. R. *J. Am. Chem. Soc.* **2015**, *137*, 14019–14022.

(3) Pratt, R. C.; Nederberg, F.; Waymouth, R. M.; Hedrick, J. L. *Chem. Commun.* **2008**, *1*, 114–116.

(4) Camara, F.; Benyahya, S.; Besse, V.; Boutevin, G.; Auvergne, R.; Boutevin, B.; Caillol, S. *Eur. Polym. J.* **2014**, *55*, 17–26.

CHAPTER FOUR

DYNAMIC DISULFIDE EXCHANGE IN REPROCESSABLE CROSS-LINKED POLYHYDROXYURETHANES

4.1 Abstract

Polymer networks that are cross-linked by dynamic covalent bonds often sacrifice the robust mechanical properties of traditional thermosets in exchange for rapid and efficient reprocessability. Polyurethanes are attractive materials for robust, yet reprocessable, cross-linked polymers because of their widespread use and ease of synthesis; however, their synthetic routes typically rely on harmful isocyanate precursors. The use of polyhydroxyurethanes (PHUs) derived from amines and cyclic carbonates is a promising alternative synthetic approach, but the rapid and efficient reprocessing of rigid, cross-linked PHUs is difficult. Herein, we report the use of cystamine as a co-monomer in cross-linked PHUs, which exhibit the most rapid catalyst-free reprocessing protocol reported for PHU resins to-date. These materials show rapid stress relaxation and have characteristic relaxation times as low as 30 s at 150 °C. Furthermore, their cross-link densities can be quantitatively recovered after only 30 min of elevated-temperature compression molding. This protocol is a promising approach toward the application of sustainable, cross-linked, isocyanate-free PHU resins.

This work was performed in collaboration with Rachel Snyder.

4.2 Introduction

Thermosets are cross-linked polymers with excellent mechanical properties and chemical and thermal stability. Their covalent cross-links typically preclude repair or reprocessing; however, dynamic covalent bonds have recently been introduced into cross-linked polymer networks to impart plasticity at elevated temperatures while maintaining robust mechanical properties under service conditions.[1–7] If these materials can maintain mechanical properties competitive with traditional thermosets while displaying rapid reprocessing and flow, these combined properties will enable new technologies and increase the sustainability of cross-linked polymers. Vitrimers are a class of dynamic covalent networks in which exchange reactions that occur within the polymer networks impart a gradual Arrhenius-type change in viscosity,[2–5] resulting in materials that can be directly reprocessed without depolymerization to small molecules. Many vitrimer exchange chemistries take advantage of associative exchange mechanisms, which allow the bonds and polymer architecture to rearrange without depolymerization of the network. Inspired by this approach, many dynamic covalent reactions have been employed in vitrimer networks, but further study remains of high interest to enable simultaneous control of the mechanical properties, reprocessing rates, and thermochemical stability of these materials.

Polyurethanes (PUs) are the sixth most abundant class of polymers[8] and the most prevalent cross-linked polymers in use; therefore, they are key targets for novel reprocessing methods. Despite their widespread application, traditional isocyanate-based PUs have significant drawbacks owing to the hazards of isocyanates, which are used in their synthesis.[9] Therefore, the development of isocyanate-free PUs or other

urethane-like materials is a growing opportunity for polymer chemists. The addition of polyfunctional cyclic carbonates with amines to generate polyhydroxyurethanes (PHUs) have received significant attention[10–12] and have yielded isocyanate-free thermoplastics and thermosets,[13,14] thermoplastic elastomers,[15,16] and coatings.[17]

We and others have developed PHU-based reprocessable cross-linked polymers by exploiting the inherent dynamic reactivity of the urethane linkages via transcarbamoylation in the presence of hydroxyl moieties. Cross-linked PHUs derived from six-membered cyclic carbonates have excellent mechanical properties and can be reprocessed via compression molding at elevated temperatures, albeit with long reprocessing times (4–8 h at 160 °C) and incomplete recovery of mechanical properties (typically ca. 75%).[18,19] Torkelson and co-workers[20] reprocessed cross-linked PHUs using catalytic 4-dimethylaminopyridine, and fully recovered the cross-link density of the materials as measured by dynamic mechanical thermal analysis (DMTA). The time scale for reprocessing these materials was roughly 1 h, although this was only demonstrated for loosely cross-linked, elastomeric samples. We hypothesized that PHU resins containing more dynamic disulfide linkages would exhibit faster and more complete repair. Disulfides undergo both radical-based[21] and base-mediated[22] exchange processes, and the rate of exchange can be tuned by altering the substituents on the sulfur atoms.[23–25] Many researchers have explored strategies to control the dynamics of disulfide bonds in cross-linked elastomers,[26–28] inspired by the presence of disulfide linkages in commercial tires. While the application of these strategies to rigid materials is less explored, incorporation of aromatic disulfides into rigid epoxy resins gives materials with rapid and efficient reprocessability at elevated temperatures,[29,30] although

changes were observed in the modulus measured by DMTA[29] after reprocessing. Therefore, we developed a synthetic strategy that allows the easy incorporation of disulfide bonds into cross-linked PHUs (Figure 4.1).

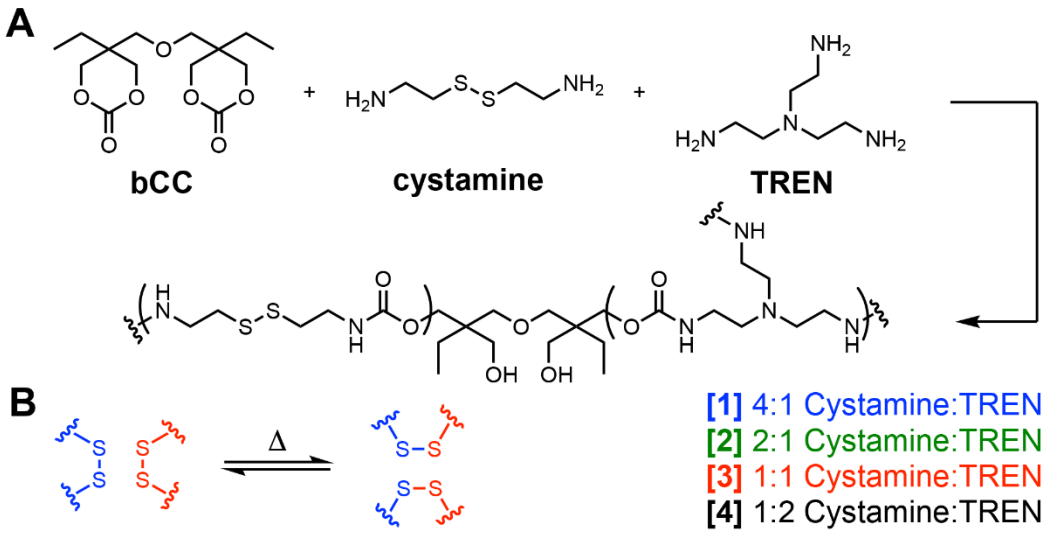

Figure 4.1. A. Polyaddition of bis(cyclic carbonate) (**bCC**) with various ratios of cystamine and tris(2-aminoethylamine) (**TREN**) to yield cross-linked polymers **1**–**4**. B. Exchange of disulfides in the polymer backbone enables reprocessing.

4.3 Results and Discussion

We identified cystamine as an accessible monomer that is compatible with the cyclic carbonate aminolysis reaction. Cystamine is a disulfide-based diamine that can be derived from the amino acid cysteine,[31] and is commonly used as a redox-responsive linker in biological applications.[32,33] However, to our knowledge, it has not been used as a feedstock for the synthesis of bulk reprocessable cross-linked polymers. To synthesize the cross-linked polymers, we reacted the free-base cystamine with bis(cyclic carbonate) and tris(2-aminoethyl)amine (TREN) as a cross-linking agent. The six-membered cyclic carbonate was chosen over the analogous five-membered cyclic carbonate because it reacts more rapidly[34] and yields PHU networks with greater

thermal stability.[19] The monomers were homogenized in CH_2Cl_2 and allowed to react at room temperature. Then, they were placed under vacuum at elevated temperature to ensure complete cross-linking and solvent removal. At a constant ratio of total amine to cyclic carbonate, we varied the ratio of cystamine/TREN to investigate the effects of cross-linking density and disulfide content on the properties of the resulting polymers.

In all cases, Fourier-transform IR (FT-IR) spectra showed the complete disappearance of the cyclic carbonate C=O stretch at 1732 cm^{-1} along with the appearance of a hydrogen-bonded urethane C=O stretch at 1688 cm^{-1}, a urethane N–H deformation at 1530 cm^{-1}, and a free hydroxyl O–H stretch at 3300 $cm.^{-1}$ These findings demonstrated that the cured polymers possessed the desired PHU structure (Figure 4.2A, Figure S4.1). High gel fractions (>0.97 in all cases; Table 4.1) obtained after swelling the polymers in CH_2Cl_2 provided evidence that the curing reaction reached high conversion and the presence of the disulfides had no effect on the cyclic carbonate aminolysis.

The DMTA results were consistent with a cross-linked architecture, as a plateau in the storage modulus was observed above the glass-transition temperature. As the ratio of TREN increased, the value of this plateau modulus at 120 °C increased from 1.24 MPa to 2.84 MPa (Figure 4.2B). This value demonstrated both that the materials were densely cross-linked and that the density of the cross-linking could be controlled by adjusting the monomer feed ratio, as expected. The results of both differential scanning calorimetry (Figure S4.2) and DMTA showed that the glass-transition temperature increased from 49 °C to 59 °C with increasing cross-link density, as is typical for cross-linked polymer networks.

Furthermore, all of the polymers displayed degradation temperatures greater than 270 °C (Figure S4.3), which are comparable to the decomposition temperatures of disulfide-free PHUs.[18,19] These results demonstrated that the disulfides do not significantly impact the thermal stability of the resins. Uniaxial tensile testing showed that the polymers had mechanical properties competitive with those of many rigid reprocessable cross-linked polymers, with Young's moduli reaching 2.0 GPa and tensile strength values surpassing 50 MPa. Increasing the cystamine loading resulted in weaker, more brittle materials, possibly due to the higher concentration of weak disulfide bonds in the networks (Figure S4.4, Table S4.1).

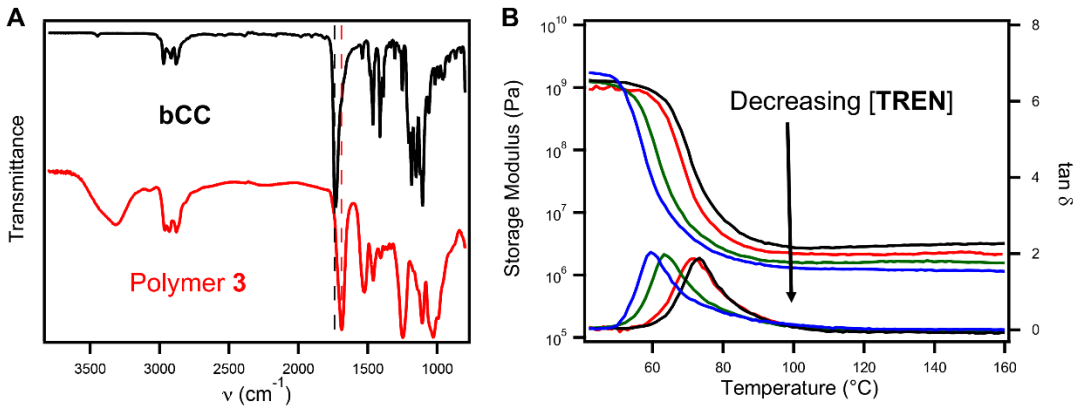

Figure 4.2. A. FT-IR spectra of **bCC** and cured polymer **3** showing the conversion of the cyclic carbonate to hydroxyurethane. B. Dynamic mechanical thermal analyses of polymers **1** (blue), **2** (green), **3** (red), and **4** (black) showing the presence of plateau storage moduli, which increased with increasing **TREN** loading.

Table 4.1. Properties of cystamine-containing polyhydroxyurethanes.

Polymer	Gel %	T_d (°C)[a]	$T_{g,DSC}$ (°C)	$T_{g,DMTA}$ (°C)	E′ (MPa)[b]	E_a (kJ/mol)[c]	T_v (°C)[d]
1	97	273	49	53	1.24	62 ± 2	–18
2	99	278	51	57	1.59	73 ± 4	9
3	99	279	56	63	2.14	78 ± 4	24
4	100	274	59	66	2.84	126 ± 7	75

a. 5% mass loss as determined by TGA *b*. E' at 120 ºC as determined by DMTA *c*. Arrhenius activation energy of stress relaxation. *d*. Topology freezing temperature, determined by the literature method.[35,36]

To analyze the dynamic nature of these networks, we performed elevated temperature stress relaxation experiments, which indicate how rapidly the cross-links reorganize in these materials. Samples were equilibrated at the desired temperature in a DMA, a rapid 5% strain was applied, and the decay of the resulting stress in the material was monitored. This process was repeated at least three consecutive times for each sample to ensure that decomposition was not prevalent under the relaxation conditions. All of the polymers displayed rapid and reproducible stress relaxation at temperatures above 120 °C (Figure 4.3, Figures S4.5-4.7), which demonstrated that the covalent bonds are dynamic under these conditions.

Notably, polymer **1** displayed a characteristic relaxation time (τ*, the time to relax to 1/*e* of the initial stress) of 29 ± 1 s at 150 °C, which is among the fastest reported for materials this densely cross-linked. The relaxation time slows with increasing TREN loading, but fast τ* values (< 80s) were still achieved at 150 °C in polymers **2** and **3**. Polymer **4**, however, displayed significantly slower relaxation of 445 ± 39 s at 150 ºC.

Analysis of the polymers by FT-IR after stress relaxation (Figure S4.1) showed no detectable change, which further confirmed that decomposition was not significantly contributing to the stress relaxation. Consistent with previous studies of stress relaxation in vitrimer systems, the relaxation rates slowed with increasing cross-link density and decreasing disulfide concentration.[37,38] This was expected as a lower concentration of disulfides coincides with a lower concentration of exchangeable linkages. The energy of activation of polymer stress relaxation (determined by applying an Arrhenius model to the temperature dependence of τ^*) also increased with increasing cross-link density, which is consistent with previous reports.[37,38] This observation provides further evidence that the kinetics of the exchange reaction are not the only factor governing the relaxation of dynamic cross-linked materials, and that the diffusion of the reactive groups, as governed by the polymer chain mobility, likely plays a role in the activation energy of stress relaxation in densely cross-linked systems. Notably, changing the cystamine/TREN ratio from 1:1 to 1:2 (*i.e.* decreasing the disulfide concentration and increasing the cross-link density) resulted in a large increase in E_a (78 to 126 kJ/mol) and significant slowing of the relaxation rate. This outcome may suggest that a significant concentration of disulfide cross-links must be incorporated to ensure rapid relaxation in these materials.

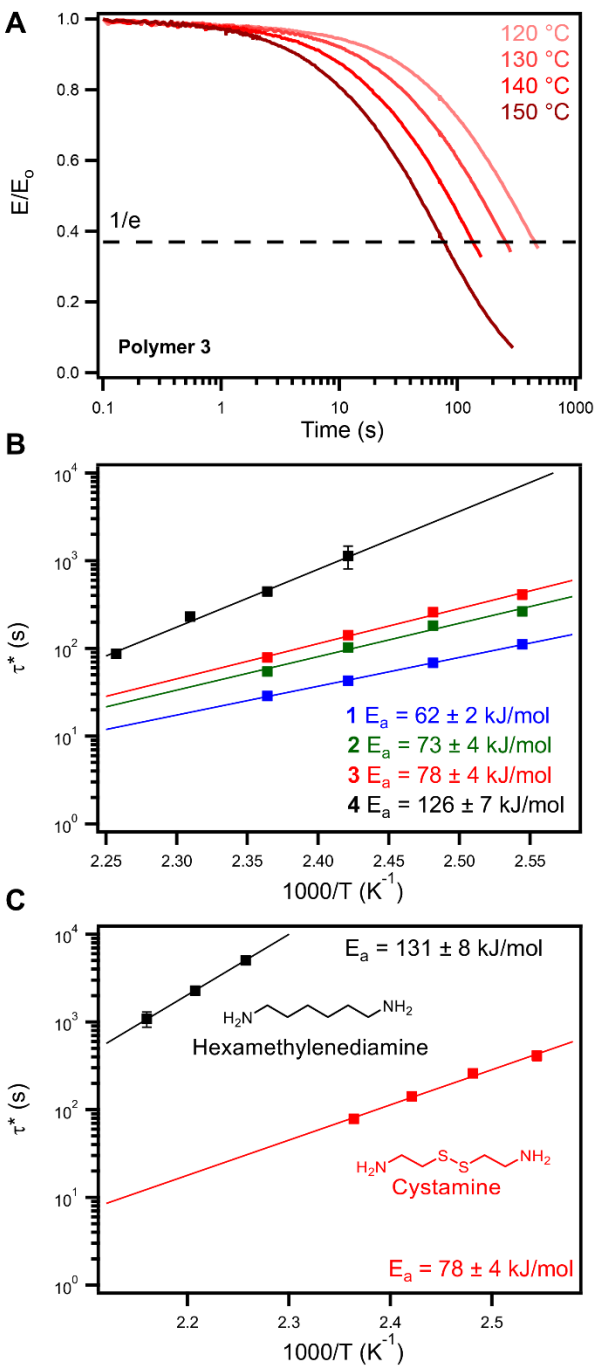

Figure 4.3. A. Representative stress relaxation curves of polymer **3**. B. Arrhenius plot relating the characteristic relaxation time, τ*, to inverse temperature; the Arrhenius energy of activation of stress relaxation increases with increasing **TREN** concentration in the networks. C. Arrhenius plot comparing the stress relaxation of polymer **3** to that of a control sample made with an identical 1:1 ratio of hexamethylenediamine:**TREN**. This comparison demonstrates the necessity of incorporating disulfides for rapid stress relaxation.

In these polymers, the cross-links may reorganize through at least two pathways: disulfide exchange or transcarbamoylation of the urethane linkages. To assess the contributions of each of these processes, we compared the original cystamine-containing polymers with identical networks in which the disulfide linkages were omitted by replacing cystamine with hexamethylenediamine. In polymers containing disulfides, stress relaxation occurred multiple orders-of-magnitude more rapidly at similar temperatures (Figure 4.3C) and with significantly lower E_a, which suggested that the disulfide exchange is dominant and the contribution of transcarbamoylation to stress relaxation is essentially negligible. The relaxation rate of these materials is also faster than that of materials based on typical aliphatic-substituted disulfide bonds, possibly because the tertiary amines in the network catalyze exchange.[22] Additional studies are required to fully understand the magnitude of these effects.

Having established the rapid dynamic nature of these networks, we sought to demonstrate that these materials could be reprocessed at significantly faster rates than those of previous PHU systems. Polymer **3** was chosen for this demonstration because it showed the best balance of robust mechanical properties and rapid relaxation times. The polymer was ground into a fine powder and heated in a compression mold under 5–10 MPa of pressure at 150 °C for 30 min to yield a homogenous, reprocessed material (Figure 4.4A). The FT-IR spectra of the polymer were indistinguishable before and after reprocessing (Figure S4.8), which demonstrated that the recycling process has no effect on the chemical composition of the network.

DMTA was used to quantitatively evaluate the efficiency of this process because it quantifies the storage modulus in the glassy and rubbery states, as well as the homogeneity of the network. The results showed very similar glassy moduli and an identical rubbery storage modulus within error (Figure 4.4B, Figure S4.9), which demonstrated that the full cross-link density of these materials is recovered in a relatively short timeframe. Furthermore, no change was observed in tan δ as a function of temperature, which suggested that full homogenization of the networks occurred within this time frame. Given the short characteristic relaxation times and thermal stability, quantitative reprocessing can likely be achieved more quickly and/or higher temperatures; however, we have not yet determined the shortest time required to achieve these efficiencies.

Reprocessing can be repeated at least three times without any detectable decrease in the storage modulus as measured by DMTA, which suggests that these materials could undergo a significant number of reprocessing cycles. Attempted reprocessing of control samples lacking disulfides under the same conditions yielded inhomogeneous materials with little evidence of polymer homogenization (Figure S10), consistent with the significantly longer relaxation times observed during stress relaxation experiments.

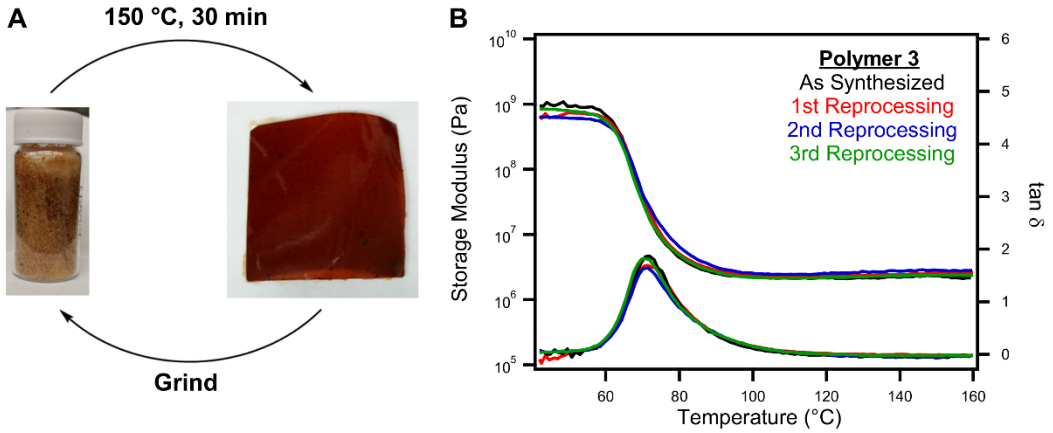

Figure 4.4. A. Ground polymer **3** and the reprocessed sample after compression molding for 30 min at 150 °C. This cycle was repeated multiple times on the same sample. B. The results of dynamic mechanical thermal analysis of polymer **3** as synthesized (black) and after one (red), two (blue), and three (green) reprocessing cycles.

4.3 Conclusions

The results reported herein demonstrate the facile incorporation of disulfide-containing cystamine into PHU networks, and show that these networks can be reprocessed with negligible changes in their chemical structure and mechanical properties. Notably, these materials show very rapid relaxation, despite their high cross-link densities, and can be reprocessed under milder conditions (150 °C, 30 min) than those required by many rigid vitrimer systems. This unique combination of mechanical robustness and rapid relaxation suggest that cystamine could be an attractive diamine feedstock for reprocessable cross-linked polymers. Additional efforts will aim to incorporate cystamine into five-membered cyclic carbonate networks, which are generally considered more sustainable,[10] and explore more industrially-viable processing techniques, such as injection molding, that take advantage of the rapid, reproducible reprocessability of these materials.

References

(1) Kloxin, C. J.; Bowman, C. N. *Chem. Soc. Rev.* **2013**, *42*, 7161–7173.

(2) Denissen, W.; Winne, J. M.; Du Prez, F. E. *Chem. Sci.* **2016**, *7*, 30–38.

(3) Imbernon, L.; Norvez, S. *Eur. Polym. J.* **2016**, *82*, 347–376.

(4) Zou, W.; Dong, J.; Luo, Y.; Zhao, Q.; Xie, T. *Adv. Mater.* **2017**, *29*, 1606100.

(5) Montarnal, D.; Capelot, M.; Tournilhac, F.; Leibler, L. *Science* **2011**, *334*, 965–968.

(6) Röttger, M.; Domenech, T.; van der Weegen, R.; Breuillac, A.; Nicolaÿ, R.; Leibler, L. *Science* **2017**, *356*, 62–65.

(7) Scott, T. F.; Schneider, A., D.; Cook, W., D.; Bowman, Christoper, N. *Science* **2005**, *308*, 1615–1617.

(8) Market Study, Polyurethanes (PUR) and Isocyanates (MDI & TDI). Cerasana January 2016.

(9) Methylene Diphenyl Diisocyanate (MDI) and Related Compounds Action Plan. United States Environmental Protection Agency 2011.

(10) Nohra, B.; Candy, L.; Blanco, J.-F.; Guerin, C.; Raoul, Y.; Mouloungui, Z. *Macromolecules* **2013**, *46*, 3771–3792.

(11) Blattmann, H.; Fleischer, M.; Bähr, M.; Mülhaupt, R. *Macromol. Rapid Commun.* **2014**, *35*, 1238–1254.

(12) Rokicki, G.; Parzuchowski, P. G.; Mazurek, M. *Polym. Adv. Technol.* **2015**, *26*, 707–761.

(13) Schmidt, S.; Ritter, B. S.; Kratzert, D.; Bruchmann, B.; Mülhaupt, R. *Macromolecules* **2016**, *49*, 7268–7276.

(14) Schimpf, V.; Ritter, B. S.; Weis, P.; Parison, K.; Mülhaupt, R. *Macromolecules* **2017**, *50*, 944–955.

(15) Leitsch, E. K.; Beniah, G.; Liu, K.; Lan, T.; Heath, W. H.; Scheidt, K. A.; Torkelson, J. M. *ACS Macro Lett.* **2016**, *5*, 424–429.

(16) Beniah, G.; Fortman, D. J.; Heath, W. H.; Dichtel, W. R.; Torkelson, J. M. *Macromolecules* **2017**, *50*, 4425–4434.

(17) Ma, Z.; Li, C.; Fan, H.; Wan, J.; Luo, Y.; Li, B.-G. *Ind. Eng. Chem. Res.* **2017**, *56*, 14089–14100.

(18) Fortman, D. J.; Brutman, J. P.; Cramer, C. J.; Hillmyer, M. A.; Dichtel, W. R. *J. Am. Chem. Soc.* **2015**, *137*, 14019–14022.

(19) Fortman, D. J.; Brutman, J. P.; Hillmyer, M. A.; Dichtel, W. R. *J. Appl. Polym. Sci.* **2017**, *134*, 44984.

(20) Chen, X.; Li, L.; Jin, K.; Torkelson, J. M. *Polym. Chem.* **2017**, *8*, 6349–6355.

(21) Tobolsky, A. V.; MacKnight, W. J.; Takahashi, M. *J. Phys. Chem.* **1964**, *68*, 787–790.

(22) Nevejans, S.; Ballard, N.; Miranda, J. I.; Reck, B.; Asua, J. M. *Phys. Chem. Chem. Phys.* **2016**, *18*, 27577–27583.

(23) Rekondo, A.; Martin, R.; Ruiz de Luzuriaga, A.; Cabañero, G.; Grande, H. J.; Odriozola, I. *Mater. Horiz.* **2014**, *1*, 237–240.

(24) Martin, R.; Rekondo, A.; Ruiz de Luzuriaga, A.; Cabañero, G.; Grande, H. J.; Odriozola, I. *J. Mater. Chem. A.* **2014**, *2*, 5710.

(25) Azcune, I.; Odriozola, I. *Eur. Polym. J.* **2016**, *84*, 147–160.

(26) Imbernon, L.; Oikonomou, E. K.; Norvez, S.; Leibler, L. *Polym. Chem.* **2015**, *6*, 4271–4278.

(27) Pepels, M.; Filot, I.; Klumperman, B.; Goossens, H. *Polym. Chem.* **2013**, *4*, 4955.

(28) Xiang, H. P.; Qian, H. J.; Lu, Z. Y.; Rong, M. Z.; Zhang, M. Q. *Green Chem.* **2015**, *17*, 4315–4325.

(29) Ruiz de Luzuriaga, A.; Martin, R.; Markaide, N.; Rekondo, A.; Cabañero, G.; Rodríguez, J.; Odriozola, I. *Mater. Horiz.* **2016**, *3*, 241–247.

(30) Ma, Z.; Wang, Y.; Zhu, J.; Yu, J.; Hu, Z. *J. Polym. Sci. Part A: Polym. Chem.* **2017**, *55*, 1790–1799.

(31) Neuberg, C.; Ascher, E. *Biochem. Z.* **1907**, *5*, 451–456.

(32) Liu, R.; Zhao, X.; Wu, T.; Feng, P. *J. Am. Chem. Soc.* **2008**, *130*, 14418–14419.

(33) Li, Y.; Lokitz, B. S.; Armes, S. P.; McCormick, C. L. *Macromolecules* **2006**, *39*, 2726–2728.

(34) Tomita, H.; Sanda, F.; Endo, T. *J. Polym. Sci. Part A: Polym. Chem.* **2001**, *39*, 162–168.

(35) Brutman, J. P.; Delgado, P. A.; Hillmyer, M. A. *ACS Macro Lett.* **2014**, *3*, 607–610.

(36) Capelot, M.; Unterlass, M. M.; Tournilhac, F.; Leibler, L. *ACS Macro Lett.* **2012**, *1*, 789–792.

(37) Snyder, R. L.; Fortman, D. J.; De Hoe, G. X.; Hillmyer, M. A.; Dichtel, W. R. *Macromolecules* **2018**, *51*, 389–397.

(38) Yu, K.; Taynton, P.; Zhang, W.; Dunn, M. L.; Qi, H. J. *RSC Adv.* **2014**, *4*, 48682–48690.

CHAPTER FOUR APPENDIX

Table of Contents

A. Materials and General Methods

Materials. All reagents were purchased from Sigma-Aldrich or Fisher Scientific. All reagents were used without further purification unless otherwise specified. Dichloromethane (CH_2Cl_2) and tetrahydrofuran (THF) were purchased from Fisher Scientific and purified using a custom-built alumina-column based solvent purification system. Other solvents were purchased from Fisher Scientific and used without further purification.

Instrumentation. Infrared spectra were recorded on a Thermo Nicolet iS10 equipped with a ZnSe ATR attachment. Spectra were uncorrected.

Solution-phase NMR spectra were recorded on a Varian 400 MHz or an Agilent DD MR-400 400 MHz spectrometer using a standard 1H/X Z-PFG probe at ambient temperature.

Gel fractions were obtained by swelling polymer samples (50-100 mg) in CH_2Cl_2 (10 ml) for at least 48 hours, then removing the swollen polymers, and drying to constant weight by heating at 80 °C under 20 mtorr vacuum, typically for 48 h.

Thermogravimetric analysis (TGA) was performed on a Mettler Toledo SDTA851 Thermogravimetric Analysis System using 10-15 mg of sample. Samples were heated under a nitrogen atmosphere at a rate of 5 °C/min from 25 ºC to 500 ºC.

Differential scanning calorimetry (DSC) was performed on a Mettler Toledo DSC822 Differential Scanning Calorimeter. Samples were heated at a rate of 10 °C/min to at least 90 °C to erase thermal history, cooled to –30 °C at 10 °C/min, and then heated to at least 110 °C. All data shown are taken from the second heating ramp. The glass

transition temperature (T_g) was calculated from the maximum value of the derivative of heat flow with respect to temperature.

Dynamic mechanical thermal analysis (DMTA) was performed on a TA Instruments RSA-III analyzer (New Castle, DE) using rectangular films (ca. 1.0 mm (T) × 5 mm (W) × 15 mm (L) and a Gauge length of 8 mm). Samples were loaded in tension and a temperature ramp was performed from 30 °C to 170 °C at a rate of 5 °C/min, with an oscillating strain of 0.05% and an angular frequency of 6.28 rad/s (1 Hz). The glass transition temperature (T_g) was calculated from the maximum value of the loss modulus (E").

Uniaxial tensile testing was conducted using dog bone shaped tensile bars (*ASTM D-1708* 1.0 mm (T) × 5 mm (W) × 25 mm (L) and a gauge length of 16 mm). Tensile measurements were performed on a Sintech 20G tensile tester with 250 gram capacity load cell at ambient temperatures at a uniaxial extension rate of 5 mm/min. Young's modulus (E) values were calculated using the TestWorks software by taking the slope of the stress-strain curve from 0 to 1 N of force applied. Reported values are the averages and standard deviations of at least four replicates.

Stress relaxation analysis (SRA) was performed on a TA Instruments RSA-III analyzer (New Castle, DE) using rectangular films (ca. 1.0 mm (T) × 5 mm (W) × 15 mm (L) and a Gauge length of 8 mm). The SRA experiments were performed with strain control at specified temperature (120 to 150 °C). The samples were allowed to equilibrate at this temperature for approximately 10 minutes, after which the axial force was then adjusted to 0 N. Each sample was then subjected to an instantaneous 5% strain. The stress decay was monitored, while maintaining a constant strain (5%), until the

stress relaxation modulus had relaxed to at least 37% (1/*e*) of its initial value. This was performed three consecutive times for each sample. The activation energy (Ea) and freezing transition temperature (T_v) were determined using the methodology in literature.[1,2]

To reprocess the materials, the polymer was ground into small pieces using a Cuisinart Grind Central© coffee grinder. The ground polymer was spread between two aluminum plates in a 1.0 mm square, aluminum mold. This assembly was placed in PHI 30-ton manual press preheated to the desired temperature and allowed to thermally equilibrate for 1 minute. The material was compressed at 5-10 MPa of pressure for 30 s, then the pressure was released, and this was repeated 2x to enable removal of air bubbles. The material was then compressed at 5-10 MPa for 30 minutes. The homogenous, square polymer was removed from the mold, and specimens for DMTA were cut using a straight-edge blade on a 150 °C hot plate.

B. Synthetic Procedures

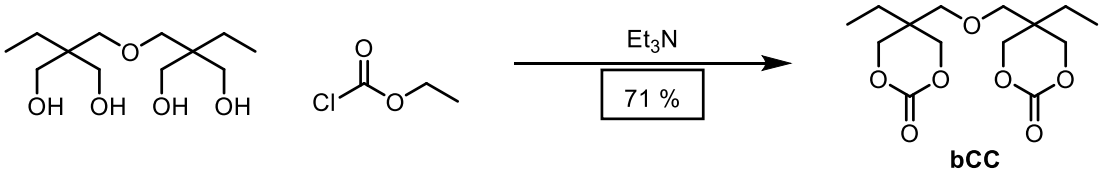

Synthesis of bCC: To a flame-dried round-bottom flask under nitrogen atmosphere was added di(trimethylol)propane (10.0 g, 40 mmol) and anhydrous THF (250 mL). To the suspension was added ethyl chloroformate (25.2 g, 232 mmol) under stirring. The mixture was cooled to 0°C, triethylamine (24.6 g, 242 mmol) was added dropwise, and a white precipitate began to form. The mixture was warmed to room temperature and allowed to stir for 3 hours. The solid was removed via filtration, and solvent was removed at reduced pressure to yield a white solid. The solid was recrystallized from THF to obtain compound **2** as a white solid (8.6 g, 71%). ^{1}H NMR (400 MHz, $CDCl_3$) δ 4.29 (d, *J* = 10.1 Hz, 4H), 4.17 (d, *J* = 10.5 Hz, 4H), 3.50 (s, 4H), 1.50 (q, *J* = 7.5 Hz, 4H), 0.91 (t, *J* = 7.6 Hz, 6H).^{13}C NMR (100 MHz, $CDCl_3$) δ 148.3, 72.8, 70.7, 35.4, 23.5, 7.34. IR (solid, ATR) 2972, 2918, 2881, 1732 (C=O stretch), 1463, 1412, 1165, 1106, 762 cm^{-1}. The characterization data match those previously reported in the literature.[3]

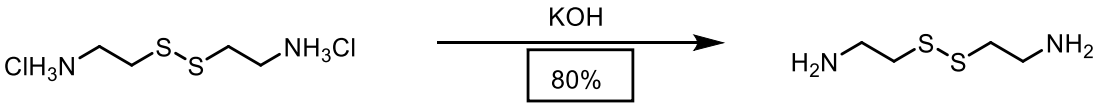

Preparation of Cystamine: In an Erlenmeyer flask, cystamine dihydrochloride (8.00 g, 35.5 mmol) was dissolved in 100 ml distilled water. Potassium hydroxide (6.00 g, 107 mmol, 1.5 eq to HCl) was added and the mixture was stirred for 10 minutes. The resulting mixture was extracted with 4 x 150 ml CH_2Cl_2, the combined organics were

dried over $MgSO_4$, filtered, and solvent was removed to yield a colorless oil (4.3 g, 80 %). The product was used immediately, as cystamine is known to decompose slowly at room temperature. ^{1}H NMR (400 MHz, $CDCl_3$) δ 1.18 (br s, 4H), 2.68 (m, 4H), 2.92 (m, 4H) ^{13}C NMR (100 MHz, $CDCl_3$) δ 40.5, 42.4. The characterization data match those previously reported in the literature.[4]

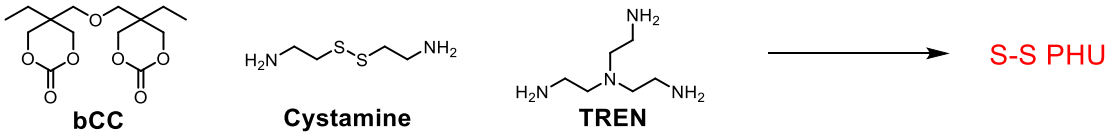

Synthesis of Cross-linked PHUs: Cystamine (1.200 g, 7.88 mmol) and tris(2-aminoethyl)amine (**TREN**) (284.1 mg, 1.94 mmol) were dissolved in 8.0 ml anhydrous CH_2Cl_2. Bis(cyclic carbonate) (3.199 g, 10.6 mmol, 0.98 eq. cyclic carbonate to amine) was added, and the resulting solutions was sonicated for one minute to ensure homogeneity, then poured into an aluminum mould (104 mm D x 15 mm H), covered with aluminum foil, and allowed to stand at room temperature for *ca*. 24 hours. Samples were cut from the resulting transparent films, and placed under reduced pressure at 90 °C and 20 mTorr for *ca*. 48 hours, then post-cured at 150 °C for one hour to ensure complete cross-linking and removal of solvent, yielding polymer **1** as a hard, orange solid.

1 IR (solid, ATR) 3312 (O-H stretch), 2931, 2880, 1688 (C=O stretch), 1526 (N-H deformation), 1461, 1250, 1109, 1030, 992, 775 cm^{-1}.

Identical procedures were performed with different ratios of cystamine:TREN to obtain the polymers as orange solids.

2 IR (solid, ATR) 3314 (O-H stretch), 2925, 1688 (C=O stretch), 1526 (N-H deformation), 1461, 1251, 1109, 1030, 775 cm^{-1}.

3 IR (solid, ATR) 3309 (O-H stretch), 2934, 2880, 1688 (C=O stretch), 1531 (N-H deformation), 1462, 1251, 1109, 1030, 774 cm^{-1}.

4 IR (solid, ATR) 3304 (O-H stretch), 2930, 2880, 1687 (C=O stretch), 1528 (N-H deformation) 1461, 1251, 1110, 1030, 775 cm^{-1}.

C. Characterization Tables and Figures

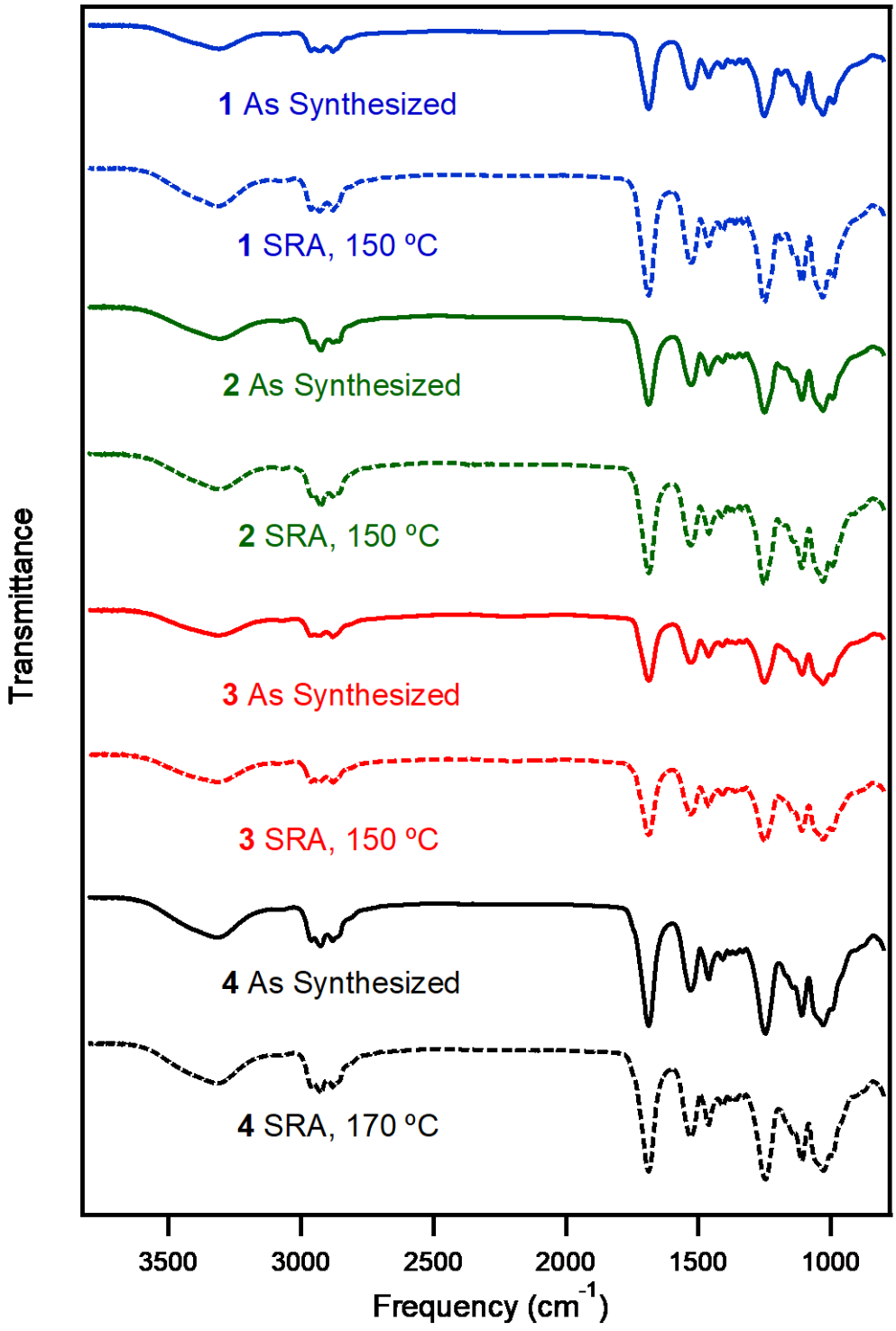

Figure S4.1. FT-IR spectra of polymers **1** (blue), **2** (green), **3** (red), and **4** (black) as synthesized and after stress relaxation analysis at highest temperature measured.

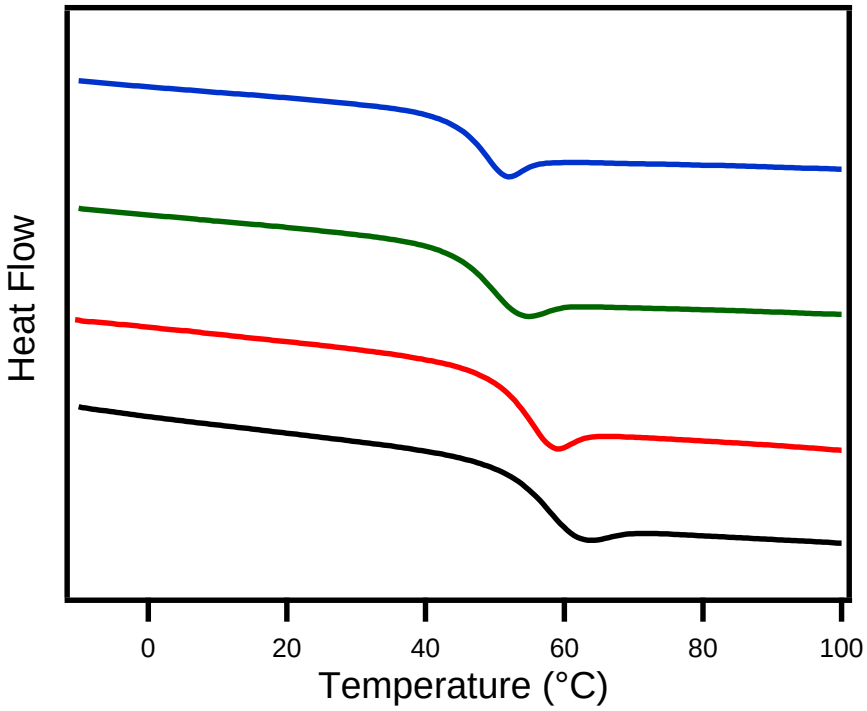

Figure S4.2. Differential scanning calorimetry traces of polymer **1** (blue), **2** (green), **3** (red), and **4** (black).

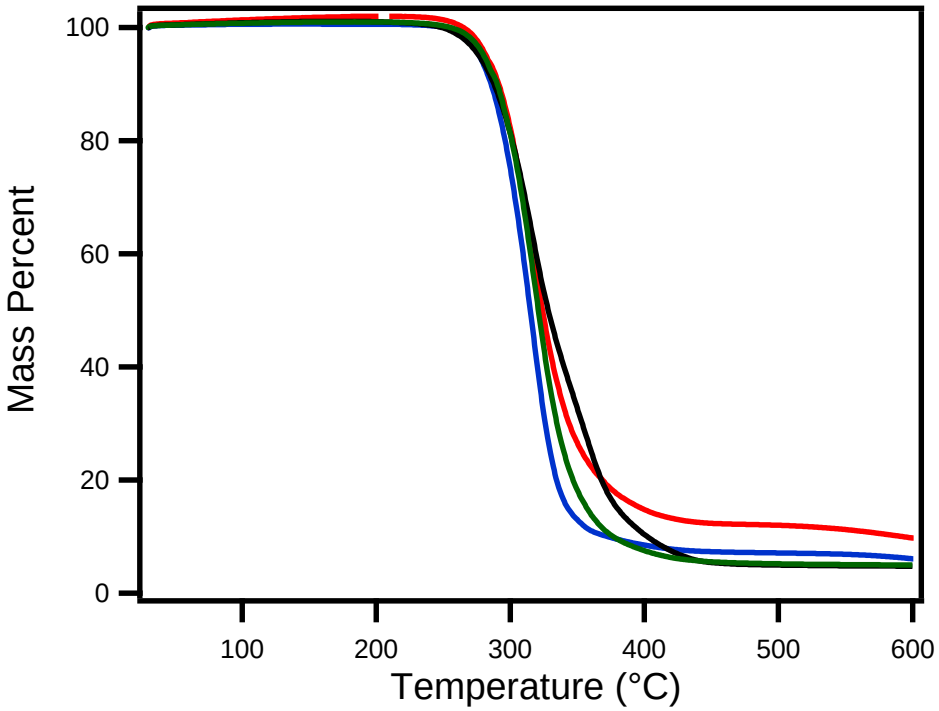

Figure S4.3. Thermogravimetric analysis of polymer **1** (blue), **2** (green), **3** (red), and **4** (black) performed under nitrogen atmosphere at a heating rate of 10 °C/min.

Table S4.1. Tensile Properties of Polymers

Polymer	Tensile Strength (MPa)	Strain at Break (%)	Young's Modulus (GPa)
1	26 ± 8	2.3 ± 1.0	1.6 ± 0.1
2	22 ± 8	2.5 ± 1.9	1.6 ± 0.3
3	54 ± 12	3.6 ± 0.7	2.0 ± 0.2
4	43 ± 7	4.9 ± 1.4	1.7 ± 0.1

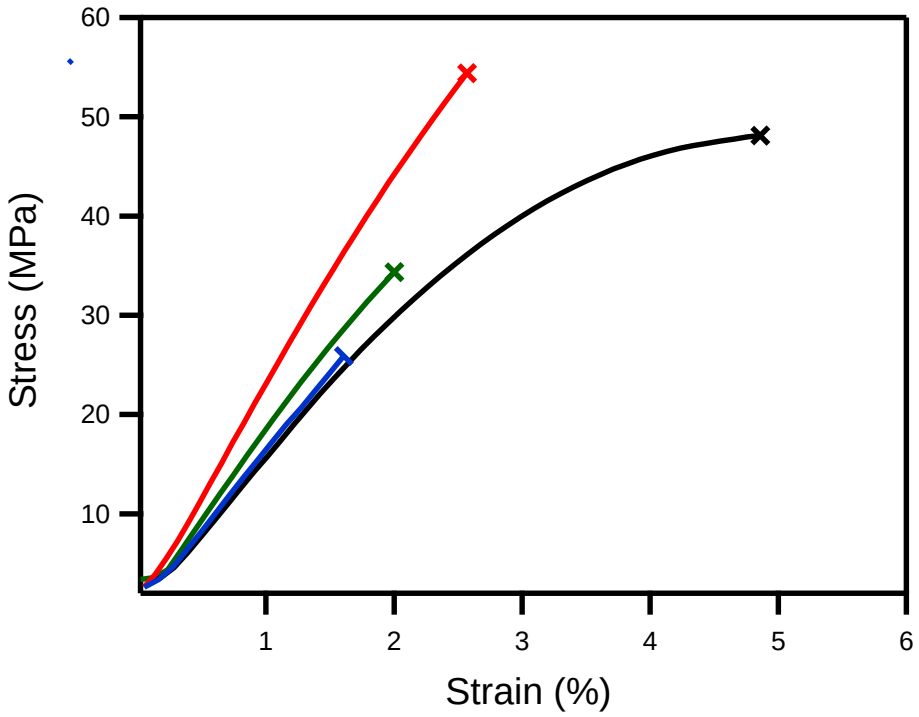

Figure S4.4. Representative tensile testing of as synthesized polymer **1** (blue), **2** (green), **3** (red), and **4** (black).

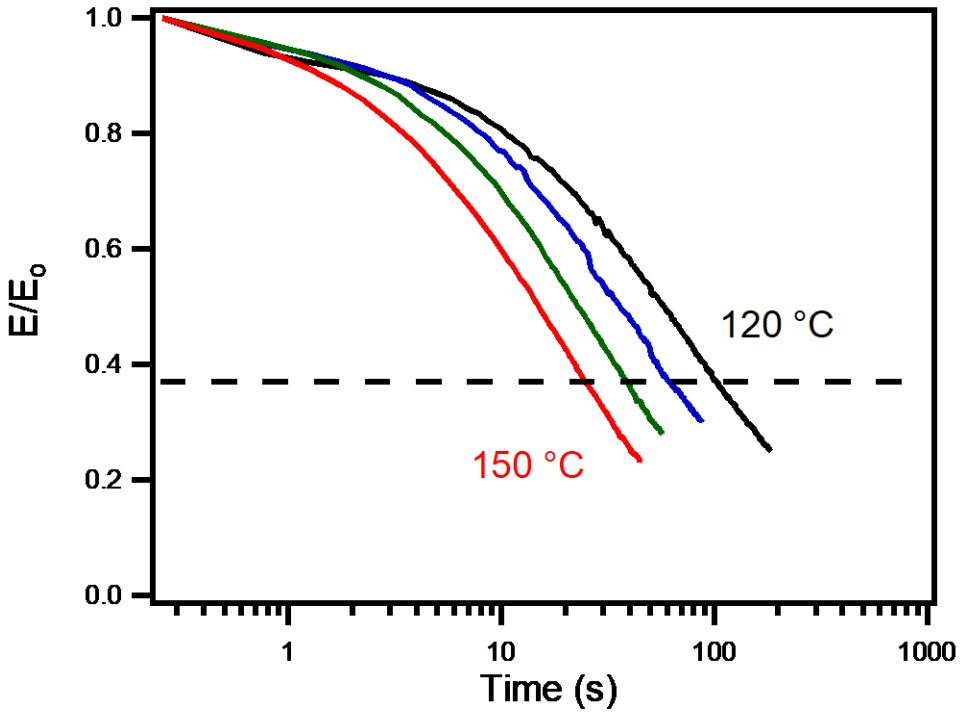

Figure S4.5. Stress relaxation analysis of polymer **1** performed 120 °C (black), 130 °C (blue), 140 °C (green), and 150 °C (red).

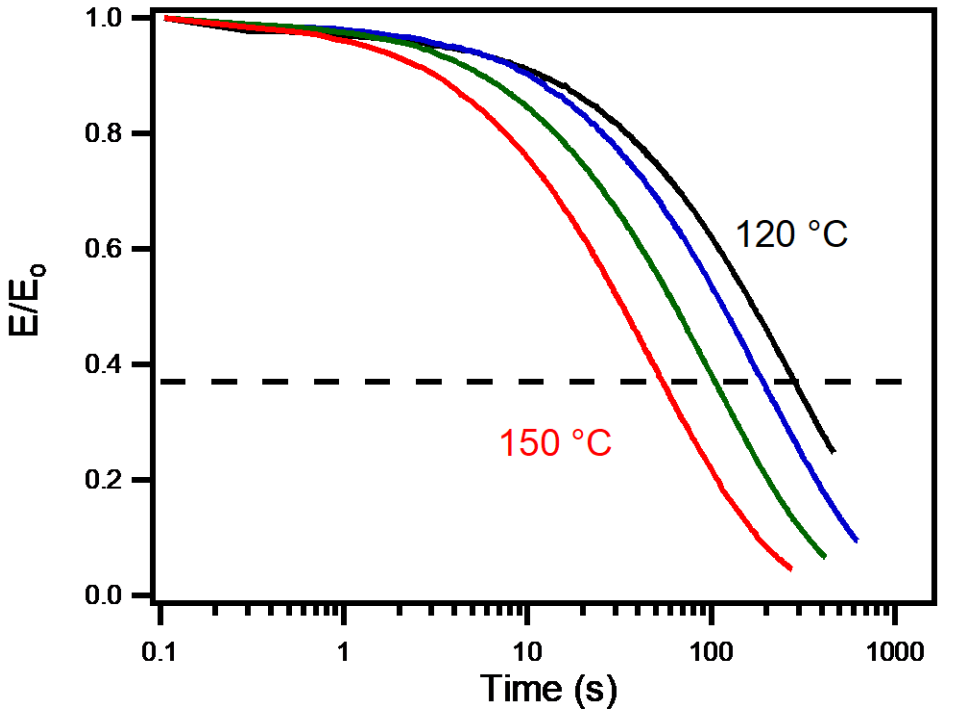

Figure S4.6. Stress relaxation analysis of polymer **2** performed 120 °C (black), 130 °C (blue), 140 °C (green), and 150 °C (red).

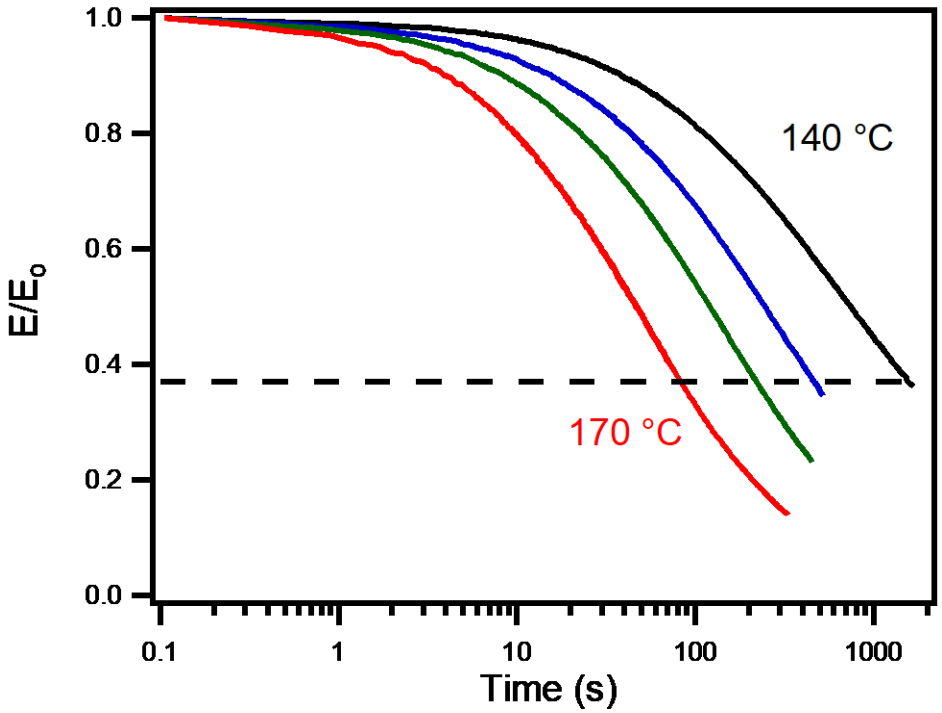

Figure S4.7. Stress relaxation analysis of polymer **4** performed at 140 °C (black), 150 °C (blue), 160 °C (green), and 170 °C (red).

Table S4.2. Characteristic Relaxation Times of Polymers at Various Temperatures

Polymer	170 °C	160 °C	150 °C	140 °C	130 °C	120 °C
1			29 ± 1 s	43 ± 2 s	68 ± 3 s	111 ± 7 s
2			54 ± 1 s	103 ± 4 s	182 ± 15 s	264 ± 26 s
3			79 ± 4 s	141 ± 8 s	259 ± 6 s	413 ± 50 s
4	87 ± 6 s	230 ± 12 s	445 ± 39 s	1137 ± 330 s		

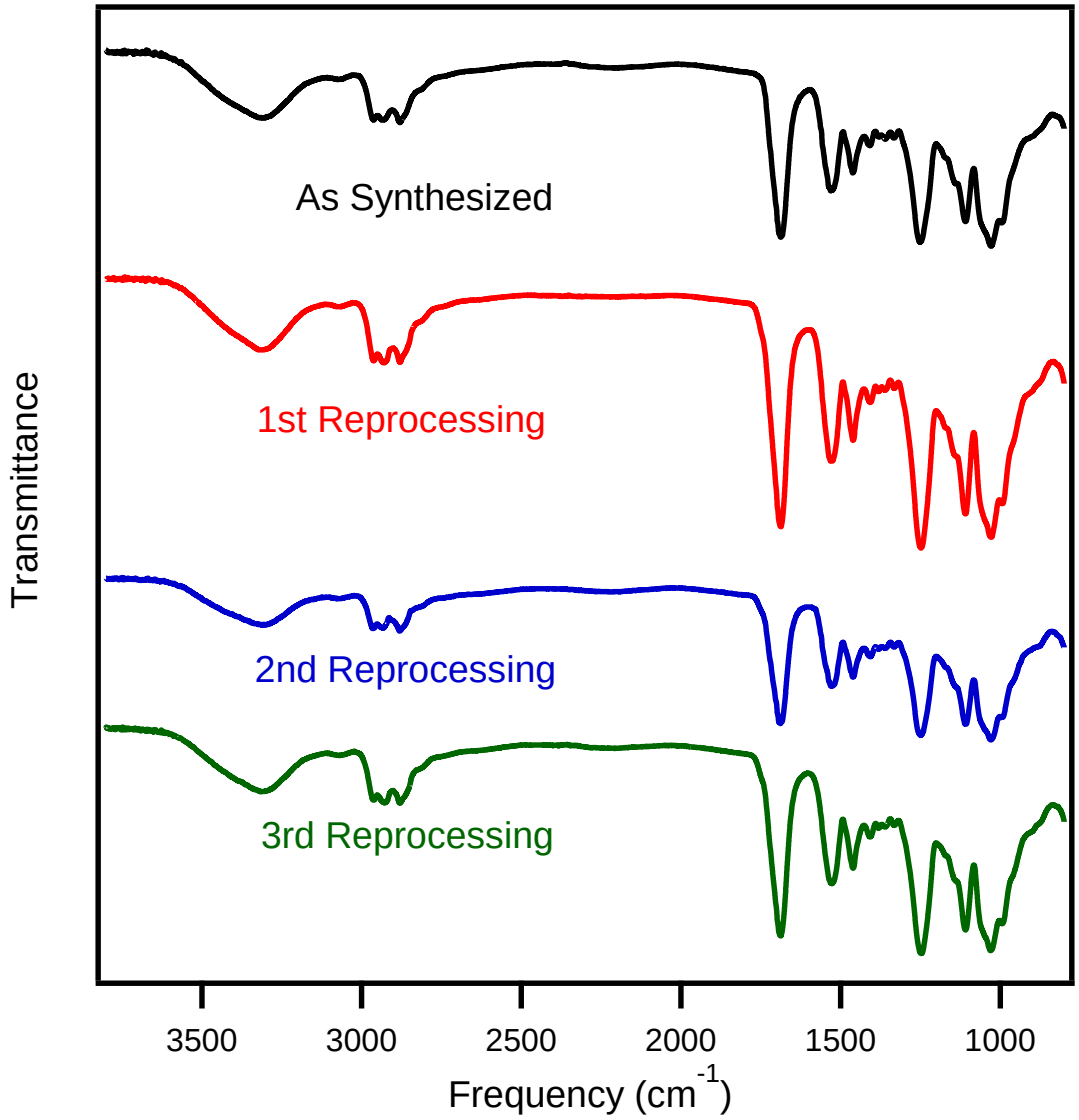

Figure S4.8. FT-IR spectra of polymer **3** as synthesized (black) and after 1 (red), 2 (blue), and 3 (green) reprocessing cycles of compression molding under 5-10 tons pressure for 30 minutes at 150 °C.

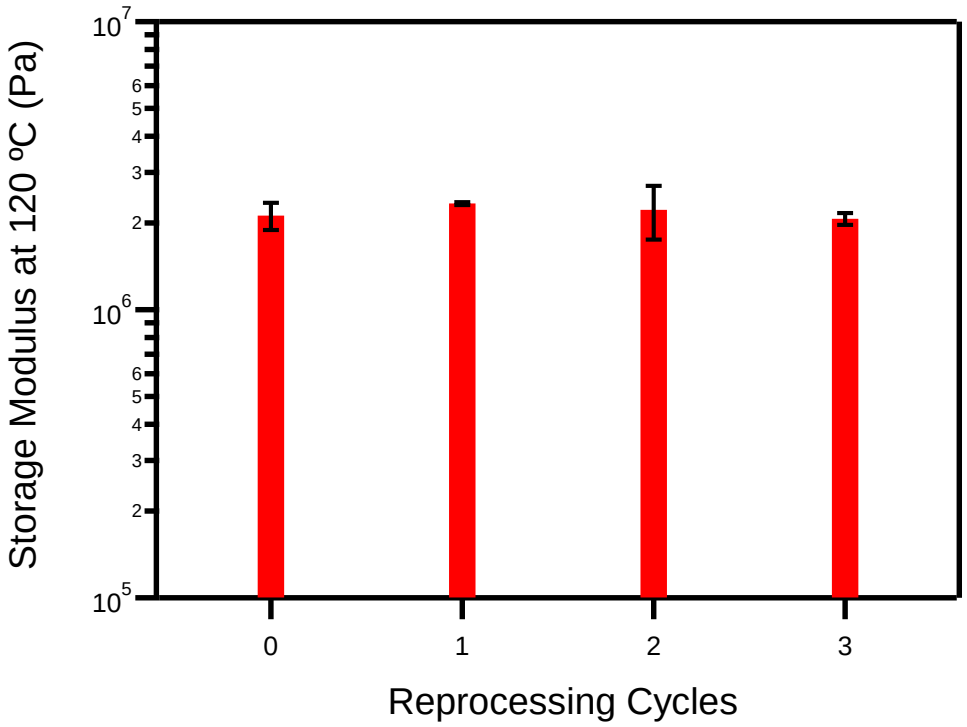

Figure S4.9. Bar graph showing plateau storage modulus of polymer 3 after each reprocessing cycle; error bars represent the standard deviation of three samples of each material.

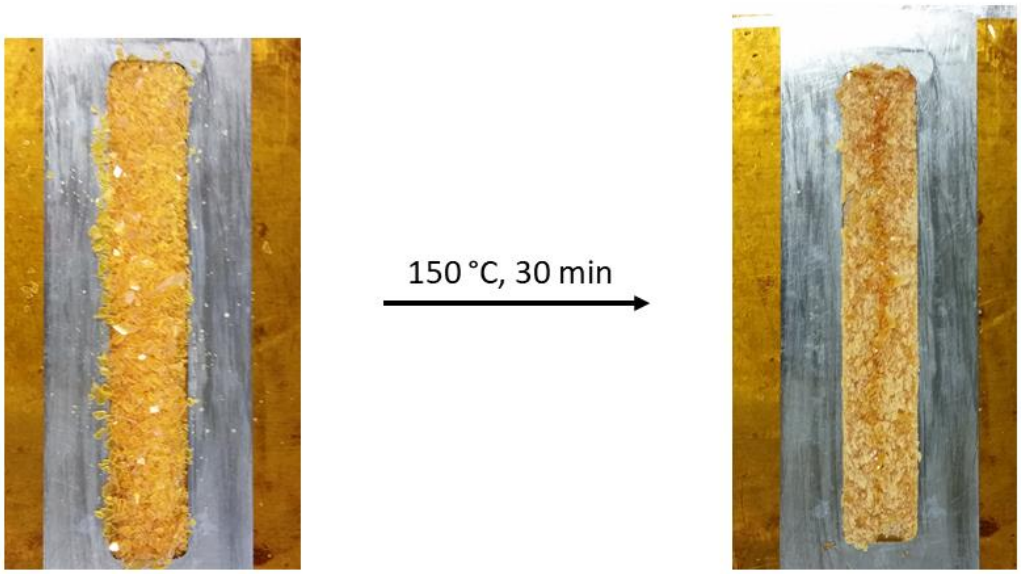

Figure S4.10. Attempted compression molding of control sample, showing no indication of reprocessability in the absence of disulfide linkages.

D. NMR Spectra

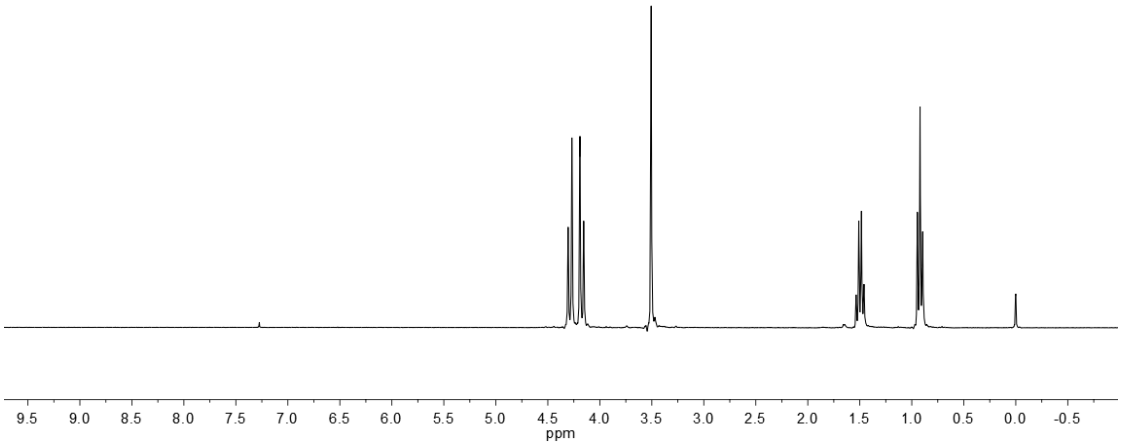

Figure S4.11. ^{1}H NMR ($CDCl_3$, 300 MHz, 298 K) of **bCC.**

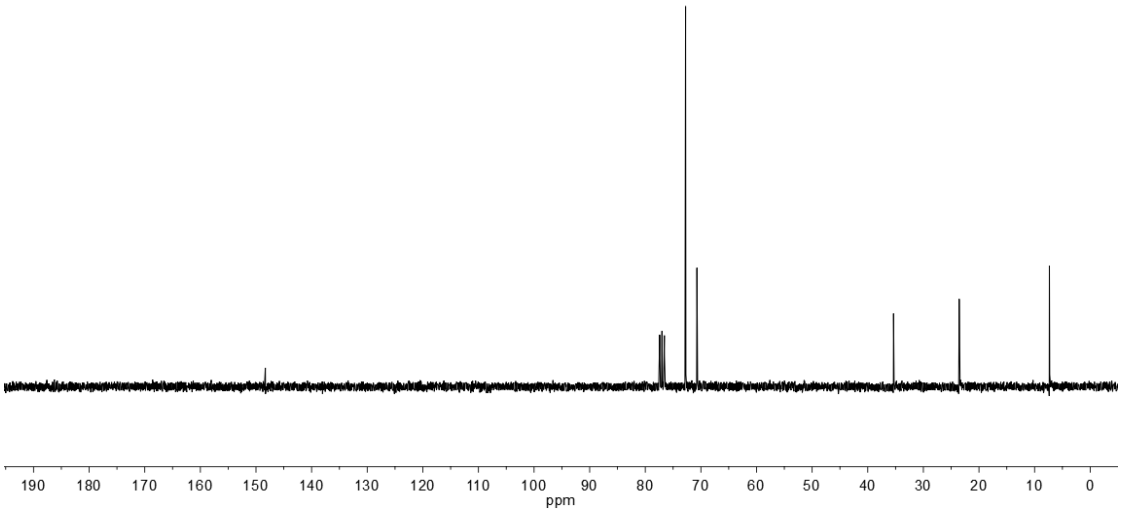

Figure S4.12. ^{13}C NMR ($CDCl_3$, 75 MHz, 298 K) of **bCC.**

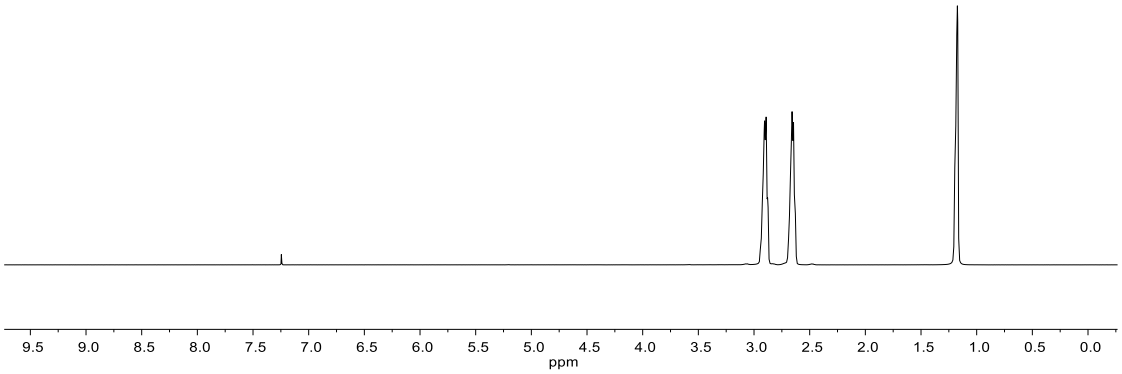

Figure S4.13. ^{1}H NMR ($CDCl_3$, 400 MHz, 298 K) of free-base cystamine.

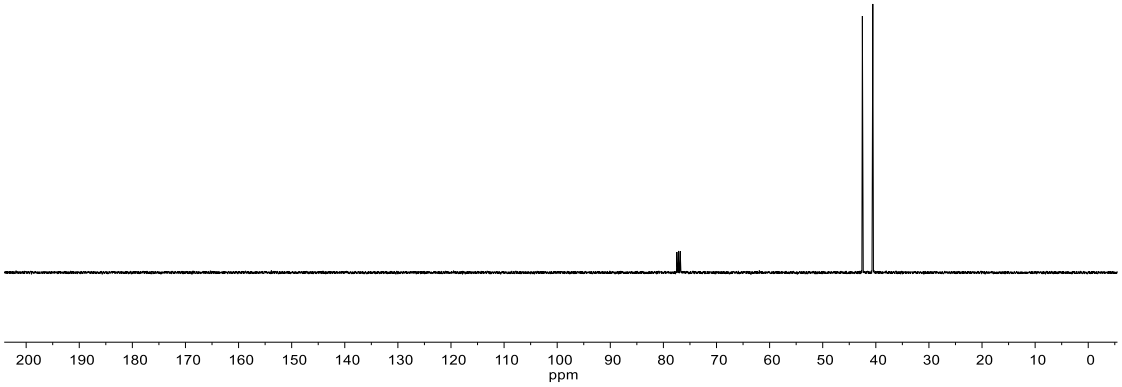

Figure S4.14. ^{13}C NMR ($CDCl_3$, 100 MHz, 298 K) of free-base cystamine.

E. References:

(1) Capelot, M.; Unterlass, M. M.; Tournilhac, F.; Leibler, L. *ACS Macro Lett.* **2012,** *1*, 789-792.

(2) Brutman, J. P.; Delgado, P. A.; Hillmyer, M. A. *ACS Macro Lett.* **2014,** *3*, 607-610.

(3) Yang, L.-Q.; He, B.; Meng, S.; Zhang, J.-Z.; Li, M.; Guo, J.; Guan, Y.-M.; Li, J.-X.; Gu, Z.-W. *Polymer* **2013**, *54*, 2668–2675.

(4) Alferiev, I. S.; Connolly, J. M.; Levy, R. J. *J. Organomet. Chem.* **2005**, *690*, 2543-2547.

CHAPTER FIVE

REPROCESSING CROSS-LINKED POLYURETHANES BY EXPLOITING THE INHERENTLY DYNAMIC NATURE OF URETHANE BONDS

5.1 Abstract

The reprocessing or recycling of cross-linked polymers by incorporating dynamic covalent cross-links has the potential to increase the sustainability associated with using these materials. Polyurethanes (PUs) are the largest class of polymers commonly used in cross-linked form; however, their direct recycling into similar value materials is not well-developed. We demonstrate that a variety of Lewis acid catalysts can mediate the exchange of urethane bonds selectively and at relatively mild conditions. Incorporating these catalysts into cross-linked polyether and polyester PUs with structures similar to commercial PUs gives cross-linked materials that relax stress very rapidly compared to most vitrimer networks at elevated temperatures. Due to their dynamic nature, these polymers can be reprocessed via compression molding to give materials with similar cross-linking densities, despite their covalently cross-linked architecture. Importantly, since these materials are based on commercially available PU monomers and simple Lewis acid catalysts, we anticipate that these discoveries will be attractive for enabling recycling of traditional thermosetting PUs and will enable new technologies requiring dynamic covalent networks.

5.2 Introduction

While cross-linked polymers are traditionally not recyclable, incorporating dynamic covalent bonds into polymer networks can lead to materials that possess mechanical properties competitive with traditional static thermosets while displaying recyclability commonly associated with thermoplastics.[1–4] Many dynamic covalent bonds, including imines,[5] boronic esters,[6] disulfides,[7] and reversible Diels-Alder adducts[8] have been incorporated into cross-linked polymer networks and been shown to enable their reprocessing. While these approaches will potentially enable new technologies or sustainable reuse of cross-linked materials, these linkages are uncommon in commodity polymers and their incorporation could represent hurdles to their large-scale implementation. Therefore, controlling the dynamic nature of linkages already prevalent in polymeric materials has the greatest potential to allow for direct reprocessing of materials already used in the marketplace. Leibler and coworkers demonstrated that incorporating a transesterification catalyst into commercially-prevalent ester-containing epoxy resins enables recycling of these traditionally thermosetting materials.[9,10] The simplicity of this approach has inspired many further studies, including the development of shape memory materials,[11,12] polymer composites,[13,14] and fundamental studies on the dynamic behavior of these materials.[15,16] Expanding this simple approach to other commodity polymers is desirable.

Polyurethanes (PUs) are the sixth largest class of polymers used worldwide, and are commonly used in cross-linked architectures as foams, adhesives, coatings, and structural components.[17] Due to their large scale use, much work has focused on the

repurposing or recycling of cross-linked PU waste, although most approaches rely on chemical recycling via glycolysis to produce new PU monomers.[18] Incorporation of other dynamic bonds into PUs is a promising strategy to directly recycle these cross-linked materials,[19–22] but controlling the dynamic nature of urethane linkages may represent a more straightforward approach to enable recycling of these materials on large scale. Tobolsky and coworkers demonstrated that urethane dissociation to isocyanates and alcohols at elevated temperatures causes cross-linked PUs to relax stress,[23,24] a phenomenon which has recently been recognized as a feature of other dynamic cross-linked polymers. More recently, Xie and coworkers showed that incorporation of catalytic dibutyltin dilaurate (DBTDL)[25] or tertiary amines[26] into cross-linked PUs causes more rapid stress relaxation via urethane exchange reactions (Figure 5.1A) and developed shape memory materials that can adjust their permanent shape (Figure 5.1B). Lei and coworkers reported that cross-linked PU elastomers containing DBTDL could be reprocessed at elevated temperatures to give materials with similar mechanical properties to the pristine materials (Figure 5.1C).[27] However, the full scope of this relaxation and reprocessing behavior remains unexplored. Therefore, we sought to more thoroughly investigate if other safer, readily available catalysts could efficiently facilitate this dynamic behavior, and whether this approach could enable efficient reprocessing of different classes of cross-linked PUs (Figure 5.1D).

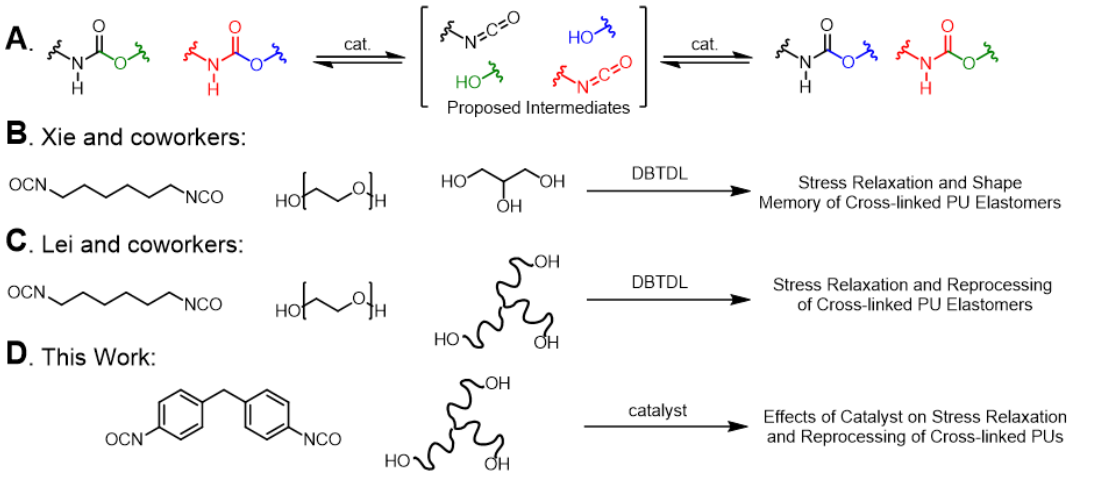

Figure 5.1. A. Schematic of urethane exchange process. B. and C. Prior investigations of dynamic urethane exchange processes in cross-linked polymers. D. This work, studying the impacts of catalyst choice on the urethane exchange process in different polyurethane networks.

5.3 Results and Discussion

Stress relaxation of cross-linked PUs has been shown to occur on slow, multiple-hour timescales in the absence of catalyst[24] or very rapidly (seconds to minutes) in the presence of DBTDL.[25,27] Incorporating DBTDL is attractive since it is a common catalyst used in the synthesis of PUs, but alkyl tin species are well-known to have harmful health and environmental effects,[28] and would not be ideal for large scale incorporation at high concentrations in PU resins. Therefore, we investigated whether tin was unique in its ability to catalyze the urethane exchange reaction. To evaluate catalyst performance, N-phenyl-O-octyl urethane and N-tolyl-O-decyl urethane were combined with 2.5 mol% of catalyst relative to urethane and heated at 140 °C for 1 hour. The mixture was then analyzed via GC-MS to determine whether the exchange products, N-phenyl-O-decyl urethane and N-tolyl-O-octyl urethane, were formed (Figure 5.2). In the absence of catalyst, only the two starting materials are observed,

consistent with slow stress relaxation observed in cross-linked PUs containing no additional catalyst.[24] Use of DBTDL as a catalyst yielded a mixture of the four urethanes, as expected for an equilibrium mixture and consistent with the prior literature reports.[25] A variety of Lewis acid catalysts and organocatalysts were screened, and many catalysts showed comparable activity to DBTDL in catalyzing this reaction. Zirconium(IV) acetylacetonate, iron(III) acetylacetonate, titanium(IV) isopropoxide, and hafnium(IV) acetylacetonate showed apparent equilibration within 1 hour (Figure 5.2, Figure S5.1). Stannous octoate and zirconium(IV) ethylhexanoate showed much lower or no conversion (Figure S5.1), suggesting that both the identity of the metal and its ligands play an important role in the catalyst's efficiency. A full study of the catalysis mechanism is ongoing, but we note a preliminary positive correlation between a given catalyst's urethane exchange activity and its reported activity for catalyzing the reaction of isocyanates with alcohols,[29] which may support a dissociative mechanism of exchange.

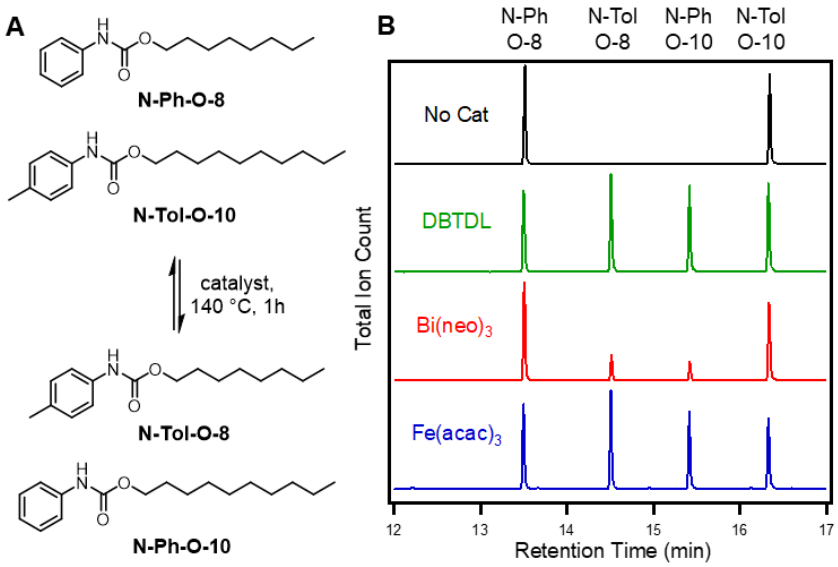

Figure 5.2. A. Urethane exchange of N-phenyl-O-octyl urethane and N-toly-O-decyl urethane to generate N-tolyl-O-octyl urethane and N-phenyl-O-decyl urethane. B. Gas chromatograms of the reaction mixture taken after heating for 1 hour at 140 °C.

We next studied the performance of these catalysts when incorporated into PU networks, using DBTDL as a benchmark for comparison due to its prior exploration in the literature.[25,27] Bismuth neodecanoate [$Bi(neo)_3$] was selected despite its lower activity in catalyst screening since it is commonly used as a catalyst in PU synthesis and has a lower toxicity than DBTDL.[30] Iron(III) acetylacetonate [$Fe(acac)_3$] was chosen as a representative example of using abundant, low-toxicity metals to catalyze this reaction.[31] Each of these catalysts was incorporated into both polyether- and polyester-based PUs, as these functional groups are most common in commercial cross-linked PU materials.

Cross-linked polyether PU elastomers were synthesized by reacting 4,4'-methylenebis(phenyl isocyanate) (MDI) with a linear polyethylene glycol (PEG, $M_n \approx$ 400 g/mol) and a 4-arm hydroxyl-terminated PEG ($M_n \approx$ 797 g/mol) in the presence of

1 mol% catalyst (Figure 5.3A). FT-IR spectroscopy of the cured polymers indicates complete disappearance of the -NCO stretching band (2285 cm^{-1}), and the appearance of both the urethane C=O stretching frequency (1690-1715 cm^{-1}, depending on the hydrogen bonding environment of the urethane) and N-H deformation (1530 cm^{-1}) (Figure S5.2). These polymers display low glass transition temperatures of ca. 10 ºC as measured by differential scanning calorimetry (DSC, Figure S5.3) and thermal stability similar to most cross-linked PUs, with decomposition onset temperatures greater than 280 °C (Figure S5.4). Dynamic mechanical thermal analysis (DMTA) shows a plateau storage modulus greater than the loss modulus above the glass transition temperature, indicative of the cross-linked architecture (Figure S5.5).

The rate of urethane exchange reactions at elevated temperatures within these networks were determined by elevated temperature stress relaxation experiments. Samples were equilibrated at a given temperature, a rapid 5% strain was applied, and the relaxation of the stress was monitored; this process was repeated multiple times for a given sample to understand the reproducibility of the process. All samples relaxed stress very rapidly and reproducibly with characteristic relaxation times (τ^*, the time required to relax to $1/e$ of the initial stress) of less than 40 s for each sample at 140 °C (Figure 5.3B, Figure S5.11-S5.13). FT-IR analysis of samples containing Bi and Sn show no change afterwards, consistent with degenerate urethane exchange reactions as the cause of stress relaxation. However, the samples containing Fe showed marked changes in functional groups present (Figure S5.9), suggesting that side reactions contribute to relaxation in these samples. Fe(III) catalysts have been reported to cause exchange or dehydration reactions of ethers,[32] so we suspect that these side reactions

contribute most strongly to the decomposition. While samples containing $Bi(neo)_3$ relaxed most rapidly at all temperatures measured, the measured relaxation rates of polymers containing each catalyst were quite similar. This contrasts the rates observed in model compounds wherein $Bi(neo)_3$ was the least efficient of the three catalysts; we suspect this could be due to presence of a different ligand environment around the metal center in the polymer, although further investigation is required to deconvolute these effects. Surprisingly, all samples relax stress with similar Arrhenius activation energies (Figure 5.3C), which strongly differs from the behavior observed in polyester vitrimers.[33] We believe this may be consistent with a dissociative mechanism, whereby the catalysts rapidly mediate the generation of an equilibrium between urethane and isocyanate/alcohol; the resulting relaxation is then governed by the equilibrium constant of the urethane dissociation process, which should be unaffected by the presence of catalyst.

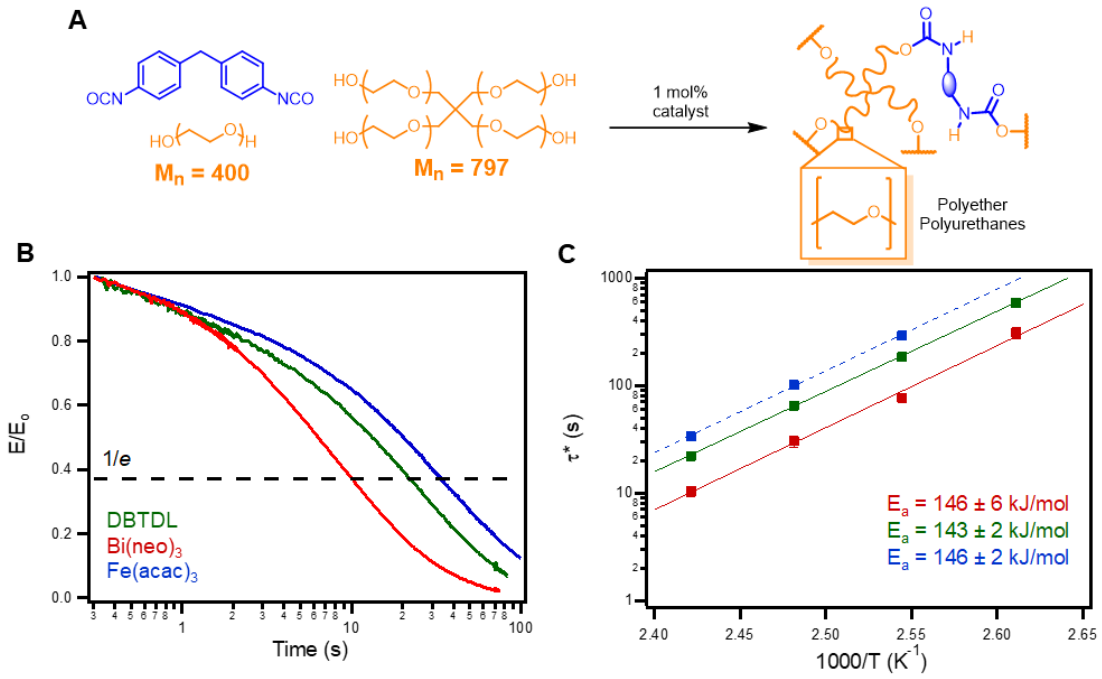

Figure 5.3. A. Synthesis of polyether PUs. B. Stress relaxation analysis of polyether PUs containing 1 mol% $Bi(neo)_3$ (red), DBTDL (green), and $Fe(acac)_3$ (blue) performed at 140 °C. C. Arrhenius plots of characteristic relaxation time of polyether PUs, the line for samples containing $Fe(acac)_3$ is dashed since decomposition occurs during the relaxation process.

To determine whether this unexpected behavior was general across multiple classes of PUs, we synthesized cross-linked polyester PUs by reacting MDI with a commercially available polyester oligomer polyol ($M_n \approx 500$ g/mol, -OH functionality ≈ 2.5) in the presence of 1 mol% of catalyst (Figure 5.4A). A control sample was synthesized in the absence of catalyst to determine its role on the properties of the material. All polymers show complete disappearance of the -NCO functionality by FT-IR spectroscopy (Figure S5.2), and swell in DCM to give relatively high gel fractions (>0.87), suggesting a cross-linked architecture. DSC indicates moderate glass transition temperatures of 45-50 °C (Figure S5.6), and TGA shows thermal stability to temperatures greater than 250 °C, even in the presence of catalyst (Figure S5.7). DMTA

shows a rubbery plateau modulus consistent with the expected covalently cross-linked architecture, and all catalysts give similar values of the rubbery storage modulus (2.14-2.31 MPa) and tan δ curves, suggesting that the different catalysts do not significantly affect the polymer curing reaction (Figure S5.8).

Elevated temperature stress relaxation experiments were again used to evaluate the dynamic nature of the polymers. In all polymers containing catalyst, rapid, reproducible stress relaxation is observed, with characteristic relaxation times of 35-47 s at 160 °C depending on the catalyst (Figure 5.4B). FT-IR analysis of polymers containing each of the three catalysts before and after stress relaxation suggests no chemical changes (Figure S5.10) and supports that even iron catalysts are compatible with polyester backbones. Remarkably similar rates and Arrhenius activation energies of stress relaxation are observed with all catalysts (Figure 5.4C). Additionally, these activation energies agree quantitatively with those obtained for polyether PU stress relaxation; this provides further support for our hypothesis that the urethane reversion process may be governing relaxation. A control sample synthesized in the absence of catalyst shows little to no stress relaxation at the same temperature (Figure 5.4B), indicating that the presence of catalyst is essential for rapid stress relaxation, consistent with our model compound studies and providing support for urethane exchange as the mechanism for relaxation in these materials.

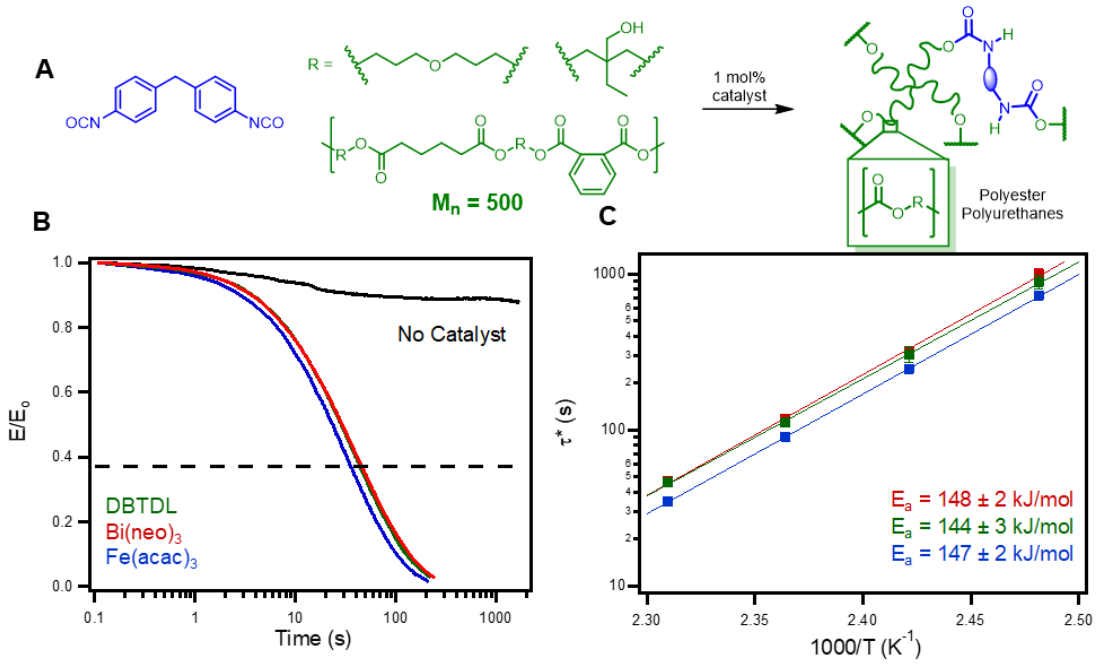

Figure 5.4. A. Synthesis of polyester PUs. B. Stress relaxation analysis of polyether PUs containing $Bi(neo)_3$ (red), DBTDL (green), $Fe(acac)_3$ (blue), or no catalyst (black) performed at 160 °C. C. Arrhenius plots of characteristic relaxation time of polyester PUs.

Given the fast and reproducible relaxation dynamics of these materials at elevated temperatures, direct reprocessing of these cross-linked materials should be possible. Polyester PU samples were ground to small pieces, and then reprocessed via compression molding at elevated temperature. In all cases, compression molding samples for 30 minutes at 150 °C gave homogeneous samples with similar properties to the virgin materials (Figure 5.5A, Figure S5.18). DMTA of the reprocessed polymers indicated similar glass transition temperatures and plateau moduli of the reprocessed samples, although slight decreases in the moduli are observed in all samples (Sn 67% recovery, Bi 90% recovery, Fe 87% recovery, Figure 5.5B). Further optimization of the reprocessing methodology is ongoing to determine if quantitative reprocessing is possible in these or other cross-linked PU systems.

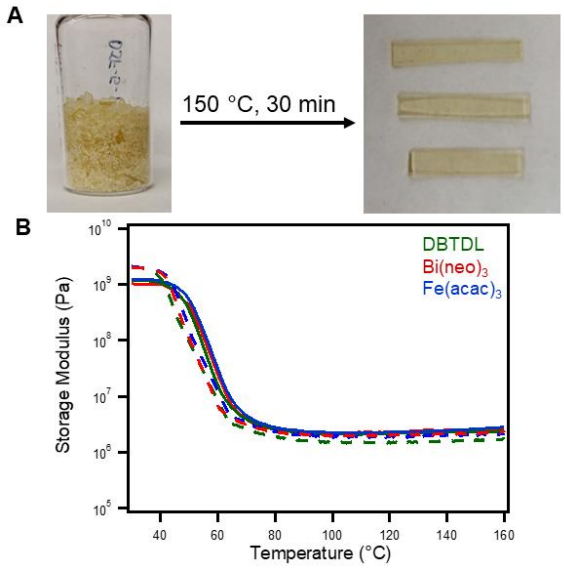

Figure 5.5. A. Photographs of ground and reprocessed polyester PUs containing 1 mol% $Bi(neo)_3$. B. DMTA of as-synthesized PUs (solid) containing DBTDL (green), $Bi(neo)_3$ (red), and $Fe(acac)_3$ (blue), and samples after reprocessing for 30 min at 150 °C (dashed).

5.4 Conclusions

In conclusion, we have demonstrated that a variety of Lewis acids catalyze the exchange of urethane bonds under relatively mild conditions. Incorporation of these catalysts into cross-linked PUs gives materials that relax stress extremely rapidly compared to many dynamic covalent networks. This methodology is compatible with both polyether and polyester-based PUs, and therefore, should be directly applicable to commercially-produced cross-linked PUs. Surprisingly, polymers with two different backbones synthesized in the presence of three different catalysts display very rapid rates of stress relaxation and similar activation energies of relaxation, which may suggest that the relaxation is governed by the urethane dissociation equilibrium, although further work is required to verify this hypothesis. Finally, we demonstrate that incorporating these catalysts enables the reprocessing of cross-linked PUs in rapid

timeframes. Further optimization of this process as well as applying more industrially-relevant reprocessing techniques has the potential to enable reprocessing of the vast amounts of cross-linked PU waste that is produced annually. We furthermore expect this to become a prevalent methodology for the synthesis of dynamic covalent networks due to the wide scope of Lewis acids and urethane monomers available to enable this methodology.

References

(1) Denissen, W.; Winne, J. M.; Du Prez, F. E. *Chem. Sci.* **2016**, *7*, 30–38.

(2) Imbernon, L.; Norvez, S. *Eur. Polym. J.* **2016**, *82*, 347–376

(3) Kloxin, C. J.; Bowman, C. N. *Chem. Soc. Rev.* **2013**, *42*, 7161–7173.

(4) Zou, W.; Dong, J.; Luo, Y.; Zhao, Q.; Xie, T. *Adv. Mater.* **2017**, *29*, 1606100.

(5) Taynton, P.; Yu, K.; Shoemaker, R. K.; Jin, Y.; Qi, H. J.; Zhang, W. *Adv. Mater.* **2014**, *26*, 3938–3942.

(6) Röttger, M.; Domenech, T.; van der Weegen, R.; Breuillac, A.; Nicolaÿ, R.; Leibler, L. *Science* **2017**, *356*, 62–65.

(7) Azcune, I.; Odriozola, I. *Eur. Polym. J.* **2016**, *84*, 147–160.

(8) Chen, X.; Dam, M., A.; Ono, K.; Mal, A.; Shen, H.; Nutt, S., R.; Sheran, K.; Wudl, F. *Science* **2002**, *295*, 1698–1702.

(9) Montarnal, D.; Capelot, M.; Tournilhac, F.; Leibler, L. *Science* **2011**, *334*, 965–968.

(10) Capelot, M.; Montarnal, D.; Tournilhac, F.; Leibler, L. *J. Am. Chem. Soc.* **2012**, *134*, 7664–7667.

(11) Pei, Z.; Yang, Y.; Chen, Q.; Terentjev, E. M.; Wei, Y.; Ji, Y. *Nat. Mater.* **2013**, *13*, 36–41.

(12) Pei, Z.; Yang, Y.; Chen, Q.; Wei, Y.; Ji, Y. *Adv. Mater.* **2016**, *28*, 156–160.

(13) Chabert, E.; Vial, J.; Cauchois, J.-P.; Mihaluta, M.; Tournilhac, F. *Soft Matter* **2016**, *12*, 4838–4845.

(14) Legrand, A.; Soulié-Ziakovic, C. *Macromolecules* **2016**, *49*, 5893–5902.

(15) Yu, K.; Taynton, P.; Zhang, W.; Dunn, M. L.; Qi, H. J. *RSC Adv.* **2014**, *4*, 48682–48690.

(16) Imbernon, L.; Norvez, S.; Leibler, L. *Macromolecules* **2016**, *49*, 2172–2178.

(17) Market Study, Polyurethanes (PUR) and Isocyanates (MDI & TDI). Cerasana January 2016.

(18) Yang, W.; Dong, Q.; Liu, S.; Xie, H.; Liu, L.; Li, J. *Procedia Environ. Sci.* **2012**, *16*, 167–175.

(19) Fortman, D. J.; Brutman, J. P.; Cramer, C. J.; Hillmyer, M. A.; Dichtel, W. R. *J. Am. Chem. Soc.* **2015**, *137*, 14019–14022.

(20) Fortman, D. J.; Brutman, J. P.; Hillmyer, M. A.; Dichtel, W. R. *J. Appl. Polym. Sci.* **2017**, *134*, 44984.

(21) Zhang, Z. P.; Rong, M. Z.; Zhang, M. Q. *Adv. Funct. Mater.* **2018**, *28*, 1706050.

(22) Heo, Y.; Sodano, H. A. *Adv. Funct. Mater.* **2014**, *24*, 5261–5268.

(23) Offenbach, J. A.; Tobolsky, A. V. *J. Colloid Sci.* **1956**, *11*, 39–47.

(24) Colodny, P. C.; Tobolsky, A. V. *J. Am. Chem. Soc.* **1957**, *79*, 4320–4323.

(25) Zheng, N.; Fang, Z.; Zou, W.; Zhao, Q.; Xie, T. *Angew. Chem. Int. Ed.* **2016**, *55*, 11421–11425.

(26) Zheng, N.; Hou, J.; Xu, Y.; Fang, Z.; Zou, W.; Zhao, Q.; Xie, T. *ACS Macro Lett.* **2017**, *6*, 326–330.

(27) Yan, P.; Zhao, W.; Fu, X.; Liu, Z.; Kong, W.; Zhou, C.; Lei, J. *RSC Adv.* **2017**, *7*, 26858–26866.

(28) Nath, M. *Appl. Organomet. Chem.* **2008**, *22*, 598–612.

(29) Schellekens, Y.; Van Trimpont, B.; Goelen, P.-J.; Binnemans, K.; Smet, M.; Persoons, M.-A.; De Vos, D. *Green Chem.* **2014**, *16*, 4401–4407.

(30) Pretti, C.; Oliva, M.; Mennillo, E.; Barbaglia, M.; Funel, M.; Reddy Yasani, B.; Martinelli, E.; Galli, G. *Ecotoxicol. Environ. Saf.* **2013**, *98*, 250–256.

(31) Egorova, K. S.; Ananikov, V. P. *Angew. Chem. Int. Ed.* **2016**, *55*, 12150–12162.

(32) Sahoo, P. K.; Gawali, S. S.; Gunanathan, C. *ACS Omega* **2018**, *3*, 124–136.

(33) Capelot, M.; Unterlass, M. M.; Tournilhac, F.; Leibler, L. *ACS Macro Lett.* **2012**, *1*, 789–792.

CHAPTER FIVE APPENDIX

Table of Contents

A. Materials and General Methods

Materials. All reagents were purchased from Sigma-Aldrich or Fisher Scientific. All reagents were used without further purification unless otherwise specified. Dichloromethane (CH_2Cl_2) and tetrahydrofuran (THF) were purchased from Fisher Scientific and purified using a custom-built alumina-column based solvent purification system. Other solvents were purchased from Fisher Scientific and used without further purification.

Instrumentation. Infrared spectra were recorded on a Thermo Nicolet iS10 equipped with a ZnSe ATR attachment. Spectra were uncorrected.

Solution-phase NMR spectra were recorded on a Varian 400 MHz or an Agilent DD MR-400 400 MHz spectrometer using a standard ^{1}H/X Z-PFG probe at ambient temperature.

Thermogravimetric analysis (TGA) was performed on a Mettler Toledo SDTA851 Thermogravimetric Analysis System using 5-10 mg of sample. Samples were heated under a nitrogen atmosphere at a rate of 5 °C/min from 25 ºC to 600 ºC.

Differential scanning calorimetry (DSC) was performed on a Mettler Toledo DSC822 Differential Scanning Calorimeter. Samples (5-10 mg) were heated at a rate of 10 °C/min to at least 90 °C to erase thermal history, cooled to –30 °C at 10 °C/min, and then heated to at least 110 °C. All data shown are taken from the second heating ramp. The glass transition temperature (T_g) was calculated from the maximum value of the derivative of heat flow with respect to temperature.

Dynamic mechanical thermal analysis (DMTA) was performed on a TA Instruments RSA-G2 analyzer (New Castle, DE) using rectangular (*ca.* 0.75 mm (T) ×

5 mm (W) × 20 mm (L) and a gauge length of 10 mm). The axial force was adjusted to 0 N and a strain adjust of 30% was set with a minimum strain of 0.05%, a maximum strain of 5%, and a maximum force of 1 N in order to prevent the sample from buckling or going out of the specified strain. Furthermore, a force tracking mode was set such that the axial force was twice the magnitude of the oscillation force. A temperature ramp was then performed from 30 °C to 200 °C at a rate of 5 °C/min, with an oscillating strain of 0.05% and an angular frequency of 6.28 rad s^{-1} (1 Hz). The T_g was calculated from the maximum value of the loss modulus (E").

Stress relaxation analysis (SRA) was performed on a TA Instruments RSA-III analyzer (New Castle, DE) using rectangular films (*ca.* 1.0 mm (T) × 5 mm (W) × 15 mm (L) and a Gauge length of 8 mm). The SRA experiments were performed with strain control at specified temperature (110 to 160 °C). The samples were allowed to equilibrate at this temperature for approximately 10 minutes, after which the axial force was then adjusted to 0 N. Each sample was then subjected to an instantaneous 5% strain. The stress decay was monitored, while maintaining a constant strain (5%), until the stress relaxation modulus had relaxed to at least 37% (1/*e*) of its initial value. This was performed three consecutive times for each sample. The activation energy (E_a) and freezing transition temperature (T_v) were determined using the methodology in literature. [1,2]

To reprocess the materials, the polymer was ground into small pieces using a Cuisinart Grind Central© coffee grinder. The ground polymer was spread between two aluminum plates in a 1.0 mm thick aluminum mold. This assembly was placed in PHI 30-ton manual press preheated to the desired temperature and allowed to thermally

equilibrate for 1 minute. The material was compressed at 5-10 MPa of pressure for 30 s, then the pressure was released, and this was repeated 2x to enable removal of air bubbles. The material was then compressed at 5-10 MPa for 30 minutes. The homogenous polymer was removed from the mold, and specimens for DMTA were cut using a straight-edge blade on a 150 °C hot plate.

B. Synthetic Procedures

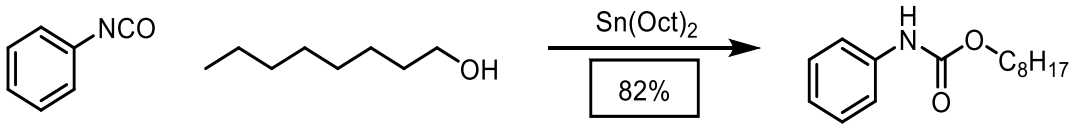

Synthesis of N-phenyl-O-octyl urethane: To a flame-dried round-bottom flask under nitrogen atmosphere was added 1-octanol (2.19 g, 2.65 ml, 16.8 mmol) and anhydrous tetrahydrofuran (20 mL). A solution of $Sn(Oct)_2$ (130 mg, 0.34 mmol, 2 mol%) dissolved in anhydrous tetrahydrofuran (1 mL) was added, followed by addition of phenyl isocyanate (2.00 g, 1.82 ml, 16.8 mmol) using a syringe. The resulting solution was stirred at room temperature for 24 h, and solvent was removed at reduced pressure to yield a white solid. The crude solid was chromatographed on silica gel in 20% ethyl acetate/hexanes to yield the product as a white solid (3.4 g, 82% yield). ^{1}H NMR (400 MHz, $CDCl_3$) δ 7.38 (d, *J* = 8.0 Hz, 2H), 7.35-7.23 (m, 2H), 7.05 (tt, *J* = 7.1, 1.2 Hz, 1H), 6.56 (br s, 1H), 4.16 (t, J = 6.7 Hz, 2H), 1.71-1.63 (m, 2H), 1.43-1.23 (m, 10H), 0.89 (t, *J* = 7.8 Hz, 3H). ^{13}C NMR (100 MHz, $CDCl_3$) δ 153.7, 138.0, 128.9, 123.2, 118.5, 65.4, 31.7, 29.19, 29.15, 28.9, 25.8, 22.6, 14.0. IR (neat, ATR) 3304, 2956, 2920, 2853, 1698, 1599, 1544, 1444, 1236, 1055, 747 cm^{-1}.

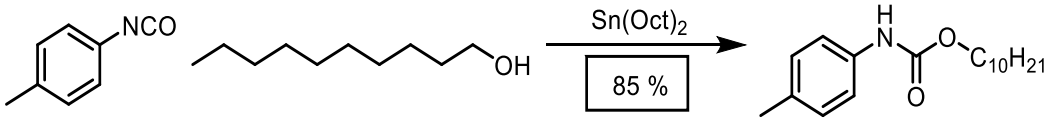

Synthesis of N-tolyl-O-decyl urethane: To a flame-dried round-bottom flask under nitrogen atmosphere was added 1-decanol (2.66 g, 3.20 ml, 16.8 mmol) and anhydrous tetrahydrofuran (20 mL). A solution of $Sn(Oct)_2$ (130 mg, 0.34 mmol, 2 mol%) dissolved in anhydrous tetrahydrofuran (1 mL) was added, followed by addition of *p*-

tolyl isocyanate (2.24 g, 2.12 ml, 16.8 mmol) using a syringe. The resulting solution was stirred at room temperature for 24 h, and solvent was removed at reduced pressure to yield a white solid. The crude solid was chromatographed on silica gel in 20% ethyl acetate/hexanes to yield the product as a white solid (4.16 g, 85% yield). ^{1}H NMR (400 MHz, $CDCl_3$) δ 7.28-7.22 (m, 2H), 7.10 (d, J = 8.3 Hz, 2H), 6.49 (br s, 1H), 4.14 (t, J = 6.7 Hz, 2H), 2.30 (s, 3H), 1.72-1.60 (m, 2H), 1.44-1.24 (m, 14H), 0.92-0.84 (m, 3H). ^{13}C NMR (100 MHz, $CDCl_3$) δ 153.8, 135.4, 132.8, 129.4, 118.7, 65.3, 31.9, 29.51, 29.50, 29.27, 29.25, 28.9, 25.8, 22.6, 20.7, 14.1. IR (neat, ATR) 3327, 2919, 2851, 1696, 1596, 1531, 1314, 1235, 1071, 814 cm^{-1}.

Model Urethane-Urethane Exchange Catalyst Screening: To a vial was added catalyst (0.059 mmol, 2.5 mol% to urethane), *N*-phenyl-*O*-octyl urethane (294 mg, 1.18 mmol), *N*-tolyl-*O*-decyl urethane (344 mg, 1.18 mmol). The resulting mixture was heated to 140 °C on a preheated aluminum heating block. Aliquots were taken after heating for 60 min, diluted with DCM, and subjected to GC-MS analysis.

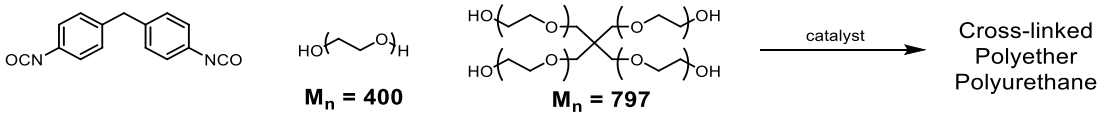

Synthesis of Cross-linked Polyether Polyurethanes: To a vial was added pentaerythritol ethoxylate (15/4 EO/OH, average $M_n \approx 797$ g/mol, 150 mg, 0.19 mmol), polyethylene glycol ($M_n \approx 400$ g/mol, 1.500 g, 3.75 mmol), and 7.5 ml anhydrous CH_2Cl_2. Solid 4,4'-methylenebis(phenyl isocyanate) (MDI) (1.033 g, 4.13 mmol) was added, and the solution was vortexed until the MDI was totally dissolved. An aliquot of a solution of catalyst (50-100 mg/ml in anhydrous CH_2Cl_2) was added to give a total

concentration of 1 mol% catalyst to total -NCO functionality. The resulting solution was vortexed for 20 seconds, then poured into aluminum pans (75 mm D x 15 mm H), covered with aluminum foil, and allowed to stand at room temperature for 16-24 h. The resulting films were cut & heated at 80 °C under 20 mtorr vacuum for 48 h. Indistinguishable FT-IR spectra were obtained with samples containing different catalysts. FT-IR (solid, ATR) 3299 (N-H stretch), 2868, 1725-1706 (C=O stretch), 1598, 1532 (N-H deformation), 1412, 1309, 1220, 1067, 946, 816, 768 cm^{-1}.

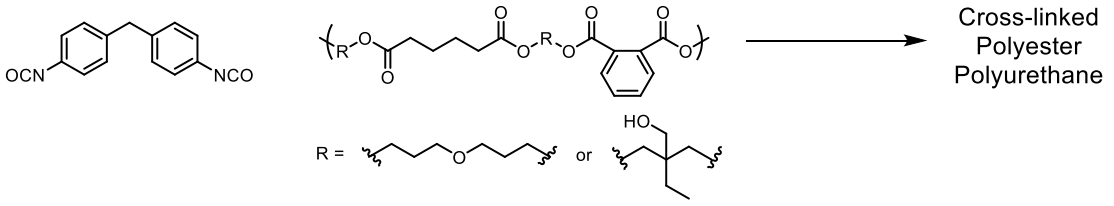

Synthesis of Crosslinked Polyester Polyurethanes with Catalyst: To a vial was added poly[trimethylolpropane/di(propylene glycol)-*alt*-adipic acid/phthalic anhydride], polyol (200 eq. wt., 3.60 g, 18.0 mmol -OH) and dissolved in 12.0 ml anhydrous CH_2Cl_2. Solid 4,4'-methylenebis(phenyl isocyanate) (MDI) (2.253 g, 9.0 mmol) was added, and the solution was vortexed until the MDI was totally dissolved. An aliquot of a solution of catalyst (50-100 mg/ml in anhydrous CH_2Cl_2) was added to give a total concentration of 1 mol% catalyst to total -NCO functionality. The resulting solution was vortexed for 60 seconds, then the mixtures were poured into an aluminum pan (104 mm D x 15 mm H), covered with aluminum foil, and allowed to stand at room temperature for 16-24 h. The resulting films were cut & heated at 80 °C under 20 mtorr vacuum for 48 h. Indistinguishable FT-IR spectra were obtained with samples containing different catalysts. FT-IR (solid, ATR) 3326 (N-H stretch), 2933, 1716-1705 (C=O stretch), 1597, 1525 (N-H deformation), 1412, 1309, 1219, 1066, 1017, 816, 766 cm^{-1}.

Synthesis of Catalyst-Free Cross-linked Polyester Polyurethane: To a vial was added poly[trimethylolpropane/di(propylene glycol)-*alt*-adipic acid/phthalic anhydride], polyol (200 eq. wt., 4.224 g, 21.1 mmol -OH) and dissolved in 8.0 ml anhydrous toluene. Solid 4,4'-methylenebis(phenyl isocyanate) (2.643 g, 10.56 mmol) was added, and the solution was heated to 60 ºC until fully dissolved. The resulting mixture was vortexed for 30 s, poured into an aluminum pan (104 mm D x 15 mm H), covered with aluminum foil, and heated at 60 ºC for 18 h. The resulting polymer was post-cured at 100 ºC for 4 h, then 140 ºC for 2 h, then 80 ºC under vacuum for 12 h to ensure full curing and removal of solvent. FT-IR (solid, ATR) 3326 (N-H stretch), 2933, 1716-1705 (C=O stretch), 1597, 1525 (N-H deformation), 1412, 1309, 1219, 1066, 1017, 816, 766 cm^{-1}.

C. Characterization Tables and Figures

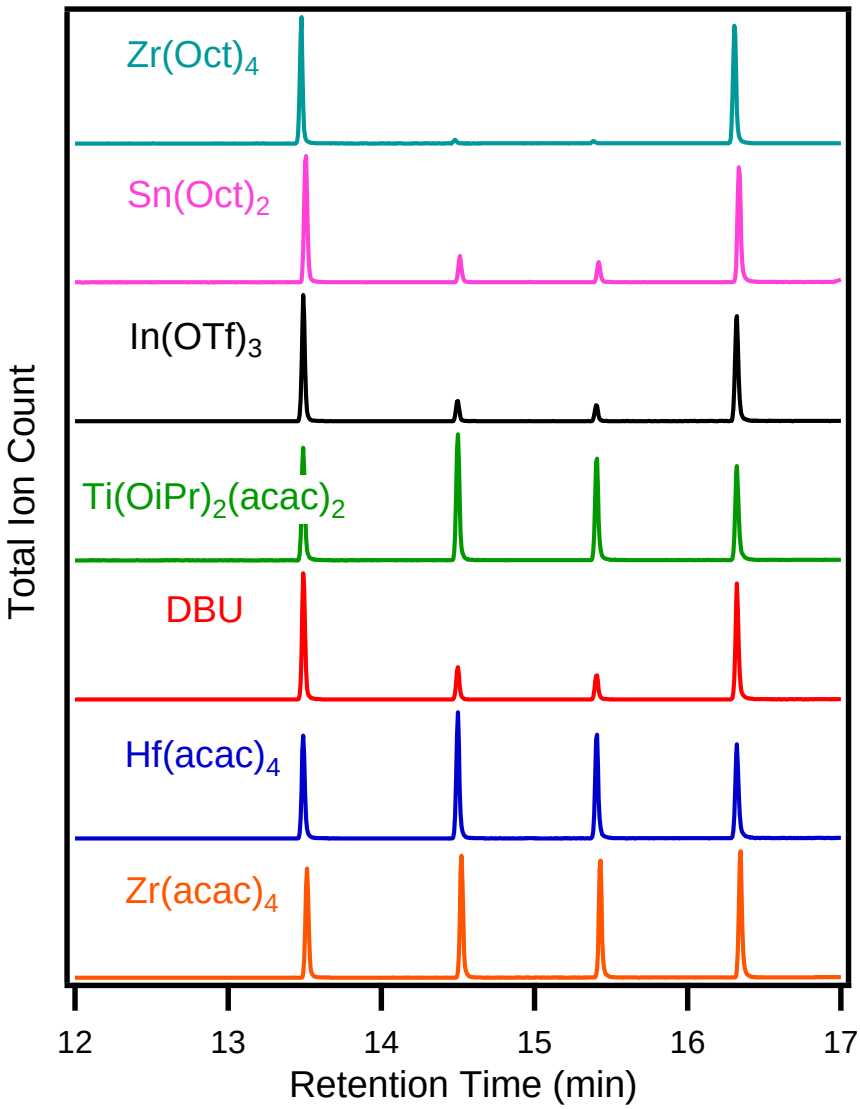

Figure S5.1. Normalized gas chromatograms of mixture of N-phenyl-O-octyl urethane (RT = 13.51 min) and N-tolyl-O-decyl (RT = 16.34 min) urethane heated to 140 °C in the presence of 2.5 mol% catalyst. The appearance of N-tolyl-O-octyl urethane (RT = 14.52 min) and N-phenyl-O-decyl urethane (RT = 15.43 min) are the result of urethane-urethane exchange.

Table S5.1. Characterization of Polyether Polyurethanes

Polymer	Gel %	T_d (°C, 5%)	$T_{g,DSC}$ (°C)	E' at 120 °C (MPa)	E_a (kJ/mol)	T_v (°C)
DBTDL	0.75	284	9	0.95	143 ± 2	49
Bi(neo)$_3$	0.86	293	10	1.07	146 ± 6	46
Fe(acac)$_3$	0.79	294	10	1.24	146 ± 2	54

Table S5.2. Characterization of Polyester Polyurethanes

Polymer	Gel %	T_d (°C, 5%)	$T_{g,DSC}$ (°C)	$T_{g,DMTA}$ (°C)	E' at 120 °C (MPa)	E_a (kJ/mol)	T_v (°C)
DBTDL	87	272	44	49	2.14	144 ± 3	71
Bi(neo)$_3$	92	282	48	51	2.31	148 ± 2	73
Fe(acac)$_3$	92	283	49	51	2.28	147 ± 2	71
No Cat	92	299	37	43	1.97	-	-

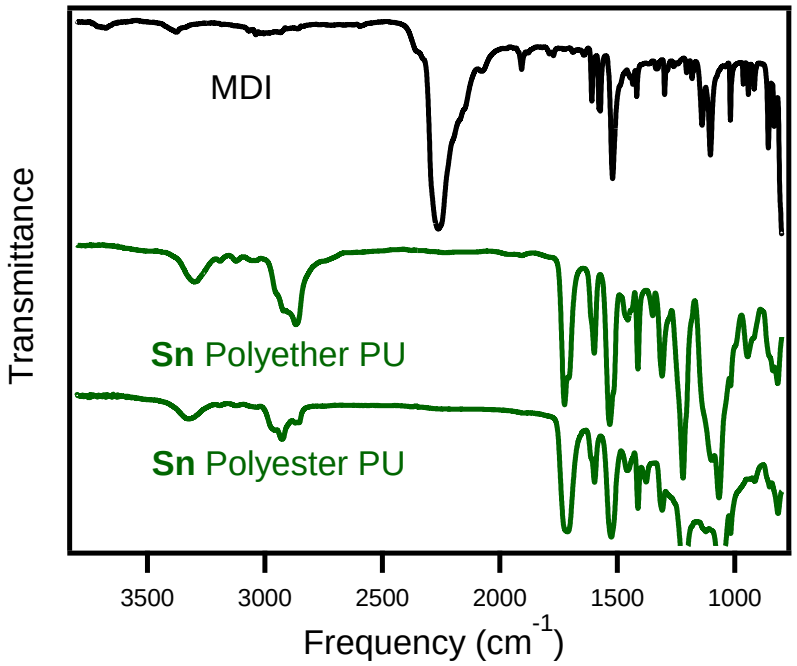

Figure S5.2. FT-IR spectra of 4,4'-methylenebis(phenylisocyanate) (black), and polyether and polyester polyurethanes synthesized with 1 mol% DBTDL (green), showing complete disappearance of -NCO stretch at 2285 cm^{-1}.

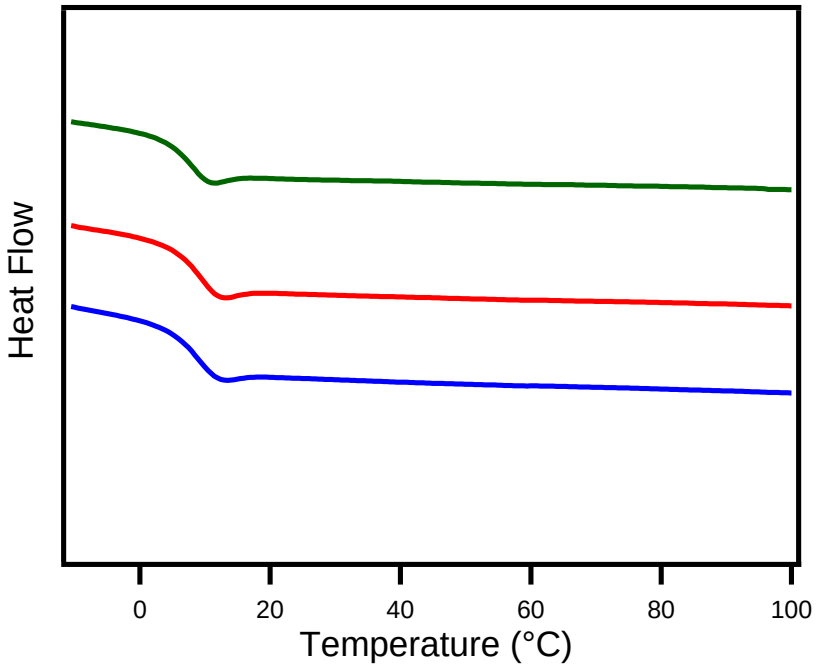

Figure S5.3. Differential scanning calorimetry traces of polyether PUs containing 1 mol% DBTDL (green), $Bi(neo)_3$ (red), and $Fe(acac)_3$ (blue) at a heating rate of 10 °C/min.

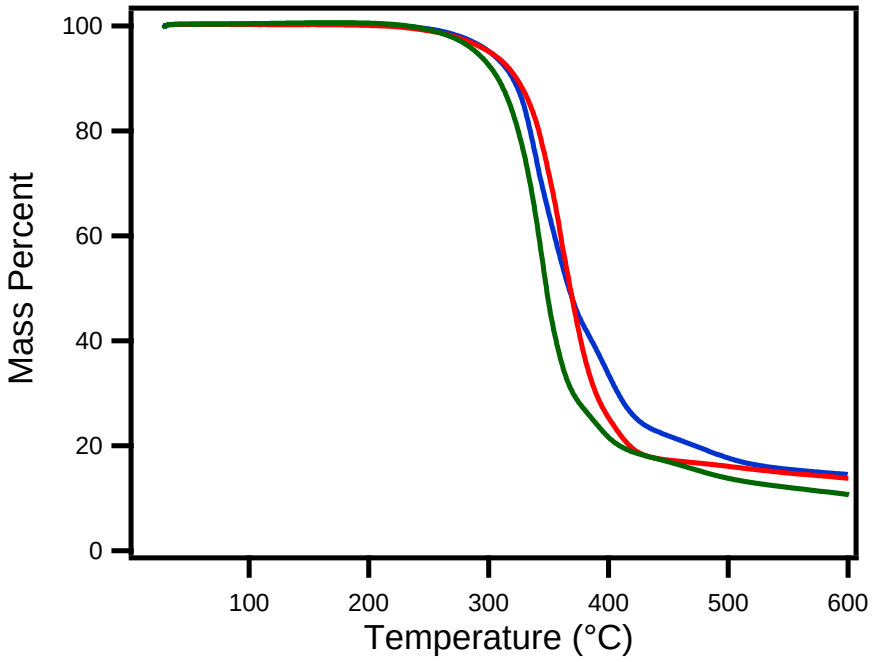

Figure S5.4. Thermogravimetric analysis traces of polyether PUs containing 1 mol% DBTDL (green), $Bi(neo)_3$ (red), and $Fe(acac)_3$ (blue) performed under nitrogen atmosphere at a heating rate of 10 °C/min.

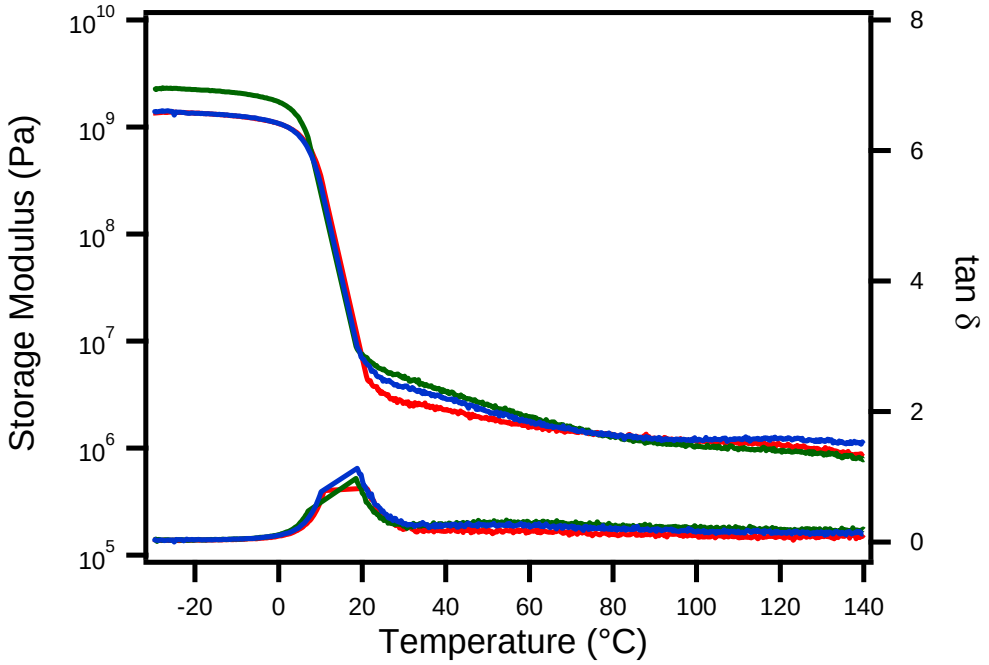

Figure S5.5. DMTA of polyether PUs containing 1 mol% DBTDL (green), $Bi(neo)_3$ (red), and $Fe(acac)_3$ (blue) performed at an oscillation frequency of 1 Hz, a minimum oscillation strain of 0.05%, and a heating rate of 5 ºC/min.

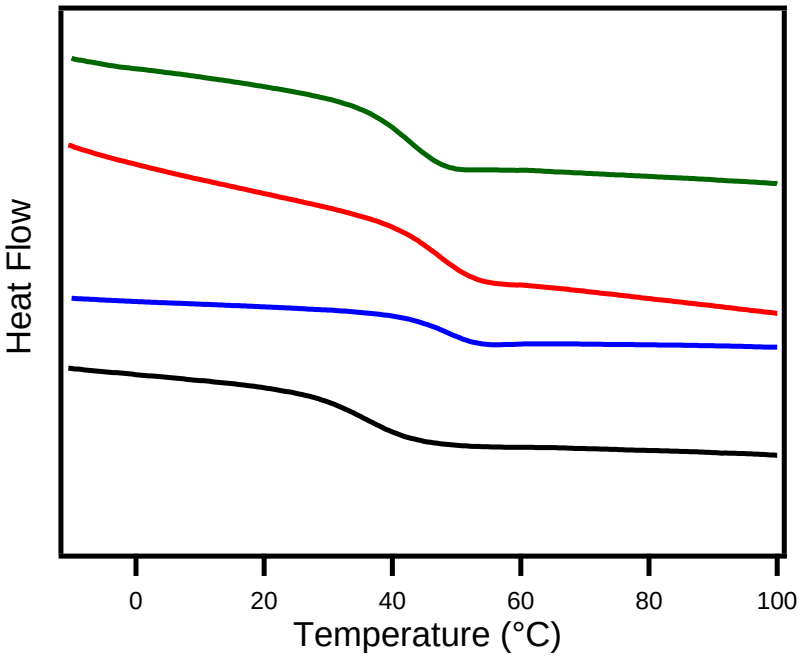

Figure S5.6. Differential scanning calorimetry traces of polyester PUs containing 1 mol% DBTDL (green), $Bi(neo)_3$ (red), $Fe(acac)_3$ (blue) or no catalyst (black) at a heating rate of 10 °C/min.

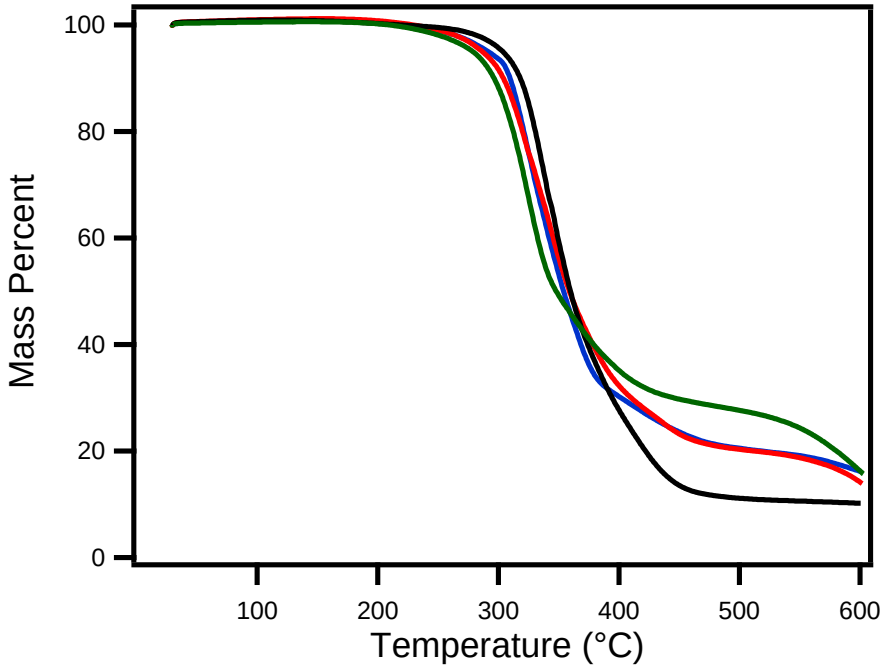

Figure S5.7. Thermogravimetric analysis traces of polyether PUs containing 1 mol% DBTDL (green), $Bi(neo)_3$ (red), $Fe(acac)_3$ (blue), or no catalyst (black) performed under nitrogen atmosphere at a heating rate of 10 °C/min.

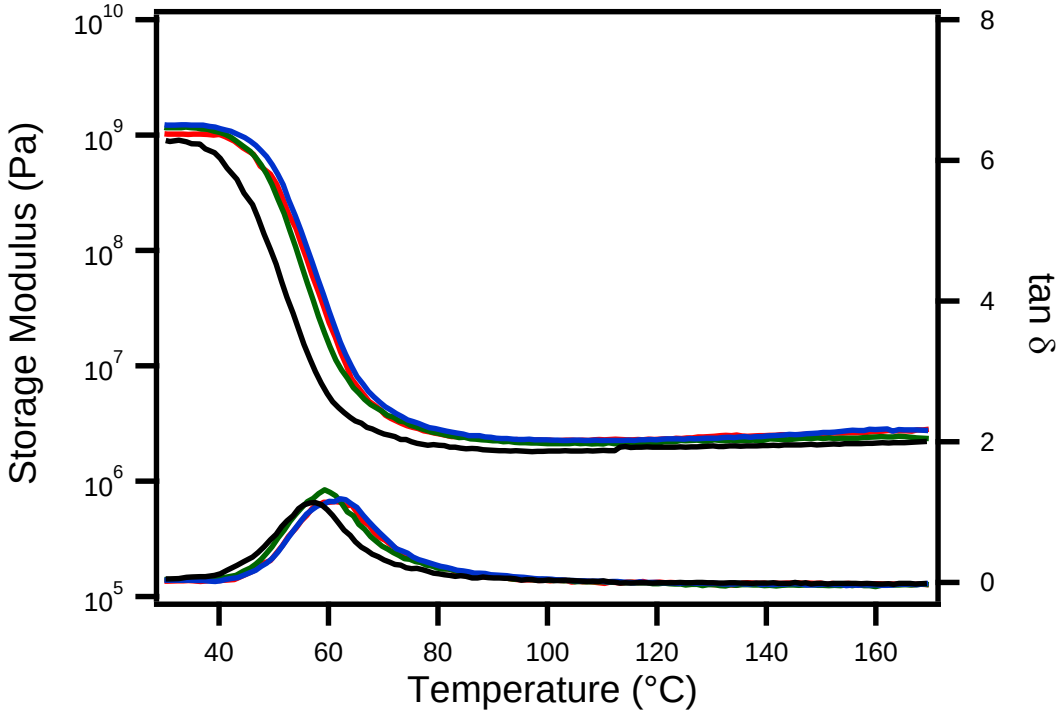

Figure S5.8. DMTA of polyester PUs containing 1 mol% DBTDL (green), $Bi(neo)_3$ (red), and $Fe(acac)_3$ (blue) performed at an oscillation frequency of 1 Hz, a minimum oscillation strain of 0.05%, and a heating rate of 5 ºC/min.

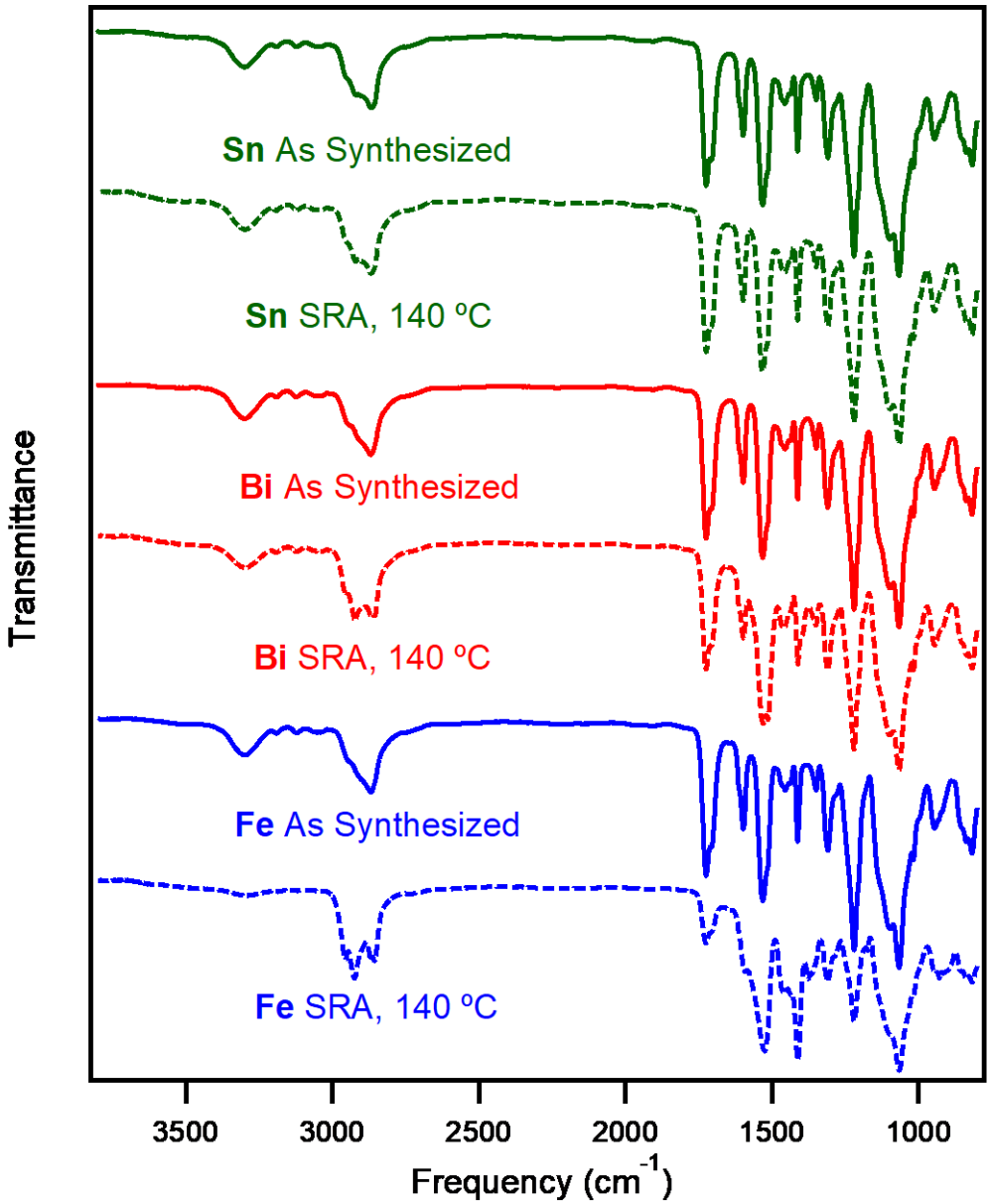

Figure S5.9. FT-IR spectra of polyether polyurethanes as synthesized (solid) and after stress relaxation analysis at highest temperature measured (dashed).

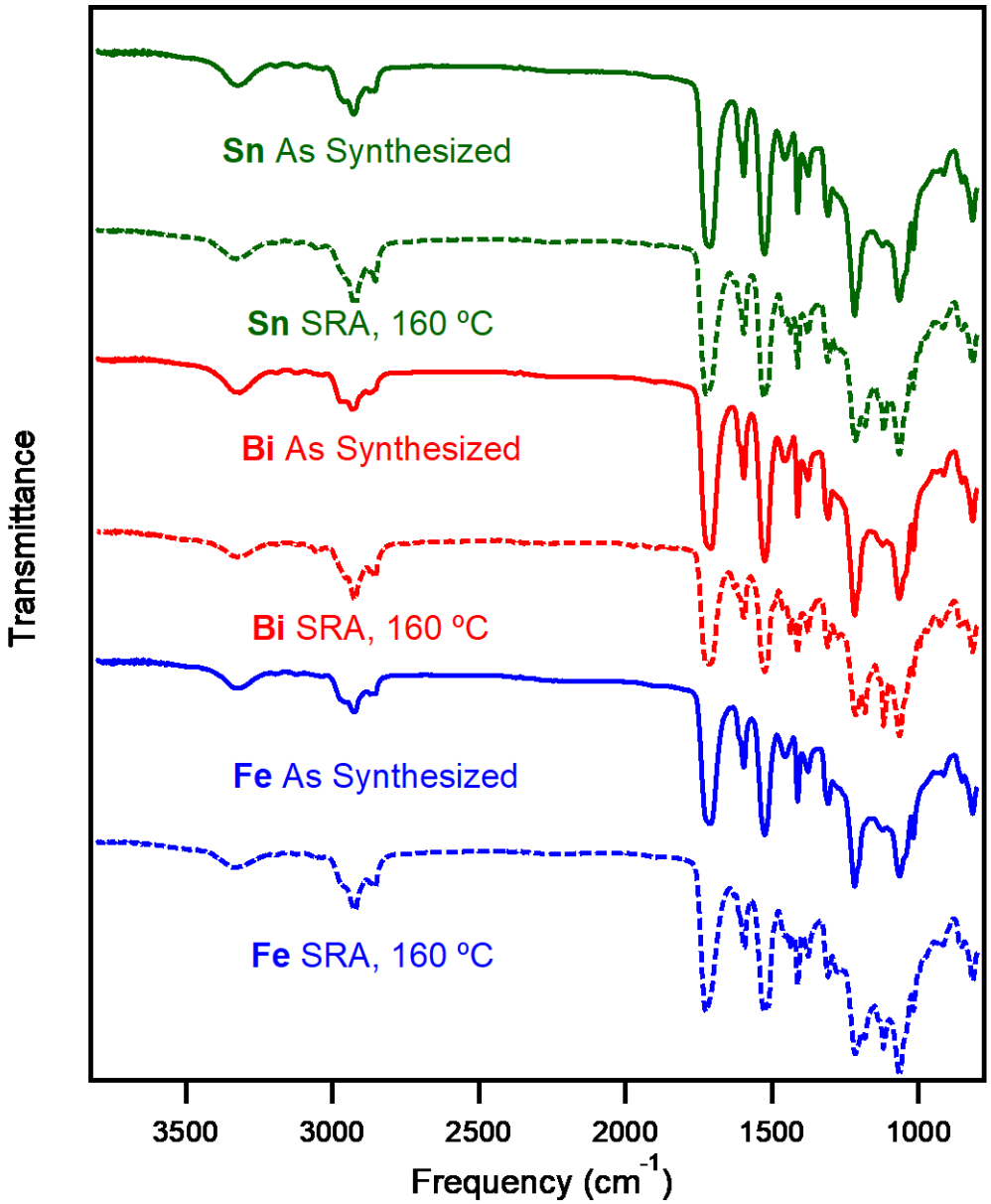

Figure S5.10. FT-IR spectra of polyester polyurethanes as synthesized (solid) and after stress relaxation analysis at highest temperature measured (dashed).

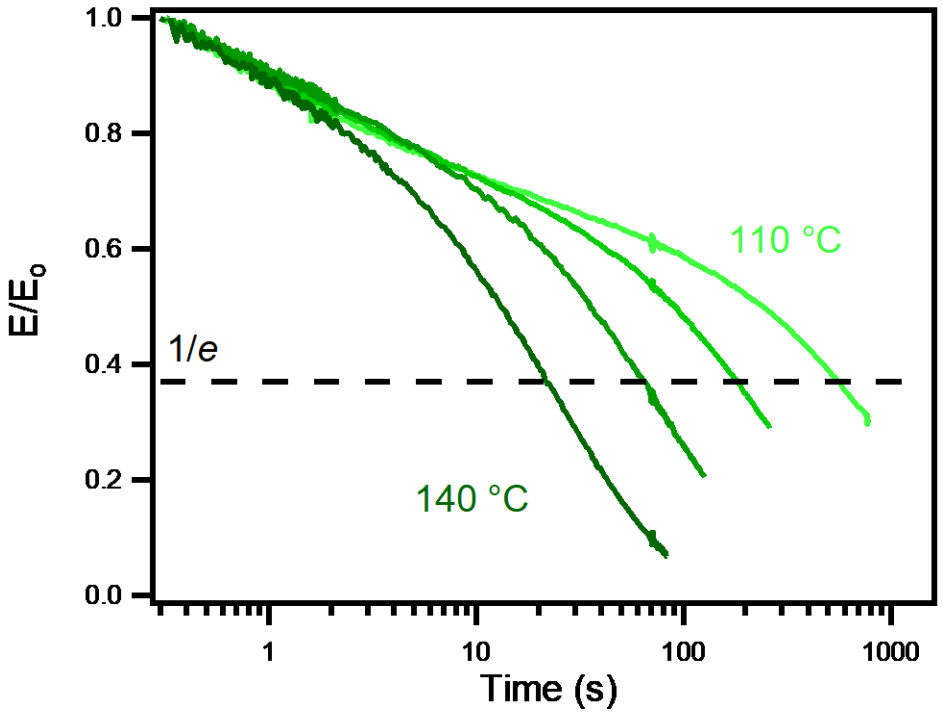

Figure S5.11. Representative stress relaxation curves of polyether PU with 1 mol% DBTDL performed from 110 to 140 °C.

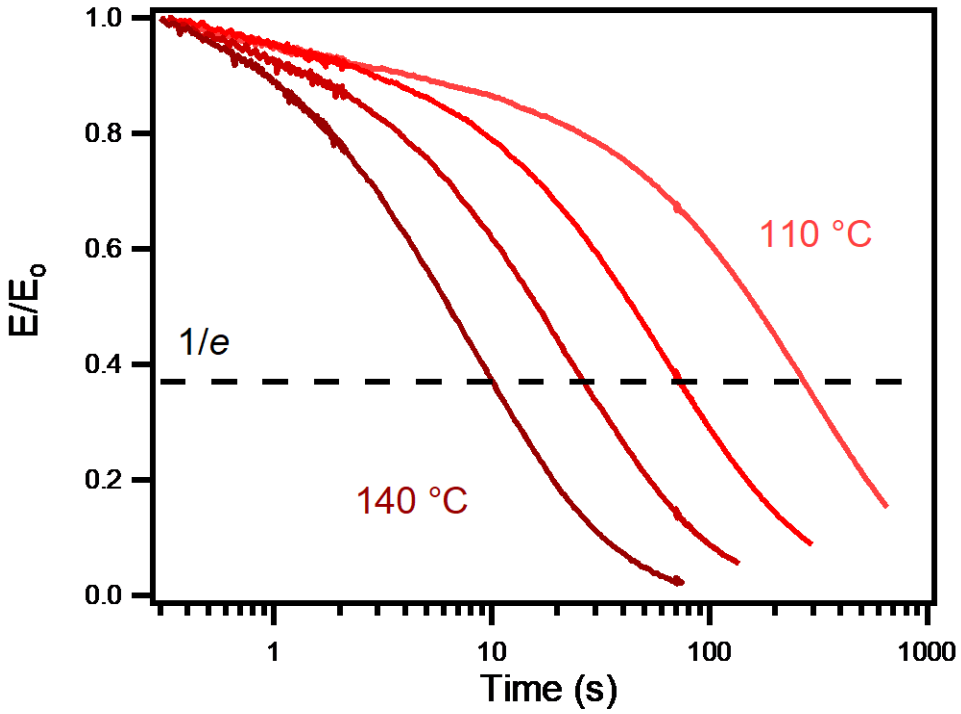

Figure S5.12. Representative stress relaxation curves of polyether PU with 1 mol% $Bi(neo)_3$ performed from 110 to 140 °C.

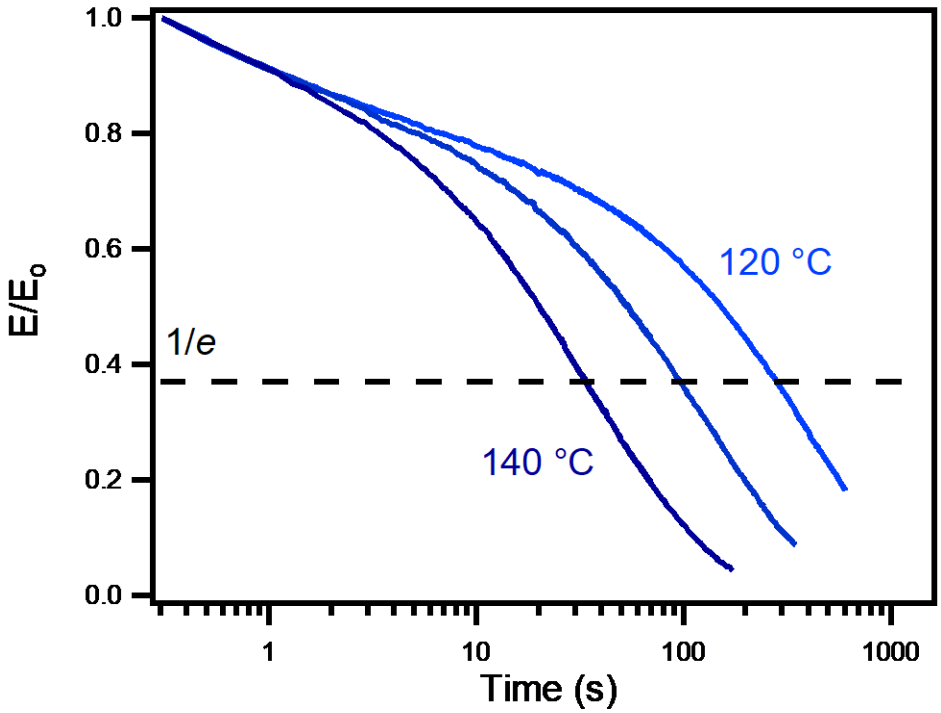

Figure S5.13. Representative stress relaxation curves of polyether PU with 1 mol% $Fe(acac)_3$ performed from 120 to 140 °C.

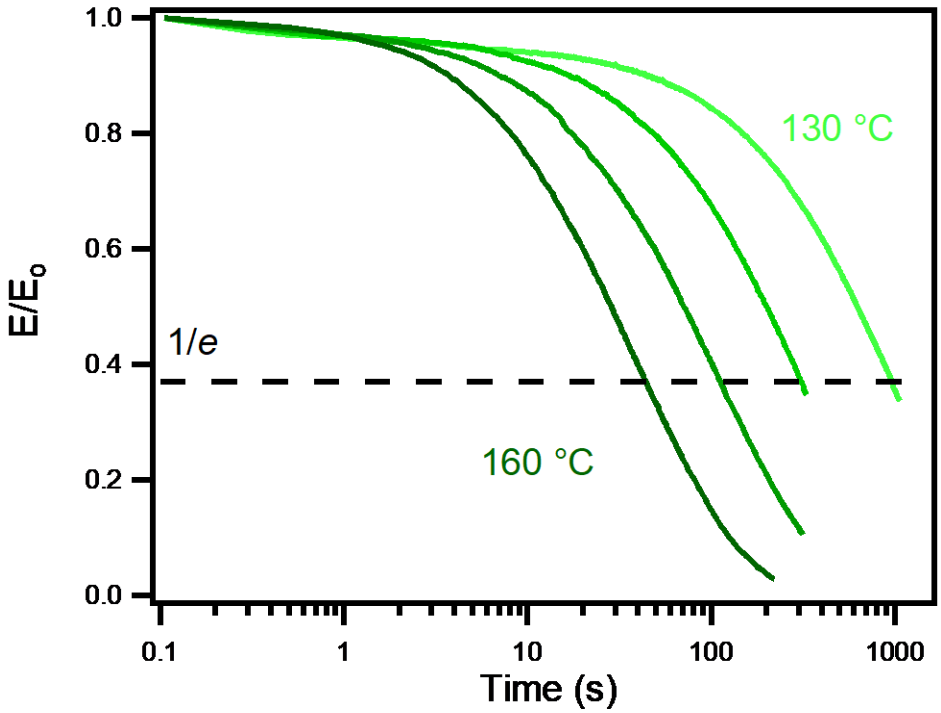

Figure S5.14. Representative stress relaxation curves of polyester PU with 1 mol% DBTDL performed from 130 to 160 °C.

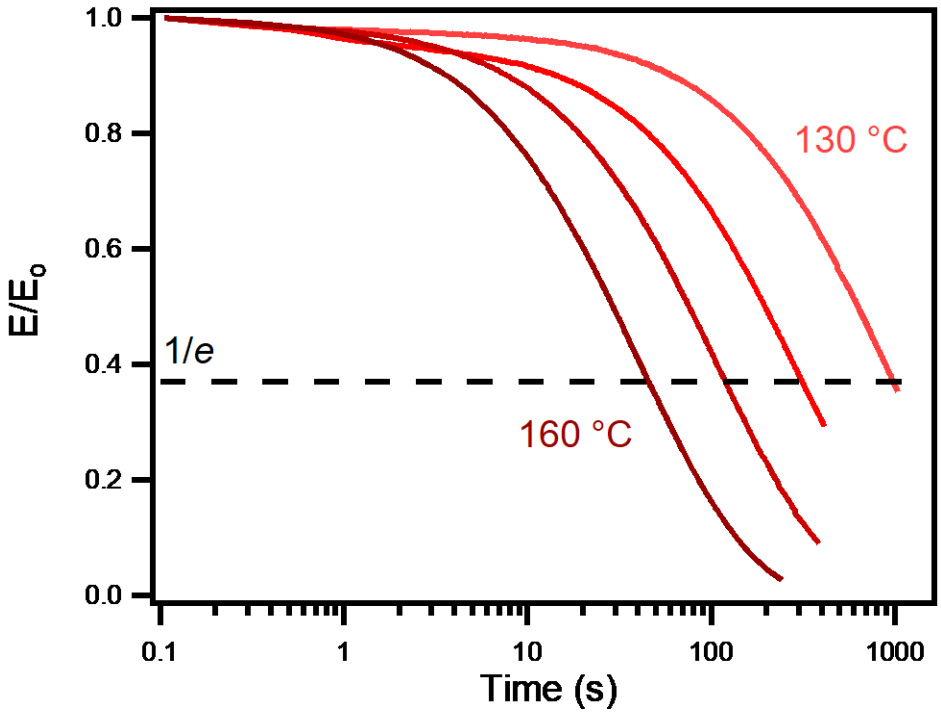

Figure S5.15. Representative stress relaxation curves of polyester PU with 1 mol% $Bi(neo)_3$ performed from 130 to 160 °C.

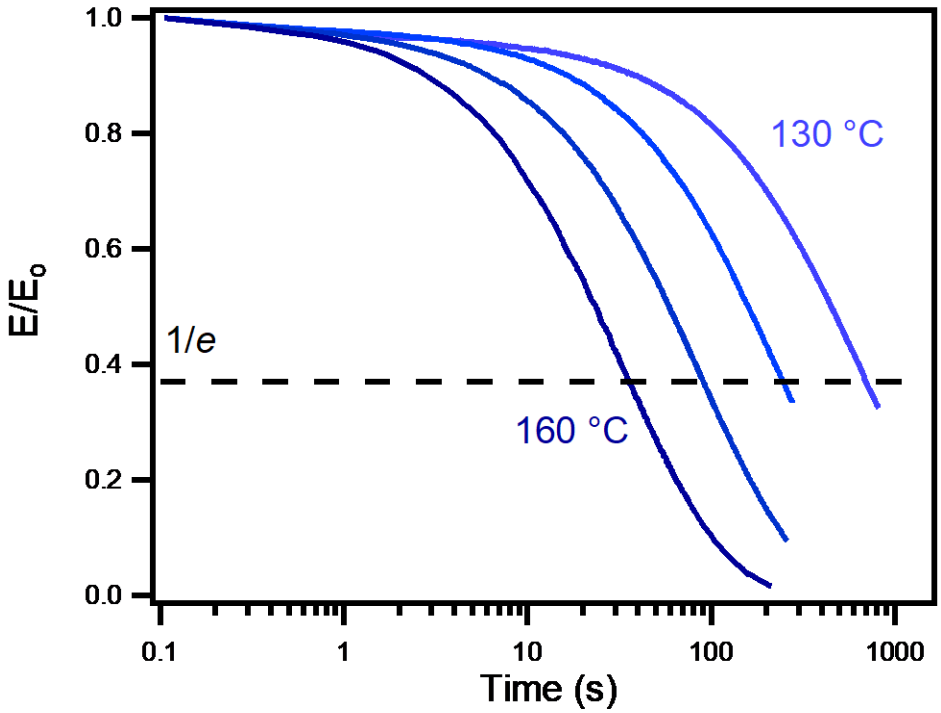

Figure S5.16. Representative stress relaxation curves of polyester PU with 1 mol% $Fe(acac)_3$ performed from 130 to 160 °C.

Table S5.3. Characteristic Relaxation Times of Polymers at Various Temperatures

Polymer	160 °C	150 °C	140 °C	130 °C	120 °C	110 °C
Ether-Sn			22 ± 1 s	65 ± 2 s	184 ± 11 s	587 ± 45 s
Ether-Bi			10 ± 1 s	30 ± 4 s	77 ± 6 s	308 ± 38 s
Ether-Fe			33 ± 1 s	101 ± 3 s	290 ± 8 s	
Ester-Sn	46 ± 2 s	111 ± 1 s	305 ± 35 s	887 ± 88 s		
Ester-Bi	47 ± 1 s	117 ± 3 s	321 ± 9 s	1006 ± 27 s		
Ester-Fe	35 ± 1 s	90 ± 1 s	246 ± 6 s	727 ± 35 s		

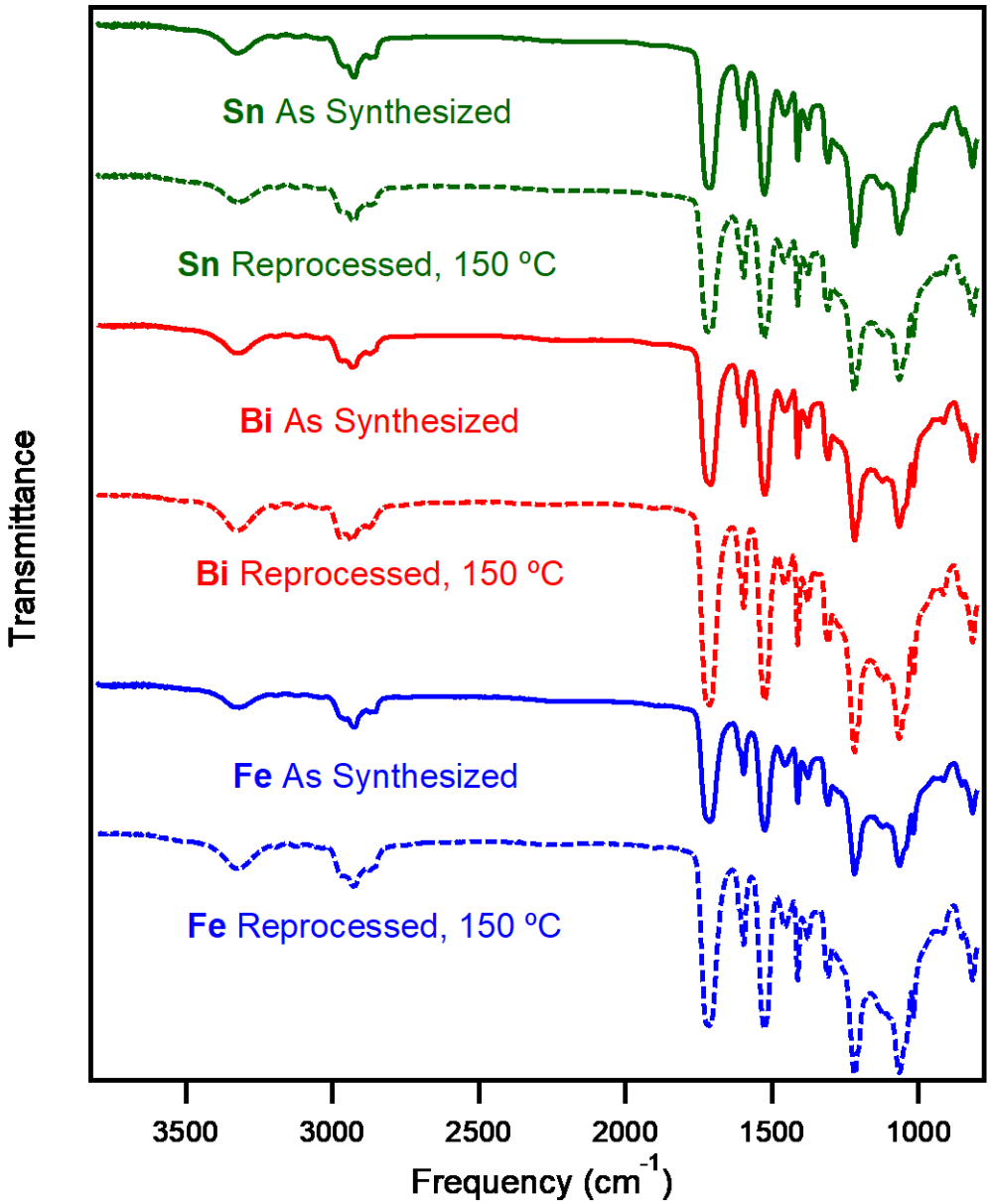

Figure S5.17. FT-IR spectra of polyester PUs as synthesized (solid) and after reprocessing (dashed) by compression molding under 5-10 tons pressure for 30 minutes at 150 °C.

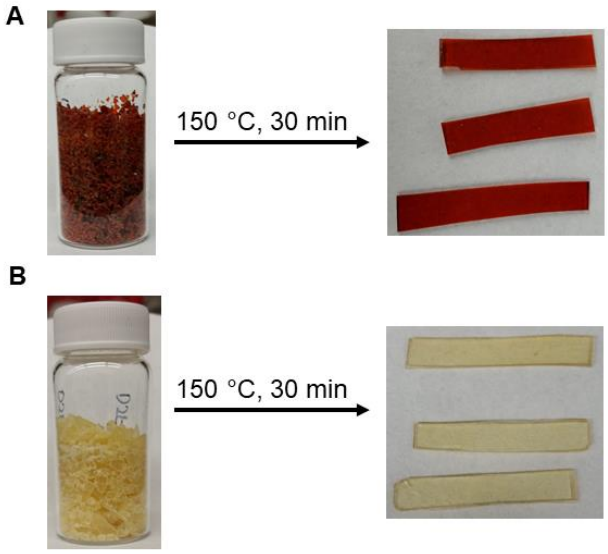

Figure S5.18. Photographs of polyester PUs containing 1 mol% A. $Fe(acac)_3$ and B. DBTDL after grinding then reprocessing via compression molding for 30 minutes at 150 ºC.

D. NMR Spectra

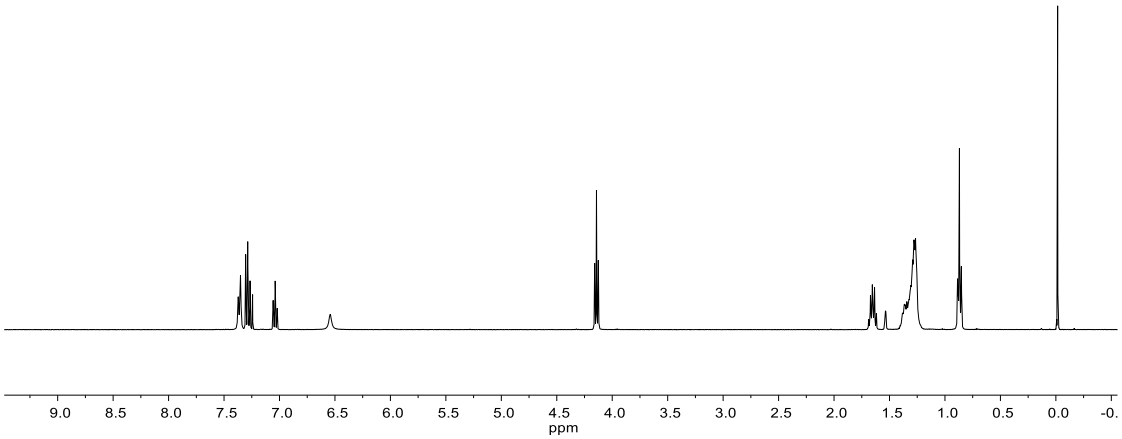

Figure S5.19. ^{1}H NMR ($CDCl_3$, 400 MHz, 298 K) of N-phenyl-O-octyl urethane

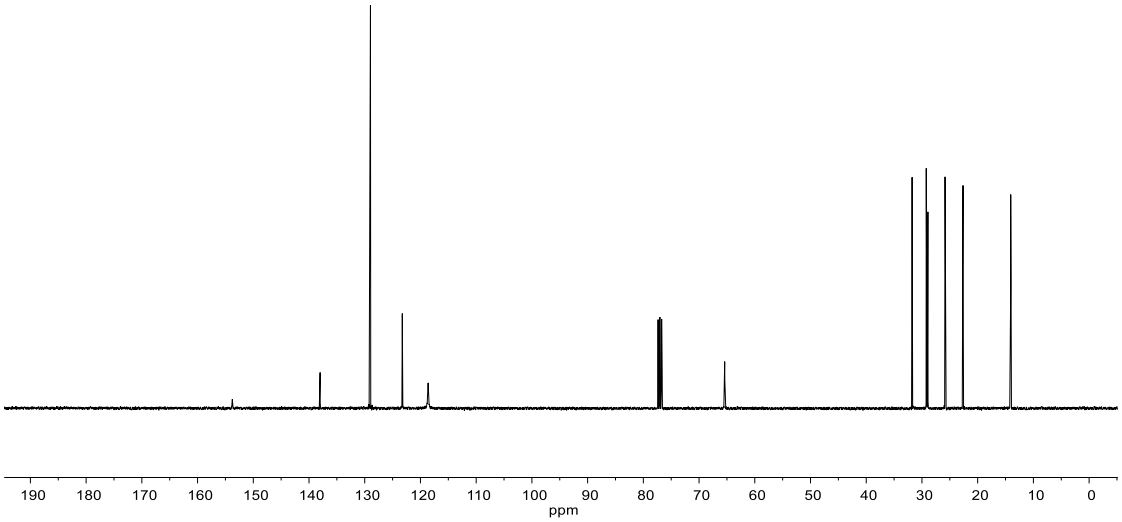

Figure S5.20. ^{13}C NMR ($CDCl_3$, 400 MHz, 298 K) of N-phenyl-O-octyl urethane.

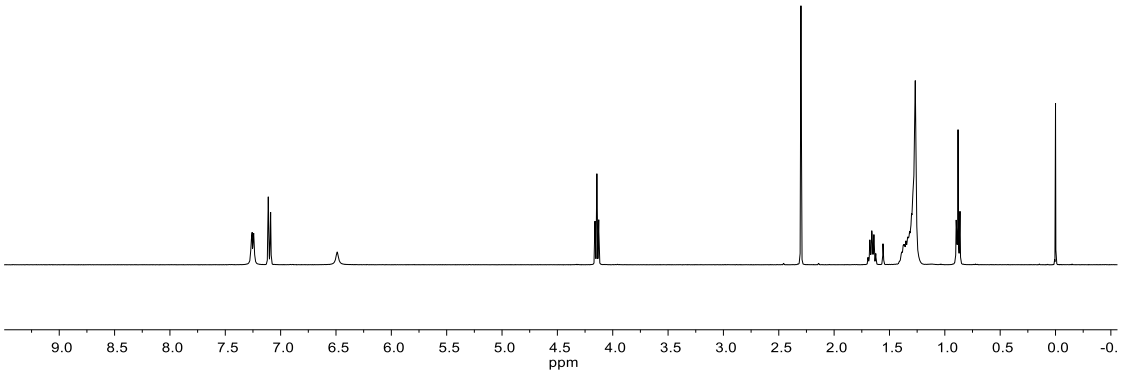

Figure S5.21. ^{1}H NMR ($CDCl_3$, 400 MHz, 298 K) of N-tolyl-O-decyl urethane.

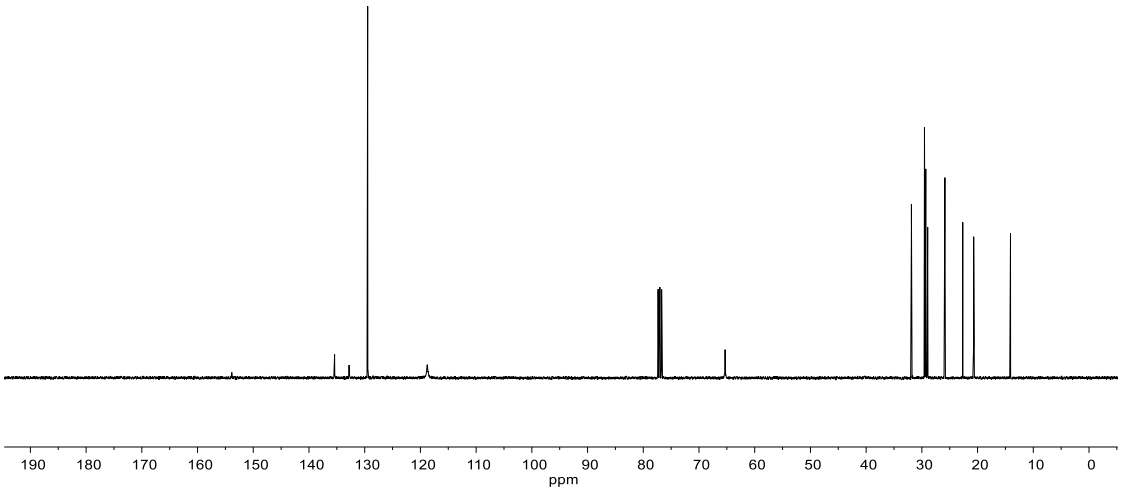

Figure S5.22. ^{13}C NMR ($CDCl_3$, 100 MHz, 298K) of N-tolyl-O-decyl urethane.

E. References:

1. Capelot, M.; Unterlass, M. M.; Tournilhac, F.; Leibler, L. *ACS Macro Lett.* **2012,** *1*, 789-792.

2. Brutman, J. P.; Delgado, P. A.; Hillmyer, M. A. *ACS Macro Lett.* **2014,** *3*, 607-610.